GFDL

Geophysical Fluid Dynamics Laboratory

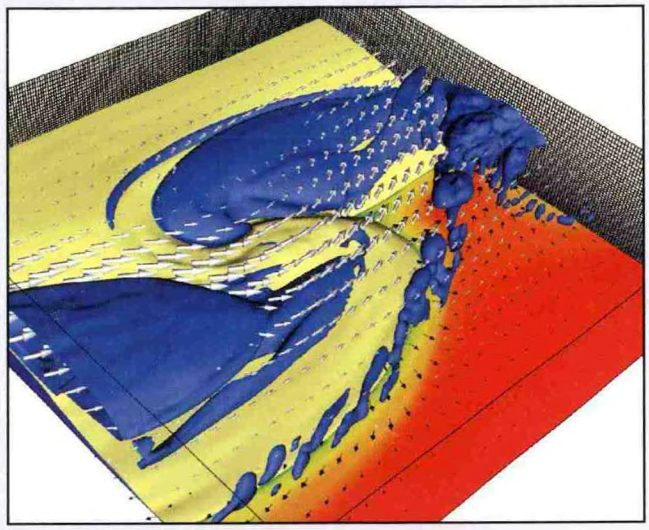

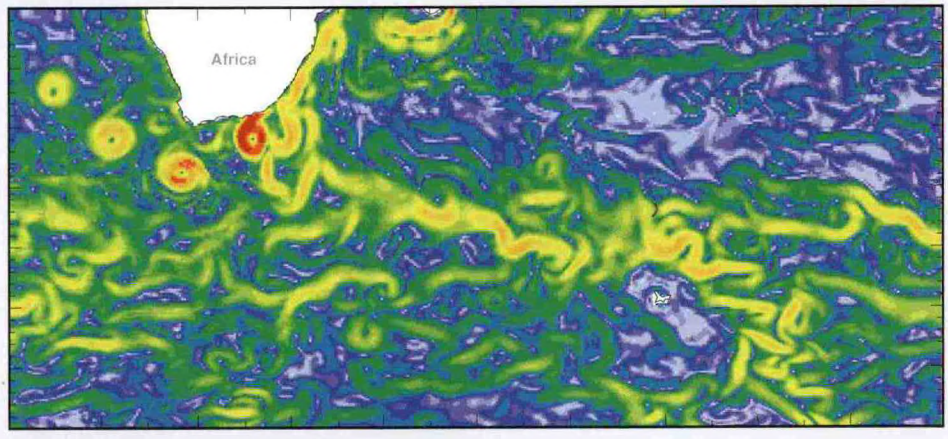

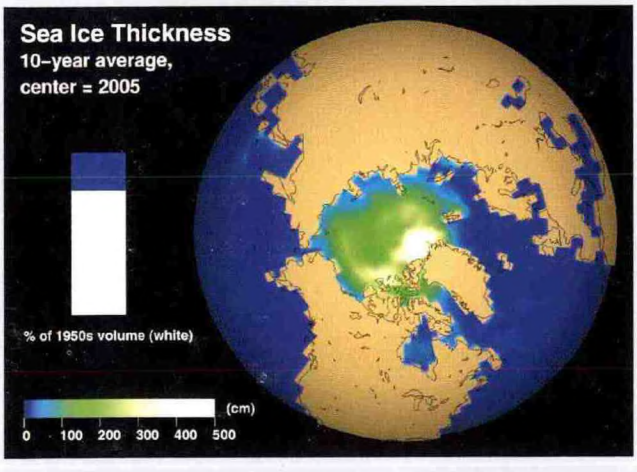

Princeton, NJ

Activities - FY00
Plans - FY01

U.S. Department of Commerce
National Oceanic and Atmospheric Administration
Environmental Research Laboratories

Front Cover:

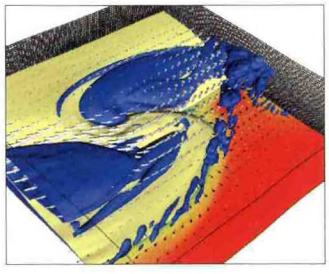

Simulation of the moist convective field associated with the development of a baroclinic wave. The isentropic surface (20°C) is shown in light green, the isosurface of liquid water (1gr/kg) is blue and the vectors show the wind pattern at 10 km (white arrows) and at the surface (black arrows). The surface temperature gradient is displayed from red (warm) to green (cold) and the mesh in the background shows the horizontal and vertical resolution used in the model. The rain band ahead of the cold front and the cloud wrapping around the cyclonic circulation are realistic features.

(Section 8.1.2)

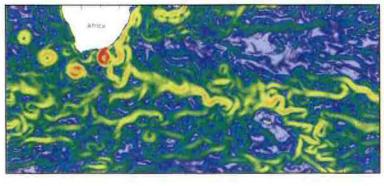

Snapshot of the velocity magnitude, averaged over the top 100 m, from a 1/4° (13.9 km resolution at 60°S) HIM ocean model run. Complete understanding of the interplay between the intense mesoscale eddies and the mean ocean circulation, and so of the general oceanic circulation itself, demands the use of numerical models with sufficiently high resolution to explicitly resolve these eddies, typically as small as 10 km in the ACC. This type of simulation will be used to assess the role of mesoscale eddies in the dynamics of the Antarctic Circumpolar Current.

(Section 5.1.2)

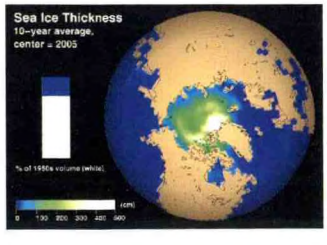

Illustration of changes in arctic sea ice thicknesses, simulated in one of GFDL's R30 atmosphere-ocean general circulation model experiments. The total volume of Arctic sea ice (i.e., sea ice poleward of 67°N) is expected to decrease by about 20% over the 50-year period extending from the 1950s to the 1st decade of the 21st century. Longer integrations show a 46% decrease by 2055. (See http://www.gfdl.noaa.gov/~kd/KDwebpages/NHice.html).

(Section 2.2.1)

GEOPHYSICAL FLUID DYNAMICS LABORATORY

ACTIVITIES - FY00

PLANS - FY01

OCTOBER 2000

GEOPHYSICAL FLUID DYNAMICS LABORATORY
PRINCETON, NEW JERSEY

UNITED STATES
DEPARTMENT OF COMMERCE

NORMAN Y. MINETA
SECRETARY OF COMMERCE

NATIONAL OCEANIC AND
ATMOSPHERIC ADMINISTRATION

D. JAMES BAKER
UNDERSECRETARY FOR OCEANS AND ATMOSPHERE

NOTICE

Mention of a commercial company or product does not constitute an endorsement by NOAA Environmental Research Laboratories. Use for publicity or advertising purposes of information from this publication concerning proprietary products or the tests of such products is not authorized.

PREFACE

This document summarizes recent research activities at the Geophysical Fluid Dynamics Laboratory (GFDL) and presents a glimpse of the planned direction of this research for the near future. The distribution of this report is intended primarily for GFDL members, Princeton University affiliates, and offices of the National Oceanic and Atmospheric Administration (NOAA), but it is also freely available to other relevant government agencies, national organizations, and interested individuals.

The organization of this document encompasses an overview, project activities and plans for the current and next fiscal year, and appendices. The overview covers highlights of the three major research areas that correspond to Strategic Plan Elements in NOAA's Environmental Assessment and Prediction Portfolio: Advance Short-Term Forecasts and Warnings; Seasonal to Interannual Climate Forecasts; and Predict and Assess Decadal to Centennial Changes, plus a category of topics which cuts across all three time scales: Basic Geophysical Processes. The body of the text describes goals, specific recent achievements, and future plans for the following major research categories: Climate Dynamics; Atmospheric Process; Experimental Prediction; Oceanic Circulation; Planetary Circulations; Climate Diagnostics; Hurricane Dynamics; and Mesoscale Dynamics. These categories, which correspond to the GFDL organization of research groups, are different from the NOAA strategic plan categories and are far from being mutually exclusive. Interaction occurs among the various groups and is strongly encouraged. The last section of the body is a description of the Laboratory's technical and computational support and its plans for the coming fiscal year.

The appendices contain the following: a list of GFDL staff members and affiliates during Fiscal Year 2000; a bibliography of recent research papers published by staff members and affiliates during their tenure with GFDL (these are referred to in the main body according to the appropriate reference number or letter); a listing of seminars presented at GFDL during Fiscal Year 2000; a list of seminars and talks presented during Fiscal Year 2000 by GFDL staff members and affiliates at other locations; and a list of acronyms.

The editors wish to acknowledge the substantial effort put forth by the GFDL staff and their Princeton University collaborators in preparing this report. Special thanks are extended to all who contributed to this work.

John P. Sheldon, Scientific Editor
Wendy H. Marshall, Technical Editor

September 2000

Geophysical Fluid Dynamics Laboratory/NOAA
P.O. Box 308, Princeton, New Jersey 08542

(609) 452-6500
http://www.gfdl.noaa.gov

TABLE OF CONTENTS

AN OVERVIEW 1
SCOPE OF THE LABORATORY'S WORK 3
HIGHLIGHTS OF FY00 AND IMMEDIATE OBJECTIVES 5
ADVANCE SHORT-TERM FORECASTS AND WARNINGS 9
SEASONAL TO INTERANNUAL CLIMATE FORCINGS 11
PREDICT AND ASSESS DECADAL TO CENTENNIAL CHANGES 15
BASIC GEOPHYSICAL PROCESSES 17

PROJECT ACTIVITIES FY00, PROJECT PLANS FY01

1. SOFTWARE INFRASTRUCTURE FOR SUPPORT OF SCIENTIFIC MODELING 25
1.1 LOW-LEVEL SUPPORT FOR MODELING 25
1.1.1 Memory Management, Communication, and I/O on Scalable Systems 25
1.1.2 Abstract Parallel Dynamical Kernels 26
1.1.3 Interpolation Between Model Grids on Scalable Architectures 26
1.2 PHYSICAL PARAMETERIZATIONS, COMPONENT, AND COUPLED MODELS 27
1.2.1 Convective Parameterizations and Diagnostics 27
1.2.2 Diagnostic Cloud Model 27
1.2.3 Global Atmospheric Grid Point Model 28
1.2.4 Dynamic/Thermodynamic Sea Ice Model 28
1.2.5 High Level Language Support for Coupled Models 28
1.3 SOFTWARE MANAGEMENT 29
1.3.1 FMS Management 29
1.3.2 Software Version Control for the Flexible Modeling System 30
1.3.3 FMS Software Releases 30
1.3.4 Web Page and Documentation Support 31
1.3.5 Optimization Team, Migration, and Evaluation 31

2. CLIMATE DYNAMICS 33
2.1 BACKGROUND FOR COUPLED CLIMATE MODELING AT GFDL CLIMATE CHANGE 33
2.2 CLIMATE CHANGE 34
2.2.1 Sea Ice and Global Warming 34
2.2.2 Water Vapor Feedback and Global Warming 36
2.2.3 Sea Level Rise and Global Warming 38
2.2.4 Response of Southern Hemisphere Winds to Global Warming 39
2.2.5 Discriminants of 20th Century Changes in Surface Temperature 40
2.2.6 Response of Climate to Natural and Anthropogenic Forcings 41
2.2.7 Climate Scenarios for IPCC Third Assessment Report 41
2.3 CLIMATE VARIABILITY AND DYNAMICS 43
2.3.1 Response of the North Atlantic Climate System to the Arctic/North Atlantic Oscillation 43
2.3.2 Observed and Simulated Multidecadal Variability in the North Atlantic 45
2.3.3 Partitioning of Poleward Heat Transport Between Ocean and Atmosphere in the Tropics 46

2.4 CLIMATE MODEL DEVELOPMENT 47
2.4.1 Coupled Climate Model Development 47
2.4.2 Development and Testing of the Land Dynamics Model 48
2.5 PALEOCLIMATE MODELING 50
2.5.1 Effects of Changes in Earth's Orbit on Climate 50
2.5.2 Simulation of Last Glacial Maximum with HadCM3 Coupled Climate Model 51
2.5.3 Effects of Fresh Water Discharge on Climate 52
2.6 HYDROLOGY AND CLIMATE 55
2.6.1 Sensitivity of River Runoff to Greenhouse Warming 55
2.6.2 Land-Process Influences on Monthly River Discharge Variability 55
2.6.3 Modeling Land Influences on Variability of Macro-Scale Water and Energy Fluxes 57
2.6.4 A Minimalist Probabilistic Description of Root-Zone Soil Water 58
2.7 PLANETARY CIRCULATION 58

3. ATMOSPHERIC PROCESSES 61
3.1 RADIATIVE TRANSFER 61
3.1.1 Solar Benchmark Computations 61
3.1.2 Shortwave Parameterizations 62
3.1.3 Diagnostic Analyses of Surface Solar Flux Measurements 63
3.1.4 Development of Radiative Parameterizations for GCMs 63
3.2 CONVECTION-CLOUDS-RADIATION-CLIMATE INTERACTIONS 65
3.2.1 Cumulus Parameterization 65
3.2.2 Limited-Area Non-Hydrostatic Models 66
3.2.3 Moist Convective Turbulence 67
3.2.4 Prognostic Cloud Parameterization 68
3.2.4.1 Parameterization Development Efforts
3.2.4.2 Diagnostic Assessment of the Simulation of Midlatitude Cloudiness
3.3 ATMOSPHERIC CHEMISTRY AND TRANSPORT 72
3.3.1 Fast Photochemical Solver Development 72
3.3.2 Ship Emissions of NOx 72
3.3.3 Tropical South Atlantic Ocean Tropospheric Ozone Maximum 73
3.3.4 Asian Impacts on Regional and Global Air Quality 74
3.3.5 GCM Simulation of Carbonaceous Aerosol Distribution 75
3.4 ATMOSPHERIC DYNAMICS AND CIRCULATION 78
3.4.1 Model Development 78
3.4.2 SKYHI Control Integrations and Basic Model Climatology 79
3.4.3 Spontaneous QBO-like Tropical Wind Oscillations in SKYHI Simulations 80
3.4.4 Low-Frequency Variability of Simulated Stratospheric Circulation 80
3.4.5 Horizontal Spectra from High-Resolution SKYHI Integrations 82
3.4.6 Parameterized Gravity Wave Drag in the SKYHI Model 82
3.4.7 GCM Simulations with an Imposed Tropical Quasi-biennial Oscillation 83
3.4.8 Observational Study of Gravity Wave Climatology 85
3.4.9 Dynamics of the Martian Atmosphere 86

3.5 CLIMATIC EFFECTS DUE TO ATMOSPHERIC SPECIES 87
3.5.1 Lower Stratospheric Ozone and Temperature Trends 87
3.5.2 Radiative Forcing Due to Ozone 88
3.5.3 Radiative Effects of Aerosol-Cloud Interactions 88
3.5.4 Radiative Effects Due to Pinatubo Stratospheric Aerosols 89
3.5.4.1 Experiments Using the SKYHI GCM
3.5.4.2 Coupled Climate GCM Simulations of Mt. Pinatubo Effects
3.5.5 Radiative Forcing Due to Changes in Stratospheric Ozone 91

4. EXPERIMENTAL PREDICTION 93
4.1 ATMOSPHERIC AND OCEANIC PREDICTION AND PREDICTABILITY 93
4.1.1 Ocean Model Development for Seasonal/Interannual Prediction 93
4.1.2 Coupled Model Development for Seasonal/Interannual Prediction 94
4.1.3 Statistical Atmospheric Model Development 94
4.1.4 Sensitivity to Horizontal and Vertical Resolution in Atmospheric Models 95
4.1.5 Impact of Land and Ocean Low-Level Tropical Clouds on ENSO Prediction 95
4.1.6 Atmospheric Model Predictability: Top of the Atmosphere Radiation Budget 97
4.1.7 Impact of MJO/WWB in the Far Western Equatorial Pacific on ENSO Forecasts 98
4.1.8 Interaction of MJO and Tropical Storms 98
4.1.9 The Nature and Predictability of Tropical Intraseasonal Oscillations 99
4.1.10 Coupled Model Potential Predictability 99
4.1.11 Indian Ocean Variability 100
4.2 DATA ASSIMILATION 103
4.2.1 Ensemble Adjustment Filter 103
4.2.2 Ocean Data Assimilation 103
4.2.3 Information Content of Surface Pressure Observations 105
4.2.4 Targeted Observations 106
4.3 OCEAN-ATMOSPHERE INTERACTIONS 107

5. OCEANIC CIRCULATION 109
5.1 WORLD OCEAN STUDIES 109
5.1.1 Modeling Eddies in the Southern Ocean 109
5.1.2 Southern Ocean Winds and the Circumpolar Current: Theoretical Studies 110
5.1.3 The ACC and the Ocean's Thermohaline Circulation 114
5.1.4 Ocean Eddy Energies, Scales, and Vertical Structure 116
5.1.5 Geostrophic Turbulence 117
5.2 MODEL DEVELOPMENT 118
5.2.1 Modular Ocean Model 118
5.2.2 Isopycnal Coordinate Model Development 120
5.3 COASTAL OCEAN MODELING AND PREDICTION 121
5.3.1 East Coast and North Atlantic Modeling and Forecasting 121
5.3.2 Turbulent Boundary Layer Modeling 122
5.3.3 Princeton Ocean Model Development and Testing 123

5.3.4 Climate Variability Studies with POM 123
5.3.5 Coastal Models of the West Coast and the Gulf of Mexico 124

5.4 GLOBAL BIOGEOCHEMISTRY AND THE CARBON CYCLE 125

5.4.1 Terrestrial Carbon Cycling 125
5.4.2 Inverse Modeling of Carbon Isotopic Ratios of CO_2 in the Atmosphere 126
5.4.3 Mixing Parameterizations, Large-Scale Ocean Circulation, and Global Biogeochemical Cycles 127
5.4.4 Air-Sea Fluxes of O_2 and CO_2 Determined by Inverse Modeling of Ocean Bulk Measurements 128
5.4.5 An Ecosystem Model for Biogeochemical Studies 129
5.4.6 Oceanic Nitrogen Cycle 129
5.4.7 Global Patterns of Marine Silicate, Nitrate, and Alkalinity Cycling 130
5.4.8 Analysis of the Ocean's Carbon Pumps 131
5.4.9 Response of Ocean Biology to Future Climate Change 132

6. CLIMATE DIAGNOSTICS 134

6.1 COMPILATION OF A TEMPORALLY HOMOGENEOUS RADIOSONDE TEMPERATURE DATASET 134

6.1.1 Sensitivity of Radiosonde Temperature Trends to Data Quality 134

6.2 ANALYSIS OF DATASETS BASED ON SATELLITE OBSERVATIONS 135

6.2.1 Decadal Variations in Tropical Water Vapor: An Evaluation of Satellite Observations and a Model Simulation 135
6.2.2 Reconciling Surface and Satellite Temperature Records 136

6.3 AIR-SEA INTERACTION 138

6.3.1 Experimentation with an Atmospheric General Circulation Model Coupled to an Ocean Mixed-Layer with Variable Depth 138
6.3.2 Atmospheric Bridge Linking ENSO to SST Variability in the North Pacific and North Atlantic 139
6.3.3 Impact of ENSO on Monsoon Systems in East Asia and Australia 140
6.3.4 Modulation of Tropical Transient Activity by ENSO 140

6.4 DEVELOPMENT OF WEB-BASED TOOLS FOR VISUALIZING AND EVALUATING MODEL OUTPUT 143

6.5 GFDL/UNIVERSITIES COLLABORATIVE PROJECT FOR MODEL DIAGNOSIS 144

7. HURRICANE DYNAMICS 145

7.1 HURRICANE PREDICTION SYSTEM 145

7.1.1 Performance in the 1999 Hurricane Season 145
7.1.2 Analysis of the Forecast Results 145
7.1.3 The 2000 Hurricane Season 146

7.2 HURRICANE PREDICTION CAPABILITY 147

7.2.1 Extended Prediction 147
7.2.2 Impact of Satellite-Observed Winds on GFDL Forecasts 147
7.2.3 Sensitivity of GFDL Track Forecasts to Initial Conditions 148
7.2.4 Evaluation of Model Forecast Errors 149

7.3 BEHAVIOR OF TROPICAL CYCLONES 150

7.3.1 Hurricane Intensity in a High-CO_2 Climate 150
7.3.2 Tropical Cyclone-Ocean Interaction 151

7.3.3 Tropical Cyclone Landfall 152

7.4 MODEL IMPROVEMENT 152

8. MESOSCALE DYNAMICS 155

8.1 ANALYSIS OF MIDLATITUDE CYCLONES AND STORM TRACKS 155

8.1.1 The Evolution and Feedback of Cyclones in Storm Track Simulations 155

8.1.2 Moist Convection in Baroclinic Life Cycles 156

8.2 TOPOGRAPHIC INFLUENCES IN ATMOSPHERIC FLOWS 158

8.2.1 Gravity-Wave Parameterizations Over the Andes 158

8.3 MODEL DEVELOPMENT 160

8.3.1 Improvements to the Nonhydrostatic Compressible Zeta Model 160

9. TECHNICAL SERVICES 161

9.1 COMPUTER SYSTEMS 161

9.1.1 Current Supercomputing Systems 161

9.1.2 High Performance Computing System Procurement 162

9.1.3 Software Development and Technical Support Procurement 164

9.1.4 Scientific Workstation Network 164

9.2 DATA MANAGEMENT 167

9.3 DATA VISUALIZATION 168

9.4 INFORMATION AND PRESENTATION RESOURCES 169

9.5 PUBLIC INFORMATION DISSEMINATION AND OUTREACH 170

APPENDIX A GFDL STAFF MEMBERS AND AFFILIATED PERSONNEL DURING FISCAL YEAR 2000 A-1

APPENDIX B GFDL BIBLIOGRAPHY B-1

APPENDIX C SEMINARS GIVEN AT GFDL DURING FISCAL YEAR 2000 C-1

APPENDIX D TALKS, SEMINARS, AND PAPER PRESENTED OUTSIDE GFDL DURING FISCAL YEAR 2000 D-1

APPENDIX E ACRONYMS E-1

AN OVERVIEW

SCOPE OF THE LABORATORY'S WORK

The Geophysical Fluid Dynamics Laboratory is engaged in comprehensive long lead-time research fundamental to NOAA's mission, both now and into the future.

The goal of this research is to expand the scientific understanding of the physical processes that govern the behavior of the atmosphere and the oceans as complex fluid systems. These systems can then be modeled mathematically and their phenomenology can be studied by computer simulation methods. In particular, GFDL research concerns the following:

- the predictability of weather on large and small scales;
- the structure, variability, predictability, stability and sensitivity of global and regional climate;
- the structure, variability and dynamics of the ocean over its many space and time scales;
- the interaction of the atmosphere and oceans, and how the atmosphere and oceans influence and are influenced by various trace constituents;
- the Earth's atmospheric general circulation within the context of the family of planetary atmospheric circulations.

The scientific work of the Laboratory encompasses a variety of disciplines including meteorology, oceanography, hydrology, classical physics, fluid dynamics, chemistry, applied mathematics, and numerical analysis. Research is also facilitated by the Atmospheric and Oceanic Sciences Program (AOSP), which is a collaborative program at GFDL with Princeton University. Under this program, regular Princeton faculty, research scientists, and graduate students participate in theoretical studies, both analytical and numerical, and in observational experiments in the laboratory and in the field. The program is supported in part by NOAA funds. AOSP scientists may also be involved in GFDL research through institutional or international agreements.

The following sections describe the GFDL contributions to three major research areas that correspond to Strategic Plan Elements in NOAA's Environmental Assessment and Prediction Portfolio, plus a broader category that supports all three.

HIGHLIGHTS OF FY00

and

IMMEDIATE OBJECTIVES

In this section, some research highlights are listed that may be of interest to those persons less concerned with the intricate details of GFDL research. Selected are items that may be of special significance or interest to this wider audience.

Most of the items in this section have been ordered according to the current NOAA Strategic Plan Elements, which are divided roughly according to time scale:

- Advance Short-Term Forecasts and Warnings
- Seasonal to Interannual Climate Forecasts
- Predict and Assess Decadal to Centennial Changes

Recognizing that much scientific progress has application to phenomena at a wide variety of time scales, a number of items have been placed into a category which cuts across the time scales represented by the previous elements:

- Basic Geophysical Processes

This avoids an awkward force-fit of certain topics into a particular time scale and highlights the fundamental role that these topics play as building blocks for progress in multiple research areas.

Note that the categories described above are organized differently than the GFDL research project areas presented in the main body of the report. This is but another reflection of the variety and interplay of activities within such a fertile research environment. As an aid in cross-referencing, the number in parentheses following each highlight refers to sections in the main body of the report.

ADVANCE SHORT-TERM FORECASTS AND WARNINGS

The need for short-term warning and forecast products covers a broad spectrum of environmental events which have lifetimes ranging from several minutes to several weeks. Some examples of these events are tornadoes, hurricanes, tsunamis, and coastal storms, as well as "spells" of unusual weather (warm, cold, wet, or dry). Benefits of these products can be measured in terms of lives saved, injuries averted, and expenses spared. NOAA's vision for improvement in this area involves operational modernization and restructuring, strengthening of observing and prediction systems, and improved applications and dissemination of products and services.

Efforts at GFDL are centered around the development of numerical models which may be used in the prediction of "short-term" atmospheric and oceanic phenomena. Simulations from these models are studied and compared with observed data to aid in the understanding of the processes which govern the behavior of the various phenomena.

With regard to tropical weather systems, efforts are aimed at understanding and forecasting the genesis, growth, and decay of tropical storms and hurricanes. In extratropical regions, interest includes the development of severe weather systems, the interaction of medium-scale atmospheric flow with that on larger scales, and the influence of the underlying topographic features. Experimental prediction of regional-scale weather parameters weeks in advance is being pursued; included in this context is the study of "ensemble forecasting." With regard to the marine environment, forecasts of coastal conditions on a day-to-day basis can be made by coupling of ocean and atmosphere models. Ocean models are also used to simulate and forecast coastal and estuarine environments, the response of coastal zones to transient atmospheric storms, and Gulf Stream meanders and rings.

ACCOMPLISHMENTS FY00

Model simulations of the Madden-Julian Oscillation (MJO) are revealing new details about the predictability of this phenomena. Analysis of the impact of the MJO on tropical storms in the model has also pointed to the potential for some skill in several week lead predictions of tropical storm activity (4.1.8).

The conversion of the GFDL modeling system to a distributed memory system was successfully completed. This ensures the efficiency of the forecast system for operational implementation at NCEP for the 2000 tropical season, as well as for future research applications at GFDL. The conversion effort was made particularly difficult because of the complex nature of the GFDL moving nested grid framework. The new design incorporates two-dimensional decomposition. Operational forecasts will now be made for 5 days instead of 3 days. Work was also completed in porting the coupled model to the new NCEP system, making the model available for the 2000 hurricane season in the Tropical Atlantic (6.1.3, 6.4).

Forecasting hurricane intensity remains a challenging goal. For the 1999 season, however, the GFDL system did exhibit skill for forecast periods of 48hr and beyond. When

adjusted for initial bias, the GFDL model showed skill relative to climatology and persistence for the entire 72h forecast period with mean errors 11, 17, and 17 knots at 24, 48, and 72hrs, respectively. This is evidence that forecast system changes made in prior years, including the addition of initial asymmetries, resulted in improvements for the 1999 season. As in the 1998 season, the coupled model achieved significant improvements in the hurricane intensity forecasts compared to the operational atmosphere-only GFDL model. The mean absolute error of the sea-level pressure forecasts was reduced by about 31%. There are indications that improvements in resolution and physical parameterizations relating to the boundary layer and cumulus convection will lead to further improvements in intensity forecasts (6.3, 6.4).

The impact of initial conditions on the quality of GFDL operational tropical cyclone forecasts was investigated in two studies. On average, the assimilation of GOES satellite winds into the GFDL regional domain led to improvements from 5-12% in track and 4-8% in intensity (6.2.2). On the other hand, the quality of GFDL forecasts was also improved by using two different global analyses: the UKMET analysis, and a test AVN analysis scheduled for operational implementation for the 2000 season. Both of these global analyses improved GFDL track forecasts by more than 20% (6.2.3). Further improvements in operational forecasts are anticipated with improved global and regional assimilation systems which optimally ingest data.

Prior studies have shown a modest increase (~5-10%) in the intensity of very strong hurricanes in a high CO_2 climate, as compared to the strongest hurricanes in a control climate. However, studies to date have neglected the effect of hurricane/ocean coupling (*i.e.*, the local SST cooling induced by the hurricane) on the intensity changes. To evaluate how a CO_2-induced enhancement of hurricane intensity could be altered by the hurricane/ocean coupling, a series of idealized hurricane experiments was performed using the GFDL Hurricane Prediction System coupled to the Princeton Ocean Model (POM). The results indicate that a CO_2-induced intensification still occurs even when the hurricane/ocean coupling effects are included; ocean coupling appears to have only a small impact on the magnitude of this intensification (6.3.1).

PLANS FY01

- Studies will continue on increasing the grid resolution of multiply-nested meshes in the GFDL hurricane model. A study of the optimal grid configuration of the nested model for distributed memory systems will be undertaken. More realistic representation of the eye and eyewall of intense hurricanes will be investigated, as well as the influence of the large-scale environmental flow.

- The initialization of the GFDL hurricane model will be improved with continued development of a four-dimensional approach in which both routine observations and supplemental storm data can be ingested into the initial condition.

- Developmental work to improve the hurricane model initialization, ocean interaction, model physics, and resolution will continue. This is critical for improved intensity

prediction skill. A significant number of case studies will be needed to evaluate the impact of these efforts on track and intensity forecast skill.

SEASONAL TO INTERANNUAL CLIMATE FORECASTS

Seasonal to interannual climate fluctuations have far-reaching consequences for agriculture, fishing, water resources, transportation, energy consumption, and commerce, among others. Short-term climate anomalies which persist from a season to several years affect rainfall distributions, surface temperatures, and atmospheric and oceanic circulation patterns. Reliable climate forecasts may be used to reduce the disruption, economic losses, and human suffering that occur in connection with these anomalies. NOAA's vision for improvement in this area is based on better predictive capability, enhanced observations, greater understanding of climate fluctuations, and assessment of impacts.

The study of seasonal to interannual climate fluctuations at GFDL is based on both theoretical and observational studies. Available observations are analyzed to determine the physical processes governing the behavior of the oceans and atmosphere. Mathematical models are constructed to study, simulate, and predict the coupled ocean-atmosphere, land-surface, sea-ice system.

Simulations based on the numerical models maintained at GFDL, in conjunction with observations, are used to study climate variations on seasonal and longer time scales. Processes under study include large-scale wave disturbances and their role in the general circulation, the effects of boundary conditions such as sea surface temperature and soil moisture, influence of clouds, radiation, and atmospheric convection, and the "teleconnection" of atmospheric anomalies across the global atmosphere. Furthermore, experimental model forecasts are used to evaluate atmospheric predictability and to assess skill in forecasting atmospheric and oceanic climate anomalies, both in general and in connection with the El Niño-Southern Oscillation phenomenon. Also, a more accurate representation of the state of the global ocean is being studied through data assimilation for better initialization of seasonal-interannual forecasts.

ACCOMPLISHMENTS FY00

Model simulations of the response of the stratosphere to the observed (1979-1997) changes in ozone and in the well-mixed greenhouse gases (carbon dioxide, methane, nitrous oxide and halocarbons) produce a pattern of temperature change similar to that observed. The response is largely due to ozone change in the polar lower stratosphere and to greenhouse gas change in the upper stratosphere (3.5.5).

GCM simulations employing the observed aerosol enhancements in the stratosphere following the eruption of Mt. Pinatubo reveal that the radiative flux anomalies induced are in good agreement with those observed, with the small residual differences attributable to deficiencies in the simulation of cloud cover variability and aerosol optical property inputs (3.5.4).

Analysis of the GFDL GCTM tropospheric column ozone, generated without the biomass burning NOx source, has shown that a reduced South Atlantic Ocean September maximum can still be produced. This suggests that the ozone phenomenon existed prior to the advent of agricultural burning by humans (2.3.3).

Episodic trans-Pacific pollution events greatly exceed background levels, with Asian contributions to episodic O3 events over the western US currently in the 3 - 10 ppbv range and growing to 40 ppbv, a factor of 4 increase (2.3.4).

Coupled models suitable for seasonal-interannual prediction are being developed using the new Flexible Modeling System. Efforts to coordinate coupled model development between all global modeling groups at GFDL are underway (4.1).

Tests with FMS atmospheric models suggests that increases of vertical and horizontal resolution may have significant impact on the quality of seasonal-interannual simulations and predictions (4.1.4).

The impact of low clouds on seasonal-interannual predictions is even larger than previously believed. Low clouds over both land and ocean regions have significant impacts on the general circulation and the seasonal cycle in the tropics. Efforts to develop improved low cloud parameterizations are continuing (4.1.5).

Expanded ensembles of one year coupled model predictions have provided further evidence that in certain years, the evolution of the sea surface temperatures in the tropical Pacific is not predictable for lead times of more than a few months (4.1.10).

Simulations of dipole sea surface temperature variability in the tropical Indian ocean have revealed new aspects of this phenomena, in particular, the sensitivity to the preconditioned state of subsurface thermal structure on the onset of this "coupled dipole mode". Potential impacts on seasonal prediction are being evaluated (4.1.11).

An ensemble adjustment filtering technique for data assimilation has been developed. The method is better than current state-of-the-art methods in low order models. As an example of the power of the assimilation method, assimilations of synthetic observations of only surface pressure in a global primitive equation model were able to reproduce many details of the circulation in the free atmosphere (4.2.1).

Initial versions of an adjoint for the MOM ocean model have been developed as a first step towards implementing four-dimensional variational data assimilation in MOM (4.2.2).

The relative contribution of land use, carbon dioxide fertilization, and nitrogen fertilization in U.S. forests has been quantified. Results show that land use is the primary factor governing the rate of carbon sequestration in U.S. forests (5.4.1).

A new terrestrial biosphere model, the Ecosystem Demography model, has been set up to examine the impact of human land-use on the terrestial carbon cycle of North America (5.4.1).

The time evolution of carbon isotopes in the atmosphere has been used to infer sources and sinks of terrestrial carbon. Results for 1993-95 indicate the presence of a terrestrial carbon sink in the mid latitudes of the northern hemisphere and a tropical carbon source (5.4.2).

Progress has been made in applying adjustments to a global network of 87 radiosonde stations so as to render their temperature time series more temporally homogeneous. These adjusted data are valuable in the study of global temperature trends (6.1.1).

Multiple satellite records of tropical-mean water vapor have been compared with a model simulation to assess our ability to monitor and predict low-frequency changes in total precipitable water, which is an important quantity for the detection of climate change. The comparison demonstrated excellent agreement between the observed variations in tropical water vapor and those predicted by the model integration (6.2.1).

A coupled model has been developed utilizing a one-dimensional ocean mixed-layer model with variable depth and a GFDL atmospheric GCM. A large suite of experiments has been completed with this model under various SST forcing scenarios. These integrations have shed new insights on the impact of ENSO on the variability of the extratropical atmosphere-ocean system and the Asian-Australian monsoons (6.3).

A decade-long effort to involve the university community in the analysis and design of GFDL model experiments has concluded. This collaboration has expanded our knowledge of the effects of anomalies in surface boundary conditions on interannual and interdecadal variability of the atmosphere, and of the dynamical and statistical nature of different types of atmospheric fluctuations (6.5).

Mesoscale (Zeta-model) simulations of realistic storm tracks have revealed different patterns of eddy structure and evolution corresponding to strong and weak zonal variations of the time-mean flow. Depending on the length of the storm track, the eddies tend to appear either in mobile wave packets or in quasi-stationary "couplets". The two patterns are most commonly observed in the Southern and Northern Hemispheres, respectively. It has been speculated that the interannual variability of the shape of the storm tracks in the Northern Hemisphere is controlled by variability in the low-level subtropical humidity. To investigate this possibility, the mesoscale simulations are now being conducted with explicit moisture and clouds, which have recently been added to the Zeta model (8.1).

PLANS FY01

- Analyses of the large number of integrations performed with various versions of the SKYHI model will continue, including integrations performed with different spatial resolutions,

QBO modes, and tracer distributions. It will also include analyzing the sensitivity of the changes in stratospheric climate to different forcings (volcanic aerosols, "QBO", ozone, well-mixed gases, water vapor, sea-surface temperatures). The changes will be compared against the "natural" internal variability of the model using the 50-year "unforced" integrations.

- Coupled models for experimental prediction using FMS will be developed and tuned in order to produce a state-of-the-art seasonal ensemble prediction system. The new model will be used to produce ensemble predictions and long simulations of the coupled climate system.

- The Hybrid statistical atmosphere coupled model will be used to evaluate the capabilities of newly developed FMS atmospheric models and will also be used to help diagnose the response of the ocean to the Madden-Julian Oscillation and Westerly Wind Bursts.

- The ensemble adjustment filter will be tested in higher resolution primitive equation models and in prediction models with fully parameterized physics. Initial application of the filter to MOM will be explored.

- A four-dimensional variational assimilation of the TAO data in the Pacific will be performed using the new MOM4 and its adjoint.

- The new Ecosystem Demography model will be used to study the importance of terrestrial biospheric feedbacks for global climate.

- A new suite of integrations under different SST forcing scenarios will be used to investigate the nature of extratropical air-sea feedbacks associated with ENSO, the atmospheric responses to SST forcing in the Indian Ocean and western tropical Pacific, and the role of tropical Atlantic SST anomalies in atmospheric variability in the North Atlantic sector.

- The process of drafting a set of review and research papers on various foci of the GFDL/Universities collaborative project for model diagnosis will be completed. The manuscripts will be edited for publication in a special issue of a scientific journal.

- The sensitivity of cyclone evolution to position within the storm track will continue to be evaluated. In particular, the mechanisms responsible for the poleward progression of low-level cyclonic eddies will be further analyzed.

- Continuing idealized storm track simulations with the spherical-coordinate models should clarify the most important processes in the development, maintenance, and decay of the storm tracks. Sensitivity studies will be undertaken to clarify the features most important to

cyclone evolution within them. The model is also being adapted to the GFDL Flexible Modeling System.

PREDICT AND ASSESS DECADAL TO CENTENNIAL CHANGES

Events such as the Sahel drought, the dust bowls in the Midwest, the Little Ice Age, stratospheric ozone depletion, and global warming may define eras in history. Events such as these have lifetimes of decades to centuries and their causes can be either natural or anthropogenic. An ability to predict such changes and to assess the causes is essential in long-range policy making. Adapting to these changes and reducing the effects of human activities will require enhanced predictive capability. NOAA's vision for improvement in this area is based on a commitment to research in climate and air quality, as well as to insure long-term climate and chemical records.

The related research efforts at GFDL require judicious combinations of theoretical models and specialized observations. The modeling efforts draw on principles from the atmospheric, oceanic, chemical, and biological sciences. One area of focus is long-term climate variability and secular change associated with the atmosphere and oceans. This area encompasses a number of topics, including the effects of changes in the concentration of atmospheric gases such as carbon dioxide, the simulation of past climates, and the variability of the oceanic thermohaline circulation. Another area of focus is the formation, transport, and chemistry of atmospheric trace constituents. This area addresses problems such as: the transport of quasi-conservative trace gases; the biogeochemistry of climatically significant long-lived trace gases; the transport, sources, and sinks of aerosols; the chemistry of ozone and its regulative trace species; the effects of clouds and aerosols on chemically important trace gases; and the impact of anthropogenic chlorofluorocarbons on stratospheric ozone amounts. Yet another area of focus relates to the modeling of the marine environment. It includes the dispersion of geochemical tracers in the world oceans, the oceanic carbon cycle and trace metal geochemistry, and ecosystem structures.

ACCOMPLISHMENTS FY00

Simulated changes in Southern Hemisphere circulation in response to global warming have been found to project strongly on the so-called Southern Annular Mode (or Antarctic Oscillation). These changes appear to be indirect adjustments of the jet and storm tracks to changes in the large-scale radiative and thermal environment. Similar circulation changes, albeit larger in magnitude, have been observed during the last 30 years (2.2.4).

Coupled climate model integrations were conducted using two of the IPCC's key scenarios of greenhouse gas and sulfate emissions. These integrations represent part of GFDL's contribution to the IPCC Third Assessment Report. Under these scenarios, the model simulates a global warming of between 2.4°C and 3.5°C during the next 100 years (2.2.7).

Motivated by the observed trend in the Arctic/North Atlantic Oscillation (AO/NAO), the oceanic response of an anthropogenically forced coupled climate model to changes in the

AO/NAO was examined. A sustained upward trend in the AO/NAO is found to delay the greenhouse gas-induced weakening of the thermohaline circulation by several decades (2.3.1).

A comparison was made between multidecadal North Atlantic climate variability simulated by a coupled model and analyses of both instrumental and proxy records. The combined instrumental/proxy data show a pattern of sea surface temperature variability that is similar to that simulated by the model. The 70-year time scale of the observed variability compares favorably with the model results, which indicate a time scale of 40-80 years (2.3.2).

In collaboration with the Hadley Centre for Climate Prediction, the first multicentury simulation of the ice age climate was conducted using a coupled atmosphere-ocean general circulation model. Interactions between the atmosphere and ocean were found to have an substantial impact on regional climate changes, particularly in the North Atlantic and eastern tropical Pacific (2.5.2).

In a coupled atmosphere-ocean model forced by a quadrupling of CO_2, runoff increased in approximately 70 percent of the world's largest river basins. River basins located in middle and high latitudes of the Northern Hemisphere typically experienced increased runoff. Decreases in runoff occurred in a smaller number of locations, including some places in the southern United States (2.6.1).

Multi-decadal control integrations of the GFDL SKYHI model have produced results with significant quasi-decadal variability. The variations in concentration of nitrous oxide indicate apparent trends in the middle stratosphere of the order of 1% per year occur over timescales of a decade or more. Since the model has no interannual variations in chemistry or any interannual changes in external forcing, all these apparent trends in stratospheric composition must result from spontaneous internally-generated changes in transport. This suggests a significant role for natural variability in explanations of observed trends in stratospheric composition (3.4.3).

An assessment of the effect of Drake Passage on the earth's climate has been carried out using an idealized coupled model. The model shows that most major features of the Atlantic thermohaline circulation and the ocean's heat transport system can be explained by the existence of Drake Passage and the Antarctic Circumpolar Current, including the observed surface air temperature difference between 50°S and 50°N (5.1.3).

PLANS FY01

- A set of climate model ensemble integrations, including natural (solar, volcanic) and anthropogenic (greenhouse gases, sulfate aerosols) forcings will be completed. These ensemble integrations will be analyzed to determine the relative contributions of natural and anthropogenic forcings to global and regional temperature trends.

- The development and testing of key coupled climate model components will continue. Construction of the atmospheric component of the current-generation coupled climate model will be completed, and the model will be ported to GFDL's new high-performance computing system.

- New simulations of the effects of freshwater discharge into the North Atlantic Ocean will be completed. The results will be compared to previous runs with a lower resolution model, with a focus on identifying possible tropical climate teleconnections similar to those suggested by paleoclimate data.

- A major study is underway to determine the role of mesoscale eddies in balancing the northward Ekman transport in the latitude band of the ACC. A series of models with progressively finer resolution will illustrate how the ACC change in response to variable winds when eddies are explicitly resolved.

BASIC GEOPHYSICAL PROCESSES

A number of the research topics at GFDL cut across the various time scales characteristic of each of the foregoing sections. Progress on these topics impacts many other research areas which depend critically on the successful representation of numerous lower-level processes which are common to problems at all scales. Topics which fall into this category include hydrological processes, radiative transfer (including the effects of aerosols and clouds), cloud prediction/specification, "teleconnection" of atmospheric anomalies across the global atmosphere, satellite data interpretation, transport processes, gravity wave effects and parameterization, model resolution effects, and many other model enhancement efforts. As these processes become better understood and more accurately represented, benefits will accrue to a multitude of other research efforts.

ACCOMPLISHMENTS FY00

All GFDL models planned for use on GFDL's next supercomputing platform have been implemented for scalable systems. The implementation was based on a memory management scheme providing domain decomposition on rectilinear grids spanning shared or distributed address (1.1).

The exchange grid software which is used to do conservative interpolation between model grids in FMS was rewritten to increase performance on scalable architectures (1.1.3).

A management structure for software development was established at GFDL. An oversight and planning committee was established to provide scientific direction for FMS priorities while a model infrastructure team was created to manage and imlement software (1.3.1).

The Flexible Modeling System software and its documentation have been placed under the CVS version control system. This allows users to access both current and previous configurations of FMS code and allows for orderly code updaes (1.3.2).

A quarterly release schedule for FMS was implemented and the first officially supported release was made in conjunction with a lab-wide meeting to introduce users to FMS (1.3.3).

The Land Dynamics (LaD) model was developed as an extension of an earlier scheme with successful application in climate modeling. The performance of this model was evaluated by forcing it with observed hydrologic data and comparing simulated and observed runoff characteristics. The LaD model matches observations better than its predecessor (2.4.2).

Analysis of high-time-resolution Baseline Surface Radiation Network observations, coupled with results from radiative transfer computations, has led to the identification of aerosol signatures in the solar flux reaching the surface (3.1.3).

Radiative-convective model simulations of lapse rate changes due to aerosol-induced solar absorption in clouds reveal a strong dependence on the vertical distribution of clouds and the amount of absorbing aerosols incorporated in them (3.5.3).

Simulations with the GFDL SKYHI model have been used to examine interannual variability of long-lived greenhouse gases in the troposphere. The effects of the stratospheric quasi-biennial oscillation on stratospheric-tropospheric exchange was shown to significantly influence the tropospheric concentrations of nitrous oxide and methane (3.4.7).

Uncertainty in the intensity and frequency of precipitation in a GCM is a major contributor to the uncertainty of the simulated atmospheric aerosol burden. While monthly mean precipitation is represented reasonably well, the episodic nature of precipitation events is not. This affects the removal of the aerosol from the atmosphere, its residence time and thereby the radiative forcing (2.3.5).

The prognostic cloud parameterization of the Flexible Modeling System has been further refined and its performance thoroughly diagnosed. The parameterization is qualitatively able to reproduce the observed cloudiness distribution with some biases (*e.g.*, too small liquid cloud drop radii and too optically thick clouds). However, the parameterization qualitatively reproduces the observed temperature dependence of low cloud optical thickness (3.2.4).

Deep convection in the intertropical convergence zone is the major mechanism acting to remove sulfate, carbonaceous aerosol, and mineral dust originating on the Indian subcontinent as it moves toward the Equator, according to studies performed with the GFDL

limited-area non-hydrostatic model. The rates at which these aerosols are removed in the model match well aerosol observations on the NOAA ship Ron Brown during the Indian Ocean Experiment, INDOEX. These aerosols modify the clouds into which they are ingested, increasing the concentration of cloud drops and ice crystals and decreasing their size (3.2.2).

Ice generated by deep convection and its associated mesoscale circulations contributes substantially to both shortwave and longwave radiative forcing. This ice generation has been parameterized by using a sub-grid distribution of vertical velocities to model cloud microphysical processes at the physically realistic scales in general circulation models. The sub-grid spatial characteristics of parameterized convective systems have been analyzed and are consistent with satellite observations of convective shields (3.2.1).

A statistical atmospheric model that can be used for efficient evaluation of the impacts of the atmosphere in coupled model simulations has been developed. The statistical atmosphere has given new insight into the deficiencies and strengths of a variety of atmospheric observational products and general circulation models (4.1.3).

A new version of MOM (MOM 4) has been created that runs faster and uses memory more efficiently on computer systems with more than 50 processors (5.2.1).

GFDL's isopycnal coordinate ocean model (HIM 1.0) was officially released. The calling interface for HIM is compatible with that of MOM 4 and HIM development is managed with modern version control software (5.2.2).

Comparison between temperature trends deduced from the Microwave Sounding Unit (MSU) and from radiosonde measurements reveals that there still remains a spurious downward drift in the MSU temperature record due to degradations in the satellite orbit, despite previous attempts to correct for this drift (6.2.2).

A long-term partnership between GFDL and PMEL has been established to facilitate the design of a user-friendly, web-based software package for visualizing and evaluating the output of FMS experiments. It is envisioned that this effort will produce a powerful and convenient tool for accessing and visualizing data sets from research centers throughout the world, and for assessing the performance of various FMS experiments to be conducted at GFDL (6.4).

Some aspects of the climate depend on the drag exerted by mountain ranges. A dynamically based parameterization of the total mountain drag has been developed and is being tested with twin experiments using the mesoscale model at coarse and high resolution. The new parameterization eliminates a certain tuning parameter and provides a much better geographical distribution of the source. The comparison between the parameterization and the resolved drag is further improved by applying a proposed nonlinear correction (8.2).

PLANS FY01

- The primary focus of FMS development will be to optimize FMS models for use on GFDL's new supercomputing system. It is anticipated that a number of simple modifications will lead to significant performance enhancements during the first six months that the new system is available.

- Design work on a single column model testing facility will be completed and the single column model will become part of official FMS releases.

- A number of enhancements to the FMS diagnostic manager will be made to support more elaborate run-time diagnostics. Among the new features will be diagnostics for limited spatial domains, better spatial averaging facilities, and the ability to output diagnostics for particular times of day.

- Quarterly releases of FMS will continue. Several major new features are planned for inclusion including a comprehensive biosphere model, a standardized coupled model as well as the new radiation code of the atmospheric processes group.

- Development and experimentation with prototypes of the atmospheric component of the next-generation coupled models will be undertaken.

- Tests of the solar and longwave radiative transfer parameterizations in the atmospheric GCM being developed in the FMS framework will continue, in particular accounting for random-maximum overlap configurations of the vertical profile of clouds.

- Examination of the impact of new radiative transfer parameterizations will cover an atmospheric model version containing the new radiation, convection and prognostic cloud parameterizations. A new gravity wave drag scheme will be incorporated into the atmospheric model. In addition to convectively-excited waves, attention will also be given to a new treatment of orographically-induced waves. The atmospheric model containing the new suite of physics will be subjected to extensive tests, both in the AMIP-style runs and "unforced" integrations.

- Analyses of solar and longwave fluxes and heating rates as obtained from the array of radiative transfer models will continue. In particular, the network of surface solar observing sites will be used to examine the climatological features of the inferred aerosol radiative effects. Radiative forcing due to atmospheric trace gases and aerosols (*e.g.*, black carbon, dust) will be further analyzed. The influences due to microphysical effects of aerosols upon their radiative properties will be examined using a hierarchy of models.

- Further diagnosis of cloud parameterizations will continue. In particular, effort will be placed on diagnosing the reasons behind the qualitatively correct temperature dependence of low cloud optical depths obtained in the model simulation.

- MOM-4 will become a part of FMS and will be integrated into all global coupled models at GFDL.

- MOM 4 will be coupled to sea ice and atmospheric models using the FMS exchange grid.

- A project will be launched with external collaborators to develop operational radiosonde products for use in near real-time diagnosis of temperature variability in the free atmosphere.

- Further intercomparisons will be performed between the radiosonde and satellite observations of upper tropospheric water vapor on a station-by-station and satellite-by-satellite basis, so as to assess their utility for climate monitoring. Particular effort will focus on identifying and quantifying discontinuities associated with radiosonde instrumentation or satellite calibration changes.

- A fully operational version of a web-based data analysis and visualization package will be adapted for laboratory-wide use within GFDL. New output from various FMS experiments will be assembled and linked to this new diagnostic tool. The multitude of data resources available through the Distributed Oceanographic Data Systems (DODS) network will be exploited to facilitate intercomparisons between model-simulated and observational data sets.

- A correction for vertical wind shear in the drag parameterization is being formulated and will be tested in the same way as the rest of the scheme, *i.e.*, with comparable high- and low-resolution experiments. The sensitivity of the drag to the treatment of the turbulent planetary boundary layer will also be examined.

PROJECT ACTIVITIES FY00

PROJECT PLANS FY01

1. SOFTWARE INFRASTRUCTURE FOR SUPPORT OF SCIENTIFIC MODELING

GOALS

To develop and maintain a centralized software infrastructure to support the creation, use, and modification of numerical models of the climate system and its components.

To provide a software framework within which specific models can be easily developed to address scientific questions of interest to GFDL scientists.

To ease the transition of GFDL models to new computer architectures and to facilitate both intramural and extramural scientific collaborations.

1.1 LOW-LEVEL SUPPORT FOR MODELING

ACTIVITIES FY00

1.1.1 Memory Management, Communication, and I/O on Scalable Systems

V. Balaji

All GFDL models planned for use on GFDL's next supercomputing platform have been implemented for scalable systems. The implementation was based on a memory management scheme providing domain decomposition on rectilinear grids spanning shared or distributed address spaces. This versatile model of memory management provides simple user interfaces for programming across a variety of scalable architectures, including clusters, distributed memory massively parallel processors (MPPs), symmetric multiprocessors (SMPs), "clusters-of-SMPs", and cache-coherent non-uniform memory access (ccNUMA) shared address space systems.

The Flexible Modeling System (FMS), as well as the other lab models, use the MPP modules developed at GFDL for memory management, communication, and I/O on scalable systems. These modules provide the message-passing and parallel I/O infrastructure for FMS and other participating lab models, including the gridpoint and spectral atmospheric GCMs, MOM3 and MOM4, and ZETANC, a non-hydrostatic mesoscale atmospheric model.

The MPP modules consist of three separate F90 programming interfaces: 1) mpp_mod, the low level interface provides basic routines for message passing; 2) mpp_domains, the

higher level interface, provides routines for defining domain decompositions and performing halo updates and data transposition across processors; 3) mpp_io, the I/O interface, provides routines for writing output in different formats (including netCDF) from distributed arrays.

The MPP modules have been stable and operational since 1999. In the last year, they have been validated and benchmarked on a variety of scalable systems, including: Parallel Vector (Cray T90); massively parallel distributed memory (Cray T3E); ccNUMA (Origin 2000 and 3000); SMP clusters (IBM-SP, Sun UE-10000); and Beowulf clusters (SGI-1200, DEC alpha cluster over Myrinet, Intel Pentium cluster on fast ethernet).

1.1.2 Abstract Parallel Dynamical Kernels

V. Balaji *R. Pacanowski*

A recent development within the MPP fabric is the development of abstract parallel dynamical kernels, called the "*distributed_grid module*". These kernels, coded in Fortran 90, describe physical quantities in terms of vector and scalar field types that contain detailed information about the distribution of the component arrays across a processor set. Operators such as dot and cross products, gradient, divergence, and laplacian can be written in a simple abstract high-level form. The operators will invoke highly optimized kernels for the actual numerics, as well as built-in detection and invocation of halo updates as needed.

The coding of model numerics in terms of abstract operators has many advantages. In particular, it permits many details of how differencing and averaging are performed on different grid types (*e.g.*, Arakawa B- and C-grid) to be hidden from the user. Thus, it may be invoked for any grid type provided that particular method is available, or can be supplied by the user, for the grid in question.

Second, since the detection and invocation of halo updates is automatic, halos of differing widths may be used as needed in different parts of the code. For instance, the barotropic solver in the ocean component of FMS is latency-bound. The *distributed_grid* module will permit the use of wide halos in this portion of the code, so that halo updates can be called less frequently.

The *distributed_grid* module has been benchmarked for a shallow water code on the Cray T90 and T3E. While there is some penalty for abstraction (about 20% on 1 processor), it exhibits its strength in its high scalability (80% scaling on 25 PEs on a 125x125 grid on the T3E).

1.1.3 Interpolation Between Model Grids on Scalable Architectures

The exchange grid software which is used to do conservative interpolation between model grids in FMS was rewritten to increase performance on scalable architectures. Only minor modifications to external interfaces were required, but communications patterns were changed to reduce bottlenecks. Additional interfaces to support disjoint longitude latitude grids for support of spectral models with hemispheric windows were implemented. Exchange grid software has been ported to NCEP (National Centers for Environmental Prediction) and

IRI (International Research Institute for Climate Prediction), where it is being used as part of coupled model developments at those institutions.

PLANS FY01

Additional optimization of the MPP modules and the exchange grid will be performed as needed to support FMS models on GFDL's new supercomputer.

The *distributed_grid* module will be implemented for testing in the B-grid atmospheric model and the MOM4 ocean model.

Versions of the exchange grid overlap interfaces to support additional grid types required by GFDL modelers will be developed.

1.2 PHYSICAL PARAMETERIZATIONS, COMPONENT, AND COUPLED MODELS

ACTIVITIES FY00

1.2.1 Convective Parameterizations and Diagnostics

M. Harrison *J. Sirutis*

A Fortran-90, modular version of the "Relaxed Arawaka Schubert 2" (RAS2) convective parameterization, which includes a downdraft parameterization and an ice phase, has been produced and is being tested in the FMS B-grid model. The same has been done with the full Arakawa-Schubert scheme which was used at GFDL for many years. Versions of the Emanuel convective parameterization that were originally obtained from GFDL FMS implementations are now being used operationally in the Navy's global prediction models.

The programs used for the tropical storm analysis, as well as the program to compute the Tibaldi/Molteni blocking index, and a number of other analysis programs have been rewritten as streamlined Fortran 90 modules.

1.2.2 Diagnostic Cloud Model

C.T. Gordon *W. Stern*

A modular version of the Gordon/Slingo diagnostic cloud parameterization scheme has been tested in single column calculations. This parameterization diagnoses cloud fraction for various cloud types, cloud optical depth of non-anvil cirrus, and specifies fixed values of cloud optical depth for other cloud types. The modular version does not yet support the diagnosis of marine stratocumulus cloud fraction and has been modestly revised to enhance scalability to finer vertical resolution. It is currently being tested in FMS in both the B-grid and spectral dynamical cores.

An empirically based relative humidity threshold cloud parameterization scheme has been designed to closely resemble the diagnostic cloud parameterization used in the Experimental Prediction spectral GCM v197. This scheme calculates cloud fractions diagnostically using relative humidity, vertical velocity, and stability. Seven cloud types and three cloud vertical layer specifications are possible, each with its associated optical properties. A concise, modular scheme written in Fortran-90 has been completed for both the calculation of fractional cloud amounts and the handling of the cloud optical properties. Column tests give very good agreement with the non-modular v197 version.

1.2.3 Global Atmospheric Grid Point Model

B. Wyman

A number of improvements have been made to the B-grid dynamical core. First, the polar filter can be used with two-dimensional domain decomposition. Second, the vertical differencing scheme has been replaced with an energy and angular-momentum conserving scheme. This scheme is also used by the spectral dynamical core. Third, the horizontal mass flux computations have been modified, reducing the two-grid-interval noise associated with the B-grid configuration so that the grid separation correction term is no longer needed. Fourth, the correction to horizontal diffusion for sloping sigma surfaces has been improved, reducing the problem of spurious precipitation over steep mountains. Fifth, the horizontal borrowing scheme for filling regions of negative tracer concentration has been improved, and lastly, a local filter option was added at the top of the model to remove undesirable modes.

Evaluation of the B-grid core is underway in several coupled model configurations. Extensive testing has been done using a 2.5 x 2.0 degrees x 18 level version of the core coupled to models providing prescribed SSTs and sea ice. Additional tests have also been made with horizontal resolutions up to 1.25 x 1.0 degrees and vertical resolutions up to 50 levels. Initial testing has begun using a version of the core coupled to MOM3 and using prescribed sea-ice.

1.2.4 Dynamic/Thermodynamic Sea Ice Model

M. Winton

Development has continued on GFDL's dynamic/thermodynamic sea ice model (renamed SIS for Sea Ice Simulator). The model was parallelized and the horizontal differencing was generalized to accommodate arbitrary horizontal coordinates. An n-category ice thickness distribution scheme was implemented and a reference document has been written. SIS has been tested with daily NCEP reanalysis forcing over the period 1948-1999, and has also been coupled into an FMS based climate model along with a spectral atmosphere, a MOM3 based ocean model, and the LaD (Land Dynamics) land model.

1.2.5 High Level Language Support for Coupled Models

M. Winton

A high level language for model coupling is being designed and implemented (a compiler is being written). This language will allow assignment of expressions on the grid of one

model to variables on another without explicit calls to exchange grid routines. A similar capability will exist for the subroutine calls that implement the component models' highest level interfaces. The high level coupling language will greatly facilitate the coupling of models to each other and to datasets.

PLANS FY01

Design work on a single column model testing facility will be completed and the single column model will become part of official FMS releases.

Further improvements to the SIS sea ice model will continue along with tests of SIS in a variety of coupled model configurations.

The high level coupling language compiler will be completed and implemented to facilitate better coupled model design at GFDL.

A number of enhancements to the FMS diagnostic manager will be made to support more elaborate run-time diagnostics. Among the new features will be diagnostics for limited spatial domains, better spatial averaging facilities, and the ability to output diagnostics for particular times of day.

Evaluation of the current FMS version of the diagnostic cloud parameterization scheme will continue. The standard parameterization and a new cloud anomaly parameterization for marine stratus cloud fraction will both be incorporated in FMS. Comparative coupled model integrations with the Klein prognostic and Gordon/Slingo diagnostic clouds will be performed.

1.3 SOFTWARE MANAGEMENT

ACTIVITIES FY00

1.3.1 FMS Management

J. Anderson *R. Hemler*
V. Balaji *P. Kushner*
R. Hallberg *R. Pacanowski*
I. Held *B. Wyman*

The Flexible Modeling System represents the first time that GFDL has embarked upon a software project of a level of complexity warranting formal management. Upon recommendation from a team of scientists involved in FMS, the director of GFDL appointed an Oversight and Planning (OP) Committee for FMS initially under his own chairmanship. The initial act of the newly founded committee was to approve a charter for FMS. The charter calls for model development to be under the direct supervision of its principal working subcommittee, the Model Infrastructure (MI) team. The MI team in turn implements the recommendations of

the OP committee. Recent activities of the OP committee include the adoption of a task list mechanism to guide GFDL in assigning activities to contracted software engineers.

1.3.2 Software Version Control for the Flexible Modeling System

V. Balaji *P. Phillipps*
P. Kushner *B. Wyman*

A significant development within FMS over the past year has been the implementation of an automated software version control system. The need for such a system is evident given the scope of FMS and the number of contributors involved. Modern software version control systems feature detailed history tracking of individual files, the ability to create and track multiple versions (branches) from a single file, the ability to group together files in a logical manner with appropriate labels, and the ability to support a broad remote community through internet-based protocols.

FMS uses GNU's CVS (Concurrent Versions System) version control system. The FMS source tree is stored in a single CVS repository that is accessible in its entirety to all users at GFDL and accessible in part to external users. Considerable effort has been made to create a repository structure and policy that will serve the needs of FMS well into the future. The repository structure is split functionally into "shared" code, which consists of utilities common to all FMS codes, "component-model" code, which consists of the core codes to run each of the dynamical cores, and "coupler" code, which consists of codes, such as the surface flux calculations and the main drivers, that couple component models together. The repository policy outlines naming conventions, requirements for introducing "branch" or "trunk" code into the repository, and the coordination of the quarterly release schedule of FMS (1.3.3) with the repository.

1.3.3 FMS Software Releases

J. Anderson *P. Kushner*
V. Balaji *B. Wyman*
R. Hallberg

The FMS development team has established a schedule of quarterly releases of the FMS code. The releases provide regular deadlines for FMS contributors to coordinate, review, communicate, and test their recent development efforts. The three-month spacing between releases is sufficiently long to complete a sizeable development project and sufficiently short that the project deadline can slip to the next release without any great loss or undue pressure on the developers involved. The release cycle begins with meetings of the MI team that establish short-term (8 to 10 week) goals and a schedule of development activities. There follows an announcement of the release and its main features, and the creation of a prerelease for testing, three to four weeks before the release deadline. Supporting documentation for the release is created in the days following the official release day, and bug fixes are appended to the release as necessary.

The releases are named by an alphabetical sequence of city names: Antwerp (5/2000), Bombay (8/2000), Calgary (11/2000), etc. The Antwerp release consisted mainly of

parallelized "benchmark" code for the GFDL computer procurement. The Bombay release featured coordinated atmospheric dynamical cores, and the introduction of the MOM3 ocean model, the LaD land surface model, the SIS sea-ice model, and enhanced web documentation.

In conjunction with the Bombay release, an FMS workshop was held at GFDL to familiarize the laboratory with the capabilities of FMS. One and a half days were devoted to a series of presentations ranging from overviews for casual users to detailed studies of low-level support modules. Representatives from nearly a dozen outside modeling institutions were invited to attend the workshop as observers, and participated in an afternoon session discussing possible ways in which GFDL could interact with the outside world using FMS.

1.3.4 Web Page and Documentation Support

V. Balaji *B. Wyman*
P. Kushner

A comprehensive web-based documentation system to support FMS is under development. Automatically generated version-specific documentation is created with each checkout of FMS code from the CVS software repository. Comprehensive documentation of updates and modifications to code are available. In addition, static documentation of FMS code and other aspects of the system are under development. Examples include a web-based start-up facility to allow new users to begin running GCMs, and a web-based bulletin board facility.

1.3.5 Optimization Team, Migration, and Evaluation

J. Anderson *J. Durachta*
V. Balaji *C. Kerr*

Until recently, FMS efficiency was considered secondary to code correctness and clarity. Now that FMS has matured and a new computer system is to be delivered, optimization issues are moving to center stage. An initial optimization team has been formed and has begun to instrument existing FMS code and document performance on existing platforms.

PLANS FY01

The primary focus of FMS development will be to optimize FMS models for use on GFDL's new supercomputing system. It is anticipated that a number of simple modifications will lead to significant performance enhancements during the first six months that the new system is available.

Continued coordination of development of different dynamical cores and component models should increase the amount of shared code and reduce maintenance burdens.

Improved coordination of run-time scripts and data archiving facilities will be explored to avoid redundant effort between scientific groups in these areas.

Quarterly releases of FMS will continue. Several major new features are planned for inclusion, including a comprehensive biosphere model, a standardized coupled model, as well as the new radiation code of the atmospheric processes group.

2. CLIMATE DYNAMICS

GOALS

To construct mathematical models of the atmosphere and of the coupled ocean-atmosphere system which simulate the global large-scale features of climate.

To study the dynamical interaction between large-scale wave disturbances and the general circulation of the atmosphere.

To identify and elucidate the physical and dynamical mechanisms which maintain climate and cause its variation, and to examine their generality in the context of paleoclimate and the atmospheres of other planets.

To evaluate the impact of human activities on climate.

2.1 BACKGROUND FOR COUPLED CLIMATE MODELING AT GFDL CLIMATE CHANGE

This section summarizes the general characteristics of two distinct coupled atmosphere-ocean climate models, both of which are in active use in research on global warming and other aspects of climate variability and sensitivity.

The R30 coupled model, which has been used extensively during the past year, has an atmospheric horizontal resolution of 3.75° longitude and 2.25° latitude, with 14 levels in the vertical. It is coupled to an ocean model with 2° horizontal resolution, a simple free-drift ice model, and a "bucket" land hydrology. The coupled model is run with adjustments to the air-sea fluxes of heat and fresh water to prevent climate drift. Two versions of the R30 coupled model have been developed, differing in their oceanic sub-grid scale diffusivities and initialization procedures. Using nomenclature taken from the IPCC Third Assessment Report, these two versions are identified as GFDL_R30_b and GFDL_R30_c. (A different nomenclature was used in A99/P00, in which these two versions were identified as R30V1 and R30V2, respectively. A more detailed description of the differences between GFDL_R30_b and GFDL_R30_c appears in A99/P00.) Several long control integrations have been performed with these models, and numerous simulations of all or part of the period 1865-2089.

The R15 coupled model has only half of the horizontal resolution of R30 in both the atmosphere and ocean. The low resolution and simplicity of this model, as well as the flux adjustment strategy, are designed to allow integrations that would otherwise be computationally prohibitive. This model has been invaluable throughout the past decade for initial studies of the variability and sensitivity of the coupled atmosphere-ocean system.

Both the R15 and R30 models have been used to simulate the evolution of the earth's climate due to past changes in greenhouse gases and sulfate aerosols, as well as to project climate change into the 21st century. In these "global warming scenario" integrations, an equivalent CO_2 concentration is used to represent changes in all of the trace greenhouse gases, and changes in aerosol loading are modeled by changing the surface albedo. The runs begin in either 1765 or 1865, depending on resolution, using historical greenhouse gas and aerosol concentrations. The runs proceed into the late 21st century with equivalent CO_2 increasing at a rate of 1% per year after 1990. All of these projections are clearly uncertain. The radiative forcing for the 20th century is also uncertain, due to uncertainties in aerosol loading (both anthropogenic and volcanic), indirect effects of aerosols on clouds, and possible changes in solar irradiance. Any climate projections must be considered with these uncertainties in mind.

2.2 CLIMATE CHANGE

2.2.1 Sea Ice and Global Warming

T. Delworth *R. Stouffer*
K. Dixon *K. Vinnikov***
*A. Robock** *M. Winton*

**Rutgers University*
***University of Maryland*

ACTIVITIES FY00

Observational evidence derived from satellites, submarines, and Arctic scientific expeditions reveal that both the areal extent and the average thickness of Arctic sea ice decreased markedly during the last few decades of the 20th century. Media reports have heightened awareness that changes in the Arctic climate can impact the region's biology and commerce. How much of the Arctic sea ice reduction may be attributable to naturally occurring climatic oscillations and how much may be the result of anthropogenically induced warming arising from the enhanced greenhouse effect? This, and related questions, are being explored in the context of GFDL's coupled climate model experiments.

Decreases in late 20th century Arctic sea ice coverage simulated in an R15 version of the GFDL coupled climate model that included transient greenhouse gas and sulfate aerosol forcing has been shown to agree well with the observations (1657). Similar Arctic sea ice trends exist in more recent, higher resolution R30 climate model simulations (GFDL_R30_c). Fig. 2.1 summarizes the evolution of sea ice distributions calculated in three R30 climate change scenario experiments. (Averaging the results of three experiments makes it easier to see the greenhouse gas-induced signal among the year-to-year noise of interannual variability.) By the year 2000, the total volume of Arctic sea ice is between 75 and 80 percent of that which was simulated to exist in the 1950s. In these experiments, the total volume of Arctic sea ice continues to decrease through the 21st century, so that only about half of that which was present in the 1950s remains in the year 2050.

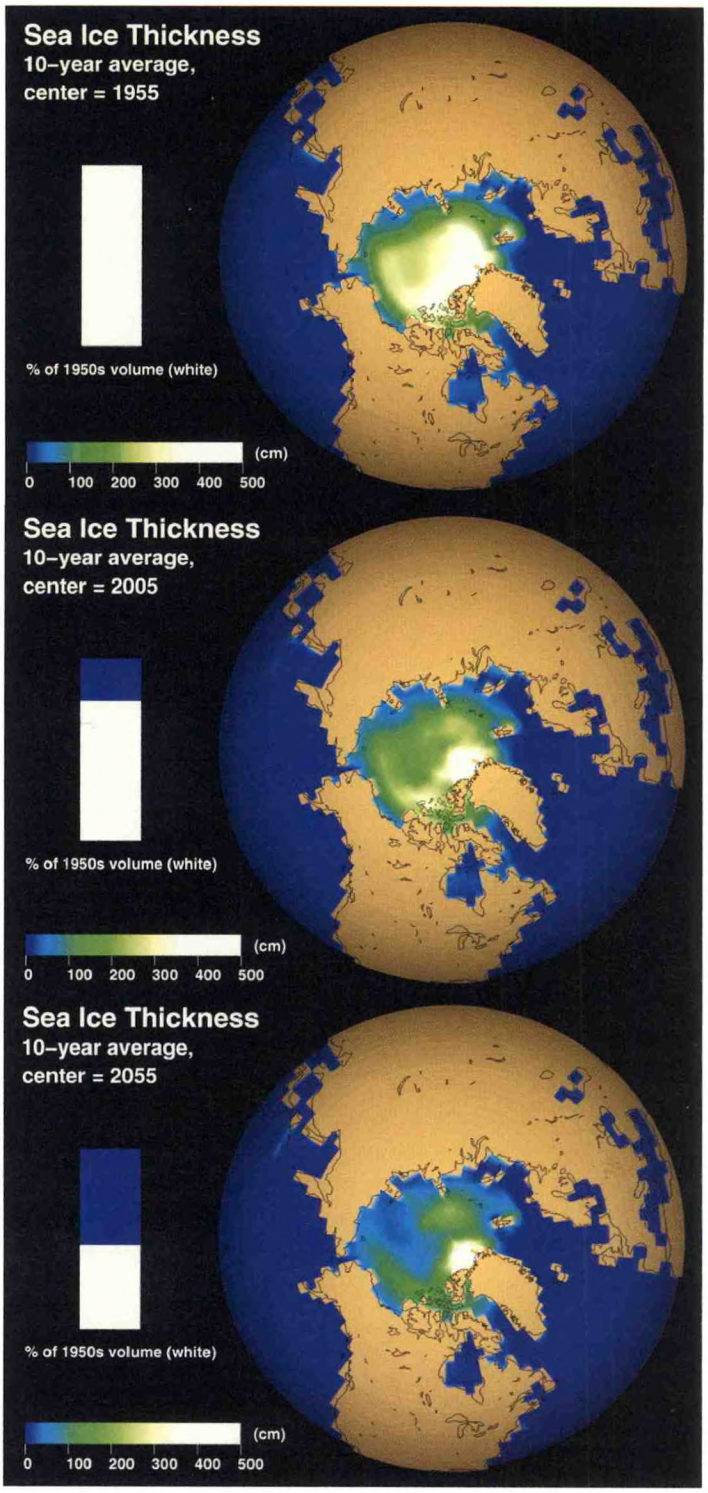

Fig. 2.1 Northern Hemisphere sea ice thicknesses as simulated in GFDL R30 climate change experiments. The projected sea ice decrease is summarized by this progression of three pictures representing decadal-mean conditions of the 1950s, 2000s, and 2050s. The values shown are ensemble means, averaged over three coupled model experiments forced by increasing levels of greenhouse gases and sulfate aerosols.

PLANS FY01

Analysis of the R30 climate model simulations of sea ice will continue. A more complete understanding of the mechanisms responsible for the low frequency variability simulated in the control (constant CO_2) experiment will be pursued. Similarly, more detailed analyses of the processes leading to the decrease in sea ice simulated under transient radiative forcing conditions are planned. A longer term goal will be to examine the sensitivity of the coupled model simulation to the sea ice model component used. Once the new sea ice model developed recently is fully incorporated into AOGCM climate change experiments, differences attributable to the choice of sea ice model will be examined.

2.2.2 Water Vapor Feedback and Global Warming

I. Held *B. Soden*

ACTIVITIES FY00

Water vapor is the dominant greenhouse gas (the most important gaseous source of infrared opacity) in the atmosphere. As the concentrations of other greenhouse gases, particularly carbon dioxide, increase due to human activity, it is centrally important to predict how the water vapor distribution will be affected. To the extent that water vapor concentrations increase in a warmer world, the climatic effects of the other greenhouse gases will be amplified. Models of the Earth's climate indicate that this is an important positive feedback which increases the sensitivity of surface temperatures to carbon dioxide by nearly a factor of 2 when considered in isolation from other feedbacks, and possibly by as much as a factor of 3 or more when interactions with other feedbacks are considered.

The question of the relative importance of different regions for water vapor feedback is a source of some confusion in the literature. This question has been reexamined as part of a comprehensive review of the current state of science and of the controversies surrounding water vapor feedback (mh). Fig. 2.2 shows an estimate of the individual contributions by water vapor (top) and temperature (bottom) to changes in the outgoing longwave radiation resulting from a spatially-uniform 1 K perturbation in temperature under the assumption of constant relative humidity. In performing these calculations, the atmosphere was divided into 10 vertical layers of equal mass, using temperature and humidity data from the European Centre for Medium Range Weather Forecasting, and cloud data from the International Satellite Cloud Climatology Project. The results presented here are zonal averages for July only.

The sensitivity of outgoing longwave radiation to temperature perturbations (Fig. 2.2, bottom) is strongly affected by the cloud distribution. Where upper level clouds are prevalent (*e.g.*, 0°-10°N), the outgoing infrared radiation is most sensitive to temperatures at the level of these emitting surfaces, and is relatively insensitive to temperatures deeper in the atmosphere. Where skies are clearer (*e.g.*, 10°S-20°S), lower tropospheric temperatures control the outgoing flux.

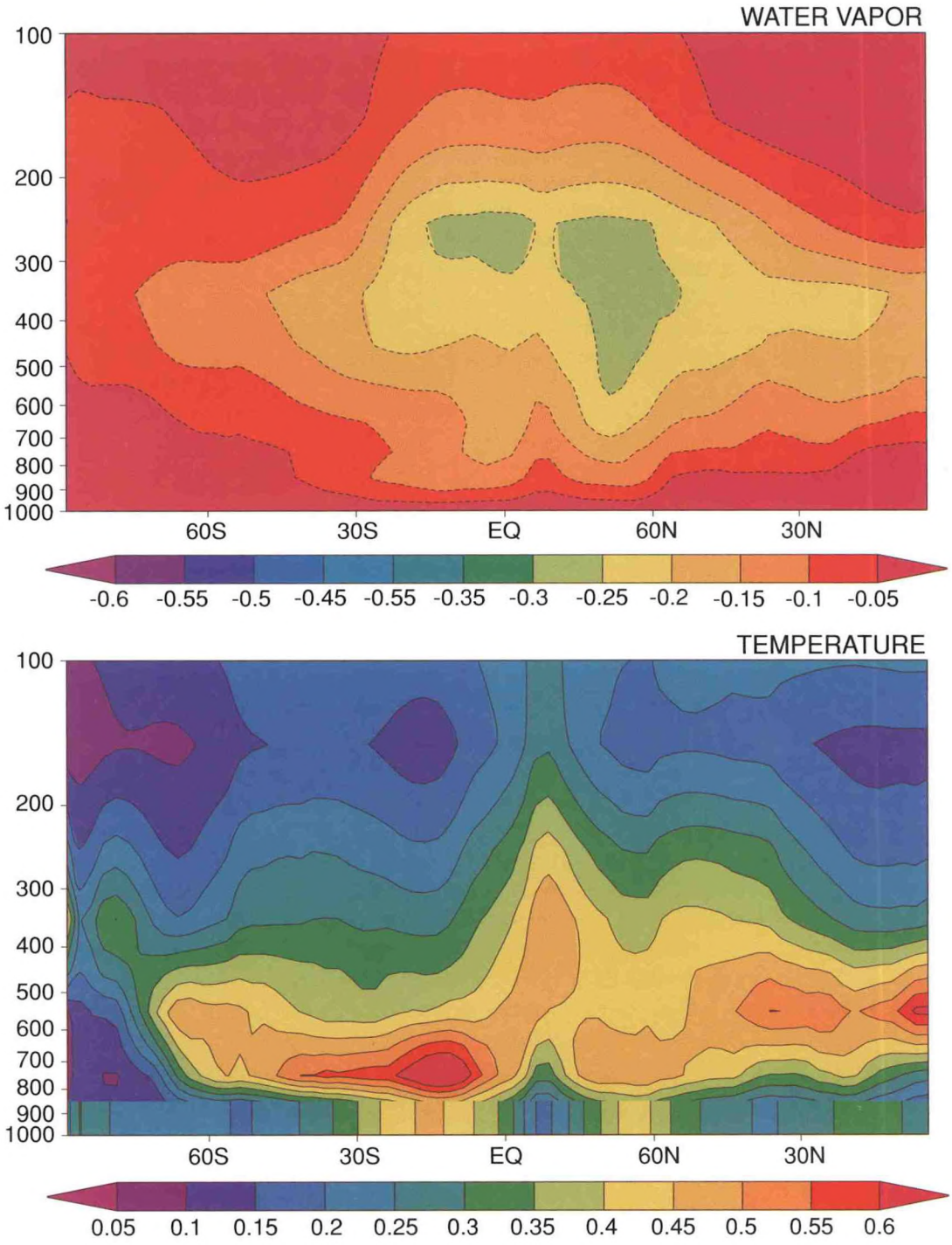

Fig. 2.2 Height-latitude cross sections of the sensitivity of the outgoing longwave radiation to perturbations in water vapor (top) and temperature (bottom) in 100 hPa thick layers. The results (expressed in units of $Wm^{-2}K^{-1}$) illustrate the importance of water vapor in the tropical troposphere above the boundary layer in determining the climate feedback by water vapor.

Figure 2.2 (top) shows that the subtropical dry zones are somewhat more important than the moister zone in the deep tropics for the strength of the fixed relative humidity water vapor feedback. This feature is a consequence of the presence of clouds. If clear skies are assumed to exist everywhere, the maximum in this figure shifts to the moister regions in the tropics. The claim that the subtropical dry zones always dominate water vapor feedback is not supported by this analysis.

If temperature changes are uniform and relative humidities remain unchanged as the climate warms, these results show that the humidity response in the free troposphere above 800 mb is responsible for almost all of the infrared water vapor feedback, with only 10% contributed by the boundary layer. Roughly 55% of the total is due to the tropical free troposphere (30°N-30°S), and 35% to the extratropics. Of this tropical contribution, about two-thirds, 35% of the total, is due to the upper half of the troposphere, from 100-500 mb.

2.2.3 Sea Level Rise and Global Warming

G. Boer
J. Church
K. Dixon
G. Flato
J. Gregory
D. Jackett
J. Lowe
J. Oberhuber
S. O'Farrell
R. Stouffer
M. Winton

ACTIVITIES FY00

Sea level rise is an important aspect of climate change because of its impact on society and ecosystems. Recently, the first international intercomparison of global mean sea level rise results from several atmosphere-ocean general circulation models (AOGCMs) was performed (os). Three climate models from GFDL (one at R30 and two at R15 spatial resolution) were included in this intercomparison. Changes in 20th and 21st century sea level (global mean and geographic variations) arising solely from changes in ocean temperatures and circulation patterns were examined. For consistency, all nine models were forced by historical estimates of greenhouse gases (GHGs) and sulfate aerosols until 1990. After 1990, forcings approximating the IPCC Is92A scenario were applied.

For the period 1910 to 1990, the time averaged rate of global mean sea level rise due to thermal expansion simulated by the different models varied between 0.3 and 0.8 mm/yr (Fig. 2.3). The observed rate for the same period is estimated to be somewhat higher (1 to 2 mm/yr), but includes contributions from melting land ice, land storage changes, etc., in additional to the ocean thermal expansion term. From 1990 to 2100, the average rate of projected global mean sea level rise due to thermal expansion accelerates, varying from 2.0-3.7 mm/yr among the different AOGCMs. Thus, the nine models simulate that the warming of ocean waters will be responsible for a 0.2 m to 0.4 m rise in global mean sea level over the period 1900 to 2100. The projected acceleration in the rate of sea level rise is consistent with increases in warming rates seen in the models' global mean surface air temperature responses. The nine models' projected 21st century warming rates vary from 2.6°C to 3.9°C.

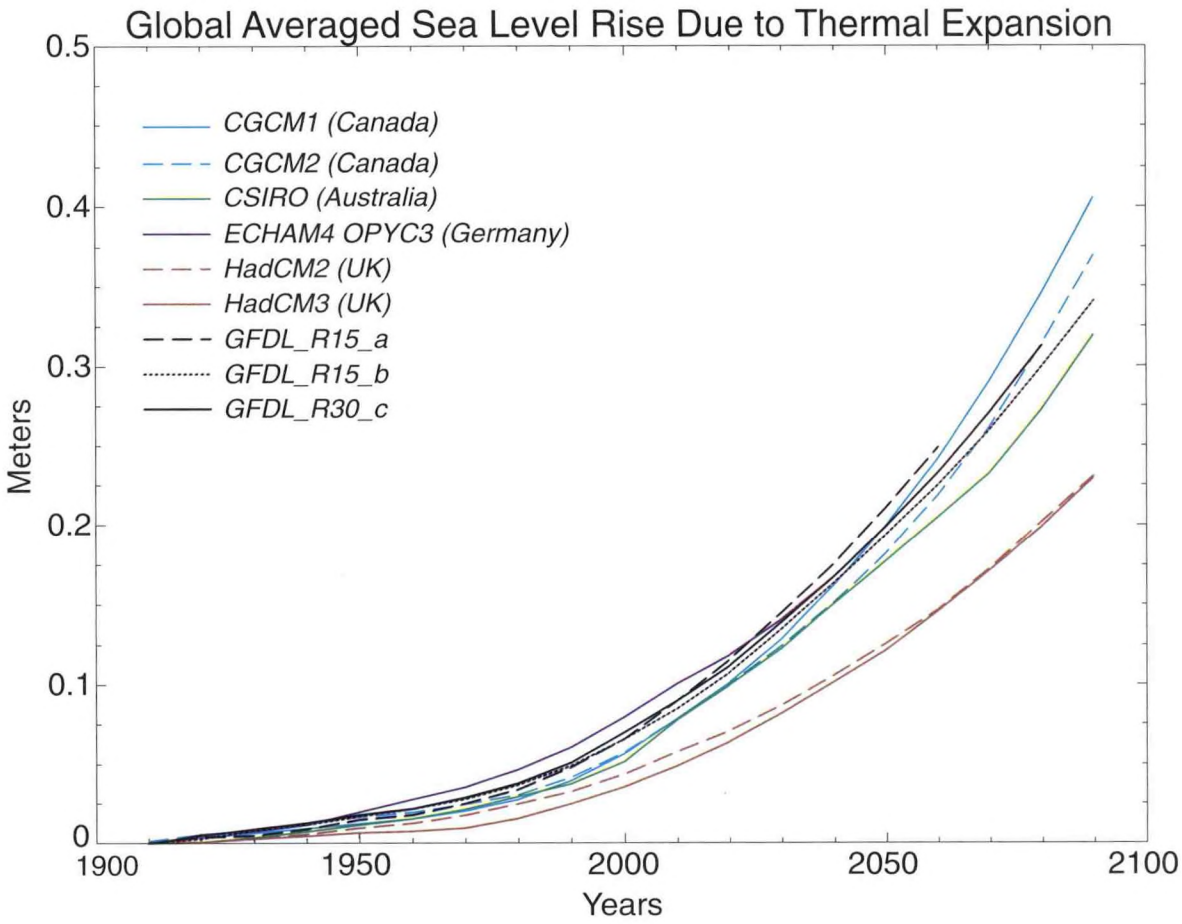

Fig. 2.3 Globally averaged sea level rise due to thermal expansion only (m). The curves have been offset on the y-axis so that they all have a mean of zero for 1900-1910. The models were forced with estimates of past and future concentrations of greenhouse gases and sulfate aerosols. Figure taken from Gregory et al., 2000.

Due to the slow penetration of heat into the oceans interior, the response time scale for sea level is very long (order of 1000 years). Therefore, sea level can be expected to continue to rise long after atmospheric GHG levels are stabilized.

2.2.4 Response of Southern Hemisphere Winds to Global Warming

T. Delworth *P. Kushner*
I. Held

ACTIVITIES FY00

Work continues on analyzing the atmospheric response to global warming in the Southern Hemisphere (mm). The circulation response can be divided into two dynamically distinct parts. The tropospheric response consists of a poleward shift of the Southern Hemisphere jet and projects strongly onto the so-called "Southern Annular Mode" (also known as the "Antarctic Oscillation"). This feature of the response is strongest in the Southern

Hemisphere summer. In the tropical upper troposphere and the model stratosphere, the response consists of a positive (*i.e.*, westerly) wind anomaly. This feature exists year round. There is also an overall increase in the depth of the troposphere, as shown by an upward shift of the eddy activity and stratification profiles. We interpret the upper-level response as being a direct response forced by changes to the large-scale radiative and thermal environment, and the Annular-Mode-like response pattern as being an indirect adjustment of the jet and storm tracks to this new thermal environment.

The response bears some resemblance to observed trends of the last 30 years in the Southern Annular Mode. This suggests that these trends are part of the atmosphere's response to greenhouse-gas loading. However, the observed trends are much stronger than the model response for the corresponding time period in the simulation. The reasons for this discrepancy are poorly understood. Possible causes are low-frequency variability in the atmospheric record, relatively coarse resolution in the stratosphere, and an absence of radiative-forcing effects associated with ozone depletion in the greenhouse warming integrations.

2.2.5 Discriminants of 20th Century Changes in Surface Temperature

I. Held *T. Schneider*

ACTIVITIES FY00

A novel analysis of observations using the statistical technique of "discriminant analysis" has been performed which isolates the dominant patterns of climate change in the 20th century surface temperature record (nf). The algorithm takes the spatially non-local covariance of the data into account and does not restrict itself to the examination of linear trends, but instead allows for nonlinear evolution in time. In discriminant analyses one divides the data into groups and looks for those linear combinations of variables or "canonical variates" that best discriminate among the different groups. Here, the groups are the surface temperature fields from different decades of the 20th century. The first canonical variate is that linear combination of surface temperatures for which the ratio of interdecadal to intradecadal variance is maximized. Higher order canonical variates maximize this ratio, subject to being uncorrelated with the lower order variates. Associated with each canonical variate is a spatial pattern obtained by regressing the data onto the time series of this variate. The ratio of interdecadal to intradecadal variability for the first variate is approximately 7 for both January and July. In comparison, for spatial mean temperatures over the area analyzed, this variance ratio is 0.7 for January and 1.1 for July. This discriminant analysis isolates interdecadal from higher frequency variability much more efficiently than a spatial mean.

The first discriminants indicate a relatively uniform and steady warming of the ocean surface, with a weak cooling over the North Atlantic being the most prominent exception. Over the continents, these patterns show regions of cooling, especially in July and typically of 1,000-2,000 km size. Most of these are in industrial regions where sulfate aerosol loadings are high. The cooling in Central Africa may be related to biomass burning. The cooling in July over North America appears to be too widespread as compared to the expected aerosol distribution centered on the Eastern states, and may be related to land surface changes. Most of the cooling centers are on scales smaller than the 5,000 km and larger scales

considered in many detection studies. New detection/attribution techniques need to be devised to distinguish climate change on these smaller spatial scales from natural variability, possibly based on the comparison of observational discriminants with ensembles of discriminants from simulations.

2.2.6 Response of Climate to Natural and Anthropogenic Forcings

A. Broccoli *T. Knutson*
T. Delworth *P. Kushner*
K. Dixon *M. Spelman*
I. Held *R. Stouffer*

ACTIVITIES FY00

A series of R30 coupled model ensemble integrations (using GFDL_R30_c) has been designed to examine the response of climate to natural and anthropogenic forcings during the period from 1865 through the present. Four ensembles will be available upon completion, each consisting of three integrations that begin from different initial conditions. The first ensemble employs only the anthropogenic forcing due to well-mixed greenhouse gases, expressed as "equivalent CO_2". The next ensemble includes forcing from tropospheric sulfate aerosols, in addition to greenhouse gases. These first two compromise the so-called "global warming" scenarios. The third ensemble adds variations in solar irradiance to the anthropogenic forcings, and a final ensemble adds the effects of volcanic aerosols. The first three ensembles have been completed, and the fourth is nearing completion.

PLANS FY01

Upon completion of the series of ensembles, the relative contributions of natural and anthropogenic forcings to global and regional climate trends in the coupled model will be examined. An important issue is whether the addition of natural forcings improves the agreement between simulated and observed climate trends.

2.2.7 Climate Scenarios for IPCC Third Assessment Report

A. Broccoli *T. Knutson*
T. Delworth *P. Kushner*
K. Dixon *M. Spelman*
I. Held *R. Stouffer*

ACTIVITIES FY00

In support of the U.S. Climate Assessment and the IPCC Third Assessment Report (2000), two integrations of the latest version of the GFDL coupled model were performed (GFDL_R30_c). For the IPCC report, six complete scenarios were developed for the future rates of emission/concentrations of the various GHGs and atmospheric aerosols. The emission scenarios varied depending on the assumptions made for the rates of population growth,

economic growth, technological development, etc. In February 2000, preliminary versions of the emission scenarios (the so-called "draft marker" scenarios) were released to the modeling community for use in their coupled models. At GFDL, integrations were made using the A2 and B2 draft marker scenarios.

The latest integrations using the A2 and B2 scenarios show that, during the next 100 years the global mean surface air temperature (SAT) increase relative to today's conditions is about 3.5°C for the A2 scenario and 2.4°C for the B2 scenario (Fig. 2.4). Despite very different

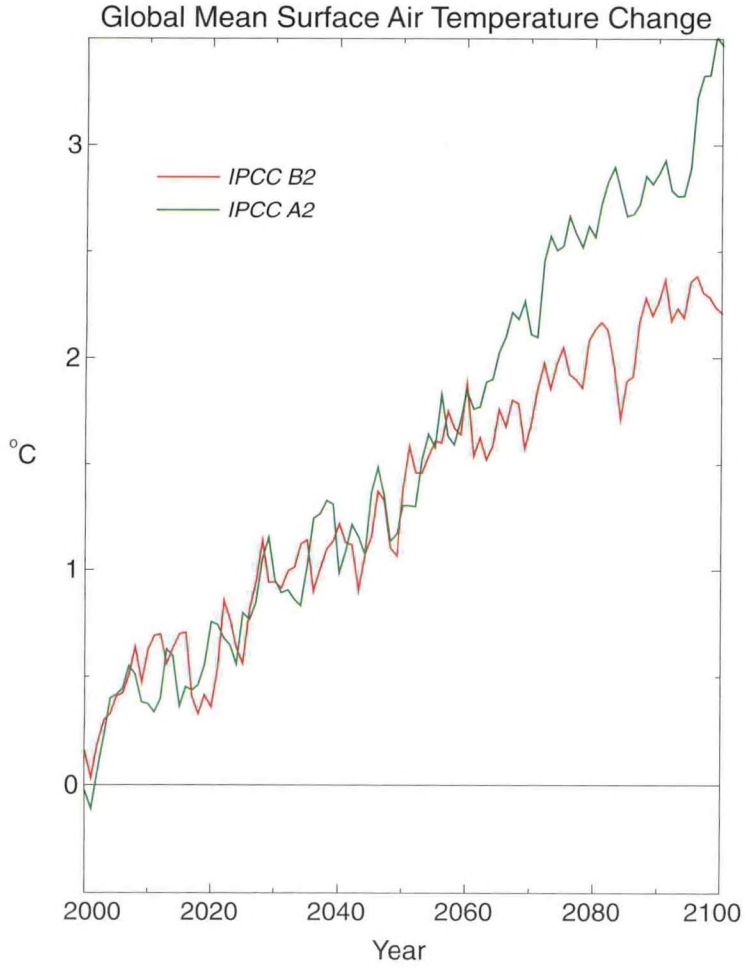

Fig. 2.4 Time series of globally averaged surface air temperature change calculated using the GFDL_R30_c coupled model. The model is forced with the latest IPCC estimates of future greenhouse gas and aerosol concentrations, the so-called A2 and B2 scenarios.

emissions for the GHG and aerosols, the increase in the global mean SAT is quite similar over the first 50 years of the integrations. The model response to the A2 scenario is also similar to the previous IPCC scenario (Is92A) over the entire 100 year simulation. These similarities in the model response are due to compensation between lower GHG concentrations and reduced aerosol loading in the newer A2 scenario, as compared with the older (Is92A) scenario. The model output from these integrations is available from the IPCC Data Distribution Center and

is being used in various studies of the societal impact of climate change by the impacts community.

2.3 CLIMATE VARIABILITY AND DYNAMICS

2.3.1 Response of the North Atlantic Climate System to the Arctic/North Atlantic Oscillation

T. Delworth *K. Dixon*

ACTIVITIES FY00

A set of experiments has been conducted (mo) using the R15 coupled ocean-atmosphere model to examine the response of the North Atlantic climate system to a sustained upward trend in the Arctic/North Atlantic Oscillation (AO/NAO). This work is partially motivated by the observed upward trend in the AO/NAO over the last 30 years.

The Arctic Oscillation denotes a tendency for out of phase sea level pressure variations between the Arctic and midlatitudes, with associated changes in the midlatitude westerly winds. An index of the Arctic Oscillation is used which is related to the difference in sea level pressure between the Arctic and midlatitude North Atlantic. This index is quite similar to the North Atlantic Oscillation (NAO) index, and hence we view the AO and NAO as effectively identical for this work.

The trend in the AO/NAO is introduced in the model by adding anomalous surface fluxes of heat, water, and momentum to the ocean component of the coupled model. These fluxes have the spatial signature of the AO/NAO, as deduced from a long control integration of the model. The amplitude of the anomalous flux pattern increases linearly over a 30 year period, corresponding to a 9 mb increase in the AO index (similar to the observed increase in the AO over the last 30 years). After that point, the amplitude of the forcing is held fixed at the elevated level.

Our primary focus is on the response of the North Atlantic thermohaline circulation (THC) to the AO/NAO trend. It is found that the stronger winds over the North Atlantic associated with the positive AO/NAO extract more heat from the ocean, thereby cooling and increasing the density of the upper ocean in the subpolar North Atlantic and thus strengthening the THC. For this model, changes in heat flux dominate over water and momentum fluxes.

Most studies of GHG-induced climate change suggest a weakening of the THC in the North Atlantic in response to increased freshening and warming in the subpolar region (1634). As described above, a sustained upward trend in the AO/NAO tends to oppose this THC weakening. The competition between these tendencies has been explored using additional ensembles of numerical experiments (Fig. 2.5). One ensemble is forced by increasing GHGs and sulfate aerosols; the second ensemble adds to this forcing the effects of the positive trend

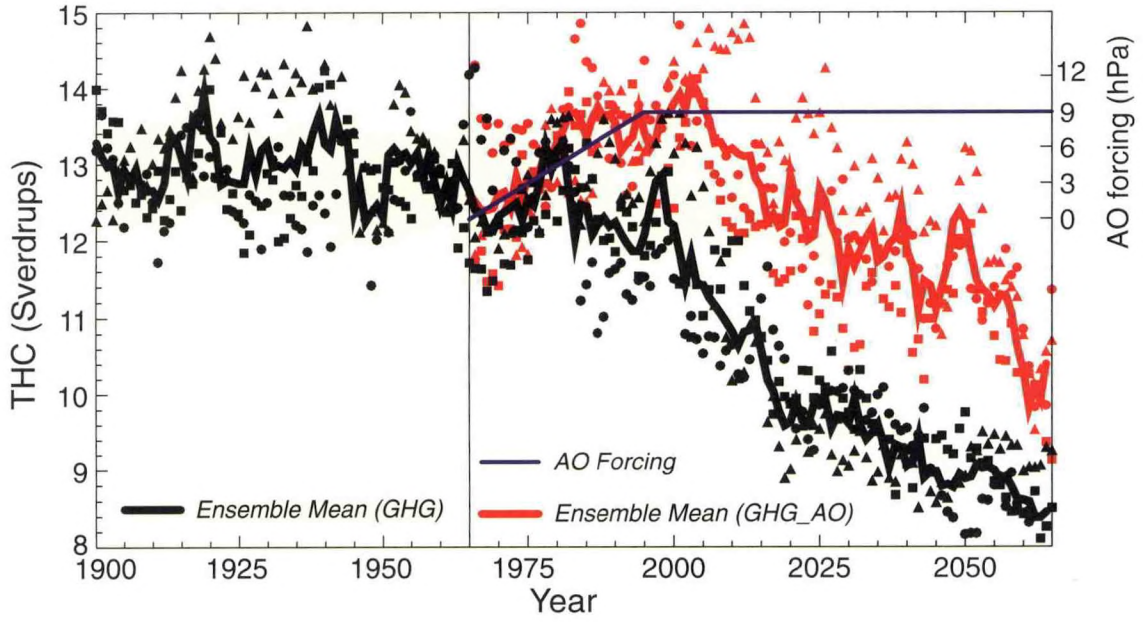

Fig. 2.5 Time series of the North Atlantic thermohaline circulation (THC) from two ensembles of experiments, indicating the effect of the upward trend in the AO/NAO on the THC. The THC is a measure of the northward flow of water in the upper layers of the North Atlantic (units are Sv, 1 Sv = 10^6 m^3 s^{-1}). The thick, black line denotes the ensemble mean from experiments incorporating increasing greenhouse gases and sulfate aerosols, while the red line denotes the ensemble mean from experiments which also include the imposed AO/NAO trend. The differences between the red and black lines are a measure of the impact of the AO-induced trend in surface fluxes on the THC. The triangles, circles, and squares are used to differentiate the members of each ensemble. The amplitude of the AO forcing imposed after 1965 is denoted by the blue line (scale on right axis).

in the AO/NAO. Differences between these two ensembles identify the influence of the AO/NAO trend. It is found that a sustained upward trend in the AO/NAO could effectively delay the GHG-induced weakening of the THC by several decades. This result is of particular importance if the positive trend in the AO/NAO is a response to increasing greenhouse gases, as has been recently suggested.

PLANS FY01

Additional analyses will be conducted to identify further impacts of the AO/NAO trends. In addition, ensembles of experiments using the R30 version of this model have been conducted and will be analyzed.

2.3.2 Observed and Simulated Multidecadal Variability in the North Atlantic

T. Delworth *M. Mann***
*R. Greatbatch**

**Dalhousie University*
***University of Virginia*

ACTIVITIES FY00

The nature of simulated and observed multidecadal temperature variability in the North Atlantic has been examined in a pair of studies. One of the motivations for such studies is the need to improve our understanding of internal variability of the coupled system on decadal to centennial time scales, which is a crucial step in the detection of climate change.

In the first study (jn), a direct comparison was made between multidecadal variability simulated by the R15 coupled model and observed variability as inferred from analyses of both instrumental and proxy records. The model variability is characterized by a large-scale pattern of sea surface temperature (SST) anomalies in the North Atlantic (Fig. 2.6), with a time scale (distinct from red noise) of 40-80 years. The instrumental record shows a spatial pattern of SST anomalies quite similar to that in the model, and with an indication of a multidecadal time scale. The shortness of the instrumental record, however, makes a determination of the timescale of variability difficult. Therefore, the simulated variability was compared to multicentury proxy records of climate variations, as deduced from tree rings, ice cores, and other indicators. Analyses of the proxy records reveal a pattern of variability in the North Atlantic which is quite similar to the simulated variability. This observed pattern has a distinct time scale (approximately 70 years) which is also similar to the model results.

In the second study (1695), experiments were conducted to investigate possible mechanisms for the simulated multidecadal variability. Specifically, the question is whether the variability involves strong, two-way coupling between the atmosphere and ocean (as is the case for ENSO), or an oceanic response to atmospheric forcing. A suite of experiments was conducted in which the ocean component of the R15 coupled model was forced with time series of surface fluxes from both the fully coupled model and from an atmosphere-only model using a prescribed seasonal cycle of SSTs. These experiments reveal that the simulated multidecadal variability is best viewed as an oceanic response to low frequency (multidecadal) atmospheric surface flux forcing. In particular, the spatial pattern of fluxes associated with the North Atlantic Oscillation is crucial in generating the oceanic variability. Interactions between the atmosphere and ocean do play a key role, however, in determining the amplitude of the simulated variability by modifying the magnitude of the air-sea heat flux variations.

PLANS FY01

Analyses will be conducted of the multidecadal variability present in a higher resolution version of this coupled model. In particular, there are preliminary indications that ocean-atmosphere interactions play a more prominent role in the higher resolution model. The

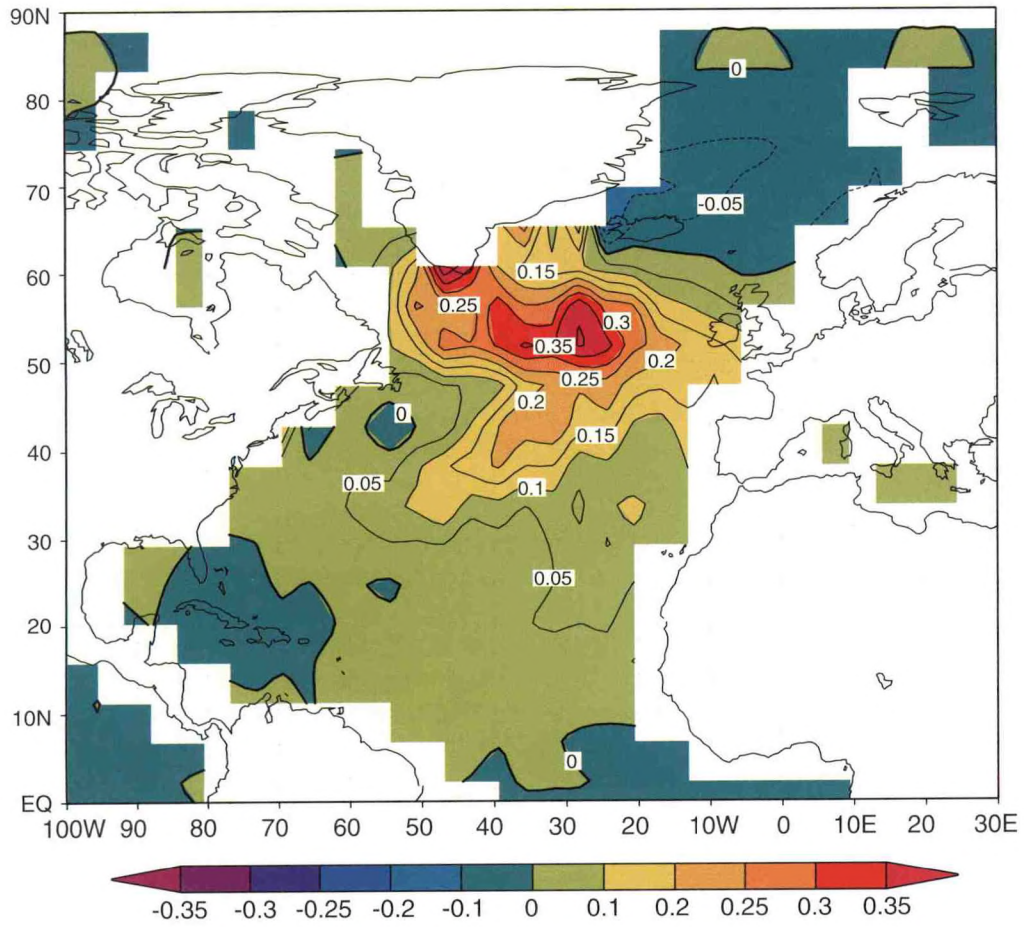

Fig. 2.6 Dominant pattern of multidecadal variability in sea surface temperature for the R15 coupled model over the North Atlantic. The quantity plotted is the linear regression coefficient at each grid point between sea surface temperature and an index of the thermohaline circulation in the North Atlantic. Units are °C Sv (where 1 Sv = 10^6 m^3 s^{-1}). The pattern thus represents the SST anomalies for a 1 Sv increase in the thermohaline circulation (the model typically displays fluctuations of 1-3 Sv).

dynamics of the variability will be studied in a series of idealized runs in which the model adjusts to a sudden imposition of NAO-like forcing, which appears to play a key role in the multidecadal variability.

2.3.3 Partitioning of Poleward Heat Transport Between Ocean and Atmosphere in the Tropics

I. Held

ACTIVITIES FY00

The tropical oceans are observed to carry a larger fraction of the poleward heat transport than the atmosphere between the equator and 20° latitude, beyond which the atmospheric eddies quickly become dominant. Analysis of simple models of the meridional heat transport by the shallow, wind-driven, overturning cells in the tropical oceans and by the

atmospheric Hadley cell has led to a theory for the partitioning of this transport between atmosphere and ocean that helps explain this oceanic dominance (mw). The theory uses the fact that the mass transport in the shallow, wind-driven, overturning cells in the tropical oceans is constrained to be close to the mass transport in the atmospheric Hadley cell, assuming that zonally integrated wind stresses on land are relatively small. It then uses simple expressions for the ratio of heat to mass transports, or the gross static stability, in the two media. The prediction is that the ratio of oceanic to atmospheric transport, averaged over the Hadley cell, is roughly equal to the ratio of the heat capacity of water to that of air at constant pressure (~4), multiplied by the ratio of the moist to the dry adiabatic lapse rates near the surface (~1/3) (yielding a ratio of ~4/3). The ratio of lapse rates is a convenient measure of the moisture content of the atmosphere. The ratio of oceanic to atmospheric energy transport is predicted to be larger than this value near the equator and smaller than this value near the poleward boundary of the Hadley cell.

2.4 CLIMATE MODEL DEVELOPMENT

2.4.1 Coupled Climate Model Development

*V. Balaji**
A. Broccoli
T. Delworth
K. Dixon
D. Golder
S. Griffies
I. Held
T. Knutson
P. Kushner
P.C.D. Milly
P. Phillipps
B. Samuels
M. Spelman
R. Stouffer
*E. Tziperman***
M. Winton

**Cray Research, Inc.*
***The Weizmann Institute of Science*

ACTIVITIES FY00

Using the framework provided by the GFDL Flexible Modeling System (FMS), two coupled climate models are under development. These are termed: 1) a current-generation coupled climate model; and 2) a next-generation coupled climate model.

The current-generation coupled model incorporates the set of physical parameterizations that have been the basis for numerous climate variability and climate change studies over the past two decades. The development of this model within FMS will insure continuity with previous work using the existing GFDL coupled climate model, facilitate systematic testing of new model physics, and provide a very efficient model code for extended paleoclimate experiments and other applications.

The next-generation coupled model will incorporate a number of important changes in physical parameterizations, including a diurnal cycle, improved boundary layer, improved land surface and sea ice models, a more comprehensive treatment of radiative climate forcings, and enhanced ocean model resolution and physics. This model will be critical to

GFDL's future climate change research program, including the laboratory's contributions to future climate change assessments.

During FY00 the development and testing of key components of these models has been a primary focus of the climate group. This effort has extended to include numerous collaborators from several groups within the laboratory. Efforts have continued in the integration and testing of model components of the coupled model framework. Through FMS, the groundwork has been laid for porting the new climate models to massively parallel computing systems. This critical task has been undertaken in preparation for the arrival of the next-generation large-scale computing system at the laboratory.

Related information on various coupled model components, including the FMS framework itself, the radiation code, the land model, the sea ice model, and the ocean model are contained elsewhere in this report.

PLANS FY01

The development, integration, and testing of key coupled climate model components will continue. Construction of the current-generation coupled model will be completed, and the model will be ported to the laboratory's new high-performance computing system. Development and experimentation with prototypes of the next generation coupled models will be undertaken on the new computing system.

2.4.2 Development and Testing of the Land Dynamics Model

The Land Dynamics (LaD) model is an extension of an earlier scheme with a record of successful application in climate modeling. The most significant changes from the original model include: 1) introduction of non-water-stressed stomatal control of transpiration, in order to correct a tendency toward excessive evaporation; 2) conversion from globally constant land parameters (with the exception of vegetation-dependent snow-free surface albedo) to more complete vegetation- and soil-dependence of all surface parameters, in order to provide a more realistic representation of geographic variations in water and energy balances and to enable model-based investigations of land-cover change; 3) introduction of soil sensible heat storage and transport, in order to move toward realistic diurnal-cycle modeling; 4) a groundwater (saturated-zone) storage reservoir, in order to provide more realistic temporal variability of runoff; and 5) a rudimentary runoff-routing scheme for delivery of runoff to the ocean, in order to provide realistic fresh-water forcing of the ocean component of a coupled global climate model.

The performance of the new land dynamics model was evaluated in stand-alone mode, using the International Satellite Land Surface Climatology Project Initiative I global dataset and a recently produced observation-based water-balance dataset for major river basins of the world. The model performance was evaluated by comparing computed and observed runoff ratios from many major river basins of the world. Special attention was given to distinguishing between two components of the apparent runoff-ratio error: the part due to intrinsic model error and the part due to errors in the assumed precipitation forcing. The

pattern of discrepancies between modeled and observed runoff ratios is consistent with the precipitation-error estimates that were produced as part of a companion study. The new model is tuned by adjustment of a globally constant scale factor for non-water-stressed stomatal resistance (Fig. 2.7). After tuning, significant overestimation of runoff is found in

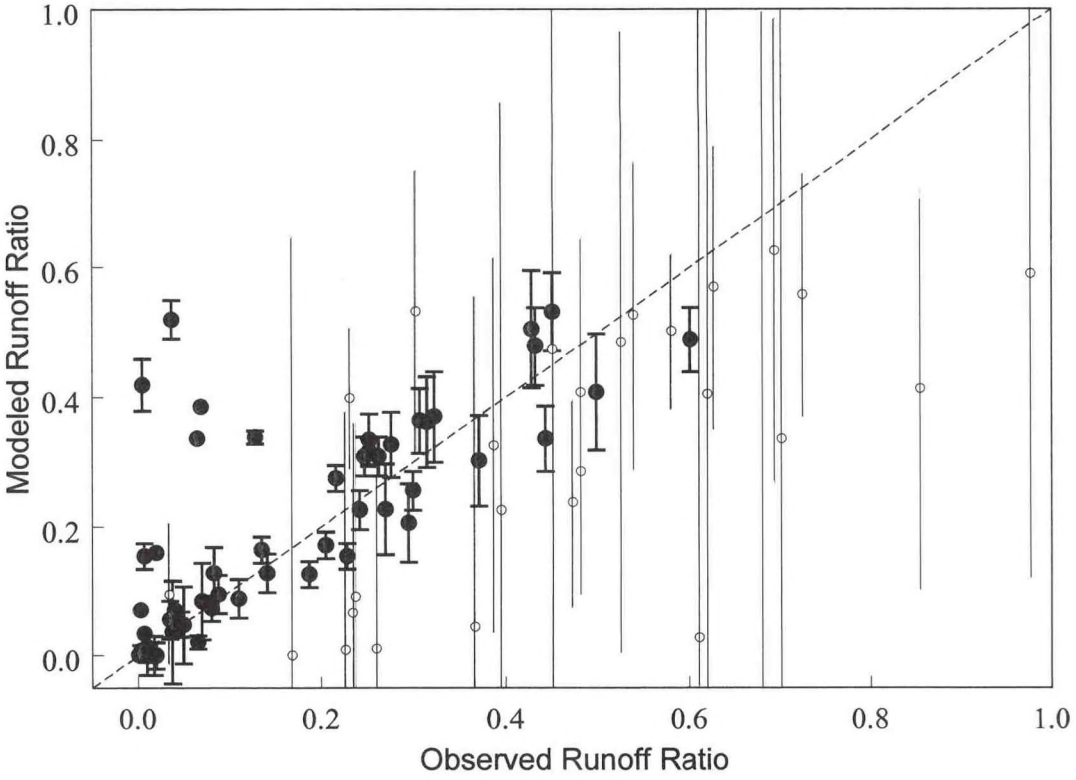

Fig. 2.7 Runoff ratio modeled by the tuned Land Dynamics (LaD) model vs. the observed runoff ratio. Each symbol represents one basin. Error bars indicate range associated with one standard deviation error in the precipitation forcing input to the model. Heavy symbols and bars are used to highlight those cases where this range is less than 0.2.

environments where an overall arid climate includes a brief but intense wet season, and this error may be explained by the neglect of upward soil-water diffusion from below the root zone during the dry season. With the exception of such basins, and in the absence of precipitation errors, the model predicts annual runoff ratios with a root-mean-square deviation from the observations of about 0.05. The new model matches observations better than its predecessor, which has a negative runoff bias and greater scatter.

2.5 PALEOCLIMATE MODELING

2.5.1 Effects of Changes in Earth's Orbit on Climate

A. Broccoli *C. Jackson*

ACTIVITIES FY00

An extended integration of an R15 atmosphere-mixed layer ocean model, in which the forcing was supplied by prescribing the variations in Earth's orbital configuration during the past 135,000 years, has been the subject of intensive examination (A99/P00). One topic of interest that emerged from this orbital forcing experiment involves the response of Arctic climate during the Holocene. Many paleoceanographic and paleoclimatic proxies indicate a cooling of this region commencing 7 to 8 ka (*i.e.*, thousands of years ago) and continuing through the preindustrial era. The cooling was rapid during the early part of this period and slowed thereafter. Many areas of elevated terrain in the Arctic, which had been glaciated during the ice age before subsequently losing this ice in the early Holocene, developed small ice caps once again as this cooling progressed.

The climate of the orbital forcing experiment responds in a manner that is qualitatively consistent with these paleodata. A period of diminished sea ice cover at 10 ka is followed by increasing sea ice toward the present, with the most rapid increase occurring from 8 to 4 ka and a more gradual increase thereafter (Fig. 2.8). The periodic changes in obliquity (*i.e.*, tilt of Earth's axis) and the precession of the equinoxes combine to yield this trend, as evident from a statistical decomposition of the model response into components associated with obliquity and precession. Obliquity peaked most recently at ~10 ka and has decreased thereafter. Because Arctic temperature is high when obliquity is high, decreases in obliquity cool the Arctic from 10 ka through the present. Because of sea ice-albedo-temperature feedbacks, Arctic temperatures are highest and sea ice least extensive when the smallest Earth-Sun distance (*i.e.*, perihelion) occurs in late spring, as it did at ~14 ka. Thus, precession also favors increasing Arctic ice from 14 ka through ~3 ka, as perihelion moved from late spring through summer into late autumn. Thus, the rapid increase in sea ice concentration from 8 to 4 ka results from the superposition of cooling effects from both obliquity and precession, and the subsequent slowing of the growth in sea ice extent occurs as the effects of precession begin to oppose the obliquity-driven cooling.

PLANS FY01

A more thorough comparison of the orbital forcing experiment with paleodata from the Holocene will be undertaken. In addition, other aspects of this experiment will be examined to identify additional mechanisms of climate response to orbital forcing.

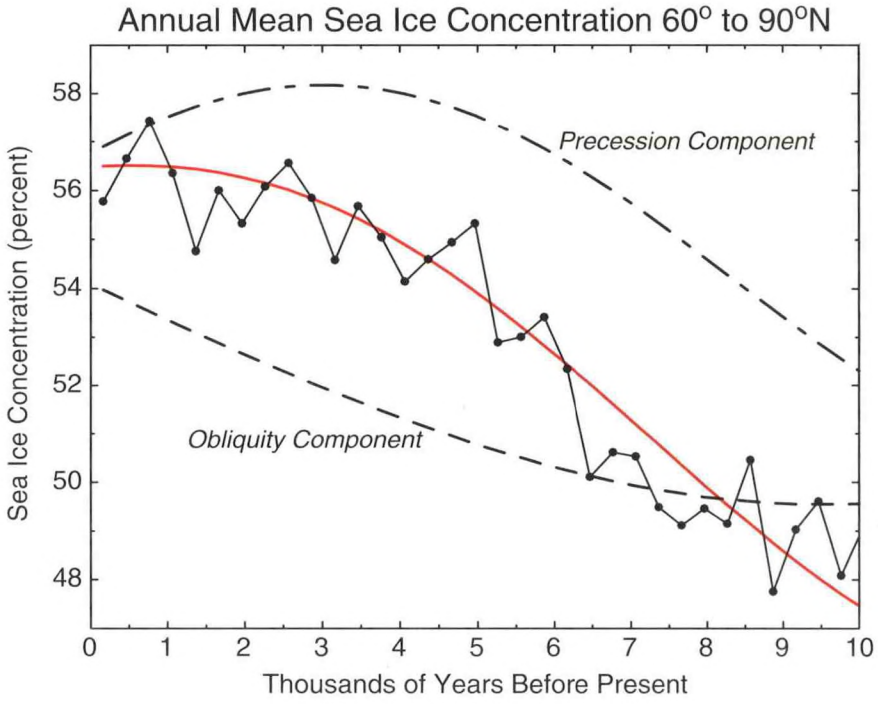

Fig. 2.8 Time series of annual mean sea ice concentration (60°N to 90°N) from a climate model forced by continually varying changes in Earth's orbital configuration over the past 10 thousand years. Also indicated are the independent effects of obliquity (dashed line) and precession (dashed-dot line) and their sum (red line) on sea ice concentration. The superposition of cooling effects from obliquity and precession are responsible for the rapid increase in sea ice concentration from 8,000 to 4,000 years ago.

2.5.2 Simulation of Last Glacial Maximum with HadCM3 Coupled Climate Model

A. Broccoli *J. Mitchell**
*C. Hewitt** *R. Stouffer*

**Hadley Centre*

ACTIVITIES FY00

In a collaboration with the Hadley Centre for Climate Prediction and Research (Bracknell, United Kingdom), a simulation of the climate of the last glacial maximum (LGM) using a three-dimensional coupled atmosphere-ocean model is underway. The LGM simulation uses HadCM3, the Hadley Centre's latest coupled climate model, as ported to GFDL's Cray T3E computer system.

To initialize the model, a strategy was devised that employed output from a LGM simulation in which a slab ocean was substituted for the oceanic component of HadCM3. Beginning from modern observations of ocean temperature and salinity, the SSTs in HadCM3 were relaxed toward the SSTs simulated by the slab ocean model for a period of 70 years. This initial period was intended to facilitate a more rapid cooling toward a glacial state. At the

conclusion of the first 70 years, the relaxation is discontinued, leaving the model free to determine a climatic state that is in equilibrium with the glacial boundary conditions. As of this writing, the model has run more than 600 additional years, during which slow changes in its dynamic and thermodynamic state have occurred.

Although HadCM3 has yet to fully equilibrate with the LGM boundary conditions, there is very clear evidence of important interactions between the atmosphere and ocean. Surface temperatures in the coupled run are substantially different from those simulated by a slab ocean coupled to the same atmosphere, particularly in the North Atlantic, as evident in Fig. 2.9, where a "tripole" anomaly pattern is found. Shifts in the position of the Gulf Stream and the regions of deep water formation are primarily responsible for this altered anomaly pattern. In the eastern tropical Pacific, enhanced equatorial cooling (relative to the slab model) has emerged during the course of the integration.

PLANS FY01

Because coupled models take a long time to reach an equilibrium state, at least several more centuries of model integration will be required to complete this experiment. In the meantime, the more stable elements of the simulated climate will be subject to additional detailed examination.

2.5.3 Effects of Fresh Water Discharge on Climate

A. Broccoli *R. Stouffer*

ACTIVITIES FY00

Abrupt climate change has been studied by imposing an additional, external fresh water source at the ocean surface (1342, 1444) in older versions of the GFDL coupled model (R15 resolution). Recently, one of the earlier experiments was repeated using a newer, higher resolution (GFDL_R30_c) coupled model. In this experiment, a 1 Sv fresh water flux is added to the model generated water fluxes from 50°N to 70°N in the North Atlantic Ocean.

In both experiments, the external fresh water flux makes the surface waters in the northern North Atlantic more buoyant, inhibiting oceanic convection. This weakening of the convection isolates the surface waters from the deeper waters leading to further freshening. The weakening of the convection also leads to a cooling of the ocean surface, since convection typically brings warmer subsurface water to the ocean's surface. The surface temperature anomalies are locally up to 12°C and the cooling covers most of the northern North Atlantic. In addition, as the surface waters become more buoyant the thermohaline circulation (THC) weakens (Fig. 2.10).

In comparing the THC response for the two models, one notes that the initial weakening is very similar in the two experiments both in terms of rate and magnitude of the weakening. However, the THC recovery in the R30 experiment is much faster than in the earlier

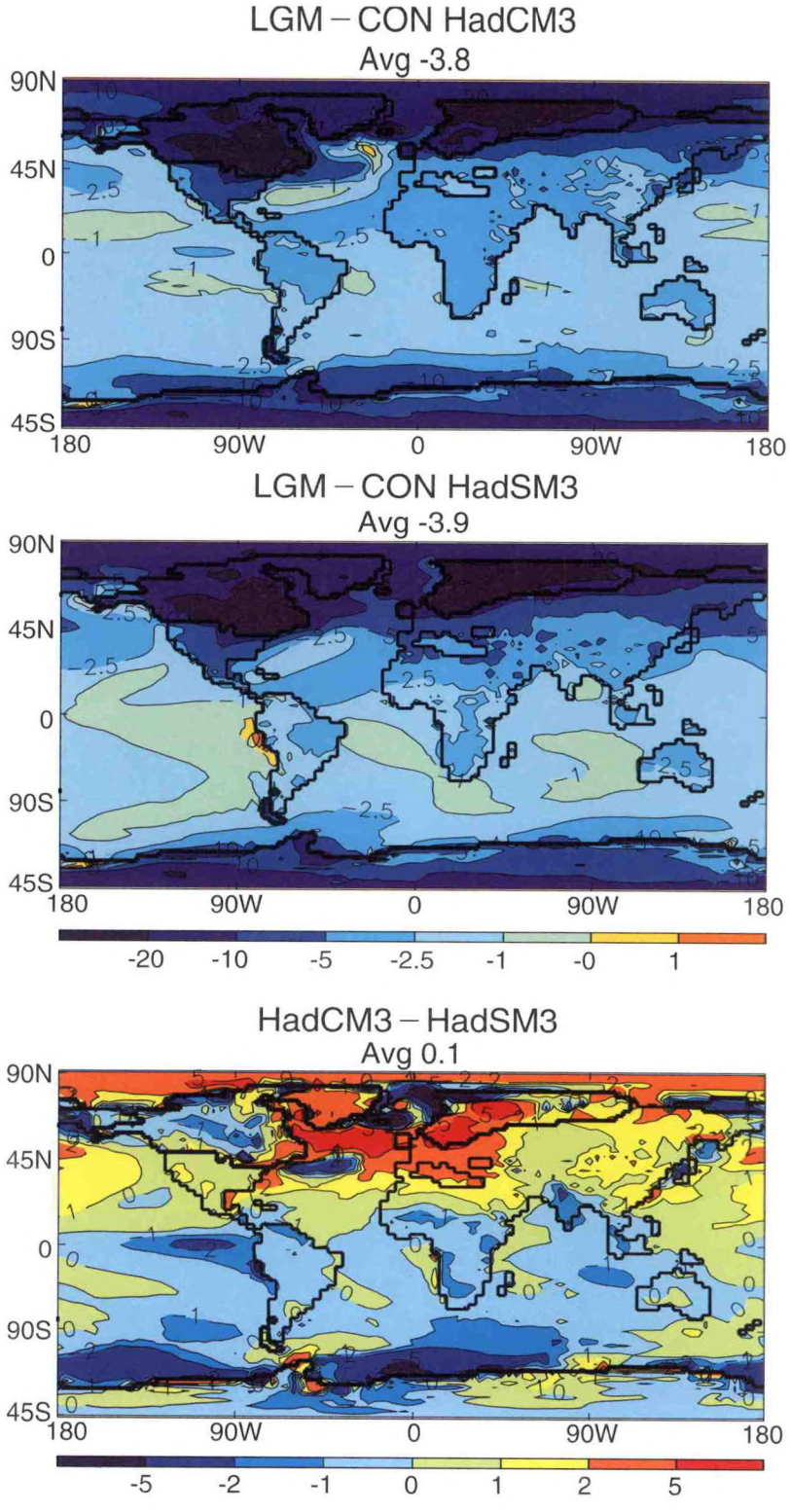

Fig. 2.9 Surface temperature differences (C°). Top: LGM minus Modern from HadCM3. Center: LGM minus Modern from slab ocean model. Bottom: HadCM3 LGM minus slab LGM. Glacial surface temperatures in the coupled run are substantially different from those simulated in the slab ocean model in a number of regions, illustrating the importance of ocean dynamics.

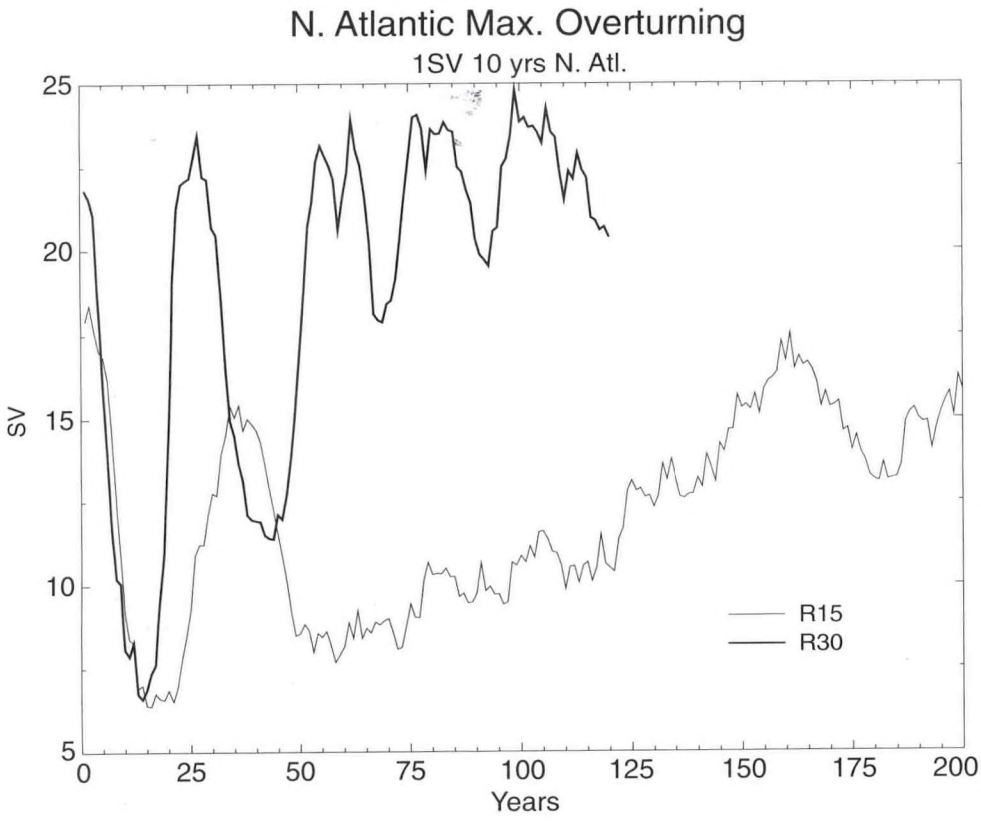

Fig. 2.10 Time series of the maximum value of the overturning streamfunction in the North Atlantic Ocean (SV). Thick line represents data from the R30 coupled model and the thin line, the R15 coupled model. The models were forced with 1SV of fresh water at the surface of the North Atlantic Ocean for the first 10 years of the integration. The overturning in the R30 integration recovers more rapidly and undergoes larger multidecadal variability during its recovery.

R15 experiment. The reasons for this difference are unclear. The rapid recovery in the R30 experiment applies not only to the THC, but also to sea surface temperature.

PLANS FY01

A new experiment is now being integrated in which the external fresh water flux is much smaller (0.1 SV) for a much longer time period (100 years). This slower rate may allow for a more comprehensive analysis of the atmospheric response to the fresh water flux in the higher resolution model. We plan to compare the results to the earlier R15 results and to paleodata, particularly the wind changes seen in the Caribbean Sea during the Younger Dryas.

2.6 HYDROLOGY AND CLIMATE

K. Dunne *A. Shmakin*
P.C.D. Milly *R. Wetherald*

2.6.1 Sensitivity of River Runoff to Greenhouse Warming

ACTIVITIES FY00

Work has continued on a project initiated in FY96 to evaluate the river discharge and its sensitivity to greenhouse warming as simulated by a general circulation model. Whereas previous efforts were concentrated on an R15 version of the model, current emphasis is placed on the GFDL_R30_b version of the coupled ocean-atmospheric model. Two integrations were examined: 1) a control integration consisting of 1000 years; and 2) an integration for 300 years where the CO_2 concentration was quadrupled. For the current investigation, the number of river basins has been increased to 184.

Figure 2.11 shows the CO_2-induced response of annual mean runoff for the 184 separate basins. According to this figure, runoff increases for approximately 70 percent of the river basins in response to the quadrupling of CO_2. From an analysis of the geographical distribution of CO_2-induced change of annual mean runoff, almost half of the negative values are produced from river basins located in various places in the southern half of the U.S. where the model indicates a general region of drying. Other river basins exhibiting negative runoff change include those located in equatorial regions of South America and Africa, India, southern Indochina and southern Europe. In general, river basins located in middle to higher latitudes in the Northern Hemisphere show an excess of river basin runoff, a result which is consistent with previous greenhouse warming studies of CO_2-induced change of land-surface hydrology.

2.6.2 Land-Process Influences on Monthly River Discharge Variability

ACTIVITIES FY00

A salient characteristic of river discharge is its temporal variability. The time series of flow at a point on a river may be viewed as the superposition of a smooth seasonal cycle and an irregular, random variation. Viewing the random component in the spectral domain facilitates both its characterization and an interpretation of its major physical controls from a global perspective. The power spectral density functions of monthly flow anomalies of many large rivers worldwide are typified by a red-noise process: the density is higher at low frequencies than at high frequencies, indicating disproportionate (relative to uncorrelated white noise) contribution of low frequencies to variability of monthly flow. For many high-latitude and arid-region rivers, however, the power is distributed relatively evenly across the frequency spectrum. The power spectrum of monthly flow can be interpreted as the product of the power spectrum of monthly, basin-total precipitation (which is typically white or slightly red) and several filters having physical significance. The filters are associated with: 1) the conversion of total precipitation (sum of rainfall and snowfall) to effective rainfall (liquid flux to the ground surface from above); 2) the conversion of effective rainfall to soil-water excess (runoff); and 3) the

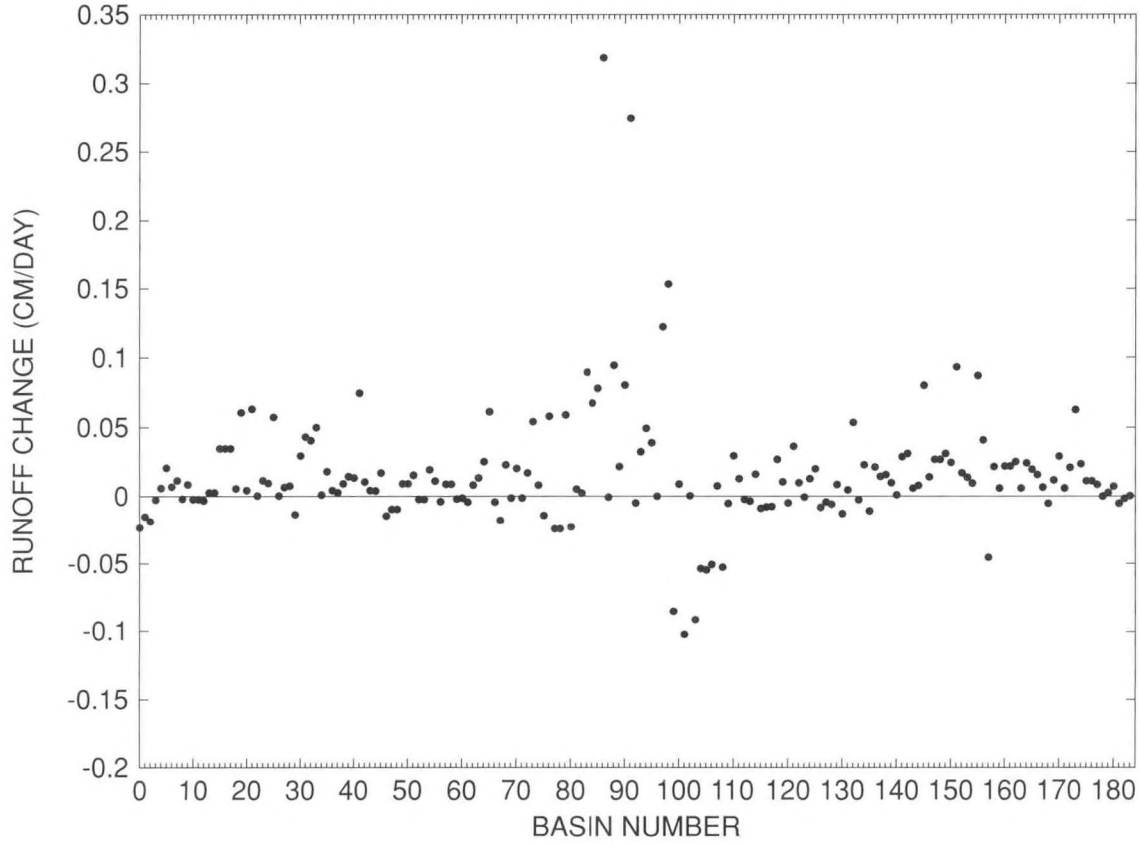

Fig. 2.11 Response of annual mean river basin runoff to a quadrupling of CO_2 by basin. The horizontal axis represents the basin number (1-184) and the vertical axis represents the corresponding change of a particular basin runoff to the quadrupling of CO_2. Basins 1-85 are located in North America; basins 86-99 are located in South America; basins 100-110 are located in Africa; basins 111-140 are located in Europe; basins 141-177 are located in Asia; and basins 178-184 are located in Australia. Units are cm/day.

conversion of soil-water excess to river discharge. The first filter causes a snowmelt-related amplification of high-frequency variability in those basins receiving significant snowfall. The second filter causes a relatively constant reduction in variability across all frequencies and can be predicted well using a semi-empirical water-balance relation. The third filter, associated with groundwater and surface-water storage in the river basin, causes a strong reduction in high-frequency variability of many basins. The strength of this reduction can be quantified by an average residence time of water in storage, which is typically on the order of 20-50 days. However, the residence time is demonstrably influenced by freezing conditions in the basin, fractional cover of the basin by lakes, and runoff ratio (ratio of mean runoff to mean precipitation). Large lake areas enhance storage and can greatly increase total residence times (100 to several hundred days). Freezing conditions appear to cause bypassing of subsurface storage, leading to smaller residence times (0 to 30 days). Small runoff ratios tend to be associated with regions where most of the runoff is produced by processes that bypass the (deep) saturated zone, leading to relatively small residence times for such basins (0 to 40 days, Fig. 2.12).

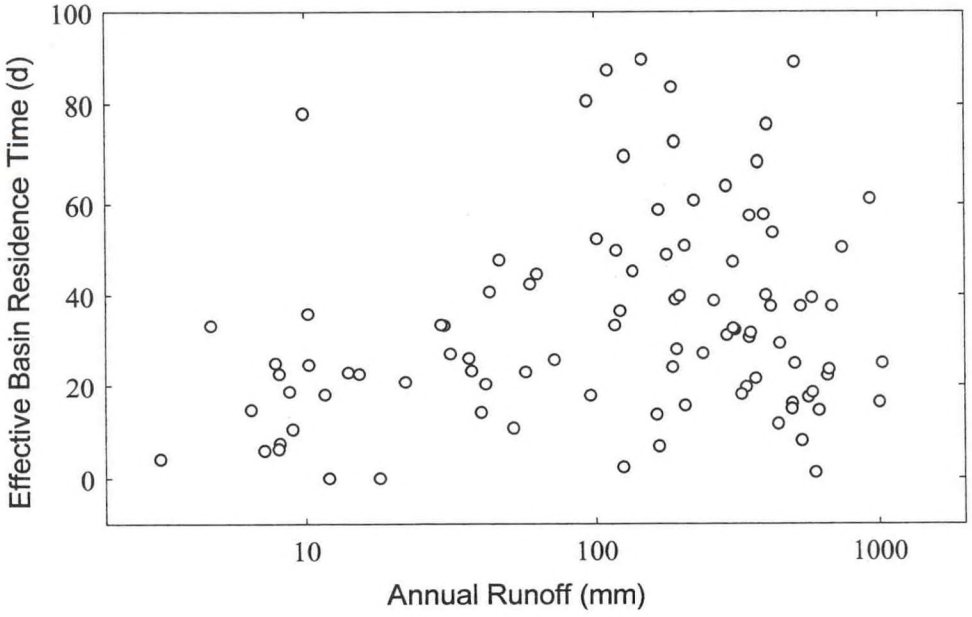

Fig. 2.12 Effective basin residence time as a function of annual runoff amount (mm). Each symbol represents one river basin.

2.6.3 Modeling Land Influences on Variability of Macro-Scale Water and Energy Fluxes

ACTIVITIES FY00

Variations in water and energy balances over land are a function of variations in the distribution of water and energy supplies as well as land characteristics. A largely untested hypothesis underlying most global models of water and energy balance is the assumption that parameter values based on estimated geographic distributions of soil and vegetation characteristics improve the performance of the models relative to the use of globally constant land parameters. This hypothesis has been tested by evaluating the improvement in performance of one land model associated with the introduction of geographic information. The ability of the model to reproduce annual runoff ratios of large river basins, with and without information on the global distribution of albedo, rooting depth, and stomatal resistance, is assessed. To allow a fair comparison, the model is calibrated in both cases by adjusting globally constant scale factors for snow-free albedo, non-water-stressed bulk stomatal resistance, and critical root density (which is used to determine effective root-zone depth). The test is made in stand-alone mode, *i.e.*, using prescribed radiative and atmospheric forcing. Model performance is evaluated by comparing modeled runoff ratios with observed runoff ratios for a set of basins where precipitation biases have been shown to be minimal.

It has been found that leaving out information on global variations in these parameters leads to a significant degradation of the ability of the model to predict the annual runoff ratio. An additional set of optimization experiments in which the parameters are examined individually reveals that spatial variations in stomatal resistance add the most predictive power to the model in stand-alone mode. Further single-parameter experiments with surface

roughness length, available water capacity, thermal conductivity, and thermal diffusivity show very little sensitivity to global variations in these parameters. Finally, it is found that the model performance exceeds that of the Budyko and generalized Turc-Pike water-balance equations, implying that the model benefits not only from information on global variations in land characteristics, but also from information on the temporal structure of the forcing.

2.6.4 A Minimalist Probabilistic Description of Root-Zone Soil Water

ACTIVITIES FY00

The probabilistic response of depth-integrated soil water to given climatic forcing can be described readily using an existing supply-demand-storage model (1180). An apparently complex interaction of numerous soil, climate, and plant controls can be reduced to a relatively simple expression for the equilibrium probability density function of soil-water as a function of only two dimensionless parameters. These are 1) the index of dryness (ratio of mean potential evaporation to mean precipitation) and 2) a dimensionless storage capacity (active root-zone soil-water capacity divided by mean storm depth). The first parameter is mainly controlled by climate, with surface albedo playing a subsidiary role in determining net radiation. The second is a composite of soil type (through moisture retention characteristics), vegetation (through rooting characteristics), and climate (mean storm depth). This minimalist analysis captures the essential features of a more general probabilistic analysis[1], but with a considerable reduction in complexity and consequent elucidation of the critical controls on soil-water variability. In particular, it is shown that: 1) the dependence of mean soil water on the index of dryness approaches a step function in the limit of large soil-water capacity; 2) soil-water variance is usually maximized when the index of dryness is close to 1, and the width of the peak varies inversely with dimensionless storage capacity (Fig. 2.13); 3) soil water has a uniform probability density function when the index of dryness is 1 and the dimensionless storage capacity is large; and 4) the soil-water probability density function is bimodal if and only if the index of dryness is less than 1, but this bi-modality is pronounced only for artificially small values of the dimensionless storage capacity.

2.7 PLANETARY CIRCULATION

G.P. Williams

ACTIVITIES FY00

The Jovian atmosphere involves basic geophysical fluid dynamical processes acting in novel arrangements and under different constraints than Earth's atmosphere and oceans. Understanding the Jovian circulation provides insights that will help to generalize and clarify our theories for these processes.

---

1. Rodriguez-Iturbe, I., Ecohydrology: A hydrologic perspective of climate-soil-vegetation dynamics, *Water Resour. Res., 36(1)*, 3-9, 2000.

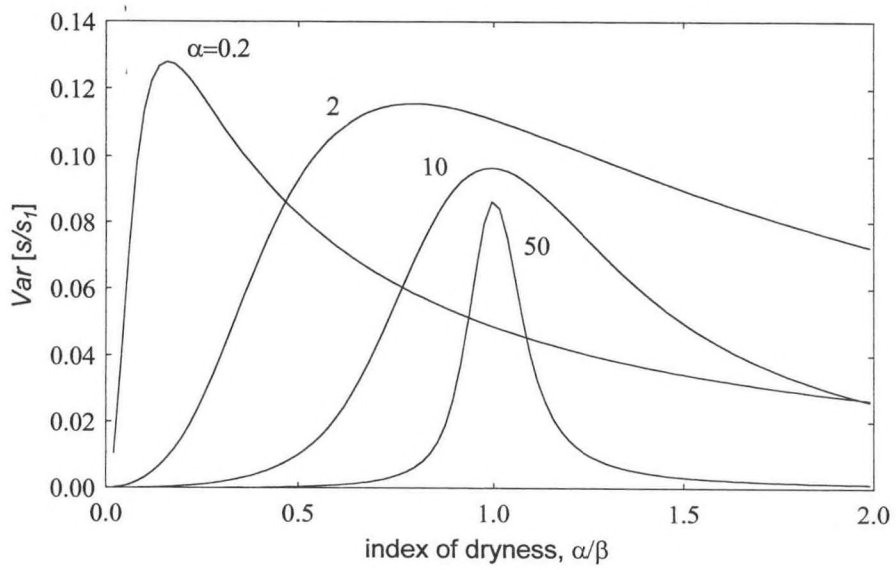

Fig. 2.13 Variance of normalized root-zone soil-water saturation as a function of dimensionless storage capacity (α) and index of dryness (α/β).

The main problem in defining Jupiter's meteorology, particularly the character of the jets and vortices, comes from the fact that the nature and extent of the motions are not generally known for the region below the clouds. To develop a theory for the circulation, 3-D primitive equation models are used to investigate the formation and coexistence of the various turbulent and coherent phenomena for hypothetical vertical structures. The main hypotheses involved - that the atmospheric circulation occurs within a relatively thin upper layer and is driven by horizontal temperature gradients - have been examined with a wide range of models. Present studies are concerned with the role of the vertical structure on the formation of vortices and jets.

In particular, studies of the dynamical response of thin atmospheric layers have been extended to examine the genesis and equilibration of multiple anticyclonic vortex sets in a Jovian context (ni). Current modeling efforts focus on the three main groups seen on Jupiter, namely, the Great Red Spot, the four Large Ovals, and the dozen or so Small Ovals that occur at latitudes of -21', -33', -41', respectively. The generation and equilibration of the vortices associated with long solitary baroclinic Rossby waves in a stratified fluid are examined numerically using a primitive equation model with Jovian parameters subject to simple heating functions. Following earlier findings (1400,1454), the motions are confined to thin upper layers by exponential vertical structures that favor absolute vortex stability. The selective character of the Rossby vortices also provides a theoretical probe of the vertical structure of the atmosphere over a wide range of latitudes.

From a wide range of calculations, it has been found that vortex sets resembling the three main Jovian groups in scale, form, and number can be simultaneously generated and maintained in a steady configuration provided that the heating components that drive the alternating jets are carefully chosen so as to make the easterly jets marginally unstable. Otherwise, more complex arrangements evolve. The vortices decrease rapidly in size and

become more numerous with latitude due to reductions both in the widths of the containing jets and in the propagation speeds. The amplitudes of the vortices depend on the strength of the baroclinic instability of the easterly jets that generate them and on the weak heating that maintains them. Vortices generally merge in the same way as those in the unheated system (1400) to explain the singularity of the Great Red Spot, while the Ovals remain multiple because of their smaller scale and mutual similarity.

Evolution of features in the model, however, are more complex in the heated system because the generation of new storms offsets the tendency to merge into fewer vortices. Regenesis can occur continuously if the jet instabilities are restored too quickly by the heating. Otherwise, weak regenesis produces weak eddies that are absorbed by existing vortices. A steady configuration requires a balance between a weak heating and a weak dissipation. Intrazonal interactions between vortices from different sets also occur and can in some situations lead to the mutual destruction of anticyclones which model the Great Red Spot and a Large Oval. They can also produce a novel form of coherence in which a large warm anticyclone occurs within a cool cyclonic zone whose flow it blocks; such storms are energized by a continuous inflow of eddy energy from the anticyclonic zone and act as a fluid dynamical "black hole".

Numerical constraints on diffusion and resolution suggest that the small eddies also contribute to the dynamical balance of the vortices and should be represented explicitly. Furthermore, the heating forms required to produce the easterly jets that generate the vortices imply that the existing heat imbalance may be more local than global and, as such, controlled by the albedo. This, in turn, implies that dynamics alone cannot explain all aspects of Jupiter's circulation, that physics must also be involved.

3. ATMOSPHERIC PROCESSES

GOALS

To develop general circulation models for understanding the interactive three-dimensional radiative-dynamical-chemical-hydrological structure of the climate system from the surface and troposphere to the upper stratosphere and mesosphere on various time and space scales.

To employ meteorological observations in conjunction with models for diagnostic analyses of atmospheric processes, and for evaluating and improving parameterizations employed in weather and climate models.

To model the interactions between clouds, convection, radiation and large-scale dynamics and understand their roles in climate and climate change.

To model the physics, chemistry and transport of atmospheric trace gases and aerosols; to investigate the impact of future emissions on regional and global air quality; and to investigate the regional and global climatic effects due to changes in natural and anthropogenic radiatively-active species.

3.1 RADIATIVE TRANSFER

S.M. Freidenreich *V. Ramaswamy*
J. Haywood *M.D. Schwarzkopf*

ACTIVITIES FY00

3.1.1 Solar Benchmark Computations

In collaboration with Phil Partain of Colorado State University, line-by-line + Monte-Carlo/Equivalence Theorem (LBL+MCET) computations were performed for overcast atmospheric conditions. Due to the computational time needed for the Monte Carlo algorithm, it is employed only once for a given set of drop single-scattering parameters. Thus, the effect of spectral variations in gas absorption are ignored in deriving cloudy layer reflection and transmission. In order to test the viability of this approximation, as well as the MCET technique in general, differences in the fluxes and heating rates derived from LBL+MCET and line-by-line + doubling-adding (LBL+DA) computations were analyzed as a function of the number of cloudy layers (geometrical thickness). Specifically, the effect of increasing the geometrical thickness in a cloud using the "CS" size distribution used in the ICRCCM (Intercomparison of Radiation Codes in Climate Models) study with a fixed total drop optical depth is examined. The fractional differences in both the absorbed flux in the cloud and the individual cloud layer heating rates increase with increasing geometrical thickness, but remain modest (3%, 5%, respectively) for even the thickest case. However, there is a growing

overestimate of the absorbed flux in the atmosphere as the geometrical thickness increases. There is likewise an increasing overestimate of heating above the cloud; the maximum fractional difference exceeds 30% for the two thickest cases. There is a corresponding increase in the underestimation of the reflected top-of-the-atmosphere (TOA) flux. These differences point out some limitations of the LBL+MCET technique as applied presently to plane parallel clouds.

3.1.2 Shortwave Parameterizations

A more realistic assessment of the stratospheric temperature changes in SKYHI (the GFDL troposphere-stratosphere-mesosphere general circulation model (GCM)) due to the improved accounting of CO_2 shortwave heating has been made possible by the completion of a 10-year SKYHI GCM integration. A control run that uses the new solar radiation algorithm with CO_2 shortwave heating included is compared against the new GCM integration that retains the same shortwave algorithm, but neglects the CO_2 heating. The results give a reasonable approximation of the effect of the improved accounting of CO_2 heating, since the older parameterization produced a very small stratospheric heating. Fig. 3.1 shows the

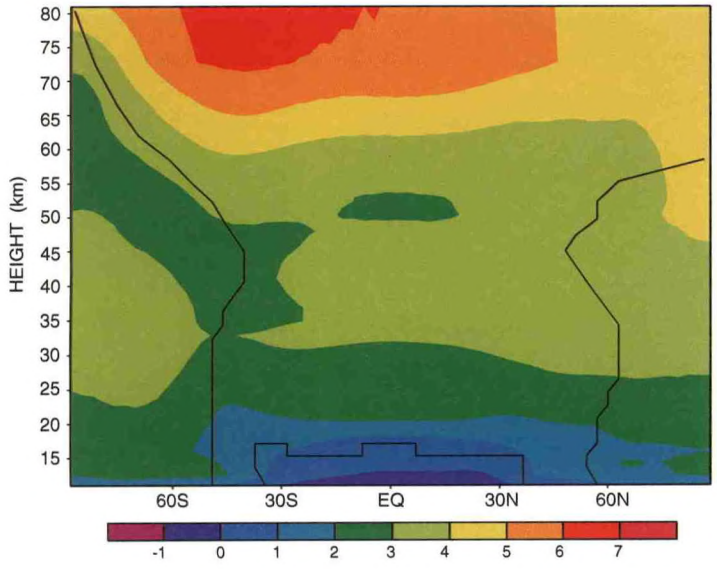

Fig. 3.1 The annually averaged temperature change in the SKYHI GCM due to the inclusion of CO_2 shortwave heating. Results are derived from 10-year integrations of the control (with CO_2) and the new (without CO_2) runs. Also shown is the contour designating regions of statistical significance > 99%. CO_2 shortwave heating exerts an important effect over most of the tropics and middle latitudes of the stratosphere.

annually averaged temperature change in the control run due to the inclusion of CO_2 heating. An increase in temperature of several degrees is seen to occur throughout most of the stratosphere with the magnitude increasing with height. Superimposed on this is the region where the statistical significance is estimated to be > 99%. Note that this covers the tropical and most of the middle-latitude stratosphere.

3.1.3 Diagnostic Analyses of Surface Solar Flux Measurements

The Baseline Surface Radiation Network (BSRN) data was further analyzed to determine differences between the measured "clear sky" surface flux for Boulder, Colorado and calculated values from a solar radiative transfer model. For the model calculations, climatological profiles of temperature and moisture are derived from daily NCEP data. Clear-sky observations are identified by stipulating that the difference in the direct surface transmission between the measurement and the model clear-sky value be less than a critical amount. This criterion is applied for all observations comprising each 30 minute time period. In Fig. 3.2 (top), the diurnal variation of the monthly-averaged total (direct + diffuse) "clear sky" surface flux derived from the observations is compared with the model value for Boulder in July 1994. Note that the measurements are consistently lower than the model value, with differences exceeding 100 W/m^2. These differences further suggest that additional attenuators, likely aerosols, need to be incorporated into the model computations to produce better agreement.

The entire record for Boulder from the BSRN dataset was archived in order to study temporal variations in the derived monthly-averaged "clear sky" surface flux. Fig. 3.2 (bottom) shows a comparison of the monthly-averaged "clear sky" total surface flux derived for all months and years (1992-1997) in the sample. The relatively small interannual variations (< 20 W/m^2) give further credence to the derived fluxes being clear-sky, since such fluxes are expected to exhibit relatively little variability. Also shown is the corresponding SKYHI clear-sky surface flux for the closest grid point to Boulder. Note that SKYHI consistently overestimates the clear-sky flux by 20-30 W/m^2 during most of the year. This confirms the fact that additional attenuators are needed to produce better agreement between calculated and observed fluxes. Smaller differences between SKYHI and the measurements are noted during the autumn season.

PLANS FY01

In collaboration with Phil Partain of Colorado State University, the LBL+MCET algorithm will be used to perform calculations for more realistic three-dimensional cloudy atmospheres. The BSRN data will be analyzed further for other stations. Available aerosol measurements will be used to make improvements in model calculated surface fluxes. Output of solar radiative quantities from the Flexible Modeling System (FMS) GCM model integrations will be analyzed.

3.1.4 Development of Radiative Parameterizations for GCMs

R. Hemler *M.D. Schwarzkopf*

ACTIVITIES FY00

The shortwave and longwave radiative parameterizations have been fully recoded in Fortran 90 modules compatible with standards of the FMS. The modules have been added to a FMS prototype ("Blue") model. A 1-column ("standalone") version of this new code has also been developed.

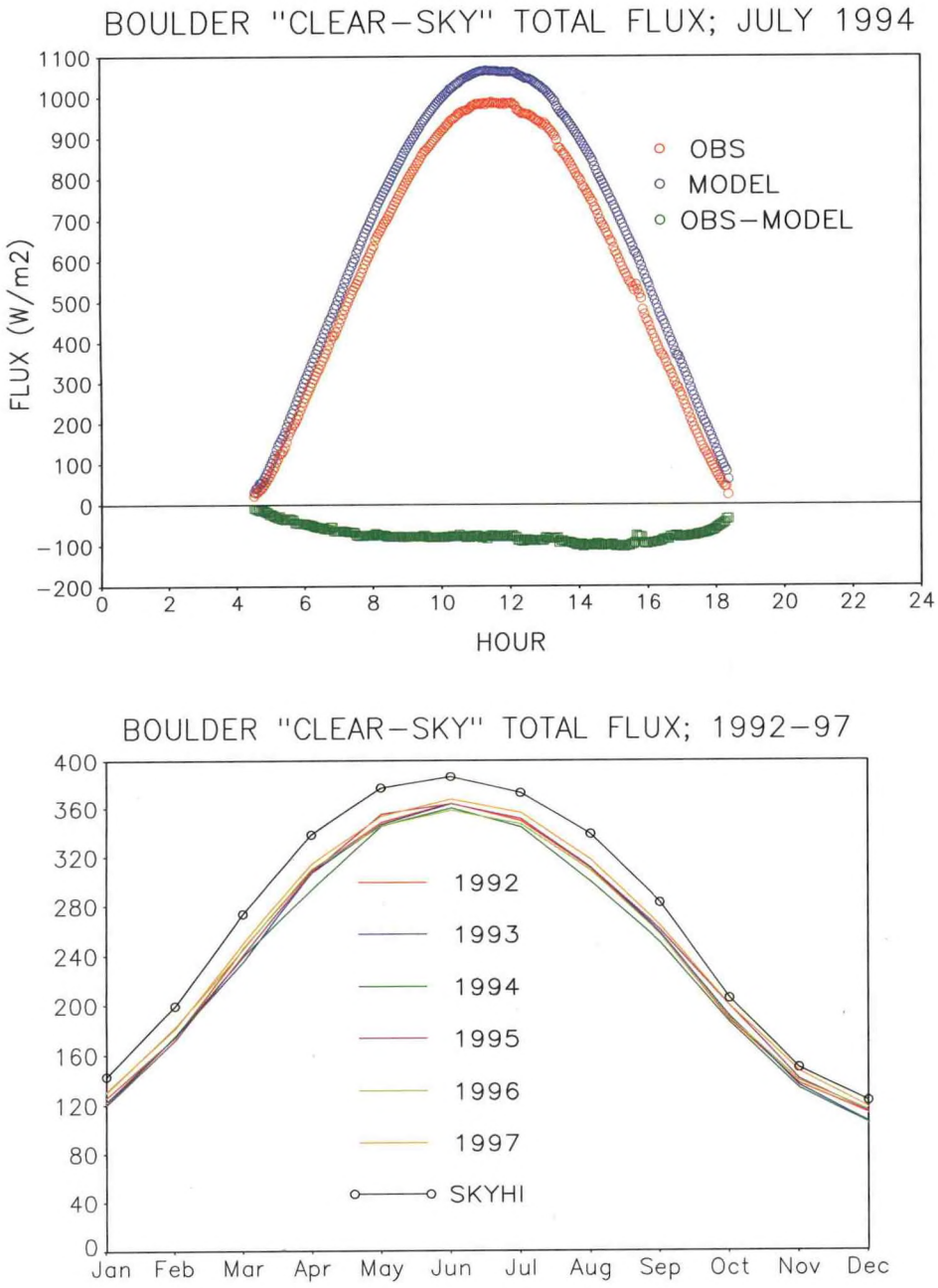

Fig. 3.2 Top: The diurnal variation in the monthly-averaged total (direct + diffuse) "clear sky" surface flux derived from the BSRN observations "OBS" for Boulder, CO in July 1994 and the corresponding value derived from the new shortwave algorithm "MODEL", using daily NCEP moisture and temperature profiles; Bottom: comparison of the monthly averaged "clear sky" total flux measurements for Boulder for all months and years with SKYHI clear sky values for the grid point closest to Boulder. The SKYHI results consistently overestimate the clear-sky fluxes, suggesting the presence of atmospheric aerosols.

A version of the SKYHI GCM with 1.2° x 1.0° longitude-latitude resolution suitable for use on the GFDL T3E system has been prepared. This version has been employed in a 1-year control integration to determine the effects of model resolution on cloud climatology (no).

PLANS FY01

The radiative algorithms in the FMS will be improved as indicated by analysis of model results. Additional changes will be made to take advantage of the resources of the new GFDL computer system.

3.2 CONVECTION-CLOUDS-RADIATION-CLIMATE INTERACTIONS

3.2.1 Cumulus Parameterization

L. Donner *R. Hemler*
*S.-M. Fan** *C. Seman*

**Princeton University*

ACTIVITIES FY00

A major, but elusive, goal in parameterizing cumulus convection for GCMs is to capture the interaction between deep cumulus towers and the mesoscale and synoptic-scale cloud systems in which they are embedded and in whose development they play important roles. The latter, spatially extensive cloud systems, are major regulators of the earth's radiant energy system. A new conceptual framework for dealing with this problem has been presented (1133). The frequently used concept of mass-flux cumulus parameterizations was extended to include a statistical treatment of the vertical velocities in cumulus convection. These vertical velocities can be used to drive microphysics at physically appropriate scales and thereby provide representations of the interactions between cumulus-scale clouds and larger-scale, radiatively important cloud systems (1349).

The impact of deep convective systems on the thermodynamic and hydrological behavior of the atmospheric general circulation has been studied using this conceptual framework, embedded in the SKYHI GCM (mn). The mesoscale cloud systems produced by deep convection in SKYHI increase upper-tropospheric water vapor and intensify the Walker circulation. The size distribution of these simulated mesoscale cloud systems is consistent with satellite observations, an important result for modeling cloud-radiative interactions realistically. The mass fluxes associated with deep convective systems, including mesoscale clouds, differ appreciably from those of deep convective systems parameterized without them, with detrainment more concentrated in the middle troposphere when mesoscale circulations are included.

Microphysical and radiative aspects of the mesoscale cloud systems have also been parameterized. Convective systems with mesoscale clouds are found to produce much larger shortwave and longwave cloud forcing than those parameterized without them.

Preliminary development of an extension to the new cumulus parameterization to include transport of chemical tracers has been completed. Based on mass fluxes produced by the parameterization when mesoscale clouds are included, it is likely that less tracer transport

to the upper troposphere will occur, correcting a problem of excessive upper-tropospheric tracer concentrations that has been noted in several studies using mass-flux parameterizations without mesoscale clouds.

PLANS FY01

Development and evaluation of tracer transport by the cumulus parameterization will be completed. GCM studies with linked cumulus and prognostic cloud parameterizations are planned. The impact of deep convection on the earth-atmosphere radiative balance will be evaluated using satellite observations (1560).

3.2.2 Limited-Area Non-Hydrostatic Models

C. Andronache *R. Hemler*
L. Donner *C. Seman*

ACTIVITIES FY00

An ongoing study of deep convection and its associated mesoscale circulations using the Lipps-Hemler (885) cloud-system model focused this year on extra-tropical, continental convection. Observations from the Atmospheric Radiation Measurement (ARM) program were used to integrate the model and evaluate its ability to produce hydrological and cloud fields in the interior United States. These experiments showed that the model is sensitive to surface fluxes, and is able to capture many observed features of continental convection.

The convection model was augmented to include aerosol chemistry and transport (1537, 1543, 1589), and used to investigate the effect of deep convection on aerosols in the region of the Indian subcontinent, using extensive observations available from the Indian Ocean Experiment (INDOEX). These studies revealed that deep convection is the major mechanism for removing aerosols originating on the Indian subcontinent from the boundary layer as they are advected toward the Equator. The aerosols subsequently modify the microphysical and radiative properties of upper-tropospheric clouds associated with deep convection.

PLANS FY01

Further studies using INDOEX data are planned. The Lipps-Hemler cloud system model will be used to evaluate cumulus parameterizations which have recently been developed for GCMs. Studies of the radiative properties of ice crystals in convective-system anvils will be used to refine the treatment of the interaction between clouds and radiation.

3.2.3 Moist Convective Turbulence

I. Held *O. Pauluis*

ACTIVITIES FY00

Analysis of the energy and entropy budgets of numerical models of radiative-convective equilibrium with explicit moist convection have led to several insights into the factors that control convective velocities and Convective Available Potential Energy (CAPE) in the tropical atmosphere. These results have led to the conclusion that: 1) a moist convecting atmosphere should be thought of as a dehumidifier, rather than as a heat engine; and 2) water vapor, not the dry air, performs most of the work in moist convection.

Surface fluxes provide energy to the atmosphere at the ground and radiative fluxes remove energy by cooling the troposphere. As the heating occurs at a warmer temperature than the cooling, entropy is lost and this reduction must be balanced in a statistically steady state by entropy production due to irreversible processes. If the dominant irreversible process is frictional dissipation of kinetic energy, one can estimate the magnitude of the kinetic energy generation, or the mechanical work performed by the atmosphere from the entropy production, as in the simplest heat engine. This is a good approximation for dry convection, but it overestimates the work performed by moist convection by an order of magnitude. In both 2-D and 3-D models of moist convection, it is found that the dominant irreversible sources of entropy are the diffusion of water vapor and the evaporation of condensate into unsaturated air. It can be argued that this is not simply a result within one particular model, but will be a property of any atmosphere in which the dominant mode of vertical energy transport is latent rather than sensible. Coupled with an earlier finding that the work performed by moist convection is primarily used to lift water and not to generate the kinetic energy of the flow (1689), this analysis implies that a theory for CAPE cannot be developed from the entropy and energy budgets alone.

An additional result emerging from this analysis is that the work performed by moist convection is primarily due to the expansion of the water vapor component of the air, despite the fact that the vapor is at most 2% of the atmosphere by weight. When air rises, the dry component expands and performs work, but most of this is cancelled during subsidence, the residual being dependent on the differences in temperature between upward and downward moving parcels. Water vapor also expands and performs work as it moves upward, but much of the vapor condenses, so there is much less cancellation during descent of the work performed during ascent. The implications of this result for our understanding of moist convective turbulence are currently being examined.

3.2.4 Prognostic Cloud Parameterization

ACTIVITIES FY00

3.2.4.1 Parameterization Development Efforts

S.A. Klein

The prognostic cloud parameterization previously incorporated into the FMS GCM has been further refined and its performance thoroughly diagnosed. The parameterization consists of a two species (cloud liquid and ice) bulk microphysics scheme coupled with a prognostic cloud fraction equation. Recent refinements include the incorporation of a physically based parameterization for the Bergeron process and a crude treatment of the plane parallel cloud albedo bias.

Initial climate simulations with this parameterization revealed significant differences with observations in the total amount of solar energy absorbed and the longwave radiation emitted by Earth. Consequently, two parameters of the cloud parameterization were adjusted until the global mean energy budget matched observations. The first parameter tuned is the threshold liquid cloud drop radius for which rain formation begins. The tuned value of the threshold radius, 7 μm, is significantly less than the observed values of 10-12 μm. This result is in common with a number of other GCMs using the same auto-conversion parameterization. The second parameter tuned is the fraction of condensed water in cumulus updrafts which becomes cloud condensate (the remaining portion becomes precipitation mass). For updrafts reaching the upper troposphere, 1% of condensed water becomes cloud condensate whereas for updrafts that only reach the lower troposphere this fraction is 50%. Although these precipitation efficiencies were tuned in the present application, in future work they will be predicted from the new cumulus convection parameterization (3.2.1) when it is coupled with this prognostic cloud parameterization.

With the tuned parameterization, the B-grid dynamical core of the FMS was integrated for 5 years over historically observed sea surface temperatures (SSTs). One field directly simulated by cloud parameterization, the amount of cloud liquid in a column of air per unit area or liquid water path (LWP), can be directly compared with satellite data, but only over oceans. An example of this is shown in Fig. 3.3, which compares the climatological mean liquid water path for the June-July-August season from the model simulation to two satellite derived observations. The cloud parameterization which, in general, has less than observed LWPs, simulates the maximums of midlatitude oceans and tropical convergence zones. However, the magnitude of the eastern tropical Pacific maximum is under-simulated by the model. This is a consequence of a very important model deficiency, namely the lack of marine stratocumulus in the eastern subtropical oceans.

Additional aspects of the cloud parameterization that can be compared to observations include the effective radius of liquid clouds, which is diagnosed in the model from the liquid water mass and an assumed number density of cloud droplets. Satellite observations suggest values of 9 to 12 μm for this parameter. However, the model's liquid cloud drop effective radii are diagnosed to be between 6 and 7 μm. This underestimate occurs

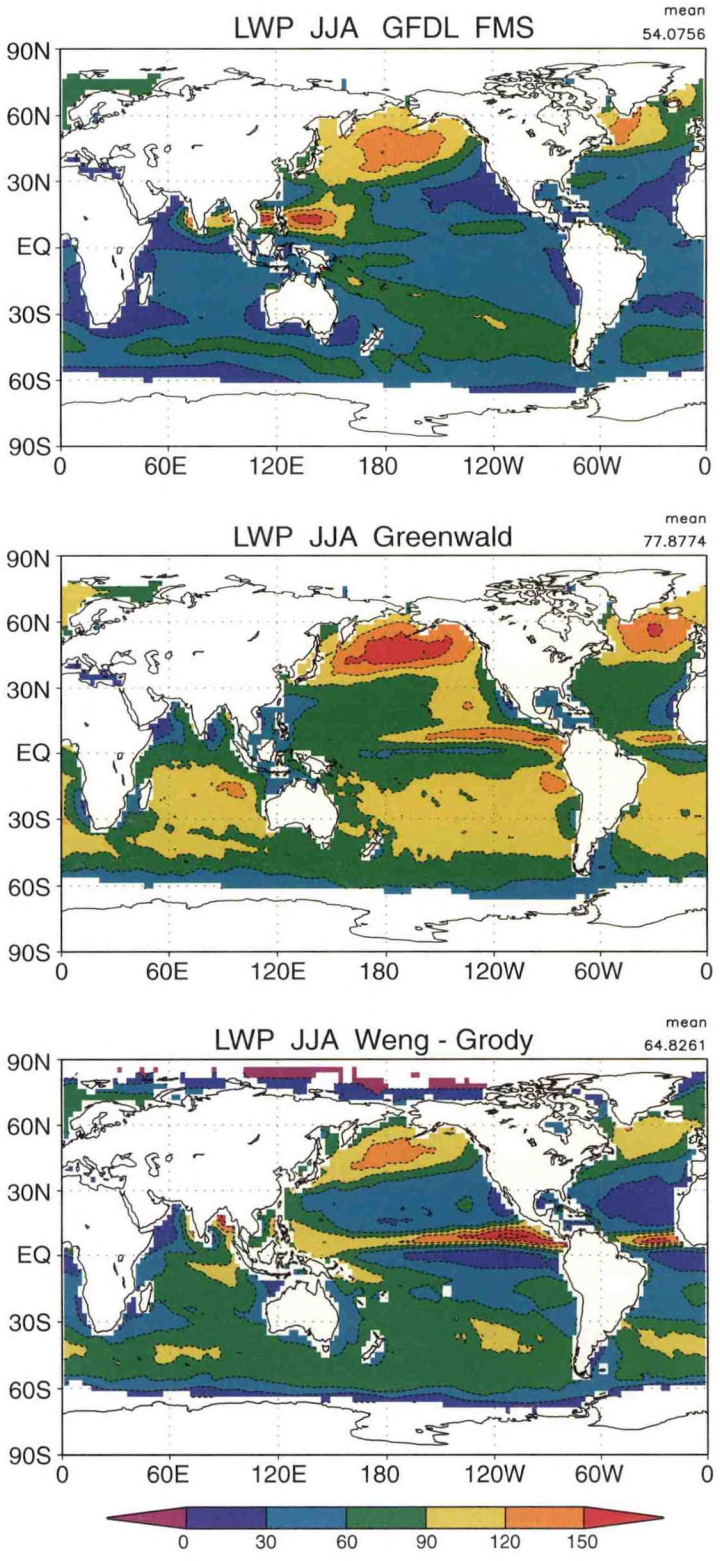

Fig. 3.3 The climatological mean liquid water path (g m^{-2}) for the June-July-August season from the FMS model with the prognostic cloud parameterization (top), and two satellite datasets (middle, bottom). Note how, despite underestimating the mean liquid water path, the FMS model qualitatively simulates the observed spatial pattern.

because the auto-conversion effectively limits the radii of the clouds to the threshold radius which is tuned to be 7 μm. This is considered an important deficiency of the cloud parameterization, as it limits the model's utility for simulating the indirect effect of aerosols on cloud properties.

Another aspect of the cloud parameterization that can be evaluated is the distribution of optical depths and cloud top pressures. Comparison of the model to satellite data reveals that at all height levels (low, medium, and high), the amount of optically thick cloud is overestimated by the model, whereas the amount of optically thin cloud is underestimated. The overestimate of cloud optical depths explains in part how the climatological radiation budget can be approximately correct with less than observed cloud amount.

If the parameterization is to be used for climate change simulations, it is important that cloud feedbacks be correctly simulated. One observed feedback is that for small increases in temperature, low cloud optical depths increase for cold clouds over land, but decrease for warmer land clouds and all oceanic clouds. Preliminary diagnosis of the temperature feedbacks of the model simulated low clouds indicates that the parameterization qualitatively reproduces this feature, despite the problems of the simulation which include a lack of marine stratocumulus clouds and cloud drop effective radii which are too small.

3.2.4.2 Diagnostic Assessment of the Simulation of Midlatitude Cloudiness

S.A. Klein *J.R. Norris*

The prognostic cloud parameterization in the FMS GCM was assessed by comparing simulated and observed cloud properties composited on 500-mb pressure vertical velocity over the summertime midlatitude North Pacific. The observed cloud properties that were used include daily Earth Radiation Budget Experiment (ERBE) cloud radiative forcing (CRF), daily NASA Water Vapor Project (NVAP) all-sky liquid water path (LWP), and 3-hourly International Satellite Cloud Climatology Project (ISCCP) cloud optical thickness and cloud top pressure. ECMWF and NCEP/NCAR reanalyses provided vertical velocity. Fig. 3.4 shows observed and simulated shortwave (SW), longwave (LW), and net (SW+LW) CRF as a function of midtropospheric vertical velocity. FMS overproduces SW and LW CRF under ascent conditions and underproduces LW CRF under subsidence conditions. FMS underproduces LWP for subsidence conditions, but this error is balanced by underproduction of cloud droplet effective radius to generate an superficially correct simulation of SW CRF. Comparison between observed and simulated frequency distributions of cloud optical thickness and cloud top pressure revealed that unlike observed cloudiness, FMS cloudiness has a bimodal distribution: large optical thickness clouds with tops in the upper troposphere and medium optical thickness clouds near the surface. FMS overproduction of SW and LW CRF in the ascent regime results from a frontal cloud shield that is too optically thick, high in the atmosphere, and horizontally extensive. FMS underproduction of LW CRF in the subsidence regime results from insufficient cloud cover. These and other errors in the relationship between meteorological processes and cloud properties need to be fixed to insure a reliable simulation of cloud feedbacks in the climate system.

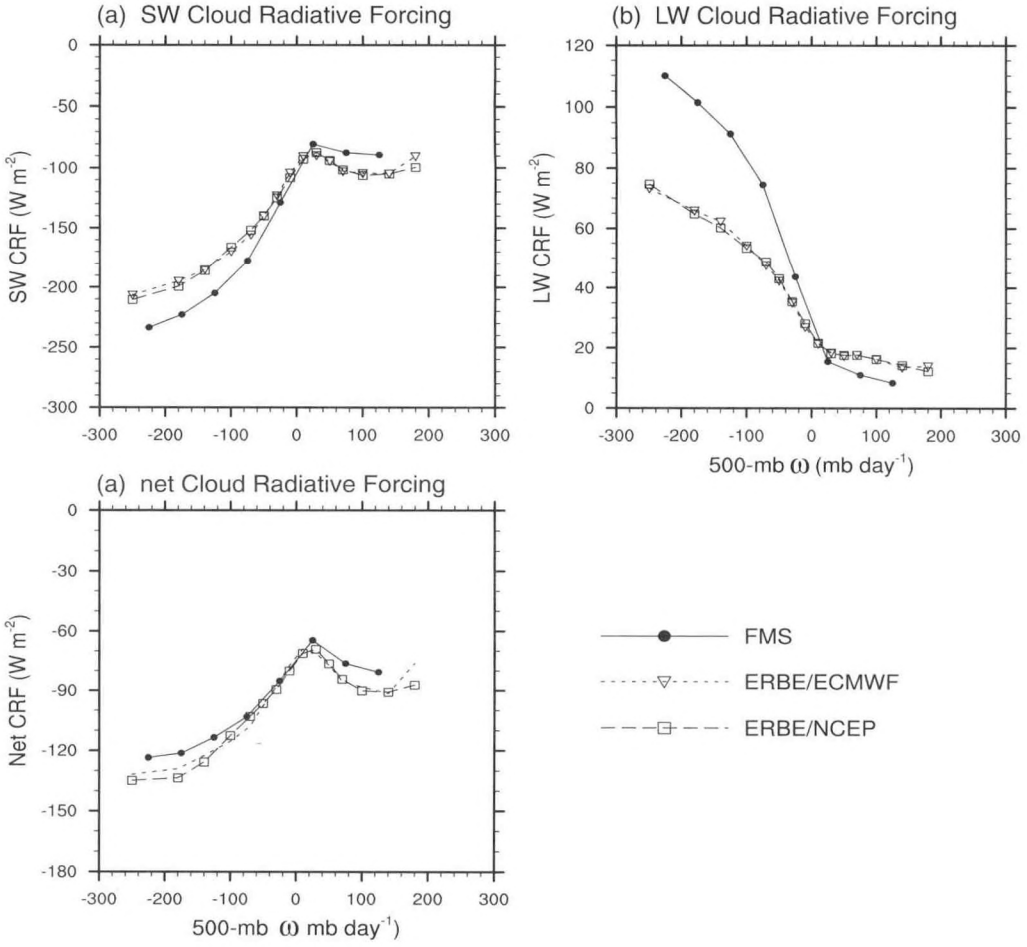

Fig. 3.4 FMS and observed daily mean shortwave, longwave, and net cloud radiative forcing as a function of midtropospheric vertical velocity over the midlatitude North Pacific during July. Note how the FMS model qualitatively simulates the observed relationship between cloud radiative forcing and vertical velocity.

PLANS FY01

Diagnosis of the cloud parameterization will continue. In particular, effort will be placed on diagnosing the reasons behind the qualitatively correct temperature dependence of low cloud optical depths.

3.3 ATMOSPHERIC CHEMISTRY AND TRANSPORT

ACTIVITIES FY00

3.3.1 Fast Photochemical Solver Development

*L. Horowitz** *W. Moxim*
H. Levy II *H. Rabitz**
*G. Li** *S.W. Wang**

**Princeton University*

A monomial preconditioning approach to constructing a fully equivalent operational model (FEOM) for chemical kinetics calculations in chemistry-transport models has been developed. This approach significantly reduces the off-line computational effort by expressing higher-order terms as linear combinations of the zeroth and first order correlated functions. A paper is in preparation.

In preparation for a future scalable supercomputer system and the incorporation of an on-line chemistry module from NCAR's "MOZART" (Model for Ozone and Related Chemical Tracers) model, the standard GFDL GCTM (Global Chemical Transport Model) was extensively re-coded. All internal input-output structure on the irregular Kurihara grid has been removed and the model now executes in CPU memory. In addition, any number of tracers can now be transported, dependent on memory and CPU speed.

A reduced form of the on-line chemistry module from NCAR's MOZART model is now being tested in a coupled CO, NOx, HNO_3, PAN, O_3 version of the GCTM. This will serve as the prototype development for the chemistry module that will be incorporated into the GFDL FMS for chemistry-climate studies.

3.3.2 Ship Emissions of NOx

*P.S. Kasibhatla** *W. Moxim*
H. Levy II

**Duke University*

GCTM simulations with and without global emissions of NOx from ocean shipping predict a significant enhancement over large regions, particularly over the northern latitude oceans. While these results are consistent with a recently published study, the resulting NOx and NOy levels are not consistent with recent measurements over the central North Atlantic Ocean and significantly exaggerate the apparent impact. Analysis suggests that the chemical evolution of ship plumes is not fully understood, and that the model's overestimate may also be due to a lack of plume dynamics and chemistry (1724).

3.3.3 Tropical South Atlantic Ocean Tropospheric Ozone Maximum

H. Levy II *W.J. Moxim*

Analysis of observed tropospheric column ozone (TCO) utilizing innovative satellite retrieval techniques has revealed the existence of a maximum TCO over the tropical South Atlantic Ocean (SAO) during September, corresponding to the time of maximum biomass burning in South America and Africa. As depicted in Fig. 3.5(a), the GFDL GCTM has successfully simulated this phenomenon.

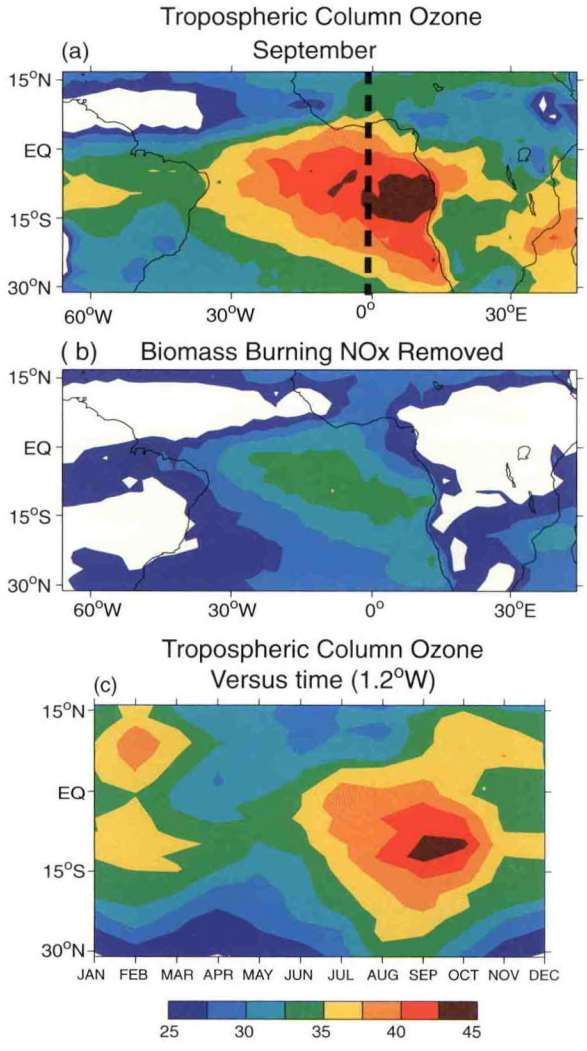

Fig. 3.5 Simulated tropospheric column ozone (TCO) in Dobson units. (a) TCO September maximum. Note that the largest values are located over the ocean distant from continental source regions. (b) TCO during September with biomass burning NOx removed from the photochemical system. A reduced oceanic maximum persists. (c) TCO monthly time series at 1.2°W (dashed line in the top figure). A general tropical maximum exists throughout the year with biomass burning enhanced values in September and February.

Initial speculation assumed that the TCO formation resulted from the emission of ozone precursors by agricultural biomass burning which were then advected from the continents to the ocean. GCTM results have shown that the maximum is produced by transport in the upper troposphere of ozone and reactive nitrogen (NOx) generated over the continents by both lightning and upward convective mixing of biomass burning products, followed by subsidence and chemical destruction of ozone in the boundary layer (1718). The dominance of lightning generated NOx (accounting for 49% of NOx over the SAO versus 36% for biomass burning) indicates a more reduced effect of human influence on tropical ozone pollution than was previously thought. To clarify this, an integration was run with the biomass burning source eliminated from the GCTM ozone photochemical system. Fig. 3.5(b) shows that even with biomass burning removed, there is still a TCO maximum isolated over the SAO. This suggests that a reduced TCO maximum existed in the SAO prior to the advent of agricultural burning, and man's influence results in an amplification of ozone pollution accumulation.

An examination of the TCO versus time (Fig. 3.5(c) from 30°S to 15°N along longitude 1.2°W (dashed line in Fig. 3.5(a)), reveals the seasonality in the SAO region. During the biomass burning dry season (July through October), there is a maximum located from the equator to 15°S, however, a general maximum is present over the SAO throughout the year, varying from less than 35 DU's in MAY to a high near 45 DU's in September. This implies that transport is acting to accumulate ozone in the SAO throughout the year and NOx from continental lightning and smaller sources provides an environment allowing chemical ozone production. An interesting secondary maximum occurs in February during the Southern Hemisphere wet season. This is a result of increased lightning and a smaller increase in biomass burning NOx transported southward from African agricultural burning north of the equator, which is depicted as a pocket of greater than 37.5 DU's at 5° to 10°N.

3.3.4 Asian Impacts on Regional and Global Air Quality

*G. Carmichael** *H. Levy II*
*M. Galanter*** *M.J. Phadnis***
*T. Holloway*** *J.J. Yienger**

**University of Iowa*
***Princeton University*

Currently, long-range transport of pollutants from Asia is known to significantly alter the composition of the remote Pacific troposphere, and there is growing observational evidence for an Asian impact extending to North America. The projected rapid increase in Asian industrialization and urbanization will lead to increased emissions of primary air pollutants, which are expected to increase tropospheric O_3 levels throughout much of the Northern Hemisphere.

GFDL/GCTM simulations find that, on average, while current Asian emissions already supply more than 20 ppbv of CO to the Northern Hemisphere, significant contributions (> 20 pptv) of NOx are only found over parts of the North Pacific and Indian Oceans. These same emissions also account for a 5-10 ppbv swath of O_3 in the boundary layer across the North Pacific, which extends to over half of the Northern Hemisphere in the middle troposphere. A

2020 "business-as-usual" emission scenario predicts that the average impact of Asian emissions on tropospheric O_3 will more than double.

Episodic trans-Pacific pollution events greatly exceed the average impact. The strongest Asian CO episodes over North America (NA), occurring most frequently between February and May, are often associated with disturbances that entrain pollution over eastern Asia and amplify over the western Pacific Ocean. With 55 ppb of Asian CO as a criteria for major events, 3-5 Asian pollution events analogous to those observed at Cheeka Peak, WA are expected in the BL all along the U.S. west coast between February and May during a typical year. In contrast to CO, Asia currently has a small impact on the magnitude and variability of background ozone arriving over NA from the west. Direct and indirect Asian contributions to episodic O_3 events over the western U.S. are generally in the 3-10 ppbv range. The two largest total O_3 events (> 60 ppbv), while having trajectories which pass over Asia, show negligible impact from Asian emissions. However, this may change. A future (~2020) emission scenario in which Asian NOx emissions increase by a factor of 4 from those in 1990 produces late spring ozone episodes at the surface of California with Asian contributions reaching 40 ppb. Such episodic contributions are certain to exacerbate local NA pollution events, especially in elevated areas more frequently exposed to free tropospheric and more heavily Asian-influenced air.

The role of nitric acid deposition in Asia relative to sulfate deposition has been explored with a regional Lagrangian chemical transport model, ATMOS, developed at the University of Iowa. Reactive nitrogen chemistry has been included in the model, with results compared with seasonal and annual deposition measurements. Sensitivity analyses have been conducted to test the model's response to variations in the rate of horizontal dispersion, the simulation of vertical transport, wet and dry deposition rates, chemical conversion rates, and emissions. Simulations from ATMOS are being used to construct a "source-receptor matrix" for the RAINS-Asia model (Regional Air Pollution Information System-Asia), a widely-used integrated assessment model for science and policy studies of regional air pollution in Asia.

3.3.5 GCM Simulation of Carbonaceous Aerosol Distribution

*W.F. Cooke** *V. Ramaswamy*
*P. Kasibhatla**

**Duke University*

The SKYHI simulation of global carbonaceous aerosol burden previously described (A99/P00) has been further analyzed. Comparisons at several locations indicate a reasonable agreement between the modeled and measured concentrations of this aerosol species (nv). The global column burdens of black and organic carbon are lower than in previous studies and can be regarded as approximately bracketing the lower end of the simulated anthropogenic burden due to these classes of aerosol. In addition to the comparison of the surface concentrations, several sensitivity tests were carried out. These included varying the time necessary for transformation of hydrophobic aerosol to hydrophilic aerosol, varying the fraction of aerosol that is emitted in the hydrophobic state and varying the wet deposition rate of the aerosol. The most sensitive parameters in the aerosol scheme, with respect to the column burden, are the wet deposition removal rate of the aerosol and the transformation rate

for hydrophobic to hydrophilic aerosol. An example of the ratio of the column burdens for the case where the transformation time is halved, as compared to the standard case, is shown in Fig. 3.6. In this case, one can see that the effect of halving the transformation time for

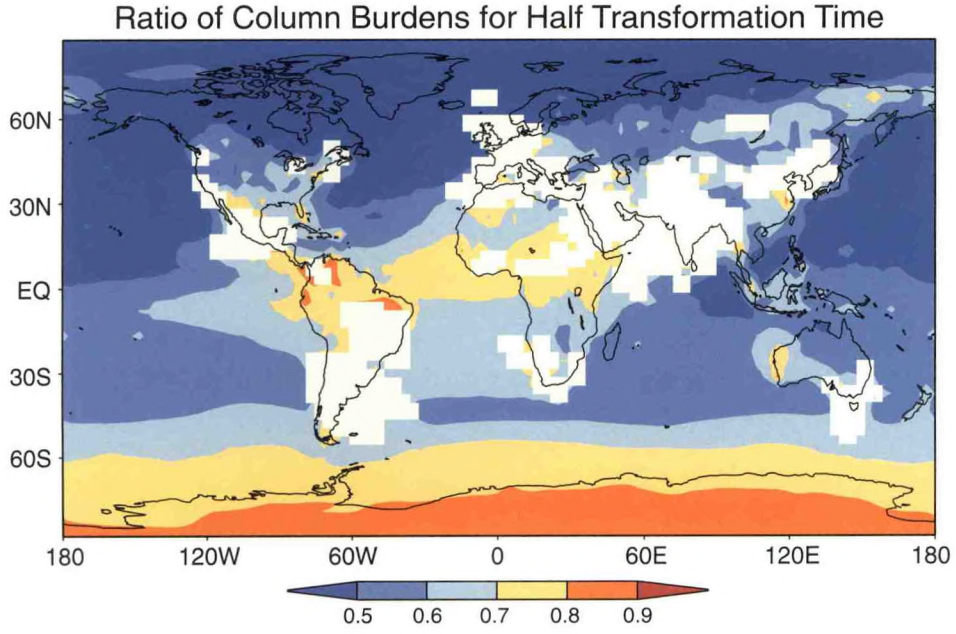

Fig. 3.6 Ratio of column burden of black carbon compared to standard distribution when the transformation time is halved. Although the global mean sensitivity is less than 25%, the regional effect can be much greater. Areas in white are where the changes are not significant at the 99% confidence level.

hydrophobic aerosol decreases the column burden of the aerosol. Although the sensitivity of the global mean column burden was less than 25% in the sensitivity tests, the regional effect can be much greater. However, as the parameter range considered for the tests here is somewhat generous, this range is likely an overestimate. In general, the most remote oceanic regions were the most sensitive to variations in the aerosol model parameters. Of the physical factors examined, the intensity and frequency of precipitation events are critical in governing the column burdens. Biases in the frequency of precipitation are likely the single biggest cause of discrepancies between simulation and observations.

The sensitivity of the mean and monthly variability in surface black carbon concentrations to halving of the wet deposition or halving of the transformation time from hydrophobic to hydrophilic state is examined in Fig. 3.7 at four different geographical locations. For reference, the results from the standard case and that from available observations are also illustrated. With respect to the standard case, the monthly mean burdens increase everywhere for a halving of the wet deposition. At Bondville, IL, which is close to sources, the maximum monthly increases are ~9% (occurs in May). At more remote locations, the monthly-mean increases are greater (range of increase at Sable Island is 11-17%, at Mace Head 24-44%, and at Mauna Loa 58-152%). These values may be compared with the global, annual-mean increase of 32%. Thus, the local and monthly sensitivities differ from that in the global, annual-mean. The modeled mean monthly values tend to show varying degrees of agreement with the available observations, with both deficiencies in the

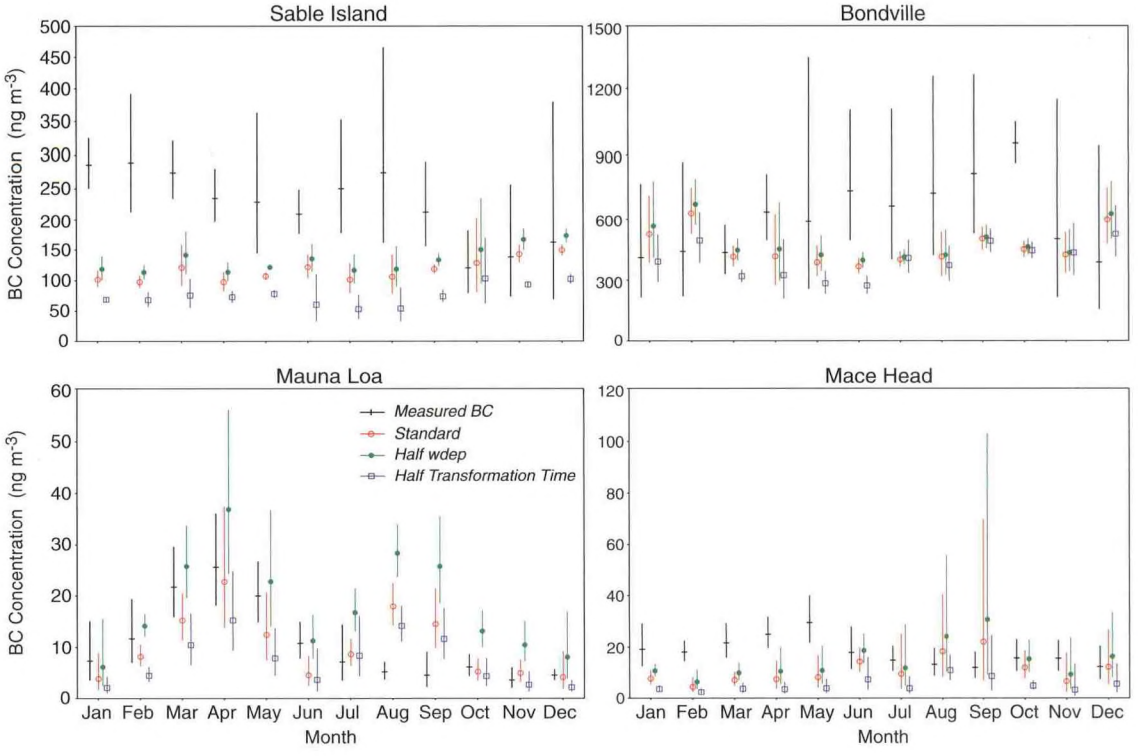

Fig. 3.7 Monthly-mean values and variability of the surface black carbon concentrations at Bondville (IL), Sable Island (Canada), Mace Head (Ireland) and Mauna Loa (HI). The standard simulation assumes a transformation timescale from hydrophobic to hydrophilic state of 1 day. Results of sensitivity tests with halving of the wet deposition and transformation time are displayed, together with the observed means and variability. There can be a substantial sensitivity of the mean and variability with respect to these parameters and considerable variation in the degree of agreement between model and observations. Both the mean and variability need to be evaluated in assessing the performance of the model.

transport and precipitation simulations playing important roles. At Sable Island and Bondville, the observed variability tends to be much greater than any of the three simulations (based on 3-year integrations in contrast to the observations, which at all sites exceed 3 years). Similarly, with respect to halving of the transformation time, while the global annual-mean burden is reduced by 25%, the monthly-mean changes in Bondville tend to be less. The sensitivity increases at the more distant locations, *e.g.*, there is a reduction of 20-50% at Sable Island, 40-61% at Mace Head and 3.5-49% at Mauna Loa. While halving the transformation time does tend to underestimate the surface concentration, it also reduces the overestimate of the variability in the monthly-means, especially at Mace Head. It is concluded that the transformation time is likely less than assumed in the standard simulation, with a value probably between 0.5 and 1 day.

PLANS FY01

The complex interactions between chemistry and transport that result in a Northern Hemisphere spring maximum in tropospheric O_3 will be explored quantitatively with the GCTM.

The relative contributions to tropospheric ozone from stratospheric ozone, ozone produced in the relatively clean troposphere, and ozone produced in the polluted boundary layer have been quantified. Global, regional, and local budgets are being constructed; and the mechanisms, both transport and chemical, by which present and future pollution impact tropospheric O_3 are being investigated.

GCTM simulations of NOx, CO, and O_3, employing present sources of CO and NOx and detailed estimates of future emissions, have been used to examine the present and future regional and global impacts, both average and episodic, of Asian emissions from fossil fuels, biofuels, and biomass burning. Specific goals include: quantifying the export of NOx, CO, and ozone from Asia's polluted BL to the free troposphere; investigating the impact of this export on the balance of ozone production and destruction over the Northern Hemisphere; quantifying the global air quality impacts resulting from the Indonesian fires in 1997; and quantifying the impact of Asian emissions on North America.

In collaboration with Princeton and Rutgers, the FEOM technique for chemical kinetics calculations will be expanded to include comprehensive atmospheric chemistry mechanisms in high-resolution global and regional simulations of tropospheric chemistry.

We will continue development of a reduced form of the on-line chemistry module from NCAR's MOZART model in a coupled CO, NOx, HNO_3, PAN, O_3 version of the GCTM.

A source-receptor matrix for reactive nitrogen oxides will be developed for the RAINS-Asia (Regional Acidification and Information Simulation - Asia) integrated assessment model, which will then be used to assess issues of future environmental policy in East Asia with a focus on China, Korea, and Japan.

The radiative forcing due to carbonaceous aerosol concentrations generated in the SKYHI GCM will be evaluated.

3.4 ATMOSPHERIC DYNAMICS AND CIRCULATION

3.4.1 Model Development

K. Hamilton *M.D. Schwarzkopf*
R. Hemler

ACTIVITIES FY00

The creation of Fortran 90 modules containing all of the model physics specific to a radiation time step (longwave, shortwave, astronomy, clouds, ozone, surface albedo) has been completed, and these modules may now be executed either within the SKYHI or FMS models or as a standalone program. Modification of these modules to include implementation options used by other research groups at GFDL is continuing, so that the new code within the FMS framework will be usable laboratory-wide.

Work is underway to convert additional physics modules previously run within the SKYHI model into Fortran 90 modules, so that they may be incorporated into the FMS.

Efforts to create a troposphere-stratosphere-mesosphere model based on the FMS are continuing. Physical and numerical parameterizations and techniques used in the existing SKYHI model, but which are not yet present in the FMS, are being examined to determine those essential features needed to produce an acceptable model climatology.

PLANS FY01

The remaining code which has been a part of SKYHI and which will be needed within the FMS will be converted to Fortran 90 modules and put in a form compliant with FMS standards. The major ongoing effort to improve the features of the FMS-based model climatology will continue. Higher horizontal resolution troposphere-stratosphere-mesosphere model experiments within the FMS will be integrated and assessed.

3.4.2 SKYHI Control Integrations and Basic Model Climatology

K. Hamilton *V. Ramaswamy*
R. Hemler *M.D. Schwarzkopf*
J.D. Mahlman *R.J. Wilson*

ACTIVITIES FY00

The extended 50 year control integration using the 40-level 3.6°x3.0° latitude-longitude version of the SKYHI model (A99/P00) has been completed. In contrast to a previous long control integration (1274), this calculation uses predicted clouds and the new longwave and shortwave radiation algorithms (1597, 1672). Improvements have also been made in the land and sea surface albedo formulations.

Results indicate the cloud climatology in the new integration is substantially more realistic than that of a corresponding simulation using prescribed clouds, although excessive cloudiness is simulated near the surface. The total cloudiness, outgoing longwave irradiances and reflected solar irradiances have been compared to ISCCP (International Satellite Cloud Climatology Project) cloud data and irradiances measured by ERBE. The interannual variability of the outgoing irradiances and the variances of temperature and moisture are greatly increased in the predicted-cloud simulation, despite the continuing constraint of specified climatological SSTs. A comparison between predicted-cloud and prescribed-cloud simulations has been completed (no).

A number of SKYHI control integrations were continued. Particularly noteworthy are a control integration with a 160-level, 1°x1.2° latitude-longitude resolution model that has now continued for 6 months, and another with an 80-level 2°x2.4° version that has run for 20 years. These represent extended model integrations with an unprecedented combination of fine horizontal and vertical resolution.

PLANS FY01

The climatology of the 3.6°x3.0° latitude-longitude simulation will be compared to that obtained using the FMS "Blue" model. Differences in the temperature and wind climatology will aid in the evaluation of the performance of the FMS model.

The results of the high-resolution integrations will be compared with available observations, including the high-resolution radiosonde data (3.4.9).

3.4.3 Spontaneous QBO-like Tropical Wind Oscillations in SKYHI Simulations

K.Hamilton *R.J. Wilson*
R. Hemler

ACTIVITIES FY00

As noted in A98/P99 and A99/P00, the SKYHI model, when run with at least 2°x2.4° horizontal resolution and 80 levels between the ground and 80 km, displays a very strong long-period oscillation in the equatorial zonal-mean circulation with some properties similar to those of the observed quasi-biennial oscillation (QBO). The integrations have been extended and additional analysis has been performed. One point emerging clearly is that the tropical mean flow oscillation is driven by eddy flux convergence associated with vertically-propagating waves. In fact, the wave forcing is typically 2-4 times larger than the realized mean flow accelerations, due to the countervailing effects of mean flow advection and parameterized diffusion. This conclusion is similar to that found in an earlier study that analyzed results from a lower resolution version of the SKYHI model that included an imposed QBO (1552). The waves responsible for the mean flow forcing in the equatorial atmosphere were found to have a rather broad spectrum in terms of both space and time scales.

PLANS FY01

The various high-resolution simulations will be analyzed in more detail.

3.4.4 Low-Frequency Variability of Simulated Stratospheric Circulation

K. Hamilton

ACTIVITIES FY00

As noted in A99/P00, long control integrations of the 40-level 3°x3.6° SKYHI model with prescribed climatological SSTs are found to display significant quasi-decadal variability in the Northern Hemisphere middle atmospheric circulation. Some of the integrations included nitrous oxide (N_2O) as a prognostic variable, and this has allowed an examination of the effects of the spontaneous dynamical variations on trace constituent concentrations in the stratosphere. Fig. 3.8 shows the time series of nitrous oxide mixing ratio for 25 consecutive December-February periods at the equator at 10 hPa in a control SKYHI simulation. The mixing

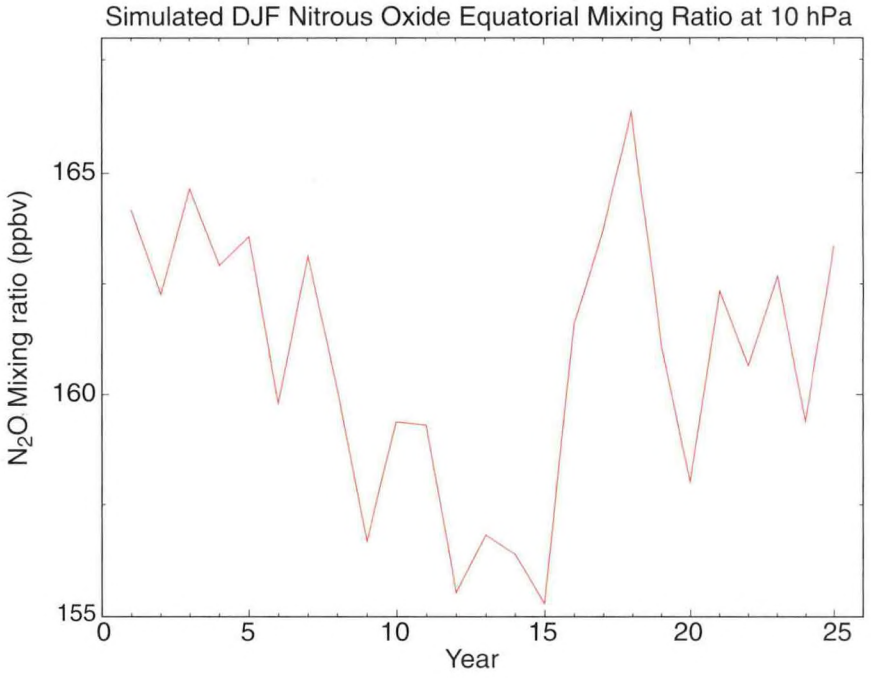

Fig. 3.8 Time series of the concentration of nitrous oxide at the equator at 10 hPa over 25 successive Boreal winters. The results are from a control simulation of the SKYHI model. Since the model includes no interannual variability in external forcing of the atmosphere or any variation in the chemistry used for the nitrous oxide, the apparent long-term trends are entirely caused by internal atmospheric transport variations. This suggests that even quite substantial decadal-scale trends in stratospheric composition, such as those seen during the 1990s in Upper Atmosphere Research Satellite (UARS) observations, may possibly be explained by natural variability.

ratio has some quasi-random year-to-year variability, but there also appears to be an overall trend, with the mixing ratio dropping by ~10% in the first 15 years and largely recovering over the last 10 years. The model has no interannual variation in the specified chemistry and no externally-forced dynamical variations. Thus, the large apparent trends seen in the figure must be caused by the transport effects of spontaneous internal dynamical variability within the model. The variations found in this model simulation are rather similar to those seen in stratospheric methane and water vapor mixing ratios in observations from the Upper Atmosphere Research Satellite (UARS) during the 1990s. The present model results suggest that natural variability may be a plausible explanation for these decadal-scale changes seen in stratospheric composition.

A review paper discussing observational and modelling issues related to interannual variability in the extratropical middle atmospheric circulation was written (Iv). Also, a contribution to an extensive review of biennial variability in the middle atmosphere (Is) was completed.

PLANS FY01

The detailed analysis of the simulated interannual variability will continue.

3.4.5 Horizontal Spectra from High-Resolution SKYHI Integrations

K. Hamilton *J.N. Koshyk**
R. Hemler *J.B. Mahlman*

**University of Toronto, Canada*

ACTIVITIES FY00

As noted in A99/P00, the 0.33°x0.4° version of SKYHI has been shown to produce a simulation of the horizontal kinetic energy spectrum in the troposphere that has a fairly abrupt transition to a shallow (close to -5/3) power-law behavior at wavelengths shorter than about 500 km, in good agreement with available observations. A detailed analysis of the spectral kinetic energy budget has been completed (ma).

Two new experiments were performed with the 0.33°x0.4° model to examine the spectral energy transfers in transient integrations. Each of the integrations started from an initial condition produced by computing a time-average of the control integration over about a day. This resulted in initial conditions that had energy levels in the mesoscale that were strongly suppressed relative to the control result. One integration used the standard version of the model. This produced a simulation in which the mesoscale energy was restored to the control value over a timescale of about 1/2 day, consistent with the earlier energy budget analysis (ma). The other integration used a model with the convective parametrization turned off. In this integration, the mesoscale energy also recovered, but only to within roughly a factor of 2-3 of that seen in the control run. This suggests that the subgrid-scale convection does play an important role in maintaining the mesoscale, but that even in the absence of the parameterized convection, the model would simulate a shallow mesoscale regime.

PLANS FY01

Work will continue to analyze the spectral budgets of potential energy and tracer variance in the high-resolution control and transient experiments.

3.4.6 Parameterized Gravity Wave Drag in the SKYHI Model

*M.J. Alexander** *K.Hamilton*
*L. Bruhwiler***

**Colorado Research Associates*
***Climate Monitoring and Diagnostics Laboratory/NOAA*

ACTIVITIES FY00

Work has continued towards incorporating a version of the Alexander-Dunkerton gravity wave drag parameterization scheme in the 3°x3.6°, 40-level version of SKYHI. The code has been rewritten to permit the drag to be calculated at intervals of several dynamical

timesteps, allowing a considerable saving of computational resources while not significantly degrading performance.

PLANS FY01

The work towards efficient implementation and appropriate tuning of the gravity wave scheme will continue. The scheme will also be implemented in the middle atmosphere versions of FMS.

3.4.7 GCM Simulations with an Imposed Tropical Quasi-biennial Oscillation

S.-M. Fan *K. Hamilton*

ACTIVITIES FY00

A 48-year integration of the SKYHI troposphere-stratosphere-mesosphere GCM was conducted with a version that included an imposed mean momentum source in the tropical stratosphere that forced a realistic quasi-biennial oscillation (QBO) in the winds and temperatures (1552). The model also included a simple treatment of the chemistry of nitrous oxide, and this allowed a study to be made of QBO effects on a long-lived trace constituent. The particular focus was on whether QBO-modulation of the upwelling through the tropical tropopause could affect the tropospheric concentration of important greenhouse gases, such as nitrous oxide and methane. Fig. 3.9 shows the rate of change of the simulated global-mean surface concentration of nitrous oxide, together with the zonal-mean equatorial zonal wind at 70 hPa over the last 45 years of the experiment. The wind timeseries clearly shows the effects of the imposed QBO. The nitrous oxide concentration also has a fairly clear QBO, although less regular than for the wind itself. The results show that the tropospheric inventory of nitrous oxide in the model is indeed systematically affected by the QBO modulation of transport. The predicted effects on nitrous oxide are probably too small to be measured with current observational networks, but a reasonable scaling of the model results for methane suggest that there should be a transport-driven QBO in tropospheric-mean methane concentration growth rates of the order of 1-2 ppbv/year. This should be detectable in the NOAA global air sampling flask network observations. The actual NOAA methane growth rate timeseries since 1983 does show a QBO variation of this size that is well correlated with the observed QBO in tropical lower stratospheric equatorial wind. While the QBO effect on methane growth rates is clearly only one component among several affecting the interannual variability, it is valuable to have a clear explanation for at least part of the variations seen in the tropospheric methane record. A paper describing these results was completed (mp).

PLANS FY01

A version of the SKYHI model is being integrated with a momentum source designed to force the tropical stratospheric zonal-mean zonal winds to agreement with the detailed time series of observed winds during the period 1989-1995. The results of these simulations will be used to study the effects of the tropical zonal-mean QBO on other aspects of the circulation. In particular, the three-dimensional structure of the stationary wave field in the model

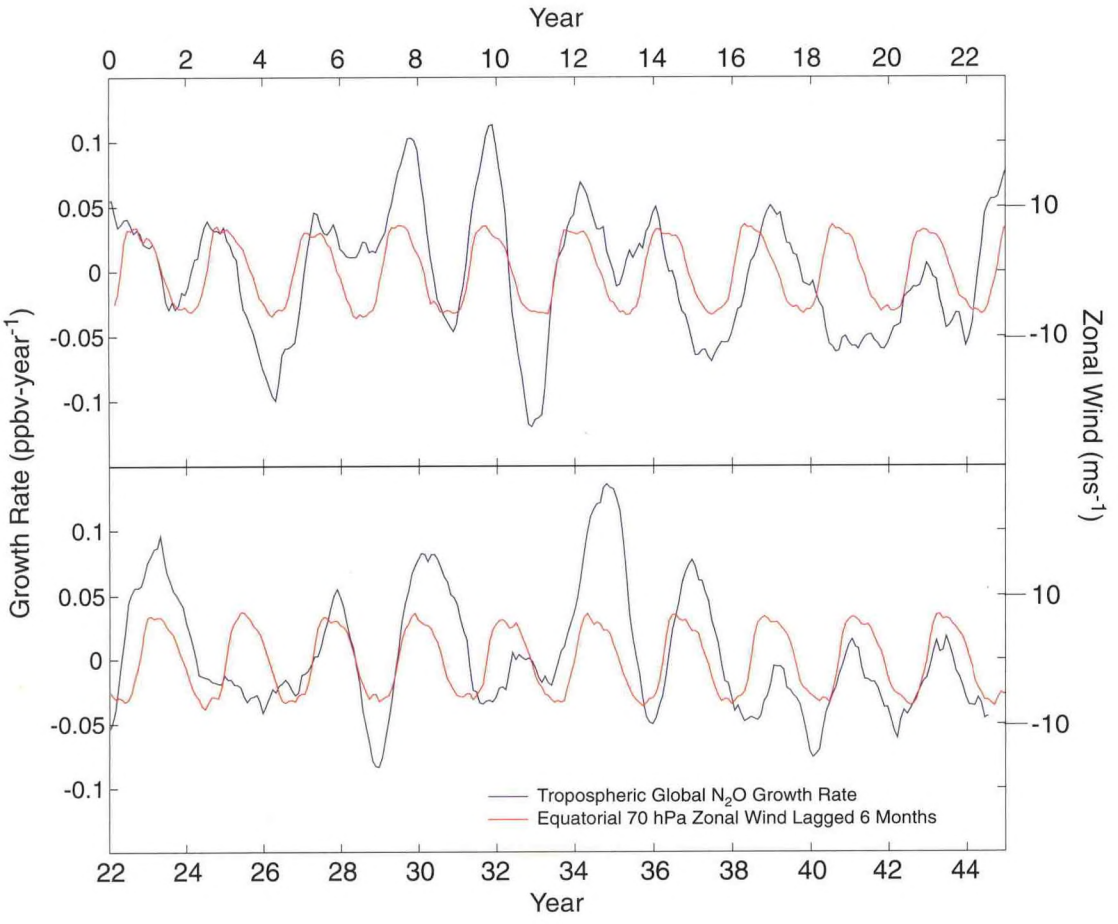

Fig. 3.9 The time series of zonal-mean zonal wind in the lower stratosphere at the equator (red) and the rate of change of global-mean surface nitrous oxide concentration (blue). Results are from the last 45 years of a long integration of the SKYHI model with an imposed quasi-biennial oscillation (QBO) in the tropical stratosphere. The wind time series plotted is lagged 6 months. The clear positive correlation between these two curves shows the effects of QBO modulation of transport on the tropospheric inventory of long-lived trace constituents. The effect is probably too small to be detected in the available nitrous oxide observations, but the same effect does appear to cause QBO variations seen in observations of the global-mean surface methane mixing ratio.

simulation will be compared in detail with the extensive wind observations taken during 1991-1995 by the Doppler radiometer instrument on the UARS.

3.4.8 Observational Study of Gravity Wave Climatology

H. Bjornnsson K. Hamilton

ACTIVITIES FY00

Collaborative work has continued on a World Climate Research Programme (WCRP) project to establish a gravity wave climatology for the lower stratosphere based on operational high-resolution radiosonde data. Data from a year of high-resolution wind and temperature soundings at Keflavik (64°N, 23°W) were obtained from the Icelandic Meteorological Service and were analyzed to determine the energy densities and dominant directions of propagation for gravity waves in the lower stratosphere. The results have been included in the worldwide climatology project along with those from almost 200 additional stations. An example of the information available is shown in Fig. 3.10. This compares

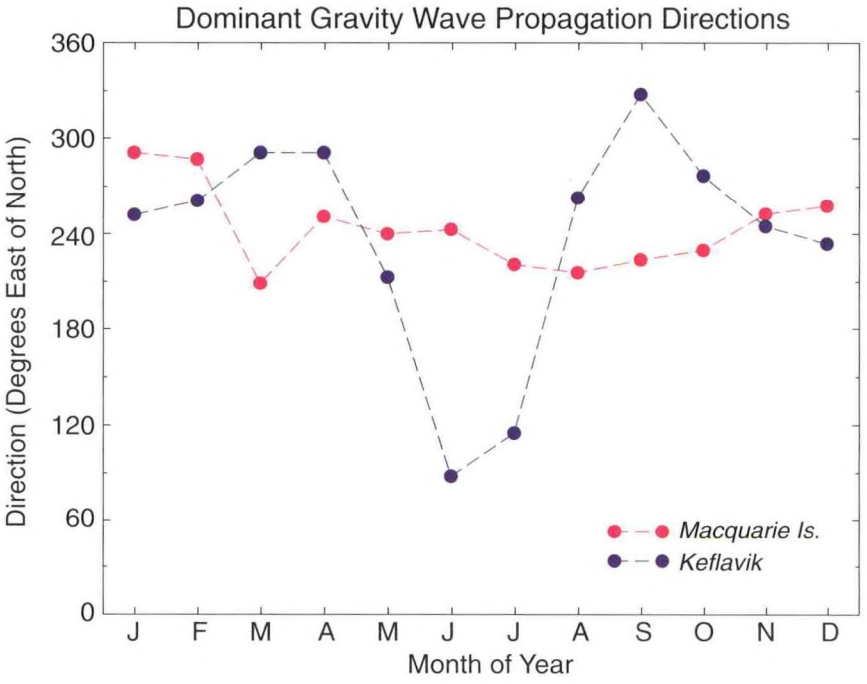

Fig. 3.10 The dominant horizontal direction of propagation for gravity waves in the lower stratosphere determined for each month of the year from an analysis of wind and temperature fluctuations in twice-daily radiosonde data. Results are shown for Keflavik (64°N, 23°W) and Macquarie (55°S, 159°E) and are expressed as an angle east of north (*i.e.*, 0° is northward, 90° eastward, 180° southward, and 270° westward). The waves at Macquarie are directed westward throughout the year, while the waves ar Keflavik are roughly westward in most of the year, but eastward in June and July. The weaker annual variation at Macquarie likely reflects a smaller seasonal signal in the mean wind at high southern latitudes than in the North Atlantic.

the dominant horizontal direction of propagation in each month of the year as determined at Keflavik and at Macquarie (55°S, 159°E), another high latitude station, but in the Southern Hemisphere. At Macquarie, the dominant wave propagation directions have a strong westward component throughout the year, while at Keflavik the waves propagate eastward

in June and July. The very different behaviors seen in the figure at the two stations probably reflect the contrast in the annual cycles of the large-scale mean flow at each location.

PLANS FY01

The analysis of worldwide high-resolution radiosonde data will continue in collaboration with the other participants in the WCRP study.

3.4.9 Dynamics of the Martian Atmosphere

R.J. Wilson

ACTIVITIES FY00

Recent results from the Mars Global Surveyor (MGS) Thermal Emission Spectrometer (TES) instrument have indicated the presence of a prominent tropical water ice belt during the relatively cold aphelion season which corresponds to the Northern Hemisphere summer. A description of water ice clouds has been included in the Mars general circulation model (MGCM) to assess the possible influence of ice clouds on the vertical distribution of dust aerosol for both the present and past Mars climates. Cloud formation is governed by a microphysics scheme based on a set of moment continuity equations (1713). The radiative effects of ice deposition on dust nuclei and the enhanced particle sedimentation velocity are also accounted for. A comparison of the simulated tropical cloud belt with the MGS TES observations indicates good agreement in the seasonal and latitudinal extent of the cloud belt. Simulated cloud opacity and particle sizes appear to be consistent with the data. Further analysis of the MGS data should permit comparisons with the vertical extent of the simulated clouds and aerosol.

Thermal tides play a much more prominent role in the martian atmosphere than in the terrestrial atmosphere and an accounting for diurnal variability is an important aspect of interpreting and comparing spacecraft observations with MGCM results. The amplitude and structure of the diurnal temperature variation is strongly dependent on the atmospheric dust opacity and the state of the zonal mean circulation (1709). The tides include westward propagating, sun-synchronous (migrating) waves driven in response to solar heating and additional non-migrating eastward and westward propagating waves resulting from zonal variations in the thermotidal forcing, most notably associated with high amplitude topography. Temperature profiles derived from MGS radio science occultations have revealed large amplitude tropical waves in the lower atmosphere that MGCM simulations suggest are thermal tides that are strongly modulated by topography. An observed large amplitude density variation in the Mars thermosphere (~130 km) has recently been identified as a diurnal period, eastward propagating Kelvin wave excited by the scattering of the migrating tide off the wavenumber 2 component of topography. Such a wave is predicted to extend from the surface to thermosphere heights with little variation in phase. This result is consistent with Viking lander surface pressure data and TES lower atmosphere temperature data.

PLANS FY01

The physics routines in the current Mars GCM will be ported to FMS and will provide an additional test of the robustness and flexibility of the new modeling system. In particular, the impact of various new tracer transport schemes on aerosol and water vapor will be examined. The Mars atmosphere also represents an opportunity to study different representations of boundary layer mixing. Further analysis of the interaction of thermal tides with topography will be carried out with an emphasis on the character of the diurnally-varying winds.

3.5 CLIMATIC EFFECTS DUE TO ATMOSPHERIC SPECIES

3.5.1 Lower Stratospheric Ozone and Temperature Trends

*M-L. Chanin** *J.D. Mahlman*
*M. Gelman*** *V. Ramaswamy*
*J-J.R. Lin*** *M.D. Schwarzkopf*

**CNRS, France*
***Aeronomy Laboratory/NOAA*

ACTIVITIES FY00

Subsequent to the compilation of a review paper on the temperature trends in the lower stratosphere (kp), it has been found that the vertical profile of cooling in the stratosphere over the 1979-1994 period in various regions closely follows that found for the 45°N region. Comparisons of temperature trends in the stratosphere, made available by the different observational platforms, has continued with the focus shifting to the seasonal trends at particular latitude zones. It is found that, as in the case of the annual-mean (A99/P00), it is the midlatitude Northern Hemisphere locations that exhibit statistically significant cooling. Other regions, such as the high latitudes in both hemispheres, as well as the tropics exhibit a lack of coherence amongst the various datasets, with the exception of the Antarctic springtime cooling. The high latitudes in the Northern Hemisphere exhibit large cooling in winter-spring, but this fails to meet statistical significance.

PLANS FY01

The temperature trend estimates from the various observing platforms will be updated, accounting for the period through the year 2000. Model-simulated temperature changes due to the observed ozone and other trace gas changes will be further analyzed, and compared with observed temperature trend estimates.

3.5.2 Radiative Forcing Due to Ozone

V. Ramaswamy *S. Solomon**
**Aeronomy Laboratory/NOAA*

ACTIVITIES FY00

As part of the IPCC (2001) assessment, the radiative forcing due to stratospheric ozone has been estimated to be -0.15 W/m^2 +/- 0.1 W/m^2. The level of confidence has advanced to the point where the confidence ranking is assigned as medium. This is, however, still well below the high confidence level accorded to the well-mixed greenhouse gases. Note that a rank of medium has also been assigned to the tropospheric ozone radiative forcing.

PLANS FY01

The seasonal temperature trends due to stratospheric ozone will be analyzed further. Temperature responses obtained using SKYHI simulations employing the observed trace gas concentrations will be compared with available temperature trends in low, middle, and high latitudes.

3.5.3 Radiative Effects of Aerosol-Cloud Interactions

C. Erlick *L.M. Russell**
V. Ramaswamy

**Dept. of Chemical Engineering, Princeton University*

ACTIVITIES FY00

In a study combining a size- and composition-resolved aerosol and cloud microphysical model with GFDL's solar radiation algorithm, it was found that microphysical changes in cloud drop distribution and composition from aerosol pollution can cause a substantive increase in cloud albedo and in absorption of solar radiation both above- and in-cloud (A99/P00). That study has been extended to include sensitivity experiments with respect to updraft velocity, updraft area fraction, particle dilution, and large particle composition. The sensitivity experiments show that cloud albedo is most strongly influenced by changes in updraft area fraction, where an increase in updraft fraction from 45% to 65% results in a 10-25% increase in cloud albedo. The albedo is also significantly influenced by particle dilution, where a 90% dilution in ship emissions reduces the albedo of a ship track by 13-18%. The modeled cloud and ship track albedos have been compared with Meteorological Research Flight (MRF) C-130 aircraft measurements from the Monterey Area Ship Track Experiment as a function of air parcel dilution, showing good agreement within the estimated uncertainties in both values (jz).

The aerosol-induced changes in cloud single-scattering albedo (ssa) predicted using the above modeling framework have been incorporated into GFDL's radiative-convective model (using the Fickian diffusion scheme) to investigate the effects of solar cloud absorption

on the surface temperature and lapse rate. When low clouds (between 890 and 660 mb) are perturbed, the surface and atmosphere remain coupled. In this case, as solar cloud absorption increases (as the ssa decreases), the surface temperature increases, with the lapse rate becoming less steep. However, no temperature inversion forms because the maximum in solar heating from the low clouds lies at or below the 3 km maximum in atmospheric emission, and the greenhouse effect prevents the formation of an inversion. The same is true if the low cloud optical depth is increased 10 times to a value of ~45. In this case, the increase in optical depth causes an overall reduction in atmospheric and surface temperature (by 20K) and a slight stabilization of the atmosphere, but no temperature inversion forms despite the increase in solar heating. When all clouds are perturbed simultaneously, distributing the perturbation in solar absorption to higher altitudes, the surface and atmosphere remain coupled down to a cloud ssa of 0.6. Only at this low value, which is unrealistic even for polluted clouds (where the minimum expected ssa is ~0.99), the atmosphere and surface decouple and a very low-lying temperature inversion forms. Here, much of the incident solar radiation is absorbed at a higher altitude and the greenhouse effect is too weak to compensate for the surface cooling.

It is found that the changes in surface temperature and lapse rate are diminished when humidity feedback is turned off. The changes in surface temperature and TOA forcing from increases in solar absorption differ considerably from those due to a doubling of CO_2 or a 4% increase in the solar constant.

PLANS FY01

Using the aerosol microphysical model, a study investigating the definition of clear sky with respect to water vapor and aerosol content in computations of solar cloud forcing will be conducted. In the radiative-convective model (RCM), a closer investigation of the difference between the Fickian diffusion and convective-adjustment schemes with respect to surface energy balance will be completed. A similar study looking at the effects of changes in solar cloud absorption and optical depth in the framework of GFDL's SKYHI GCM will be continued, focusing on changes in cloud amount as well as temperature.

3.5.4 Radiative Effects Due to Pinatubo Stratospheric Aerosols

3.5.4.1 Experiments Using the SKYHI GCM

S.M. Freidenreich *A. Robock***
*S. Ramachandran** *M.D. Schwarzkopf*
V. Ramaswamy *G. Stenchikov***

**Physical Research Laboratory, Ahmedabad, India*
***Rutgers University*

ACTIVITIES FY00

Using an updated, comprehensive monthly- and -zonal mean spectral optical properties dataset, the aerosol radiative forcing and stratospheric thermal response of the SKYHI GCM to the Mt. Pinatubo volcanic eruption was investigated (mf). This study was

performed using an ensemble of four 2-year SKYHI integrations. Another set of four ensemble runs has been completed for the purpose of investigating the tropospheric climate response to Pinatubo aerosols. Preliminary analysis of surface temperature anomalies in DJF 1991-1992 show areas of warming of up to 2 K over Eurasia and cooling of 1 K over the Middle East. Calculations have confirmed that the near-IR solar forcing due to Pinatubo aerosols contributes substantially to the total stratospheric heating.

PLANS FY01

It is further planned to study the radiative and dynamic responses in the climate system by increasing the aerosol perturbation to 10 and 100 times that of Pinatubo. These experiments are intended to isolate the mechanisms by which large natural forcings affect climate. An experiment which accounts for only the longwave effects of aerosols will also be conducted.

3.5.4.2 Coupled Climate GCM Simulations of Mt. Pinatubo Effects

*A. Robock** *B. Soden*
*G.Stenchikov** *R. Wetherald*

**Rutgers University*

ACTIVITIES FY00

A series of GCM experiments have been performed using a coupled ocean-atmosphere GCM (A99/P00, 1.1) with prescribed (seasonally-varying) cloud cover, fixed cloud optical properties, and specified stratospheric aerosol properties. The radiative effects of the aerosols were incorporated using observed aerosol optical properties specified as a function of latitude and time, beginning with the June 1991 eruption and extending for a 4-year period. The radiative anomalies predicted by the GCM were then compared to those observed from the ERBE for the same 4-year period. Since cloud cover and optical properties are prescribed in the model, the GCM simulations contain only the direct radiative effects of the aerosols, whereas the ERBE observations contain both direct and any indirect effects which may have also occurred.

The magnitude and evolution of shortwave and longwave radiative anomalies in the GCM exhibit excellent agreement with the ERBE observed anomalies. Both the model and observations show peak anomalies of ~6 W/m^2 over the tropics for ~6 months, which then slowly decay and drift towards higher latitudes. The similarity between the observed and model-simulated anomalies suggests that, at least for the case of Mt. Pinatubo, the direct radiative effect of the aerosols dominates over any indirect effects. Some regions and periods do show residual differences of 1-2 W/m^2 between the model and observations which may be attributable to indirect effects or natural variability in cloud cover. Discrepancies may also arise due to uncertainties in the prescribed aerosol optical properties (which are estimated to be ~15%). Nevertheless, even with these uncertainties, the comparison of observations and model simulations with Mt. Pinatubo aerosols offers a useful global experiment for bounding the uncertainty of indirect radiative forcing by aerosols in the upper troposphere.

PLANS FY01

Future efforts will focus on evaluating the temperature and moisture responses of the GCM simulations in comparison to the observed changes, and assessing the importance of water vapor feedback in modifying the global surface cooling that resulted from the Pinatubo eruption.

3.5.5 Radiative Forcing Due to Changes in Stratospheric Ozone

V. Ramaswamy M.D. Schwarzkopf

ACTIVITIES FY00

A study of the climatic effects of the observed changes in stratospheric ozone during the 1979-1997 period has been completed. The ozone trends dataset, derived from SAGE and TOMS satellite data[1], was provided by W. Randel. Two 10-year SKYHI calculations were performed using the model version discussed earlier (3.4.2). In the first simulation, the ozone concentrations are the climatological model ozone values plus the Randel ozone trend, but with carbon dioxide (CO_2), methane (CH_4), nitrous oxide (N_2O), and halocarbon concentrations fixed at 1980 levels. The second simulation uses the same ozone concentrations, but with the greenhouse gas (CO_2, CH_4, N_2O, and halocarbon) concentrations fixed at 1997 levels.

Results indicate that ozone decreases and greenhouse gas increases both play major roles in determining the overall pattern of stratospheric temperature change during the last two decades. Fig. 3.11 displays the annual-mean, zonal-mean temperature changes between the two perturbation simulations and the control simulation with climatological ozone concentrations and 1980 greenhouse gas concentrations. Regions with statistical significance at the 99% level are also shown. Substantial (4-6K) temperature decreases, primarily due to the greenhouse gas increases, are predicted for pressures near 1 hPa. Temperature decreases of ~2-3K (which are statistically significant in the Northern Hemisphere autumn and winter) are found in the Antarctic lower stratosphere (20-100 hPa), mostly due to the observed ozone loss. The tropical (30°N-30°S) region between 5-10 hPa shows a small temperature decrease, with substantial cancellation between positive temperature change due to ozone and negative temperature change due to the greenhouse gases. The annual-mean, zonal-mean pattern of temperature change is similar to observed stratospheric temperature trends (1631); the simulation with the greenhouse gas and ozone perturbations appears closer to the observations in tropical latitudes. Both simulations give substantially different results from the previous simulation (A93/P94; 1394) in which ozone change was restricted to the region below ~30 km.

---

1. Randel, W.J., and F. Wu, A stratospheric ozone trends data set for global modeling studies. *Geophys. Res. Lett.*, 26, 3089-3092, 1996.

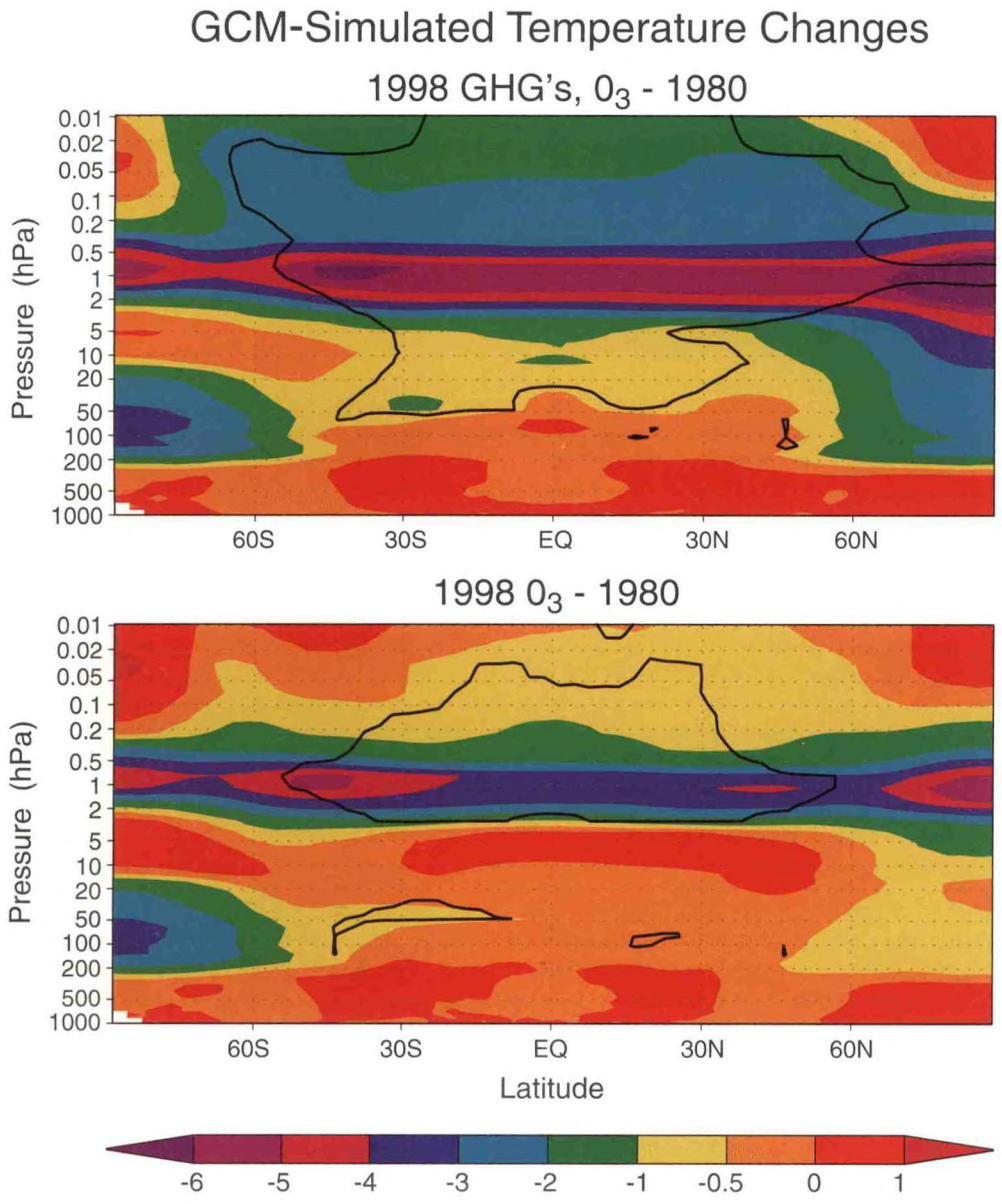

Fig. 3.11 The annual-mean, zonal-mean temperature change between the control simulation and the simulation with 1998 values of well-mixed greenhouse gases and ozone (top), and between the control simulation and the simulation with 1980 greenhouse gas concentrations, but 1998 ozone values (bottom). The regions within the black line have a statistical significance of 99%. Results indicate that changes in both ozone and greenhouse gas concentrations are important in determining the pattern of temperature response.

PLANS FY01

A simulation including the effects of the observed stratospheric water vapor change, together with the above changes in ozone and greenhouse gases will be completed. Analyses of the water vapor simulation and of the two ozone simulations will improve the understanding of the relative importance of changes in each of the radiatively active gases in determining the observed stratospheric temperature change.

4. EXPERIMENTAL PREDICTION

GOALS

To develop methods of stochastic-dynamic prediction capable of extracting as much useful forecast information as possible from numerical prediction models given imperfectly observed initial conditions.

To develop and improve numerical models of the atmosphere-ocean-land system in order to produce useful forecasts with lead times of several weeks, months, seasons or years.

To understand the limits of predictability of the ocean-atmosphere system with emphasis on quantifying the amount of useful forecast information that could be available at lead times of several weeks, months, seasons or years.

To develop methods for the assimilation of observations into dynamical models in order to improve predictions of the ocean and atmosphere.

4.1 ATMOSPHERIC AND OCEANIC PREDICTION AND PREDICTABILITY

ACTIVITIES FY00

4.1.1 Ocean Model Development for Seasonal/Interannual Prediction

S. Griffies *A. Rosati*
M. Harrison

The advent of more powerful computers will permit the next generation of ocean climate models to have a grid resolution necessary for studies of seasonal-to-interannual prediction. Consequently, over the past year the ocean model development efforts of the Climate Dynamics group have been closely coordinated with members of the Experimental Prediction group. The past year has seen prototype studies of ocean grid resolution and ocean parameterizations which are useful to both groups. Most notably, such work expands the domain of the experimental prediction group's ocean model into the Arctic.

This development work represents part of a multi-year effort aimed at enhancing the realism of GFDL's ocean simulations (1535, 1536, 1676). In particular, this new ocean model will facilitate study of longer term phenomena, such as decadal fluctuations of ENSO and variations in the thermohaline circulation.

4.1.2 Coupled Model Development for Seasonal/Interannual Prediction

J. Anderson *A. Rosati*
C.T. Gordon *J. Sirutis*
S. Griffies *R. Smith*
R. Gudgel *W. Stern*
S. Klein *M. Winton*
M. Harrison *B. Wyman*
J. Ploshay

A new coupled model to be used for seasonal/interannual forecasting is under development. The configuration of the atmospheric component has not yet been determined. However, using Bombay release versions of the Flexible Modeling System (FMS) (1.3.3), an atmospheric model has been assembled with the following features: N45L18 B-grid dynamical core, 4th-order advection, Klein predicted clouds (3.2.4), diurnal variation of radiation, and RAS (Relaxed Arakawa Schubert) convection. The ocean component is MOM3 and is also used as the base model for a comparison project with the International Research Institute for Climate Prediction/Applied Research Centers (IRI/ARCS). This model is nearly global (no Arctic Ocean) with one degree resolution increasing to one-third degree meridional resolution within ten degrees north and south of the equator. The vertical resolution is 40 levels with a constant 10 m resolution to 200 m. The physical parameterizations include K-Profile Parameterization (KPP) vertical mixing, Smagorinsky viscosity (1720), Gent-McWilliams (GM) diffusion for horizontal mixing (1536), and an explicit free surface. The coupling between component models uses the FMS coupling framework (1.1.3). Modifications to pass fluxes to MOM and sea surface temperatures (SSTs) to the atmosphere, required because MOM3 is not a compliant FMS component model, have been completed. Preliminary coupled forecast experiments using this system are being run, although only rudimentary tuning has been done. Early indications are that the mechanics of the coupling are working, although considerable tuning will be required to produce acceptable simulations and predictions.

4.1.3 Statistical Atmospheric Model Development

M. Harrison *A. Rosati*

A statistically-based atmospheric model has been developed using SST anomalies as predictors and ocean surface fluxes of heat, momentum, and freshwater as predictands. The model was initially developed using the National Centers for Environmental Prediction (NCEP) and European Centre for Medium Range Weather Forecasting (ECMWF) Reanalyses and the GFDL Atmospheric Model Intercomparison Project (AMIP) 2 model used for seasonal to interannual prediction. The model is capable of generating sustained oscillations when coupled with an ocean model without additional tuning. Considerable differences have been observed between atmospheric products (1624, na); for instance, the statistical version of the ECMWF Reanalysis model yielded sustained coupled oscillations, while the GFDL statistical model was highly damped when coupled to the ocean model. Subcriticality in the coupling between atmosphere and ocean resulted in diminished forecast skill, as measured by Niñ o3 SST correlation and RMS error.

4.1.4 Sensitivity to Horizontal and Vertical Resolution in Atmospheric Models

C.T. Gordon *J. Sirutis*
R. Gudgel *W. Stern*
A. Rosati *B. Wyman*

The impact of vertical and horizontal resolution in the B-grid atmospheric model (1.2.4) is under investigation in an attempt to determine the required resolution for improved coupled predictions. Initial results are focusing on the quality of simulations of basic atmospheric quantities. As an example, Fig. 4.1 shows the 1980-1981 mean winter and summer zonal jets from the NCEP reanalysis, and corresponding 2-year integrations from N45L18, N45L30, and N90L18 model simulations. Evaluation of many additional diagnostic quantities, aided by the capabilities of the GFDL web-based diagnostic facility (6.4) will determine the most cost-effective resolution.

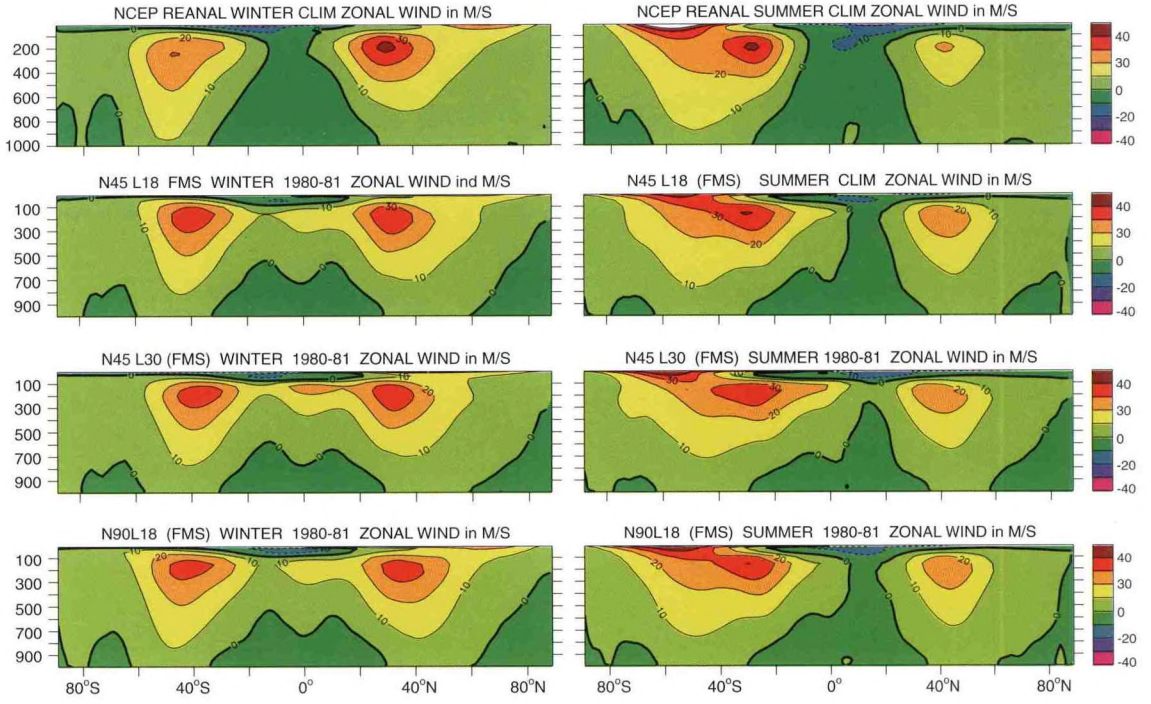

Fig. 4.1 Mean zonal wind values in m sec^{-1} averaged for 1980-1981 time for December-January-February (left) and June-July-August (right). From top to bottom are the NCEP Reanalysis, an N45L18, an N45L30, and an N90L18 model simulation to demonstrate impacts of model resolution.

4.1.5 Impact of Land and Ocean Low-Level Tropical Clouds on ENSO Prediction

C.T. Gordon *A. Rosati*
R. Gudgel

The role of tropical land and ocean low-level clouds in the ability of a coupled atmospheric-ocean general circulation model (AOGCM) to predict ENSO has been studied (nl) through a set of ten 12-month model integrations. In the tropics, a strong bias in a GFDL

Experimental Prediction AOGCM is evident in the western tropical Pacific, where overly strong convection diminishes the SST warm pool, reducing the east-west SST gradient, and effectively weakening the trade winds. This bias is exacerbated by the poor simulation of tropical marine stratocumulus clouds (MSc) in the eastern equatorial Pacific, which are essential to a proper SST annual cycle. The sensitivity of the AOGCM simulation of the tropical circulation to prescribing low-level clouds obtained from the International Satellite Cloud Climatology Project (ISCCP) was studied. The results showed that the combined prescription of global ocean and tropical land low-level clouds in the AOGCM resulted in the best simulation of the Walker circulation. The improved tropical circulation was accompanied by an improvement in the one-year prediction of ENSO by the AOGCM. It was determined that the combination of more realistic MSc in the eastern tropical Pacific and more realistic tropical land surface heating led to the improvements.

The top panel in Fig. 4.2 depicts ENSO hindcast skill in the Niño3 region. The skill scores show that the addition of the low-level ISCCP clouds over the oceans alone (CMIO) has indeed resulted in an improvement in model skill compared to the fully predicted cloud

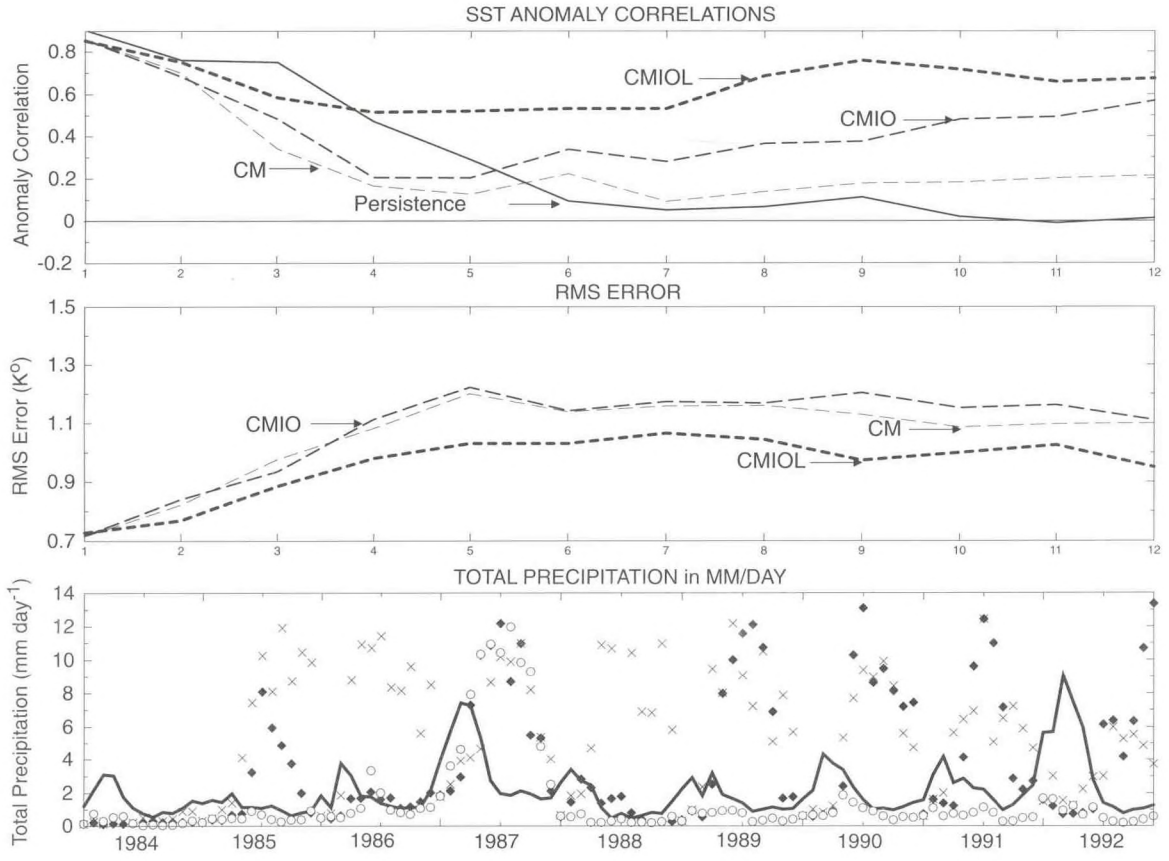

Fig. 4.2 Top: Mean Niño3 SST anomaly correlations with Reynolds observed SSTs as function of forecast lead to 12 months for 1984-1993 for persistence (thick), and for coupled models with fully predicted clouds (CM, thin), prescribed ISSCP low-level clouds over the oceans (CMIO, medium dashed) and prescribed low-level ISSCP clouds over the oceans and tropical land (CMIOL, thick dashed). Middle: Niño3 rms errors for all but persistence. Bottom: Niño3 total precipitation in mm - day^{-1} for observations (thick solid), CM (X's), CMIO (diamonds) and CMIOL (circles). In general, prescribing clouds improves the coupled model performance.

experiment (CM). The CMIOL experiment (prescribed clouds over both ocean and land) shows even more skill for the entire 12-month period. The experimental rms errors, shown in the middle panel of Fig. 4.2, indicate that only the CMIOL experiment separates itself from the other experiments as having reduced error. It follows that although the ocean low-level clouds are assisting the CMIO experiment to simulate the correct sign of the SST anomaly, these clouds alone are not sufficient to simulate the amplitude of the ENSO events. The lower panel of Fig. 4.2 shows that the CMIOL experiment has a more realistic simulation of precipitation than the other experiments, though it does err on the side of underpredicting precipitation.

Multi-year simulation experiments with low (as well as multi-level) ISCCP cloud fractions and optical depths were performed with a newer version of the coupled model. However, relative to results obtained with the previous model (1719), the SSTs in the tropical Pacific cooled a few degrees and displayed much weaker interannual variability in the equatorial belt. Moreover, what variability remained was not ENSO-like in character, *e.g.*, was not linked to a delayed oscillator mechanism. On the contrary, it appeared to be driven by westward propagating variations in surface heat flux associated with the ISCCP low clouds in the eastern tropical Pacific. This behavior is presumably due to one or more new features of the new coupled model: MOM3 instead of MOM2, RAS with a re-tuned threshold parameter instead of the full Arakawa-Schubert convective parameterization, variable high cloud emissivity, diurnally-varying radiation, and elimination of the 10% proportional surface evaporative flux correction.

4.1.6 Atmospheric Model Predictability: Top of the Atmosphere Radiation Budget

L. Donner *W. Stern*
C.T. Gordon

Bruce Wielicki of NASA/Langley is comparing several AGCM (Atmospheric GCM) simulations of the earth's tropical radiation budget to Earth Radiation Budget Experiment (ERBE) and to Clouds and the Earth's Radiant Energy System (CERES) satellite observations. GFDL has provided results that are relevant to evaluating the ability of GCMs to simulate interannual variability as well as secular trends. Two sets of AGCM runs with specified SSTs from 1997/1998 were analyzed: the single AMIP 2 run; and a 10-member ensemble of 28-month Monsoon Modeling Intercomparison Project (MMIP) integrations started from the AMIP 2 run.

Both the phase and amplitude of the outgoing longwave radiation (OLR) and net absorbed shortwave anomaly fields (calculated with respect to the 1985-1989 monthly and 2-month means) verified extremely well compared to observations. Results from the 10 MMIP ensemble members indicated that the El Niño signal was very robust. In fact, the "GFDL-EP" model (in contrast to the GFDL climate model) was among the top performers. These excellent interannual variability results may be attributed to the ability of the diagnostic cloud parameterization scheme to discriminate between anvil cirrus and non-anvil cirrus clouds in terms of cloud optical depth and emissivity. On the other hand, none of the models captured the apparent trend in global mean OLR suggested by a comparison of the CERES observations with earlier ERBE observations.

4.1.7 Impact of MJO/WWB in the Far Western Equatorial Pacific on ENSO Forecasts

M. Harrison *A. Rosati*

The influence of the Madden-Julian Oscillation (MJO) on ENSO is an intriguing and controversial issue. Extraordinary MJO events coincided with the onset of the 1997/1998 warm event, which was unusual in its magnitude and rapidity of onset. In order to gain a quantitative understanding of the role of MJO and westerly windburst (WWB) events in ENSO prediction, a hybrid coupled model (HCM) forecast system was applied. The ocean model is MOM3 with 1 degree zonal and 1/3 degree meridional resolution. The statistical atmosphere (4.1.3) is based on ECMWF reanalysis surface windstress, evaporation, and radiation fluxes regressed to SST anomalies. The experimental design included ocean initial conditions from the GFDL ocean data assimilation system and control forecasts using the HCM for the 1980-1998 period. Another experiment was run using the observed wind time series within a region bounded by 120°E-165°E and 5°S-5°N. This case gave much better predictions of the large events in 1982-1983, 1988, and 1997, resulting in significantly better skill scores. The 1982 and 1997 El Niños were amplified by wind events from the preceding March. While the model predicted these warm events without the patch winds, the amplitude was significantly underestimated. The wind events were found to trigger ocean Kelvin waves which result in deepening of the thermocline in the Eastern Pacific with subsequent SST warming and amplification by coupled interactions.

4.1.8 Interaction of MJO and Tropical Storms

J. Sirutis

A number of observational studies have indicated the existence of a relationship between the frequency of tropical storm occurrence and the MJO. Tropical storm formation appears to be enhanced during the convectively active phase of the MJO. Data from a 20-year AMIP 2 run made with the experimental prediction AGCM have been analyzed and indicate that there is indeed a relationship. For 16 of the 19 years analyzed, over 50% of the tropical storms in the model formed during the convectively active phase of the MJO; for 7 of the 19 years, more than 70% formed during the convectively active phase of the MJO. This relationship was strongest in the west Pacific during the 1980s. During the 1990's the signal was stronger in the east Pacific and the Atlantic. During El Niño years the relationship seems to be weak or non-existent. The MJO also has an impact on the intensity of tropical storms in the model. During the 19 years analyzed, 75% of the tropical storms that reached hurricane intensity (maximum winds exceeding 75 mph) occurred during the convectively active phase of the MJO. In 7 of the 19 years, all of these "hurricanes" formed during the convectively active phase of the MJO.

4.1.9 The Nature and Predictability of Tropical Intraseasonal Oscillations

R.Smith *D. Waliser**
W. Stern

**Marine Sciences Research Center, SUNY*

Results from both AMIP (1540) and coupled GCM integrations are being used to investigate tropical intraseasonal oscillations (TIO). As part of the Monsoon Modelling Intercomparison Project, a comparison of TIO/MJO behavior in the 1982-1983 and 1997-1998 ENSOs was performed using 10-member ensembles of AGCM integrations forced by observed SSTs. Longitude-time plots and power spectra indicate a difference in MJO behavior between the onset and mature phases of both ENSO events. Statistical tests indicate that some of the MJO interannual variability is significant, especially in the west-central equatorial Pacific Ocean. Considerable TIO activity is also seen in the Asian monsoon region and appears to be associated in part with northward propagation from the equatorial Indian Ocean. An association between equatorial MJO activity and Monsoon rainfall intensity is being sought.

Results from Coupled Model Ensemble Prediction (CMEP) coupled GCM are being analyzed to better understand TIO as a coupled atmosphere-ocean phenomenon. Fig. 4.3 shows evidence of a robust TIO in the model using the first extended EOF of bandpassed (20-100 day) 200 hPa velocity potential. This EOF compares favorably to those from the NCEP/NCAR reanalysis, but it is stronger. By forcing the atmospheric AGCM with SSTs generated by the CGCM and comparing these results to those obtained using a weakly interacting slab mixed-layer ocean, a better understanding will be gained of how interactive ocean processes impact the behavior of TIO.

4.1.10 Coupled Model Potential Predictability

J. Anderson *J. Ploshay*

To increase understanding of the prediction and predictability (1539) of the coupled GCM and the coupled atmosphere-ocean system (ke), an ensemble of one-year forecasts was run with members differing only in small perturbations to the 850 mb temperatures in the atmospheric initial conditions. These results complement earlier results from the CMEP experiments in which somewhat larger initial condition perturbations were used. The spreads in the predicted SST anomalies over the east-central Pacific Ocean are as large as in the forecasts produced from initial conditions with much larger differences. For several of the years investigated, SST spreads of several degrees can appear in the tropical Pacific within a few months of the start of the forecast. This implies that predictions of the thermal structure of the tropical Pacific cannot be viewed as deterministic, even for lead times as short as one or two seasons, at least for certain ocean initial conditions.

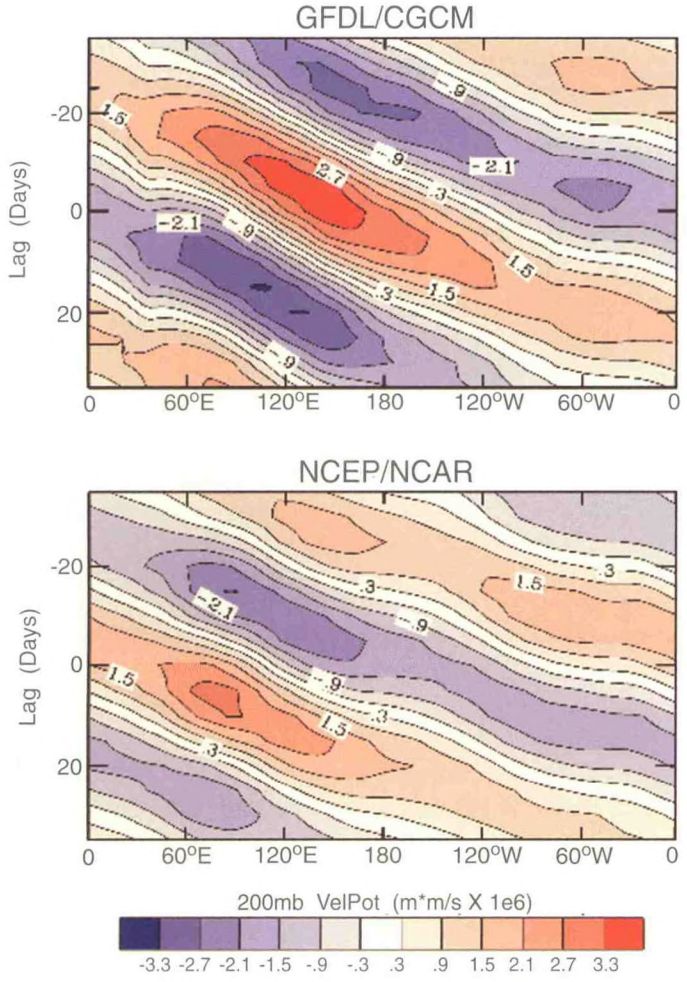

Fig. 4.3 First mode extended EOF time-longitude diagrams of bandpassed (20-100 day) equatorial (10°N-10°S) 200 hPa velocity potential from the GFDL CGCM (top) and the NCEP/NCAR reanalysis (bottom). This plot suggests that the propagating features of the MJO in the GFDL model are consistent with observations while the strength appears to be somewhat greater.

4.1.11 Indian Ocean Variability

M. Harrison *D. Sengupta*
A. Rosati

For the tropical Pacific and Atlantic Oceans, internal modes of variability that lead to climatic oscillations have been recognized, but in the Indian Ocean a similar interannual climate variability caused by air-sea interaction has not yet been found. However, recent observational analyses have suggested that the interannual variability of the Indian Ocean consists of a dipole mode in SST. These analyses further argue that the dipole mode is independent of ENSO and is the result of internal dynamics. The dipole mode has important implications for climate variability, as the shift of the convergence zone leads to floods in east Africa and drought in Indonesia. A 1/4 degree ocean model that covers the Indian Ocean basin was used to simulate the ocean during 1997/1998. Preliminary results indicate the importance of both the ocean dynamics and surface fluxes in the evolution of this mode.

Fig. 4.4 shows the large subsurface temperature anomalies for November 1997 associated with the dipole mode. Investigations of the sensitivity to various forcing products and heat flux formulations are underway. These results are to be compared to the GFDL ocean data assimilation for verification and understanding.

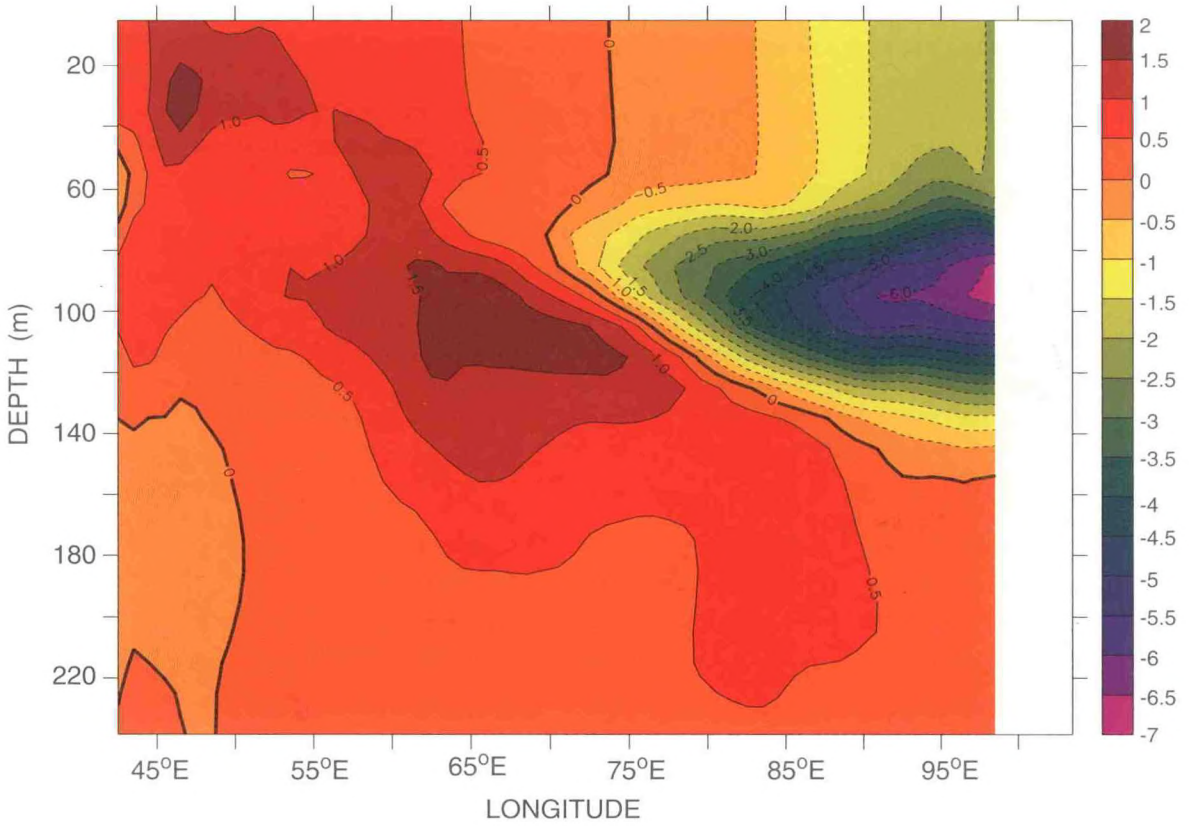

Fig. 4.4 Vertical section of anomalous temperatures along the Equator in the Indian Ocean during November 1997 from the model simulation. Only temperatures in the top 250m are important for climate changes on seasonal time scales. The eastern Indian Ocean was 7 C colder than usual at 80m depth. Such large anomalies are very unusual. The changes in the subsurface water may give some predictability to the dipole mode in the Indian Ocean.

PLANS FY01

A key focus will be on developing the components of a coupled forecast system that will produce simulations and coupled predictions that are superior to those that were available from the models used for seasonal prediction experiments in the past five years. Initial efforts will focus on development of improved individual component models, particularly for the atmosphere. Model resolution, the choice of physical parameterizations, and the tuning constants available in existing parameterizations are all candidates for change. A coordinated diagnostic effort making use of new tools available at GFDL (6.4) along with the capabilities of the FMS (Section 1) are expected to facilitate model improvements. As component model improvements occur, they will be tested in a fully-coupled model with a final goal of producing an improved coupled model.

MOM4's diagnostic capabilities and subgrid scale parameterization suite will be expanded and MOM4 will become the ocean model of choice for coupled model development.

As improved coupled models are developed, they will be integrated for several decades and used to produce ensembles of forecasts from 1980-2000 to assess ENSO forecast skill. The primary focus will be on the tropical circulation and the use of physically based metrics for evaluating model performance. Among the metrics are: ENSO variability and forecast skill; MJO; monsoon circulation; tropical storm frequency and distribution; and precipitation patterns.

The Hybrid-Coupled Model work will be extended to make additional comparisons between atmospheric models developed at GFDL and the IRI/ARCS community. An evaluation will be made of the relative merits of an anomaly coupled forecast system versus a fully coupled system in the context of ENSO prediction; *i.e.*, are there significant and predictable air-sea interactions which are not captured by a diagnosed linear relationship to SST in any of the atmospheric models considered ?

Further work using the Hybrid Coupled Model will focus on trying to gain an understanding of the relation between the ocean state and its response to MJO/WWB events. The impact of an event and its relation to the seasonal cycle will be investigated.

The ability to perform integrations with ISCCP low and/or multi-layer cloud fractions and cloud optical depths will be added to the coupled FMS model, and reference integrations with ISCCP low clouds will be performed.

An analysis will be performed of the sensitivity of the interannual variability (as well as the climatology) of the top of the atmosphere earth radiation budget in the FMS model to the diagnostic and prognostic cloud parameterizations.

Many aspects of the onset and development of the Indian Ocean dipole mode remain to be investigated. Some of the questions to be studied are: Is there a preferred background state? Are there regime shifts that account for why there was no dipole in the 1980s but two in the 1990s? Is the dipole a coupled mode? How does it grow and decay? Is there a possible relationship with ENSO?

4.2 DATA ASSIMILATION

ACTIVITIES FY00

4.2.1 Ensemble Adjustment Filter

J. Anderson

An established theory (1658) exists for generating an estimate of the complete probability distribution of the state of a model given a set of observations. This non-linear filtering theory unifies the data assimilation and ensemble generation problem that have been key foci of prediction and predictability research for numerical weather and ocean prediction applications. A novel Monte Carlo approximation to the fully non-linear filter has been developed and applied in perfect model experiments in a low order model, a non-divergent barotropic model in both perfect model and real data applications, and in a dry global primitive equation model. This ensemble adjustment method is able to produce assimilations with small ensemble mean errors while providing accurate measures of uncertainty in the assimilated variables. The filtering method uses information from an ensemble of model integrations to obtain an estimate of the covariance between model state variables and observations. Each available observation is then allowed to impact the prior distribution for each state variable independently. However, the way in which the required product of the observational error distribution and the prior state distribution is computed maintains much of the information about covariances of the prior state variables. The method is able to assimilate observations with a nonlinear relation to model state variables, and has also been demonstrated to be effective in using observations to adjust the value of unknown model parameters. The method is shown to have significant advantages over four dimensional variational assimilation in low order models (Fig. 4.5) and scales easily to much larger applications.

4.2.2 Ocean Data Assimilation

*E. Galanti** *R. Pacanowski*
*R. Giering*** *A. Rosati*
M. Harrison *E. Tziperman*

**The Weizmann Institute of Science*
***NASA/Jet Propulsion Laboratory*

A nearly global, 40 level ocean model (MOM3) with 1 degree zonal resolution and 1/3-1 degree meridional resolution is being used for seasonal to interannual prediction at GFDL. Ocean initial conditions are generated by a statistical interpolation algorithm[1] which assimilates ocean profile data to depths of approximately 400 meters. These ocean initial conditions and model configuration are being shared with several collaborators as part of an IRI/ARCS forecasting effort.

---

1. Derber, J., and A. Rosati, A Global Oceanic Data Assimilation System, *Journal of Physical Oceanography, 19(9)*, 1333-1347, 1989.

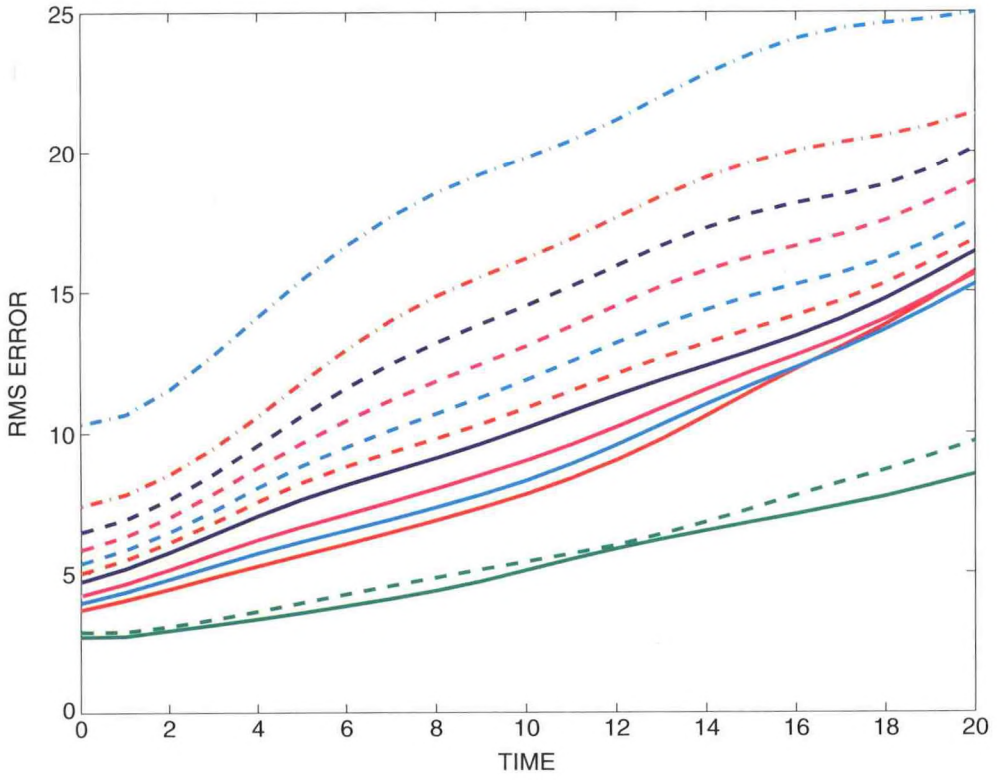

Fig. 4.5 RMS error as a function of forecast lead time for assimilations and forecasts in a 40-variable low order model (lead time 0 is the error of the analysis) for ensemble adjustment filters with a 10-member ensemble (- -) and a 20-member ensemble (—) and for four-dimensional variational assimilations that use the model as a strong constraint to fit observations over a number of observing times. In generally descending order, the number of observation times used by the variational method is two (_._.), three (_._.), four (- -), five (- -), six (- -), seven (- -), eight (—), ten (—), twelve (—), and fifteen (—). The filter methods are seen to be qualitatively superior to viable variational methods in this model.

Bi-weekly ocean initial conditions have been distributed to groups at IRI, NCEP, COLA (Center for Ocean, Land and Atmosphere studies), and NCAR for the period January 1980 through January 2000. The ocean model has been ported to parallel computational platforms at the respective centers. Comparisons of forecasts using identical ocean model and initial conditions but different atmospheric models are being made.

Currently, monthly-averaged data from the ocean analysis are available on the web (data1.gfdl.gov) through interactive browsing software developed at PMEL by Steve Hankin. In addition to the ocean assimilation, a simulation which does not make use of subsurface data can be viewed in arbitrary latitude/longitude/depth/time sections and downloaded for further analysis. Other ocean assimilation products from Ming Ji and Dave Behringer at NCEP and Jim Carton at University of Maryland are also available.

A four-dimensional ocean assimilation system using a version of MOM4 coupled to a statistical atmospheric model is currently being developed in collaboration with Eli Tzipermann and Eli Galanti at the Weizmann Institute in Israel. The tangent linear and adjoint versions of this model have been generated using a compiler developed by Ralf Geiring.

4.2.3 Information Content of Surface Pressure Observations

J. Anderson S. Zhang

The ensemble adjustment filter (4.2.1) has been applied in a dry global primitive equation model to evaluate the information content of observations of surface pressure in a perfect model experiment. A control integration of the model is used to generate observations of surface pressure at a set of 600 randomly located points on the surface of the sphere every six hours. Using only these observations, the filter is able to reconstruct the structure of the free atmosphere (Fig. 4.6). Without the impact of the surface pressure observations, the ensemble

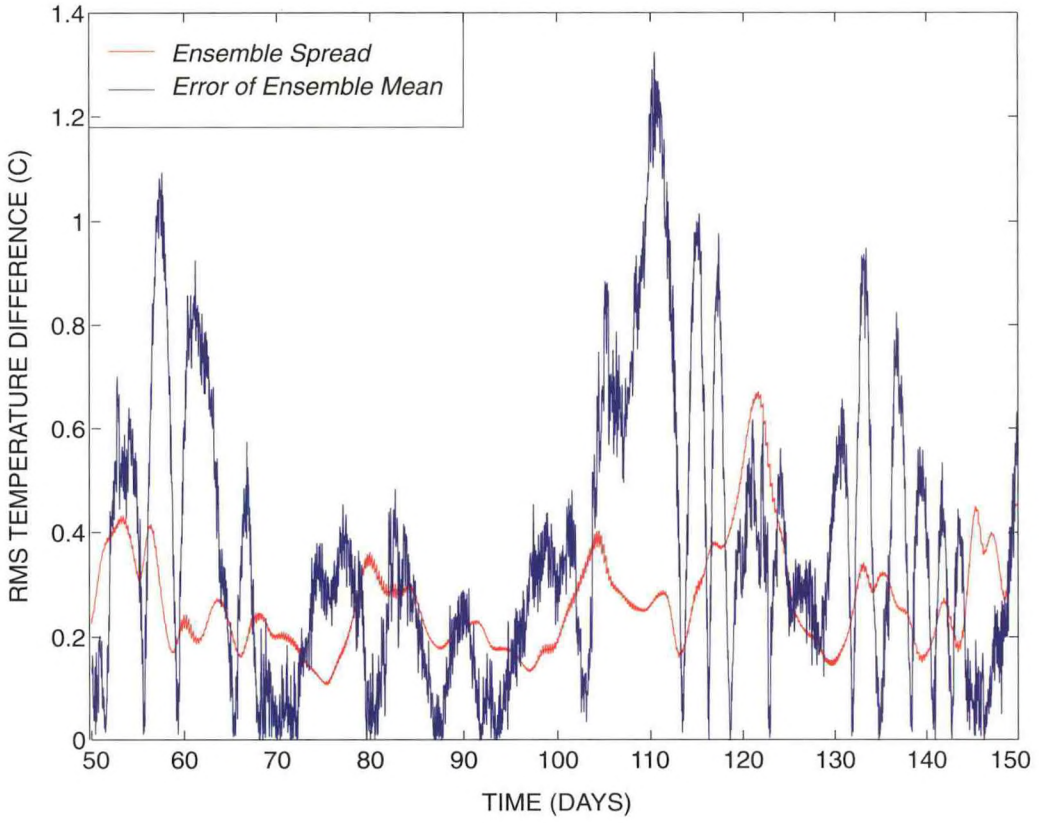

Fig 4.6 Root mean square error and ensemble spread for temperature at a point in the midlatitude middle troposphere in a perfect model adjustment filter assimilation using a global primitive equation model. The filter only has observations of surface pressure at 600 randomly distributed points on the sphere with an imposed observational standard deviation of 1 mb. Nevertheless the filter is able to produce an analysis of the temperature in the middle of the free atmosphere with mean errors of less than 0.5 C.

has an error doubling time of roughly 5 days and error saturates to climatological values which are several orders of magnitude larger than the RMS error of the assimilated ensemble mean after about 25 days. Applying the adjustment filter allows much more efficient use of data than most other known data assimilation methods and should improve our estimates of the predictability of the atmosphere.

4.2.4 Targeted Observations

J. Anderson S. Khare

The "targeted observation problem" tries to determine the location at which an additional observation should be taken some time in the future in order to improve significantly a forecast of some quantity at a time even further in the future. A number of heuristic methods using operational ensemble predictions have been used to attack this problem in recent years. The ensemble adjustment filter method (4.2.1) for ensemble assimilation and prediction provides a framework in which the targeted observation problem can be addressed. The filtering method uses information from an ensemble of model integrations to obtain an estimate of the covariance between model state variables and observations. Each available observation is then allowed to impact the prior distribution for each state variable independently. There is no reason that the impact of observations must be limited to those available at the present time. The impact of observations from previous times can also be computed in this filter using the information available from the time history of the ensemble of assimilations. Likewise, the impact of a hypothetical future observation on a forecast even further in the future can also be approximated. Initial results in a low order dynamical system have suggested that the ensemble adjustment filter targeted observation method is significantly superior to other methods currently available.

PLANS FY01

The ensemble adjustment filter will be tested in high resolution primitive-equation models both with and without comprehensive physical parameterizations. Further study of the information content of surface pressure observations in more realistic models should lead to an understanding of operational implications. Initial application of the adjustment filter will be attempted in MOM. Strategies for targeted observations in both low order and realistic models will be refined.

Additional ocean assimilation runs are being planned in collaboration with Mike Tippett at IRI using a reduced empirical orthogonal function (EOF) space estimate of model error. Forecasts using this technique will be compared to the current ocean analysis.

Current plans are to assimilate data from the TAO array in the equatorial Pacific and wind data from the NCEP Reanalysis using the adjoint method. Working in collaboration with Geiring, his compiler is being updated to be Fortran 90 compliant in concert with the latest developments of MOM4 (4.1.1). Developing the ocean model and its adjoint compiler simultaneously is a key to this effort.

4.3 OCEAN-ATMOSPHERE INTERACTIONS

J. Boccaletti *G. Philander*
A. Federov *B. Winter*
S. Harper *A. Wittenberg*

ACTIVITIES FY00

Although there has been considerable progress in our understanding of climate fluctuations on seasonal, interannual, and decadal time-scales, a wide gulf still seems to separate observational, theoretical, and modeling studies. Evidence of this divide includes the following.

Theoretical studies of El Niño focus on the natural modes of oscillation and, therefore, take an eigenvalue approach. Measurements, on the other hand, pay essentially no attention to the theoretical results and describe the development of El Niño, of 1997 for example, in terms of westerly wind bursts that initiate an event, treating the evolution as an initial value problem. In a recent debate about the possible effect of global warming on El Niño, the various arguments being presented all concern statistical issues; no one is appealing to theoretical results to anticipate how global warming will affect El Niño. Numerous groups are developing coupled ocean-atmosphere GCMs and are simulating a bewildering variety of interannual oscillations. It is not at all clear how the available theoretical results can contribute to the development of realistic complex models. The remedy for these various problems is a stability analysis that establishes how the properties of the Southern Oscillation (its period, growth rate, etc.) depend on the background state described in terms of readily measurable quantities, such as the spatially averaged depth of the thermocline, the temperature difference across the thermocline, and the time-averaged intensity of the trade winds. Preliminary results from such an analysis have already been published (1710) and a more detailed analysis has been completed (ab). This past year, attention focused on application of these results to the interpretation of a realistic simulation of oceanic conditions over the past fifty years with a GCM, and to factors that can effect gradual (decadal) changes in the background state. The distinctiveness of each El Niño was another topic that was explored.

Decadal changes in the depth of the thermocline and in the intensity of the time-averaged zonal winds along the equator can account for certain observed changes in the properties of El Niño from the 1960s to the 1980s. The period of the Southern Oscillation, for example, increased from approximately 3 years to 5 years, but does not explain why El Niño was prolonged and weak in 1992, but brief and intense in 1997. Westerly wind bursts near the date-line appear to have played a central role in the development of El Niño in 1997, but similar wind bursts were present on other occasions and failed to generate any El Niño. Up to now, studies of these wind bursts have concerned either their atmospheric aspects (whether they are associated with certain sea surface temperature patterns, for example) or the oceanic response they generate. Surprisingly, no one has investigated the response of the coupled ocean-atmosphere system to these winds. A study of the ocean-atmosphere interactions generated by westerly wind bursts, by means of a simple Cane-Zebiak type coupled model, indicates that the impact of the winds depends critically on the phase of the Southern Oscillation, if one is present. A swinging pendulum subjected to blows at random

times is a good analogy. Westerly wind bursts can amplify El Niño enormously, if they occur when the Southern Oscillation is in the early stages of its El Niño phase, but have the opposite effect when they occur during La Niña. This result has the important implication that, although it should have been possible to anticipate El Niño of 1997 on the order of a year in advance, it was not possible to anticipate its enormous amplitude until the westerly wind bursts had actually occurred. Given this role of unpredictable westerly wind bursts, El Niño has very limited predictability. A long-term forecast can at best sound an alert that conditions are ripe for an intense El Niño should the appropriate wind bursts materialize. To make such a statement, the best quantity to monitor is the available potential energy (1694) of the tropical Pacific which is highly correlated with sea surface temperatures in the eastern tropical Pacific, but has the advantage of being a global rather than a local quantity.

A realistic General Circulation Model of the ocean (MOM), forced with the winds observed over the tropical Pacific Ocean since 1950, provides data that permit a detailed study of both gradual, decadal, and rapid event-to-event changes in the properties of El Niño. Preliminary results indicate that the differences between one event and the next can indeed be attributed to the impact of random westerly wind bursts. Those winds contributed to the great intensity of El Niño in both 1982 and 1997. A further contributing factor was the change in the background state from the 1960s to the 1980s. The easterly winds weakened over that period, and the thermocline gradually deepened. This caused the structure of the Southern Oscillation to become closer to that of the delayed oscillator in which sea surface temperature variations in the eastern tropical Pacific are controlled mainly by vertical movements of the thermocline in response to winds near the dateline. (During the 1960s and 1970s, local winds in the eastern tropical Pacific had a stronger influence on sea surface temperatures.) Thus, even if the structure of westerly wind bursts remained unchanged over the decades, their impact increased in the 1980s and 1990s because of the preferred mode during that period.

The extent to which oceanic exchanges between the tropics and subtropics contribute to the decadal variations in the background state is a topic of continuing interest. Experiments with a realistic oceanic GCM indicate that the disturbances that reach the equator come predominantly from the Southern Hemisphere.

PLANS FY01

Studies planned for the coming year include the use of an intermediate coupled ocean-atmosphere model, composed of an oceanic GCM coupled to a statistical atmosphere in which the winds correspond to that component of the observed winds correlated with tropical sea surface temperature changes. The goal will be to explore the validity of the stability analysis which was obtained by means of a very simple coupled model with a great number of adjustable parameters in a more realistic setting. The strategy will be to focus on certain extreme situations where the differences between the possible modes are very large: the delayed oscillator mode that is favored when the thermocline is deep and the winds are intense, versus the local mode when the thermocline is shallow. (In the local mode sea surface temperatures depend not on vertical movements of the thermocline, but primarily on entrainment across the thermocline and on zonal advection.) The coupled model will also be used to explore how changes in the structure of the equatorial thermocline, induced by tropical-subtropical exchanges, affect ocean-atmosphere interactions.

5. OCEANIC CIRCULATION

GOALS

To predict the response of the World Ocean to changing atmospheric conditions through the use and development of detailed three-dimensional ocean circulation models.

To understand the critical role of the oceans in climate variability, regional climate change, and climate change impacts.

To identify practical applications of oceanic models to human marine activities by the development of a coastal ocean model.

To understand the biogeochemistry of the ocean through the use of coupled carbon-cycle/ocean models.

5.1 WORLD OCEAN STUDIES

5.1.1 Modeling Eddies in the Southern Ocean

A. Gnanadesikan *K.S. Smith*
S. Griffies *J.R. Toggweiler*
R. Hallberg *G.K. Vallis*
B. Samuels

ACTIVITIES FY00

The Southern Ocean in general, and the Antarctic Circumpolar Current (ACC) in particular, are emerging as centrally important players in both the general circulation of the ocean and the earth's climate system. For this reason, the Ocean Group at GFDL has embarked on an ambitious, multi-year effort to numerically simulate the Southern Ocean, with sufficient horizontal and vertical resolution to resolve the ubiquitous energy containing mesoscale eddies.

The Southern Ocean is unique in containing latitudes that are not blocked by land. Consequently, the leading-order dynamic balances (*e.g.*, Sverdrup balance) do not obviously dictate the general structure of the ACC, unlike most of the other ocean currents. The northward Ekman transport in the unblocked latitudes must be balanced by the combination of the upwelling of waters from great depth and meridional eddy mass fluxes. The meridional density gradients associated with the ACC are intimately tied to the mean stratification of the entire ocean to the north of the ACC, and it is becoming increasingly evident that the dynamics of the Southern Ocean are crucial in determining the stratification and overturning circulation of the entire ocean (1313, 1595, 1700, 1728).

Complete understanding of the interplay between the intense mesoscale eddies and the mean ocean circulation, and so of the general oceanic circulation itself, demands the use of numerical models with sufficiently high resolution to explicitly resolve these eddies, typically as small as 10 km in the ACC. These processes are being studied through simulations of the Southern Hemisphere oceans using GFDL's z-coordinate model (MOM) and GFDL's isopycnal-coordinate model (HIM). Fig. 5.1 shows a comparison of instantaneous velocities in the ACC near the tip of Africa. The top two panels show results from HIM and MOM at 1/2° resolution (25 km at 60°S). The bottom panel shows results from HIM at 1/4° resolution (13.9 km resolution at 60°S). The ACC flows toward the east between 40° and 45°S. The strong flow along the coast of Africa is the Agulhas current flowing toward the southwest. The Agulhas current in the real world is known to join the ACC south of Africa by retroflecting back to the east. It is also known to break up into eddies which propagate westward into the Atlantic. Fig. 5.1 shows that both HIM and MOM capture the retroflection at 1/2° resolution, but only the 1/4° model in the bottom panel is able to simulate the production of Agulhas eddies.

Wind stress perturbations are being applied to both models over a range of resolutions to study the sensitivity of the dynamic balances between the mean circulation, eddy fluxes, and the diabatic circulation in the Southern Ocean. The complete suite of experiments at 1/2° resolution is nearing completion.

The Southern Ocean provides an ideal test-bed for exploring the effects of eddy-flux parameterization schemes and the still more basic scientific issue of geostrophic turbulence in the ocean. Parameterizing (and therefore understanding) oceanic mesoscale eddies is necessary for properly representing the ocean in long-term coupled ocean-atmosphere climate simulations. The re-entrant channel geometry of the ACC makes it possible to pose the problem in a relatively clean form and, taken together with the inclusion of sub-tropical gyres and intense western boundary currents in the proposed simulations, allows the problem to be studied with unprecedented detail.

PLANS FY01

Sensitivity studies with both MOM and HIM will be analyzed at 1/2° (isotropic) resolution. Remaining calculations, including wind stress perturbations, at 1/4° resolution will be carried out. A similar series of simulations at a resolution of 1/6° or 1/8° will be initiated. More idealized geometries will also be used to understand the dynamics.

5.1.2 Southern Ocean Winds and the Circumpolar Current: Theoretical Studies

A. Gnanadesikan R.W. Hallberg

ACTIVITIES FY00

A number of theories have been advanced to predict how the Antarctic Circumpolar Current should respond to changes in the wind stress over the Southern Ocean. According to one theory, the strength of the Circumpolar Current should respond to the mean wind stress within the open latitudes of Drake Passage. According to another, the meridional gradient of

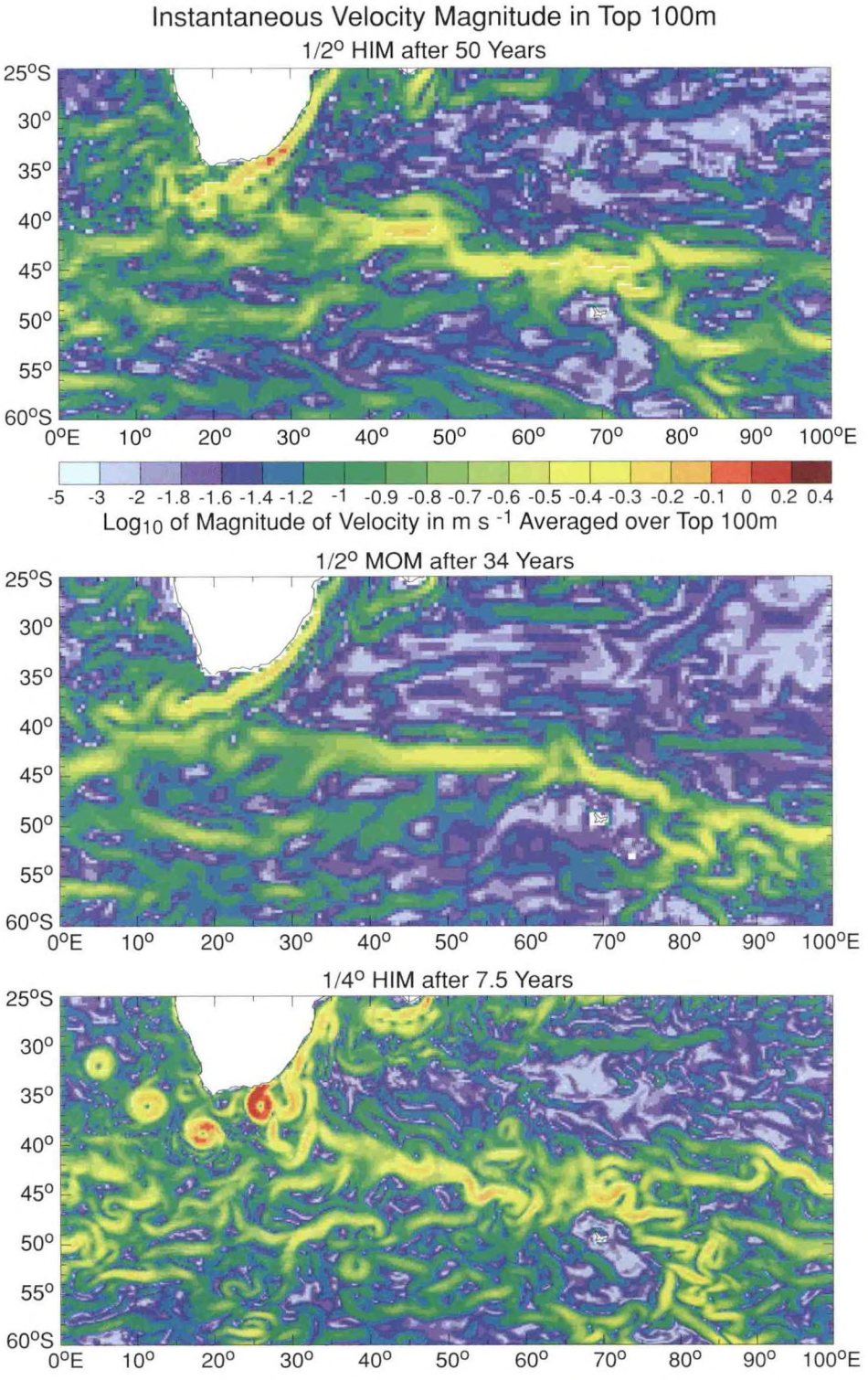

Fig. 5.1 Snapshots of the velocity magnitude, averaged over the top 100 m, from HIM and MOM run in the MESO configuration, at two resolutions. The eddy field is much more realistic at the higher resolution. The higher of these resolutions (and still finer resolution simulations) will be used to assess the role of mesoscale eddies in the dynamics of the Antarctic Circumpolar Current.

the wind stress should be the most important factor. Still another theory predicts that the strength of the ACC is saturated, *i.e.*, additional energy input from the wind simply makes for more energetic eddies. Until recently, none of these theories considered the impact of heating and cooling north and south of the ACC.

A recent study (1728) suggests that any theory which purports to explain the response of the ACC to the wind must consider the buoyancy forcing north and south of the ACC as it pertains to the north-south pressure gradient across the current. Fig. 5.2 shows schematically

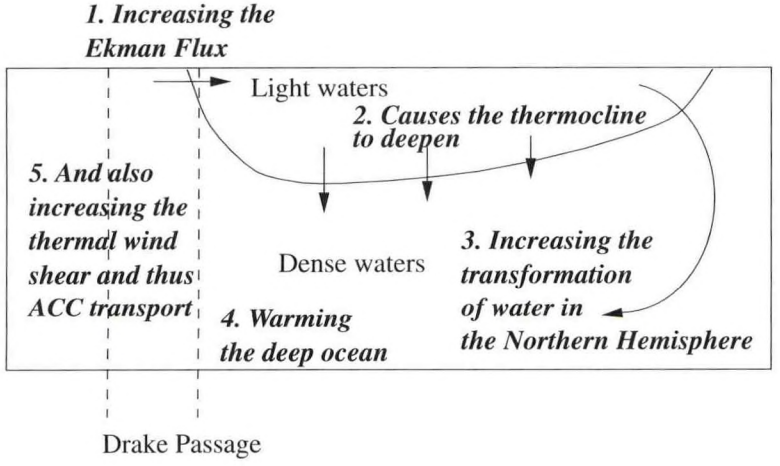

Fig. 5.2 Illustration of how an increase in Southern Ocean winds causes an increase in the transport of the Circumpolar Current by causing an increase in the north-south pressure gradient (1728).

that upwelling in the south forces a conversion of dense deep water into lighter thermocline waters. This leads to an increase in the depth of the light-water pool in low latitudes and a larger north-south pressure gradient in the upper part of the water column. This pressure gradient increases the overturning in the Northern Hemisphere leading to warmer and lighter deep waters in the north. Insofar as the density of deep water in the Southern Ocean remains basically unchanged, the result is a larger north-south pressure gradient at all depths across the ACC and an increase in the transport of the Circumpolar Current.

The picture is complicated by the presence of mesoscale eddies in the ACC. Eddies allow for a southward mass flux of relatively light water which replaces some of the dense water being upwelled from the deep ocean by the winds. Eddies thereby reduce the mass conversion and northern overturning depicted in Fig. 5.2. An idealized theoretical study to examine the effects of eddies has been carried out using a two-layer isopycnal primitive-equation model (nc). The model setup allows for strong topographic effects and the resolution of baroclinic eddies. A key parameter is the ratio between the Ekman flux, which lifts the interface between the two layers, and the diapycnal mass flux, which converts water from one density type to the other. When this ratio is small, *i.e.*, the circumpolar current is relatively weakly forced by the wind, the conversion of dense upwelled water into lighter surface water dominates and the strength of the circumpolar current increases with a stronger wind stress. An increase in the wind stress is partly compensated by increases in the pycnocline depth and

overturning at the northern wall, partly compensated by an increase in eddy fluxes. However, when the Ekman flux dominates at the point of instability, *i.e.*, the conversion of dense upwelled water into lighter surface water can't keep up with the Ekman flux, increases in wind stress are compensated almost entirely by increases in the eddy flux.

Figure 5.3 illustrates the importance of this non-dimensional ratio in governing the dynamics of a circumpolar current. It shows two realizations of an idealized ACC, both with the same ratio of Ekman flux to diapycnal flux. The idealized ACC in the top panel is forced with a

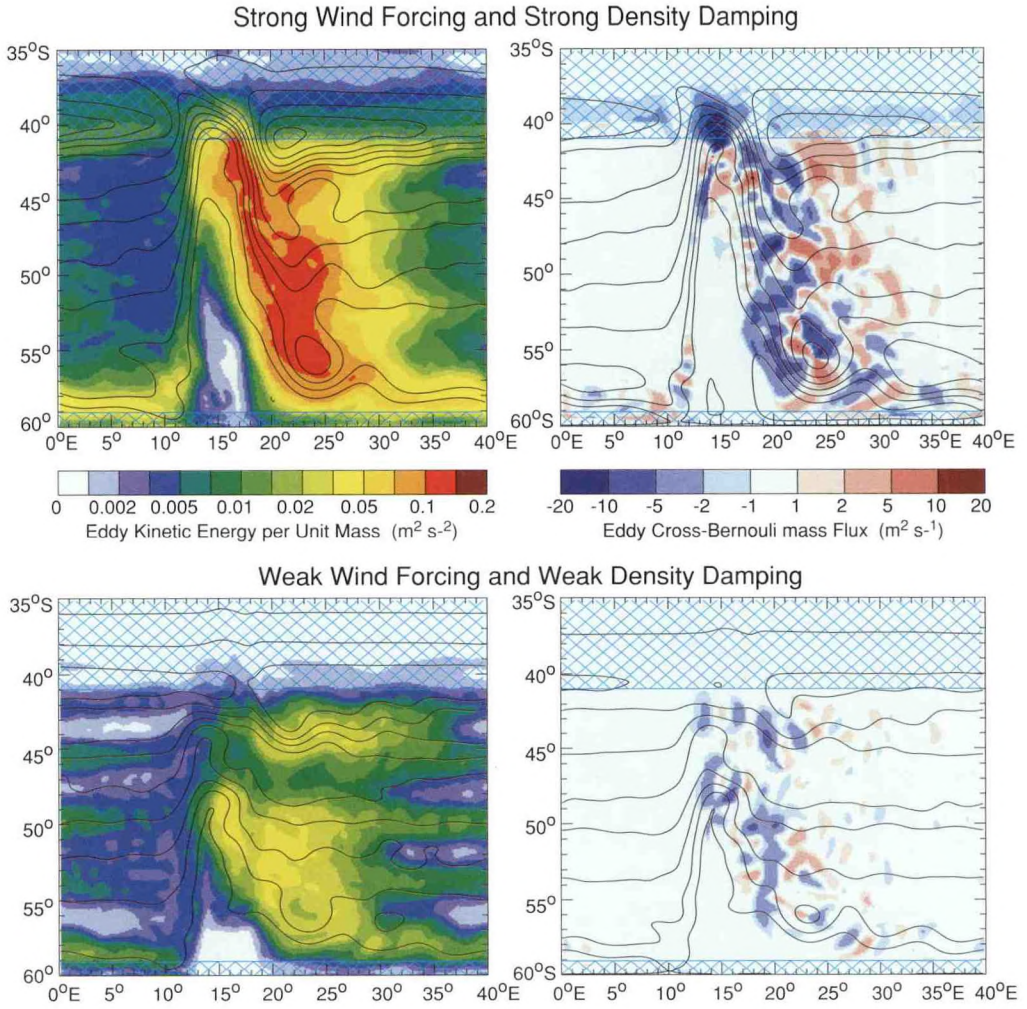

Fig. 5.3 Illustration of the dependence of a circumpolar current on topography and eddies. Results shown are from a two-layer, eddy resolving model set in a re-entrant zonal channel with a north-south topographic ridge (centered at 15°E in the figure). The top panels show results from a run with a high wind stress and high thermal damping in the (blue-hatched) sponge regions. The bottom panels show results from a run with a fourfold weaker wind stress and fourfold weaker thermal damping. In the two panels on the left, eddy kinetic energy is overlaid with contours of stream function. In the two panels on the right, the cross-stream eddy transport is overlaid on contours of the Bernoulli function. The circumpolar transport is almost identical in the two runs, but the structure of the current and associated eddy fluxes are very different. The eddy mass flux is about fourfold larger in the more energetic case and is concentrated downstream of the topography.

strong wind stress and a high rate of thermal damping in the sponge regions to the north and south. The ACC in the bottom panel is forced with a weaker wind stress and less thermal damping. The ACC transport is almost identical in the two runs, but the structure of the ACC and associated eddy fluxes are very different.

PLANS FY01

As illustrated in Fig. 5.3, the eddy mass flux should be more energetic downstream of large topographic features, such as the Scotia Arc or Campbell Plateau. Homogeneous parameterizations of eddy fluxes, like the widely used Gent-McWilliams parameterization, are unlikely to be able to reproduce this asymmetry. It is unclear whether this will have important effects on their ability to predict the large-scale structure and dependence of the Circumpolar Current. Simulations will be carried out in which various parameterizations are included in a coarse-resolution version of the eddy resolving model. Results will be compared with the fully eddy-resolving calculations.

5.1.3 The ACC and the Ocean's Thermohaline Circulation

H. Bjornsson *R. Hotinski*
S. Carson *B. Samuels*
A. Gnanadesikan *J.R. Toggweiler*

ACTIVITIES FY00

Much of the meridional heat transport into the earth's temperate and sub polar zones is carried by the ocean's thermohaline circulation. It has long been supposed that this circulation is maintained by diabatic heating in the interior brought about by the downward mixing of heat in low and middle latitudes. Given the central role of diabatic heating in the theory, the thermohaline circulation has been thought to carry tropical heat poleward toward both poles. The archetypal thermohaline circulation in today's ocean, seen in the Atlantic Ocean, does not readily conform to expectations. Both the warm upper branch and the cold lower branch of the Atlantic thermohaline circulation extend across the equator into the circumpolar region in the south such that much of the heat carried northward into the North Atlantic comes from outside the Atlantic basin. The cross-equatorial overturning in the Atlantic weakens the poleward ocean heat transport in the Southern Hemisphere, while it strengthens that of the Northern Hemisphere. The old theory requires special factors, *e.g.*, extra salt in the Atlantic, to account for the interhemispheric nature of the Atlantic overturning.

Earlier studies (1313, 1562) showed that the Atlantic's thermohaline circulation could very well exist without diabatic heating if it operates in conjunction with a wind-driven ACC in the far south. From this perspective, the ocean's dominant thermohaline circulation is interhemispheric by definition, and it owes its existence to Drake Passage, the gap between South America and Antarctica which allows the ACC to exist. An idealized coupled model has been created in which the climatic effects of an open Drake Passage can be explicitly simulated (1714). The model describes a mostly water-covered earth in which a full ocean GCM (MOM) is coupled to an energy balance model of the atmosphere. Land consists of a thin barrier which extends north and south between two Antarctica-like polar islands. The

opening of Drake Passage is simulated by removing a section of the barrier near the south polar island. Air temperatures and oceanic SSTs are prognostic variables of the coupled system; no restoring boundary conditions are used.

Results from the "water planet" model show that all the major features of the Atlantic thermohaline circulation and the ocean's heat transport system suddenly appear with the opening of Drake Passage. The high latitudes of the Southern Hemisphere cool down by some 3°C while the high latitudes of the Northern Hemisphere warm up by about the same amount, in accord with the observed temperature differences between the North and South Atlantic. A relatively warm, salty deep water mass forms next to the north polar island and flows southward across the equator at mid-depths much like North Atlantic Deep Water (NADW) in the real world. The deep water forming next to the north polar island is inherently salty in relation to deep water formed elsewhere.

Virtually all the extra heat given up to the atmosphere in the high latitudes of the Northern Hemisphere comes from the high latitudes of the Southern Hemisphere, where cold water upwelled by Ekman divergence south of the model's ACC is warmed as it moves northward under the influence of the Southern Hemisphere westerlies. According to the old theory, the thermohaline circulation should cool the tropics as it transports tropical heat poleward. The tropics in the water planet model actually warm slightly and contribute no extra heat to the Northern Hemisphere when Drake Passage is opened. The pattern of warming and cooling generated by an open Drake Passage is proportional to the wind stress applied in the latitude band of the model ACC. Stronger winds thicken the thermocline north of the model's ACC in accord with the simple predictive scheme in (1595). Stronger winds enhance the amount of warm water that comes into contact with the atmosphere near the north polar island and thereby enhance the flux of oceanic heat to the atmosphere.

PLANS FY01

This approach to the ocean's heat transport suggests that the earth's climate should be particularly sensitive to tectonic changes that open and close critical ocean gateways. It is hypothesized, for example, that the equable climates of the Cretaceous and early Cenozoic were maintained, in part, by the enhanced ocean heat transport caused by a circumglobal current, analogous to the ACC, that circled the earth in the latitude band of the northern tropics. Preliminary work with the water planet model shows that the opening of a Drake Passage-like gap in the northern tropics cools the entire tropical ocean by some 2°C and boosts the northward oceanic heat transport out of the tropics up to 4×10^{15} W.

5.1.4 Ocean Eddy Energies, Scales, and Vertical Structure

S. Griffies *S. Smith*
*T. Huck** *G. K. Vallis*

**Universite de Bretagne Occidentale, Brest, France*

ACTIVITIES FY00

Turbulent motions comprise a significant fraction of the oceanic energy budget and transport, yet remain at the edge of what computer models can resolve. Parameterization of such motions is thus a continuing effort, but one for which only intermediate solutions currently exist, all of which have deficiencies. A particular approach pioneered by Held and Larichev (1362) is based on the fundamental aspects of fully developed geostrophic turbulence generated by baroclinic instability, and is thus most likely applicable in regions of highly unstable flow - a fair characterization of much of the world's ocean. A new project extends the Held and Larichev formalism to incorporate the effects of arbitrary stratification and shear. The modified theory specifies a vertical structure for the eddy diffusivity which automatically ensures conservation of the appropriate material properties. In particular, the theory specifies a form for the northward eddy potential vorticity flux, v'q', shown in Fig. 5.4, which always

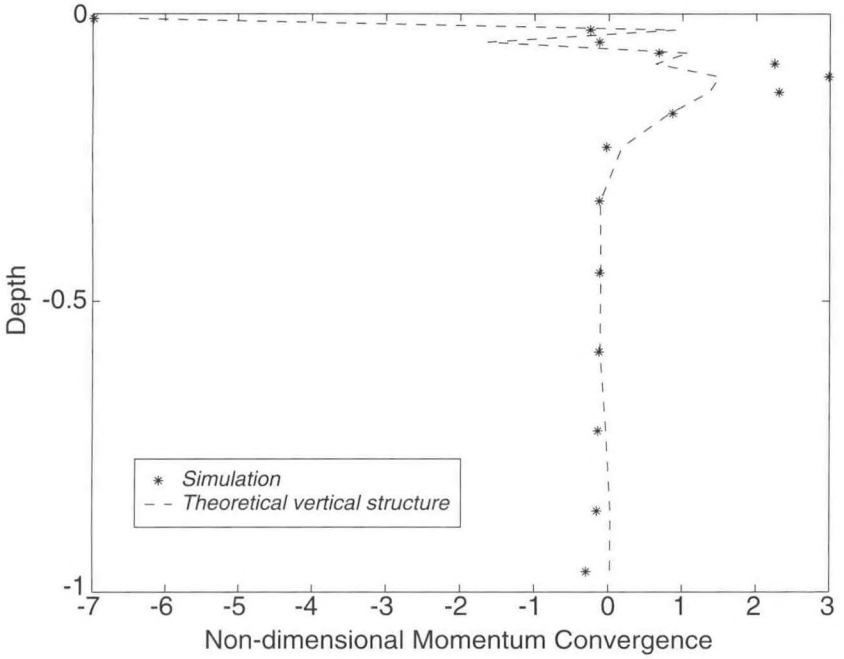

Fig. 5.4 Simulated profile of horizontally averaged northward eddy potential vorticity flux v'q' (asterisks) compared to the theoretical prediction (dashed line). Both curves integrate to 0, a necessary constraint for momentum conservation.

integrates to 0, thereby ensuring that the parameterization conserves momentum. The modified theory has been tested in a multi-layer homogeneous quasi-geostrophic turbulence model with realistic stratification and mean shear with encouraging results.

PLANS FY01

The proposed parameterization presumes that an eddy producing flow is highly unstable. While this is likely the case, no specific analysis of ocean climatology has addressed this question specifically. Moreover, alternate theories exist which are likely more appropriate for the weakly unstable limit. In order to determine the degree to which regions of the global ocean are stable, weakly unstable or strongly unstable to both baroclinic and barotropic instability, a linearized balanced model appropriate for large scale and frontal regions will be used to assess the regional instability of oceanic currents. By comparing these results to measurements of the four-dimensional spectrum of mesoscale variability throughout the ocean, an assessment will be made regarding the degree to which various regions are controlled by linear or non-linear processes, leading to the determination of appropriate eddy closure schemes for each region. Plans are underway to test the modified theory in an isopycnal primitive equation model (HIM) and to extend the theory to incorporate the effects of non-zonal flow, surface buoyancy flux and topographic roughness.

5.1.5 Geostrophic Turbulence

G. Boccalletti *I. Marinov*
C. Cartwright *S. Smith*
*A. Fournier** *C.-Y. Tam*
N. Griannik *G.K. Vallis*
I. Held

**Dept. of Geosciences, Princeton University*

ACTIVITIES FY00

An interesting research project emerged from a graduate class taught in the fall of 1999. In lieu of a final exam, the students worked on various computational/theoretical problems in geostrophic and two-dimensional turbulence. These projects were of sufficient interest and originality that they have been extended and focussed. The common theme of the work is the inverse cascade in forced-dissipative turbulence. The inverse cascade is of particular oceanographic significance, because it is one means whereby mesocale eddies interact with the large-scale circulation, potentially providing natural variability at the gyre scale. Here, we will highlight just a few of the results that have emerged so far in this idealized, homogeneous framework.

Ocean general circulation models typically use a linear Rayleigh damping on the bottom layer vorticity to simulate Ekman drag. Because baroclinic modes are primarily surface trapped, bottom drag acts primarily to damp the barotropic mode. The degree and mechanism by which drag is involved in setting the observed eddy scales is an open question. Two-dimensional turbulence is an approximation of the ocean's barotropic mode, thus a simplified two-dimensional model can be used to selectively examine the dynamics of linear drag on non-linear transfers. A theory which predicts the steady-state energy spectrum of this system has been devised and tested against a simulation of two-dimensional turbulence in a doubly periodic domain forced at high wave number (Fig. 5.5). Given the highly non-linear character of these flows, it is remarkable that the theory predicts not only the mean scale of

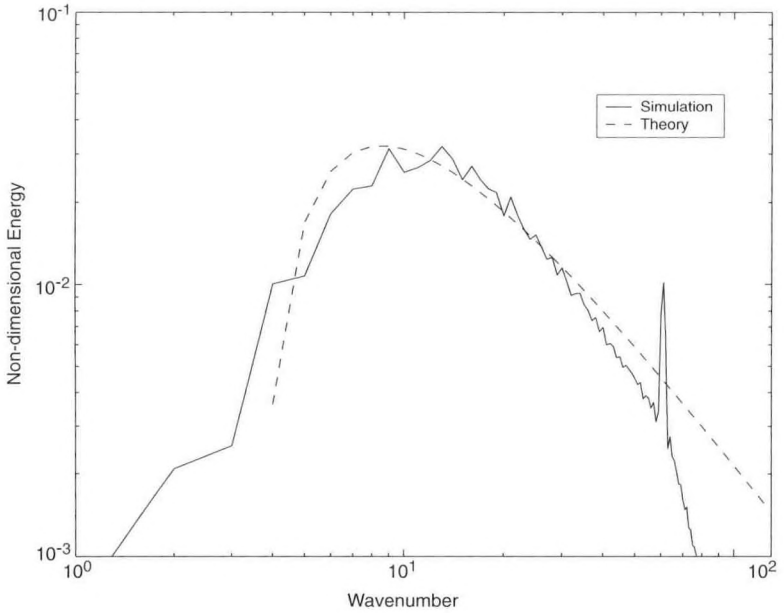

Fig. 5.5 Steady state energy spectrum of forced homogeneous barotropic turbulence with linear vorticity drag showing how the scaling theory predicts the horizontal scale and magnitude of the most energetic eddies. The simulation (solid line) is from a spectral model with 256x256 equivalent horizontal grid points. The theoretical prediction is given by the dashed line.

the eddies, but their magnitude and energy distribution as well. Ongoing research will address the combined effects of more realistic quadratic drag, differential rotation and finite radius of deformation on eddy energies and scales, as well as on tracer variance distributions, which approximate baroclinic mode energy at large scales.

5.2 MODEL DEVELOPMENT

5.2.1 Modular Ocean Model

V. Balaji *R. Pacanowski*
S. Griffies *A. Rosati*

ACTIVITIES FY00

Version 3 of GFDL's Modular Ocean Model (MOM 3) was developed and optimized for use on vector computers such as the CRAY T90. It can also run on distributed memory systems like the CRAY T3E. Model performance suffers in two respects, however, when MOM3 is run on distributed memory systems. First, the amount of memory required per processor is not reduced as more processors are used to attack a problem. This means that large models may not be able to fit in available memory even though the computational domain is divided among many processors. The second deficiency is an inadequate increase in speed when the work load is spread across a large number of processors. Because of the way that arrays are laid out in memory, it is impossible to address these deficiencies within MOM 3.

A new version of MOM (MOM 4) has been created to address these deficiencies. MOM 4 has been written in Fortran 90 syntax and is structured so that it can use generalized curvilinear coordinates. Early tests indicate that MOM 4 memory requirements and speed scale significantly better than in MOM 3 on the CRAY T3E. Better scaling of memory has been achieved by eliminating MOM 3's memory window and allocating all arrays to the size of the local domain on each processor which is determined at run-time.

Better scaling of model speed across multiple processors has been realized due to the two-dimensional domain decomposition used in MOM 4. Fig. 5.6 shows a comparison of model

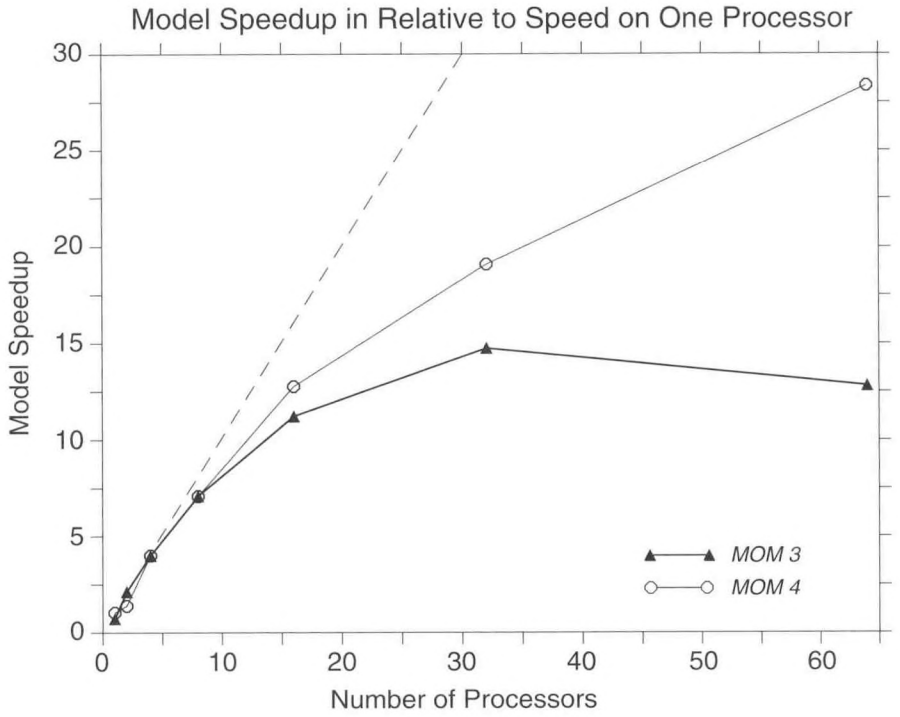

Fig. 5.6 Comparison of the relative speedup of MOM 3 and MOM 4 as more and more processors are applied to a sample problem run on a Cray T3E. MOM 3 fails to show improvement when the number of processors approaches the number of latitude rows. MOM 4 is able to subdivide its computational domain to much greater degree and can thereby make productive use of many more processors.

speedup versus number of processors in MOM 3 and MOM 4. The test configuration used 64 rows of latitude, 120 longitudes, and 15 vertical levels. Both versions of the model were run on 2, 4, 8, 16, 32, and 64 processors of the GFDL CRAY T3E and execution times were normalized by the execution time on 1 processor. The circles indicate the speedup over one processor using MOM 4 and the triangles represent the speedup over one processor using MOM 3. The speedup in MOM 3 peaks at 32 processors and then declines while the speedup in MOM 4 on 64 processors is still increasing. In absolute terms, the execution time of MOM 4 on 64 processors is a little less than one half of the execution time of MOM 3 on 64 processors.

Coding complexity has also been reduced by removal of the memory window and by the use of averaging and derivative operators. Further improvements in speed are expected

to follow once operators have been optimized for better use of cache and registers. MOM 4 is compliant with the Flexible Modeling System (FMS) and will be added to the FMS repository once the driver for interfacing MOM 4 to the atmosphere and ice models has been written. After MOM 4 has been added to the FMS repository, MOM 4 will be available for addition of physics modules.

PLANS FY01

Future plans include further optimization of speed once the new GFDL computer system is in place. Parameterizations such as Redi-diffusion and Gent McWilliams skew flux will have to be rewritten. An adjoint of MOM 4 will be built using the Giering TAF compiler. MOM 4 will be coupled to ice and atmosphere models using the FMS exchange grid.

5.2.2 Isopycnal Coordinate Model Development

R. Hallberg *J. Stephens*

ACTIVITIES FY00

Isopycnal coordinate ocean models offer several potentially important advantages over traditional level models. But disadvantages (such as the difficulty of representing the nonlinear equation of state, the need to use a nonlinear and nonlocal treatment of vertical mixing especially in dense flows over sills, and the difficulty of representing mixed layer dynamics in the detraining phase) have in the past been limitations for this class of model. Many of these difficulties have now been addressed.

GFDL's isopycnal coordinate ocean model (HIM1.0) was officially released to the community this past year. New technical features include run-time specification of many parameters, flexible registration style temporal averaging and determination of the output fields, full support of NetCDF-based input and output, and run-time determination of parallel processor count. HIM may be run in parallel using a one- or two-dimensional domain decomposition, and this past year HIM was ported to 8 different parallel computers without having to change a single line of code. Also, the calling interface of HIM1.0 is now essentially compatible with that of MOM 4. HIM development is now managed with modern version control software.

The effects of the nonlinear equation of state of seawater are particularly tricky to incorporate into a model which uses a density-like vertical coordinate. In the past year, all of the effects of the nonlinear equation of state, including thermobaricity and cabbeling, have been incorporated into HIM. Potential density referenced to an interior pressure (typically 2000 dbar) is used as the vertical coordinate. But various other terms involving density gradients use different, locally appropriate measures. Gradients of *in situ* density (adjusted by a function of pressure only) are used to calculate pressure gradient accelerations. Locally referenced potential density is used to estimate the shear-Richardson-number-dependent diapycnal mixing (1707). Cabbeling is included by advecting potential temperature and salinity, and adjusting the vertical mixing to restore the coordinate density of each layer towards its target

value. Mixed layer dynamics use potential densities referenced to the surface to evaluate the mixed layer turbulent kinetic energy balances (although convective adjustment is also done if the coordinate variable is unstably stratified). In short, by separating the role of density as the coordinate variable from its other dynamic roles, all of the effects of the nonlinear equation of state of seawater can be described within an isopycnal coordinate ocean model.

PLANS FY01

Improved treatments of the mixed layer dynamics will be explored. These may include depictions of Ekman-driven mixed layer stratification, baroclinic instability within the mixed layer, penetrative short-wave radiation, and rotational constraints on convective efficiency. The use of HIM as the ocean component of a coupled model will be tested. Hybrid pressure-density vertical components and alternative horizontal grids will also be examined.

5.3 COASTAL OCEAN MODELING AND PREDICTION

5.3.1 East Coast and North Atlantic Modeling and Forecasting

T. Ezer *G.L. Mellor*
H.-C. Lee

ACTIVITIES FY00

A 6-year simulation of the Atlantic Ocean, west of 55°W, has been carried out using the sigma coordinate Princeton Ocean Model with a curvilinear grid. A comparison between experiments with and without surface fluxes shows that the effect of the surface wind stress and heat fluxes on the Gulf Stream path and separation is closely related to the intensification of deep circulations in the northern region. The separation of the Gulf Stream and the downslope movement of the Deep Western Boundary Current (DWBC) are reproduced in the model results. The model DWBC crosses under the Gulf Stream southeast of Cape Hatteras and then feeds the deep cyclonic recirculation east of the Bahamas. The model successfully reproduces the cross-sectional vertical structures of the Gulf Stream, such as the asymmetry of the velocity profile and the eddy activity of the Gulf Stream. Entrainment of the upper layer slope current into the Gulf Stream occurs near the cross-over point; the converging cross-stream flow is nearly barotropic.

Using the same model, the Loop Current and deep circulation in the Gulf of Mexico has been described. A deep cyclonic circulation, bounded by the deep basin in the eastern Gulf, is shown to be spun up by the Loop Current. The Loop Current also induces deep anticyclonic columnar eddies in the eastern Gulf which decouple from the upper layer Loop Current. The westward translation speed of a Loop Current Ring is about 2.5-6 cm/s. Lower layer eddies have a higher speed and lead the rings into the central Gulf. The time-average surface circulation of the Gulf of Mexico basin is anticyclonic, mainly due to the transport of anticyclonic vorticity by Loop Current Rings in the surface layer. An average lower layer cyclonic circulation occurs along the continental slope of the basin.

The Data Assimilation and Model Evaluation Experiments in the North Atlantic Basin (DAMEE-NAB), supported by the Office of Naval Research (ONR), has been completed with the publication of a special issue that includes an intercomparison between six different ocean models (1716). Sensitivity studies evaluate the effect of open boundary conditions, horizontal diffusivity, and model resolution on model variability and Gulf Stream dynamics (1715).

PLANS FY01

Future research will focus on the dynamics of the Loop Current and the deep circulation in the Gulf of Mexico. A coastal forecasting system based on a higher resolution version of the extended east coast model will be tested.

5.3.2 Turbulent Boundary Layer Modeling

T. Ezer *G.L. Mellor*

ACTIVITIES FY00

An improved surface boundary layer formulation has been developed to improve the Mellor-Yamada boundary layer model (ky). Unlike the situation in three-dimensional simulations or in the real ocean, the kinetic energy in one-dimensional surface layer models can build up and artificially enhance local mixing. Adding a sink term to the momentum equations counteracts this behavior. The sink term is a surrogate for energy divergence available to three-dimensional models, but not to one-dimensional models. The new sink term tends to exacerbate problems with overly warm summertime surface temperatures. A Richardson number dependent dissipation term yields a favorable improvement in the comparison between model calculations and observations.

Further testing of the modified Mellor-Yamada turbulence scheme with a three-dimensional North Atlantic Ocean model (1717) shows improvement in the simulations of the seasonal mixed-layer depth. The mixed layer in the three-dimensional model is shown to be strongly influenced by errors in the surface heat flux, the frequency of the forcing wind stress and most importantly, by penetration of short wave radiation, making the evaluation of the new turbulence scheme in three-dimensional models much more difficult than it is in one-dimensional models.

PLANS FY01

Future work will incorporate the effects of surface waves in both the surface boundary layer and bottom boundary layers in shallow water.

5.3.3 Princeton Ocean Model Development and Testing

T. Ezer *G.L. Mellor*

ACTIVITIES FY00

The Princeton Ocean Model (POM) users group has continued to grow. It now includes more than 700 users from 54 countries. User support and code development continues (for more detail consult the POM web page - www.aos.princeton.edu/WWWPUBLIC/htdocs.pom). Some of the new features that have been tested with POM during the last year include: a) a modified Mellor-Yamada turbulence scheme (1717, ky) that improves the simulation of vertical mixing and surface layers; b) a vertical generalized coordinate system that can accommodate z-level, sigma-level or other vertical discretizations (ip); c) a multidimensional positive definite advection transport algorithm; and d) a sixth-order accuracy combined compact difference scheme that significantly reduces pressure gradient errors. A parallel version of POM is currently being tested.

PLANS FY01

A new ONR-supported initiative will foster a collaboration between the POM developers and other ocean model developers from Rutgers University in order to develop and improve terrain-following ocean models and community support.

5.3.4 Climate Variability Studies with POM

T. Ezer *G.L. Mellor*

ACTIVITIES FY00

Sigma coordinate ocean models, originally developed for regional coastal studies and prediction, are now being used for long-term climate simulations. Attention is given to surface and bottom boundary layers which may play an important role in surface heat exchange and in deep water formation processes. Observed decadal variations in the North Atlantic Ocean during the period 1950-1989 have been successfully simulated with an Atlantic Ocean version of POM (1663) and compared favorably with a simple wind-driven Rossby wave model (ny). The simulations demonstrate the important role played by westward propagating planetary waves in affecting the subtropical gyre and Gulf Stream variations. An interesting finding was that, on decadal time scales, the ocean model responds in a linear fashion to the combined effect of surface temperature and wind stress anomalies. Simulations of the response of the ocean to heat and fresh water flux anomalies in high latitudes, a result of possible future climate change, show an adjustment process that takes a few decades (nz). Spatial climatic changes in circulation patterns and in coastal sea level will be studied in detail.

PLANS FY01

Research will focus on the interaction between climatic changes in the open ocean and variability in the coastal ocean. The effect of bottom boundary layers and the way they are formulated in ocean models on deep water formation will be further studied.

5.3.5 Coastal Models of the West Coast and the Gulf of Mexico

H.-C. Lee *M. Wei*
L.-Y. Oey

ACTIVITIES FY00

Research on the coastal observing systems off the west coast of the U.S. have started up recently as part of the National Ocean Partnership Program (NOPP). This work shows that details of the wind field, particularly the local wind curl, can be an important forcing to coastal circulation (1611). Studies based on coastal observations and models that continue to deploy sparse arrays of wind stations and coarse-resolution wind products (*e.g.*, NCEP or ECMWF) may therefore be incomplete. Hindcasts of the coastal variability in the Santa Barbara Channel, carried out in collaboration with the Scripps Institute of Oceanography, show that the high-resolution wind fields give the best results.

Observations have suggested that episodic subsurface current events in the Gulf of Mexico are caused by topographic Rossby waves (TRW) forced by Loop Current pulsation (north/south extrusion and retraction) and eddy shedding in the eastern Gulf. However, the existence of TRWs in coastal forecast models has never been rigorously established. A ten-year simulation has been analyzed to isolate the TRWs. Over 70% of the simulated subsurface energy was observed to reside in the 20 to 100 day periods in narrow bands over the continental slope and rise. Bottom intensification has been shown to exist in these high-energy bands. While the modeled TRWs are unambiguously forced by variability induced by the Loop Current and Loop Current Eddies, precise mechanism(s) through which energy is transmitted to lower layers is not yet understood.

PLANS FY01

High-resolution simulations of coastal variability along the west coast and Gulf of Mexico will continue.

5.4 GLOBAL BIOGEOCHEMISTRY AND THE CARBON CYCLE

5.4.1 Terrestrial Carbon Cycling

S.-M. Fan *S. Pacala**
*G.C. Hurtt** *J.L. Sarmiento*
P.C. Milly *E. Shevliakova***
P. Moorcroft

**Institute for the Study of Earth, Oceans, and Space, Univ. of New Hampshire*
***Dept. of Ecology and Evolutionary Biology, Princeton University*

ACTIVITIES FY00

Through a detailed analysis of forest inventory data, the relative contribution of land use, carbon dioxide fertilization, and nitrogen fertilization to carbon sequestration in U.S. forests has been quantified. Results show that land-use is the primary factor governing the rate of carbon sequestration in U.S. forests. This conclusion is further supported by a second analysis that compares U.S. carbon budgets obtained through inventories of forests and other components of the terrestrial carbon cycle with U.S. carbon budgets obtained through inverse modeling of CO_2 flask sample measurements. The findings of this study support the conclusion that changes in land-use account for most of the carbon being sequestered within the U.S., and reconciles a longstanding perceived inconsistency in the estimates obtained by these different methods.

The first implementation of a new terrestrial biosphere model, the Ecosystem Demography model (ED model), has been documented. A second implementation of the off-line model that examines the impact of human land-use on the terrestrial carbon cycle of North America is currently being completed. The results of this study show how historical changes in patterns of land-use across the continent during the past three centuries account for the spatio-temporal distribution of carbon stocks and fluxes during this period and how these effects are likely to continue into the next century.

The ED model has also been successfully coupled to a mesoscale model of the atmosphere (MM5 V3.3), and significant progress has been made towards integrating ED into GFDL's new FMS. Energy and moisture exchange parameterizations in MM5 have been modified to account for the sub-grid heterogeneity in vegetation distribution predicted by ED. The sub-grid scale heterogeneity includes ecosystem age and species type, and vertical profiles of plant canopy characteristics, in particular, the Leaf Area Index (LAI) and stomatal closure. The coupled ED-MM5 model is being used to explore the role of vegetation structure on diurnal patterns of fluxes between land surface and the lower atmosphere. Preliminary results obtained using the original OSU-ETA soil hydrology model show that the diurnal mode is able to capture the diurnal pattern of moisture and heat fluxes between atmosphere and biosphere in the tropical region.

A canopy interface that couples the atmosphere with vegetation and soil processes modeled by ED has also been developed. In this parameterization, sensible heat and moisture

fluxes from leaves and soil surface are calculated using a multiple resistance parameterization and turbulent mixing inside the canopy is assumed to be dominated by gusts with a size characteristic of the height of canopy. Mass and energy are transported directly from leaf surfaces to the top of the canopy, while diffusion between leaf layers is assumed to be small and thus neglected. Effective canopy air temperature and moisture content near the top of the canopy are calculated as linear combinations of temperature at the bottom layer of the atmosphere, ground temperature and leaf temperature through the canopy.

PLANS FY01

The ED model will be integrated with forest inventory and land-use history data to complete a global, off-line implementation. The MM5-ED model will be used to: 1) analyze the impact of anthropogenic land use practices on the regional distribution and dynamics of CO_2 sources and sinks; and 2) understand the role of plant rooting depth on the biophysical feedback to local climate. This research will explore a range of perturbations to the land atmosphere system that represent scenarios of land-use and vegetation succession in different regions. Once incorporated into FMS, ED will form the terrestrial component of a global, land-atmosphere-ocean model that we will use to study the importance of biospheric feedbacks for global climate. A particular focus will be the identification of regions where ecosystem dynamics have a significant impact on the regional climate.

5.4.2 Inverse Modeling of Carbon Isotopic Ratios of CO_2 in the Atmosphere

S.-M. Fan *J.L. Sarmiento*
*E.M. Gloor**

**Max-Planck Institute for Biogeochemistry, Jena, Germany*

ACTIVITIES FY00

Over the past two years, the steady-state distribution of carbon isotopic ratios in atmospheric CO_2 has been modeled using the GFDL Global Chemical Tracer Model (GCTM), which uses a year-long record of wind fields generated previously by a general circulation model. Prescribed air-sea isotopic fluxes without seasonal variability are used to force the model over the oceans. The annual isotopic fluxes due to terrestrial net primary production and respiration were estimated for three land regions (Eurasia, North America, and the tropics and Southern Hemisphere) by inversions of atmospheric observations of the isotopic ratios. The inversion results suggest for the 1993-1995 period the presence of a terrestrial carbon sink in the midlatitude Northern Hemisphere and a terrestrial carbon source in the tropics. The terrestrial carbon source and sink were estimated previously for the 1980s and 1990s from inversions of atmospheric CO_2 mixing ratios

PLANS FY01

The goal of this work is to estimate, using inverse models, the isotopic carbon fluxes between air and ocean, as well as between air and land. The isotopic fluxes are caused by net oceanic CO_2 uptake and by the existence of an air-sea disequilibrium due to a lagged

isotopic Suess Effect in the ocean. On-going global ocean general circulation and biogeochemistry model simulations by the Carbon Modelling Consortium (CMC) will be used to predict the net CO_2 uptake and the disequilibrium isotopic carbon fluxes from the pre-industrial times to the present. The inversion results will be combined with ocean models to improve the estimate of the oceanic uptake of CO_2 and the estimate of the terrestrial carbon fluxes for different geographical regions. A time-dependent inverse model of atmospheric carbon dioxide and its isotopic ratios may be developed towards this goal.

5.4.3 Mixing Parameterizations, Large-Scale Ocean Circulation, and Global Biogeochemical Cycles

A. Gnanadesikan *J.L. Sarmiento*
*N. Gruber** *R. Slater*
I. Marinov *P.S. Swathi*

**Dept. of Atmospheric Sciences, UCLA*

ACTIVITIES FY00

It has been shown that the large-scale pycnocline depth can be explained by multiple combinations of wind stress, Southern Ocean eddy fluxes, and low-latitude diffusion (1595). However, different combinations of vertical and lateral mixing result in very different pathways for vertical exchange. A suite of model runs was performed in which the vertical and lateral diffusion were changed in a way that produced a similar pycnocline depth. In one case (with low vertical and lateral mixing) relatively little upwelling of deep water occurred through the low-latitude pycnocline. In a second case (with high vertical and lateral mixing) about 18 Sv of upwelling occurred through the low-latitude pycnocline. The high and low mixing cases are quite similar in their thermal structure, but the high mixing case has slightly higher uptake of CFCs and anthropogenic CO_2, and a new production which is twice that of the low mixing case (pc). This is because the high mixing model has more upwelling at low latitudes and more convection at high latitudes. Additional model runs were made with high vertical mixing only in the Southern Ocean. In these runs, the amount of convection in high latitudes increased, but the low-latitude upwelling was essentially unchanged.

PLANS FY01

Analysis of the suite of model runs will continue. Particular attention will be paid to the effect of nutrient fertilization on anthropogenic CO_2 uptake and low-latitude production. Development of the ocean general circulation model will continue with a focus on improving the deep circulation.

5.4.4 Air-Sea Fluxes of O_2 and CO_2 Determined by Inverse Modeling of Ocean Bulk Measurements

*E.M. Gloor** *J.L. Sarmiento*
*N. Gruber***

**Max-Planck Institute for Biogeochemistry*
***Dept. of Atmospheric Sciences, UCLA*

ACTIVITIES FY00

A method has been developed to estimate the air-sea fluxes of gases from their observed distributions in the interior of the ocean. An ocean circulation model is used to establish a relationship between a unit air-sea flux in a given region of the surface ocean and the concentration at any point in the interior of the ocean. The surface ocean is divided into 15 regions, each of which contributes to the interior concentration at any location in the ocean. The tracers are linear (*i.e.*, additive), so the model predicted concentration in any given region is equal to the sum of the 15 components. In a final step, the Singular Value Decomposition is used to estimate the actual magnitude of the air-sea fluxes in each of the 15 regions by requiring that the predicted interior concentrations fit the observations.

The method has been applied to estimating the air-sea flux of heat, water, O_2, and CO_2. Before the method could be applied to O_2 and CO_2, the observed concentrations had to be corrected for the changes in water column chemistry that are due to biological cycling. This was done using the observed phosphate, nitrate, and alkalinity distributions, and assuming that the stoichiometric oxygen and carbon to phosphate ratios in organic matter are constant. The observed CO_2 distribution must also be separated into a pre-industrial component, which is assumed to be at steady state, and an anthropogenic component. This separation enables estimation of both the pre-industrial air-sea flux distribution, and anthropogenic carbon uptake.

PLANS FY01

Estimates of CO_2 uptake will be made as more estimates of anthropogenic CO_2 become available from the World Ocean Circulation Experiment.

5.4.5 An Ecosystem Model for Biogeochemical Studies

*R. Armstrong** *N. Gruber***
C. Deutsch *J.L. Sarmiento*
A. Gnanadesikan *R. Slater*

**Marine Sciences Research Center, SUNY-Stony Brook*
***Dept. of Atmospheric Sciences, UCLA*

ACTIVITIES FY00

A simplified ecosystem model has been developed for use in biogeochemical studies. The ecosystem model is simple in the sense that it has few state variables, yet advanced in the sense that it captures fundamental features concisely. The production model consists of two state variables representing small and large producer organisms. These are parameterized in a way that captures the difference between small and large phytoplankton, as well as the production and temperature dependent behavior of the f-ratio. The model is simple enough that four of the parameters needed for its specification can be estimated from the f-ratio data, and the other two can be estimated from fits to Levitus nutrient data.

PLANS FY01

The ecosystem model simulations will be compared with local patterns of seasonal variation in nutrients and chlorophyll at long term study sites (the Bermuda Atlantic Time Series and Ocean Weather stations), as well as satellite chlorophyll data and primary production estimated from these data. These comparisons give a measure of the ability of the model to reproduce seasonal and interannual patterns of production, as well as identifying regions where additional biogeochemical processes such as iron limitation will need to be added. Future development of the model will include splitting of production among taxonomic categories (diatoms, calcium depositors, and other algae) to match observed latitudinal patterns in silicate, phosphate, and alkalinity.

5.4.6 Oceanic Nitrogen Cycle

C. Deutsch *J.L. Sarmiento*
*N. Gruber**

**Dept. of Atmospheric Sciences, UCLA*

ACTIVITIES FY00

An analysis of nitrogen cycling in the Pacific has recently been completed based on nutrient data from the World Ocean Circulation Experiment (WOCE). The analysis uses the tracer N* (nitrate - 16◊·phosphate) to identify regions where nitrogen fixation and denitrification occur (1497). The analysis shows the basin to contain sources and sinks of fixed nitrogen with magnitudes that are significant on the global scale (about 50 TgN/yr of water column denitrification - a sink, and about 60 TgN/yr of newly fixed nitrogen).

PLANS FY01

Work is currently under way to prepare gridded fields from the high quality nutrient dataset provided by the WOCE program, with the aim of diagnosing the spatial patterns and rates of nitrogen fixation and denitrification by damping an OGCM toward those observed nutrient fields. This will allow exploration of a number of hypotheses regarding what controls the rates and locations of nitrogen inputs and outputs to the ocean. It will also enable diagnostic models of ocean carbon uptake to account for carbon transports that are associated with source and sink pathways in the marine nitrogen cycle.

5.4.7 Global Patterns of Marine Silicate, Nitrate, and Alkalinity Cycling

A. Gnanadesikan *J.L. Sarmiento*
*N. Gruber** *P.S. Swathi*
R.M. Key

**Dept. of Atmospheric Sciences/UCLA*

ACTIVITIES FY00

The large-scale field of nutrients has been used to identify regions where particular functional groups of plankton (in particular, silicifying organisms such as diatoms) are important. Typical diatoms have a silicate to nitrate molar uptake ratio of approximately 1:1. This observation is used to define a tracer Si* = (Si) - (N) of excess silicate concentration relative to the needs of such diatoms (Fig. 5.7). The dominant feature of deep ocean Si* is an increase along the pathway of the deep thermohaline circulation from a low of 0 to 10 μmol kg^{-1} in the North Atlantic to highs in excess of 100 μmol kg^{-1} in the deep North Indian and Pacific Oceans. This increase results from the well-known preferential dissolution of silicate in the deep ocean.

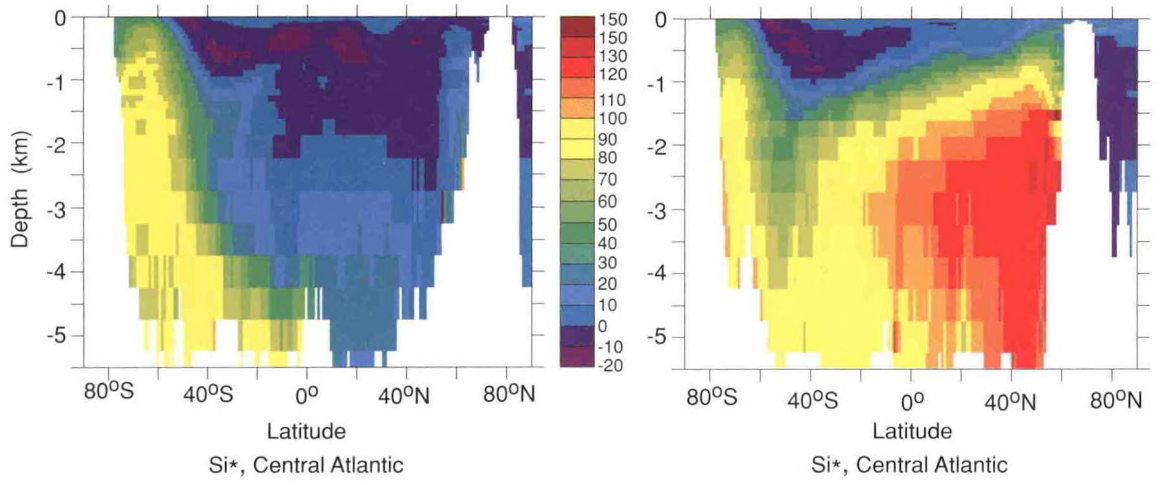

Fig. 5.7 Si* (dissolved silicate - nitrate in μmoles/kg) as a function of latitude in the Atlantic (left) and Pacific (right). All low and middle latitude surface waters in the ocean have less silicate than nitrate, *i.e.*, negative Si*. This feature is shown to originate in the Southern Ocean where silicate is preferentially stripped out by diatoms. Low-Si* water then penetrates equatorward as a plume of intermediate-depth water at about 600 m.

The high Si* waters of the abyss reach up to the surface in the Southern Ocean south of the Antarctic Polar Front. There the silicate is preferentially stripped out by diatoms with a Si:N ratio of approximately 5:1, consistent with this being an iron limited region. This generates a broad 20°-wide band of negative surface Si* around the entire Southern Ocean that subsequently penetrates to the north at the depth of the Subantarctic Mode Water (SAMW). The negative Si* supplied by the SAMW is the dominant feature of the upper kilometer of all ocean basins except the North Pacific, which is the only other place in the world where high Si* waters of the deep ocean are able to reach the surface. Consequently, most areas of the ocean outside the North Pacific and Southern Ocean have a deficit of silicate relative to nitrate. Within the North Atlantic, the low Si* water is swept downward with North Atlantic Deep Water. A more detailed examination of Si* shows how other processes such as shallow remineralization of nitrate relative to silicate modify the above overview. Of particular interest is the fact that there is no clear indication of a high Si:N drawdown in the iron limited North Pacific.

PLANS FY01

The global analysis will be extended to look at the effects of calcifying organisms. The goal is to identify regions where coccolithophorids are dominant producers using the water mass distribution. Results will be compared with satellite estimates for calcification under way at other institutions. A key product will be an estimate of the fraction of new production associated with these functional groups. Simulations which evaluate the effects of changes in the relative fraction of carbonate and silicate producing organisms on the carbon cycle will then be carried out.

5.4.8 Analysis of the Ocean's Carbon Pumps

S. Carson *J.L. Sarmiento*
A. Gnanadesikan *J.R. Toggweiler*
*R. Murnane**

**Bermuda Biological Station for Research*

ACTIVITIES FY00

It is almost axiomatic that temperature anomalies imposed on the ocean near the poles will have a greater effect on the partitioning of CO_2 between the ocean and atmosphere than temperature anomalies imposed in low latitudes. This is true because most of the ocean's volume comes into contact with the atmosphere through cold polar outcrops. Two influential papers published during the last two years[1,2] have shown that this polar temperature sensitivity is not nearly as strong in GCMs as it is in box models. Broecker and Archer suggest that this is true because vertical mixing in GCMs allows the solubility effect of warm surface temperatures to be felt well down in the interior of the ocean. Broecker and

1. Broecker, W. S., J. Lynch-Stieglitz, D. Archer, M. Hofman, E. Maier-Reimer, O. Marchal, T. Stocker, and N. Gruber, How strong is the Harvardton-Bear constraint?, *Global Biogeochem. Cycles, 13*, 817-820, 1999.
2. Archer, D., G. Eshel, A. Winguth, W. Broecker, R. Pierrehumbert, M. Tobis, and R. Jacob, Atmospheric CO_2 sensitivity to the biological pump in the ocean, *Global Biogeochem. Cycles*, in press.

Archer imply that the mixing effect in GCMs carries over to the other "carbon pumps" in the ocean, namely those involving the production and remineralization of organic particles and $CaCO_3$.

A new method has been devised for disaggregating the carbon pumps in ocean models to explore these issues. The results show that the critical distinction between box models and GCMs has less to do with mixing than with the relative areas over which atmosphere-deep ocean communication is allowed to occur. GCMs have less polar sensitivity than box models because the high-latitude gas exchange that allows CO_2 to move between the deep ocean and atmosphere is restricted by limited areas of convection and deep water formation. The polar boxes in box models tend to be fairly large, typically occupying 5-10% of the overall ocean area. With such a large area, the effect of gas exchange in box models is less limiting. It is found, furthermore, that the effect of limited gas exchange is different for the thermal solubility effect than it is for the CO_2 pumped down into the deep ocean by organic particles. This is because the critical region where limited gas exchange influences CO_2 solubility is in the North Atlantic while the critical region for the organic carbon pump is in the Southern Ocean.

PLANS FY01

The new method for disaggregating carbon pumps described above has been applied so far only to one GCM-based biogeochemistry simulation (1617). In the coming year, the new method will be used to examine other GCM simulations and data from the real ocean.

5.4.9 Response of Ocean Biology to Future Climate Change

J.L. Sarmiento R. Stouffer
R. Slater

ACTIVITIES FY00

In collaboration with modeling groups at CSIRO (Australia), the Hadley Center (United Kingdom), Max Planck Institute (Germany), the Institute Pierre et Simon Laplace (France), and NCAR, six different coupled climate model simulations of future climate change are being examined to determine the range of behavior of those aspects of global warming simulations that are relevant to the ocean biological response. The overall response inferred from examining the physical response of the ocean to global warming is decreased biological production in low latitude upwelling regions and the poleward half of the subtropical gyres, and increased production in the polar regions.

Wind-driven upwelling is the dominant mechanism of nutrient supply along the highly productive western margins of the continents and in the equatorial regions. Models predict widely varying results, but the general tendency is towards a reduction of upwelling in these regions, from which it is inferred that biological production would decrease. The dominant mechanism for nutrient supply in the subtropical gyres poleward of the subtropical

convergence zone is wintertime convection. These regions tend to become more stratified with future climate change, which reduces the depth of wintertime mixing. The expectation, supported by model predictions, is that this would result in reduced biological production. The polar regions generally have a high supply of nutrients due to upwelling and convection, but can suffer from low productivity due to low light supply in deep mixed layers. Increased stratification, which occurs in most models, though with a complex pattern, would thus tend to increase biological production. Exceptions to this would be where low levels of micronutrient supply by dust limit the production, such as is thought to be the case in the Southern Ocean and North Pacific, or where the decreased mixing reduced the nutrient supply to less than the potential biological uptake.

The mechanism of nutrient supply to regions between the equatorial upwelling bands and subtropical convergence is poorly understood and poorly simulated in most models. It is difficult to determine how these regions will respond to future climate change. The changes described will also very likely lead to changes in ocean ecology, as the major phytoplankton groups such as diatoms, coccolithophorids, flagellates, Phaeocystis, and nitrogen fixers are sensitive to water column stratification, as well as nutrient content.

PLANS FY01

The analyses made to date are local analyses, and do not consider impacts of changes in one part of the ocean on other parts of the ocean. In the coming year, special attention will be paid to this question. A particular area of interest is the effect of increased high latitude production on nutrient supply to the low latitudes.

6. CLIMATE DIAGNOSTICS

GOALS

To determine and evaluate the physical processes by which the earth's climate and the atmospheric and oceanic general circulations are maintained in the mean, and by which they change from year to year and from decade to decade, using all available observations.

To compare results of observational studies with similar diagnostic studies of model atmospheres and model oceans developed at GFDL and thereby foster an enhanced understanding of both observed and simulated climate systems.

6.1 COMPILATION OF A TEMPORALLY HOMOGENEOUS RADIOSONDE TEMPERATURE DATASET

ACTIVITIES FY00

6.1.1 Sensitivity of Radiosonde Temperature Trends to Data Quality

*D. Gaffen** *J.R. Lanzante*
S.A. Klein

** Air Resources Laboratory*

Progress has been made in applying adjustments to a global network of 87 radiosonde stations so as to render their temperature time series more temporally homogeneous. Adjustment is needed due to artificial discontinuities introduced when instruments or recording practices were changed. These adjusted data are intended for use in the study of long-term climate variability, particularly with regard to global temperature trends. This effort builds on progress made recently (1699) in quantifying the sensitivity of various factors involved in the process of making adjustments and estimating trends.

The laborious task of identifying artificial change-points (abrupt changes in time series) has been completed. This procedure entailed visual examination and consideration of all data and a variety of ancillary information on a station by station, level by level basis. The tools employed were a unique compilation of station history meta-data (created at ARL), diurnal differences in the temperatures, vertical temperature structure, and non-temperature measures of climate variability, among others.

A complex algorithm for adjusting the data has been developed and coded, along with related graphical tools. The scheme employed attempts to make adjustments in such a way as to preserve the natural vertical coherence of the temperature data. This is accomplished by making adjustments using "reference levels" from the same station (*i.e.*, vertical levels which do not require adjustment and, excluding the effects of any artificial

discontinuities, correlate highly with the level to be adjusted). After a level has been adjusted it can potentially serve later as a reference level. This scheme is an attempt to remove the artificial component of change while retaining the natural component. In a minority of cases when suitable reference levels are not available, adjustment is made by a method which assumes that the difference in mean temperature across the change-point is entirely artificial.

After completing the identification of artificial change-points, the newly developed adjustment method was applied to the radiosonde station data. This process was repeated more than once in order to create different "scenarios" of adjusted data based on either various levels of confidence in the identification of artificial change-points or other procedural differences. Such an approach allows for testing the sensitivity of low frequency variability (especially trends) to some of the details of the identification and adjustment processes. Having completed these initial steps, various analyses involving internal sensitivity and consistency checks, comparisons with other observed datasets, and comparison with model (GCM) data were started.

ACTIVITIES FY01

The effort to create and examine a more temporally homogeneous radiosonde temperature data base will continue. The adjusted data will be used to assess long-term trends and compared to a number of observational and GCM datasets for the assessment of global change. It is anticipated that the observed data used for comparison will include Microwave Sounding Unit (MSU), surface station, and NCEP/NCAR Reanalysis temperature data. An additional project involving wider external collaboration will be initiated and will focus on development of operational radiosonde products for use in near real-time diagnosis of temperatures in the free atmosphere.

6.2 ANALYSIS OF DATASETS BASED ON SATELLITE OBSERVATIONS

ACTIVITIES FY00

6.2.1 Decadal Variations in Tropical Water Vapor: An Evaluation of Satellite Observations and a Model Simulation

B.J. Soden *S.R. Schroeder**

** Texas A & M University*

It is widely believed that water vapor amounts will increase in response to global warming. Climate models predict that the column-integrated water vapor, or total precipitable water (*W*), will increase by ~7% per 1°C increase in surface temperature. Consequently, if the global warming in response to a doubling of CO_2 approaches the upper range of current model predictions (~4.5°C), water vapor amounts could increase in excess of 20% during the next half century. This amplified moistening of the atmosphere in response to a surface warming not only highlights the importance of water vapor feedback in determining the climate sensitivity of GCMs, but also underscores the importance of long-term monitoring of water vapor to the detection and attribution of climate change.

Despite its obvious importance, there have been relatively few observational studies of the long-term variations or trends in water vapor. Moreover, there have been few, if any, attempts to compare observed trends against model-predicted trends, or to inter-compare observed trends from different observing systems. To address this issue, multiple satellite records of tropical-mean water vapor were compared with a general circulation model (GCM) simulation to assess our ability to monitor and predict low-frequency changes in *W* (1741). Particular attention was focused on the drying between 1979-1995 recorded by a TOVS-statistical retrieval which is calibrated to radiosondes. A version of the GFDL GCM integrated with observed time-varying SST forcing, as well as observational estimates based on microwave and TOVS-physical retrievals, show no sustained drying in the last two decades (Fig. 6.1). This discrepancy is consistent with a previous assertion that the TOVS-statistical

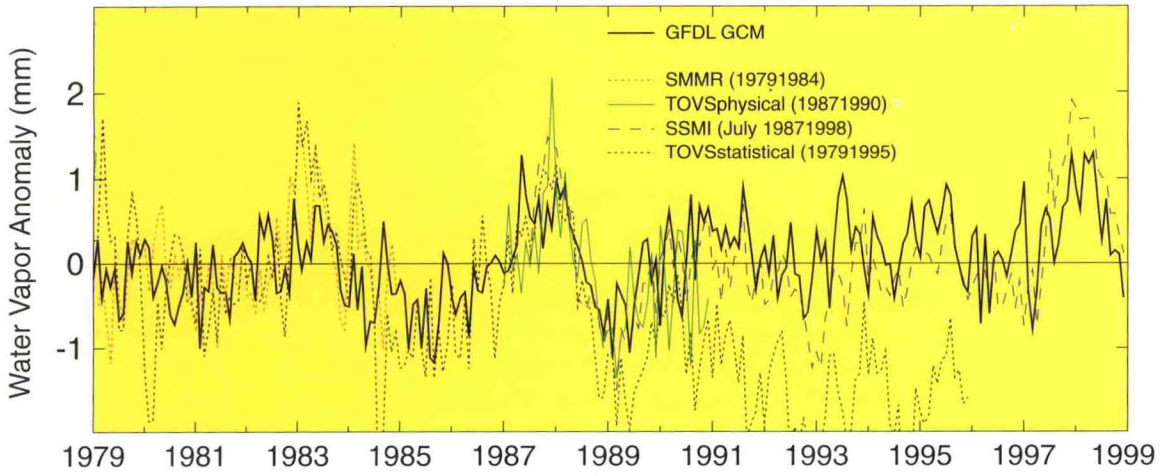

Fig. 6.1 Comparison of the interannual anomalies of tropical-mean precipitable water from GCM simulations (black) with satellite observations (colored) for the period 1979-1998. A version of the GFDL GCM, integrated with observed time-varying SST as the lower boundary condition, successfully captures the observed interannual-to-decadal fluctuations in tropical water vapor concentrations.

algorithm is vulnerable to radiosonde instrumentation changes over this period, which introduce an artificial drying trend into the retrieval. The comparison also demonstrated excellent agreement between the observed variations in tropical water vapor over the 1979-1999 period and those predicted by the GCM integration.

6.2.2 Reconciling Surface and Satellite Temperature Records

B.J. Soden

The nature of temperature trends in the lower troposphere is a subject of considerable debate. Satellite observations from the Microwave Sounding Unit (MSU) channel 2LT exhibit little warming over the period of record (1979-present), in contrast to the distinct warming trend evident in surface records. A key point of debate in interpreting the MSU temperature records centers on the ability to correct for known degradations in the satellite orbit, which have been shown to introduce a spurious cooling trend in the record. While attempts have been made to correct for these spurious drifts, comparison with radiosonde temperature

records suggests that a cooling drift, consistent with that expected from changes in the satellite orbit, still remains in the MSU record.

Figure 6.2 compares the globally averaged difference in the lower tropospheric temperature between MSU and an objectively-analyzed radiosonde dataset. The MSU record exhibits a distinct cooling trend over the period 1979-1994 relative to the radiosonde data. Also shown in this figure is the expected spurious trend in the MSU lower tropospheric temperature record based upon known changes in satellite orbit. A notable similarity between the two time series is discernible, suggesting that there still remains a spurious downward (cooling) drift in the MSU temperature record.

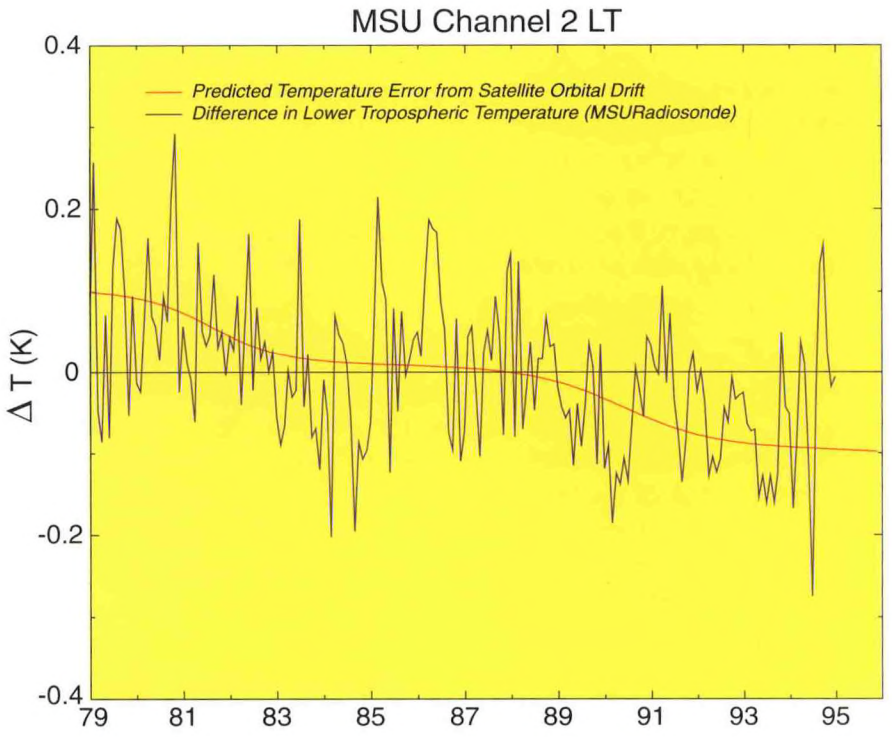

Fig. 6.2 Difference in global mean lower tropospheric temperatures as estimated using MSU satellite measurements and radiosonde observations (blue) and the expected spurious drift in MSU temperature measurements due to decay of the satellite orbit (red). The close similarity between the two curves suggests that there still remains a spurious downward (cooling) drift in the MSU temperature record due to changes in satellite orbit.

PLANS FY01

Future intercomparisons will be performed between the radiosonde and satellite observations of upper tropospheric water vapor on a station-by-station and satellite-by-satellite basis, so as to assess their utility for climate monitoring. In order to construct a homogeneous record of water vapor for trend detection, particular effort will focus on identifying and quantifying discontinuities associated with radiosonde instrumentation or satellite calibration changes.

6.3 AIR-SEA INTERACTION

ACTIVITIES FY00

6.3.1 Experimentation with an Atmospheric General Circulation Model Coupled to an Ocean Mixed-Layer with Variable Depth

M. Alexander M.J. Nath*
*J.R. Lanzante J. Scott**
N.-C. Lau

**Climate Diagnostics Center/NOAA*

A coupled model has been developed utilizing a one-dimensional ocean mixed-layer model (MLM) developed at the Climate Diagnostics Center (CDC) and a GFDL atmospheric GCM. The mixed-layer in the oceanic component has a variable depth, with computations of temperature and salinity changes at 31 levels in the vertical. The ocean model considers fluxes through the air-sea interface and vertical re-distribution in the column, but excludes any horizontal communication in the ocean. The atmospheric component is a full GCM with horizontal resolution of R30 and 14 levels in the vertical.

Having completed the initial testing of this new coupled model, several ensembles of experiments were conducted using different spatial configurations of the ocean model. Since the main goal of this project is to assess the impact of El Niño-Southern Oscillation (ENSO) on global sea surface temperature (SST) variations, all of the experiments entail prescription of SST anomalies in the deep tropical eastern Pacific (DTEP, defined as the region between ~173°E and the South American coast, and within ~15°N-15°S) as observed in the 1950-1999 period. These experiments will henceforth be referred to as the Deep Tropical Eastern Pacific Ocean-Global Atmosphere (DTEPOGA) runs.

The "standard" experiment uses the SST forcing in DTEP, with the MLM employed elsewhere in the World Oceans. A sixteen-member ensemble of this experiment has been completed, with each run being initiated from an independent set of atmospheric conditions. To compliment this model scenario, a set of eight "control" integrations has been completed in which the MLM was not used; instead, seasonally varying climatological SSTs (computed from the "standard" DTEPOGA runs) were specified outside of DTEP. Finally, an eight-member ensemble of the "North Pacific" (NP) experiment has been completed. In this scenario, the MLM was employed only in the North Pacific Ocean, and observed climatological SSTs were specified elsewhere outside of DTEP. The purpose of the NP experiment is to isolate the influences of ENSO on SST variability in the North Pacific through changes in the overlying atmospheric circulation. The data generated by the coupled model has been distributed to external collaborators. In particular, a large subset of the model output was sent to CDC.

The DTEPOGA experiments have been analyzed in conjunction with a previous series of integrations based on coupling of the same R30L14 atmospheric GCM to an oceanic mixed layer model with a constant depth of 50 m. The domain of SST prescription in the model

runs using fixed mixed layer depth extends across the entire width of the tropical Pacific between ~25°N and ~25°S. Integrations with the 50-m mixed layer incorporated at all ocean grid points outside of the tropical Pacific are referred to as the TOGA-ML runs; whereas the corresponding control experiment (*i.e.*, with climatological SST conditions prescribed outside of the tropical Pacific) is labeled as the TOGA experiment. Four-member ensembles of the TOGA-ML and TOGA experiments have been completed for the 1950-1999 period.

6.3.2 Atmospheric Bridge Linking ENSO to SST Variability in the North Pacific and North Atlantic

*M. Alexander** *N.-C. Lau*
*I. Blade*** *M.J. Nath*
J.R. Lanzante

**Climate Diagnostics Center/NOAA*
***Universitat Politècnica de Catalunya, Barcelona, Spain*

Both observational data and output from the TOGA-ML experiment (6.3.1) indicate that the imposed ENSO forcing during mid-winter is accompanied by prominent atmospheric circulation changes over the North Pacific and Atlantic. These teleconnection patterns in turn alter the heat exchange across the local sea-air interface. The extratropical SST anomalies generated by this "atmospheric bridge" mechanism (1393) typically attain maximum amplitudes in late winter or early spring.

Detailed diagnoses of the monthly evolution of the surface heat budget during ENSO episodes at selected sites have been performed (nk). The simulated SST response exhibits a 1-2 month delay relative to temperature changes in the overlying atmosphere. This lag relationship results in a polarity change of sea-to-air gradients in temperature and water vapor mixing ratio in late winter. From late autumn through mid-winter, the action of the climatological wind on these gradients results in enhancement of the developing SST anomalies. In the months thereafter, the reversed gradients are accompanied by attenuation of the SST signal. Shortwave radiative fluxes associated with variations in cloud cover play an important role in SST variability at some of the subtropical sites.

The nature of sea-air feedbacks in the extratropics has been studied by contrasting the output from the TOGA-ML and TOGA experiments (6.3.1). Incorporation of sea-air coupling in TOGA-ML is seen to enhance the persistence of the ENSO-related atmospheric anomalies in the extratropics through late winter and early spring. Comparison with results from previous studies on midlatitude sea-air interactions suggests that part of the atmospheric signal in TOGA-ML may be attributed to forcing from extratropical SST anomalies produced by the atmospheric bridge mechanism.

Preliminary diagnosis of the output from the DTEPOGA experiments (6.3.1) confirms the principal findings based on the TOGA-ML and TOGA runs. Comparison between the results from the "standard" and "NP" scenarios (6.3.1) reveals that the atmospheric signals in the latter scenario are stronger, thus suggesting the presence of negative interferences from

atmospheric responses to SST anomalies generated in the Indian Ocean or tropical western Pacific through tropical atmospheric bridges.

6.3.3 Impact of ENSO on Monsoon Systems in East Asia and Australia

N.-C. Lau *B. Wang**
M.J. Nath

**University of Hawaii*

Previous observational studies have indicated that warm ENSO events are accompanied by the development of a wintertime near-surface anticyclone over the Philippine Sea region. The southwesterly wind anomaly on the northern flank of this circulation feature is opposite to the climatological northeasterly (dry) winter monsoon over East Asia. The resultant weakening of the monsoon flow brings about above-normal precipitation and temperature in that region. The air-sea interaction associated with the Philippine anticyclone is also known to influence the SST conditions in the South China Sea and tropical western Pacific. Such altered conditions could affect the subsequent development of the Meiyu/Baiu rainbands over eastern China and Japan in the following spring and early summer.

Diagnosis of both the TOGA and "control" DTEPOGA experiments (6.3.1) illustrates that the GCM simulates the above-mentioned ENSO influences on the East Asian winter monsoon with a high degree of fidelity. In accord with the observations, the composite model anomaly near the surface in the control DTEPOGA integration is characterized by an anticyclone over the Philippines during warm events (Fig. 6.3). The southerly flow to the west of the anomalous high pressure center leads to warmer and wetter conditions than normal. The reduced wind speeds and cloud cover over the South China Sea result in considerable warming of the oceanic mixed layer, whereas the enhanced northeasterly circulation to the east of the anomalous anticyclone is conducive to oceanic cooling. Both the atmospheric and oceanic anomalies over the subtropical western Pacific exhibit a tendency to migrate eastward during the spring season.

Also noteworthy in the patterns of Fig. 6.3 is the appearance of the anticyclone off the eastern Australian coast, which exerts a considerable influence on the summertime circulation in that sector. The salient symmetry about the equator of the anomalous features over the western Pacific is suggestive of a Rossby-wave response to reduced near-equatorial convective heating in that sector, when the ascending branch of the Walker Cell is displaced eastward during warm ENSO events.

6.3.4 Modulation of Tropical Transient Activity by ENSO

N.-C. Lau *C.-Y. Tam*

The impact of ENSO events on the geographical distribution and intensity of tropical atmospheric variability on synoptic (~several days) and intraseasonal (30-60 days) time scales has been examined using both NCEP/NCAR reanalyses and output from the TOGA experiment (6.3.1). The preferred sites of eddy activity, propagation behavior and

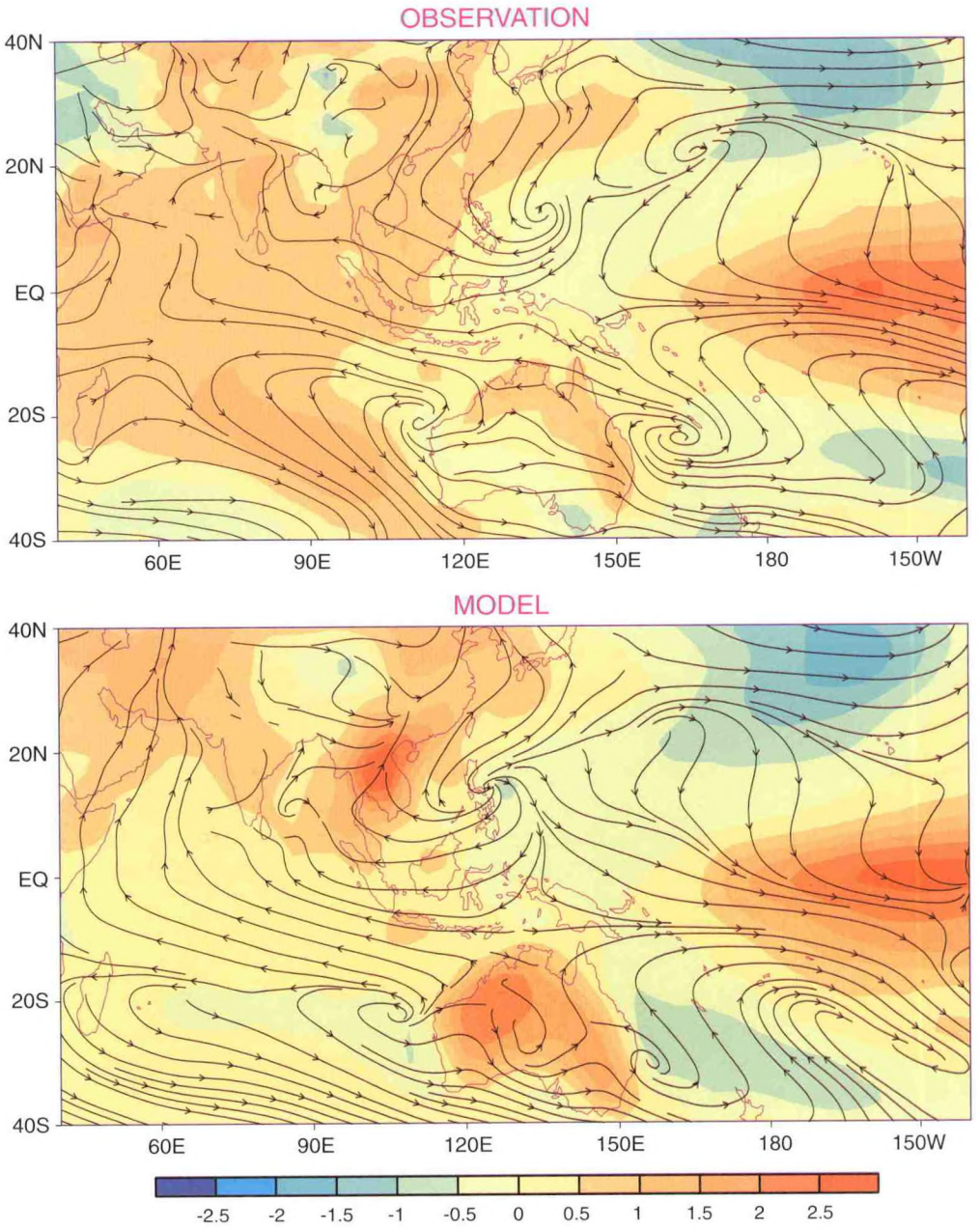

Fig. 6.3 Distributions of the near-surface circulation (streamlines) and temperature (color shading, see scale at bottom), as obtained by subtracting the composite data over nine cold ENSO events from those over nine warm events in the 1950-1999 period. The top panel is based on NCEP/NCAR observational reanalyses. The lower panel is based on the eight-run ensemble average simulated in the "control" DTEPOGA experiment. These panels portray the typical atmospheric response during El Niño episodes. Note, in particular, the circulation and temperature anomalies in the vicinity of the Philippines and off the eastern Australian coast.

growth/decay characteristics of these disturbances have been identified using lagged regression statistics, variance analysis, and complex empirical orthogonal functions. It has been demonstrated that the GCM is capable of reproducing the essential regional and

seasonal characteristics of the observed transient activity in the tropics. The results also indicate that the occurrence of ENSO has noticeable effects on the propagation speed, as well as locations of growth and attenuation, of the these disturbances. Further analysis suggests that such influences are attributable to spatial shifts in convective zones accompanying the development of ENSO events, and to changes in the atmospheric steering flow when such events occur.

PLANS FY01

With the integration of the coupled oceanic mixed-layer model/atmospheric GCM having been completed, future efforts will be devoted to more detailed examination of the model output, with particular emphasis on remote atmospheric and oceanic responses to ENSO forcing, and on local air-sea interactions in the extratropics.

The relative contributions of enhanced persistence and positive dynamical air-sea feedbacks to the springtime atmospheric signals associated with ENSO will be further investigated using the suite of DTEPOGA integrations. The nature of the atmospheric responses in the North Pacific to SST forcing in the Indian Ocean and western tropical Pacific will be studied. The role of tropical Atlantic SST anomalies in atmospheric variability in the North Atlantic sector will also be analyzed.

The relationships between ENSO-related processes and the Asian-Australian monsoon systems will be further delineated using the available observational and model datasets. Particular emphasis will be placed on the origin of the variability of the air-sea coupled system on biennial time scales, and on extratropical influences of monsoon fluctuations during the summer season.

The characteristics of air-sea interactions accompanying the passage of atmospheric disturbances on synoptic and intraseasonal time scales will be documented using output from the TOGA-ML and DTEPOGA experiments. The teleconnections between extratropical flow features and tropical Madden-Julian Oscillations will be examined.

6.4 DEVELOPMENT OF WEB-BASED TOOLS FOR VISUALIZING AND EVALUATING MODEL OUTPUT

ACTIVITIES FY00

*M. Alexander** *S.A. Klein*
A.J. Broccoli *P.J. Kushner*
*J. Collins** *N.-C. Lau*
M.W. Crane *M.J. Nath*
K.W. Dixon *J.J. Ploshay*
K.P. Hamilton *A.J. Rosati*
*S. Hankin*** *J. Scott**
M. Harrison *H. Vahlenkamp*

**Climate Diagnostics Center/NOAA*
***Pacific Marine Environment Laboratory/NOAA*

Continued efforts have been made to design and improve a user-friendly web-based software package for visualizing and validating the output of the future FMS. The graphical and model evaluation tools assembled in a preliminary version of this package have been introduced to the GFDL community.

This project has been substantially reorganized to include applications to oceanic datasets, and to incorporate the advanced features in the data display and management toolkit maintained by the Thermal Modeling and Analysis Project at the Pacific Marine Environmental Laboratory (PMEL). A long-term partnership between GFDL and PMEL has been established to facilitate this collaboration. The latest version of the PMEL Live Access Server (LAS), which is a web-based interface to data sharing, visualization and analysis, has been successfully installed and tested at GFDL. Plans to link existing model evaluation tools to this framework have been formulated. Enhancements and modifications to LAS aimed at improving its functionality in displaying both meteorological and oceanographic fields have been made. It is envisioned that the LAS facility, in conjunction with the generalized Internet-wide approach to data sharing through the Distributed Oceanographic Data Systems (DODS) network, will constitute a powerful and convenient tool for accessing and visualizing datasets from research centers throughout the world, and for evaluating the performance of various FMS experiments conducted at GFDL.

PLANS FY01

With the assistance of the PMEL staff, a fully operational version of LAS, with appropriate connections to various standard model evaluation routines, will be adapted for laboratory-wide use within GFDL. New output from various FMS experiments will be assembled and linked to this new software package. The multitude of data resources available through the DODS network will be exploited to facilitate intercomparisons between model-simulated and observational datasets.

6.5 GFDL/UNIVERSITIES COLLABORATIVE PROJECT FOR MODEL DIAGNOSIS

J.L. Anderson *M.J. Nath*
I.M. Held *P.J. Phillipps*
N.-C. Lau

ACTIVITIES FY00

The primary goals of this collaborative effort are to involve the university community in the analysis and design of numerical model experiments at GFDL for identifying the effects of anomalies in surface boundary conditions on interannual and interdecadal variability of the atmosphere, and to develop procedures for insightful analysis and comparison of GCM predictions of regional climate anomalies. The efforts of this collaboration are focussed on the mutual interactions between stationary eddies, low-frequency variability and storm tracks, the maintenance of regional climates and their sensitivities to ocean surface temperature, and the applications of these results to atmospheric predictability. Since 1990, this collaboration has received financial support from the Climate and Global Change Program of the NOAA/Office of Global Programs. The present group of extramural investigators include scientists from CDC, University of Washington, University of Illinois, Florida State University, University of Wisconsin at Milwaukee, and Pennsylvania State University. The final workshop for this decade-long effort was held in September 2000 at GFDL, at which the progress of our understanding of various scientific issues was reviewed, and the future continuation of cooperative arrangements among interested scientists was considered.

Significant achievements by GFDL investigators associated with this collaborative project during the past year include the completion of a comprehensive suite of 50-year (1950-1999) long experiments in which a variable-depth ocean mixed layer model is coupled to the atmosphere under different scenarios (6.3.1), improved understanding of the role of air-sea coupling in enhancing the persistence of extratropical atmospheric anomalies associated with ENSO (6.3.2), and identification of the impact of ENSO on tropical monsoon systems and transient activity (6.3.3, 6.3.4). Progress has also been made in summarizing the principal findings of this collaborative effort in a set of review articles to be published in a special issue of a journal.

PLANS FY01

The drafting process of the set of review papers on various research foci of this collaborative project will be completed. The manuscripts will be edited for publication in a scientific journal.

Efforts will be made to sustain this collaboration through identification of appropriate scientific problems and interested scientists, and consultation with funding agencies.

7. HURRICANE DYNAMICS

GOALS

To understand the genesis, development and decay of tropical disturbances by investigating the thermo-hydrodynamical processes using numerical simulation models.

To study small-scale features of hurricane systems, such as the collective role of deep convection, the exchange of physical quantities at the lower boundary and the formation of organized spiral bands.

To investigate the capability of numerical models to predict hurricane movement and intensity, and to facilitate their conversion to operational use.

7.1 HURRICANE PREDICTION SYSTEM

ACTIVITIES F00

7.1.1 Performance in the 1999 Hurricane Season

M.A. Bender *R.E. Tuleya*
T. Marchok

The 1999 Atlantic hurricane season, comprising 12 storms, turned out to be another busy year for the GFDL model. More than 290 forecasts were made at NCEP for the National Hurricane Center (NHC) at four initialization times per day. In the Eastern and Central Pacific, the GFDL model was run at NCEP for 162 cases for the NHC. As in past years, the U.S. Navy continues to run their separate GFDL forecast system to support requirements in the Northwest Pacific, Indian Ocean, and various Southern Hemispheric Basins. In addition, during the 1999 Atlantic season the Navy ran the "GFDN" version of the GFDL model after the NCEP fire to provide support to the NHC when NCEP forecasts were not available.

7.1.2 Analysis of the Forecast Results

M.A. Bender *R.E. Tuleya*
T. Marchok

Skillful forecasts of intensity have been a challenging goal in hurricane forecasting. For the 1999 season, however, the GFDL system did exhibit skill at 48hr and beyond. When adjusted for initial bias, the GFDL model showed skill relative to SHFR (climatology and persistence) for the entire forecast period with mean errors 11, 17, and 17 knots at 24, 48, and 72hrs, respectively. This is evidence that forecast system changes made in prior years, including the addition of initial asymmetries (FY99), resulted in improvements for the 1999 season. There are indications that improvements in resolution and physical parameterizations, such as ocean

coupling, boundary layer and cumulus convection will lead to further improvements in these intensity forecasts (6.3, 6.4).

On the other hand, the GFDL track forecast error in the 1999 season was again strongly affected by the difficulties in NCEP's near-storm tropical analysis. Implementation of the higher resolution T170L42 analysis/forecast system was delayed until the 2000 season. Nevertheless, the GFDL forecast errors of 68,124 and 187 nautical miles at 24, 48, and 36hr exhibited considerable skill and were competitive with the Navy and UKMET global model guidance. After the 1999 season, NCEP corrected and improved their near storm analysis and the GFDL model was rerun for the cases of Dennis, Floyd, and Gert with dramatic improvements: for 63 cases, the GFDL 72h forecasts from the reanalysis yielded skill 50% better than climatology and persistence compared to only 35% for the GFDL operational run. It is anticipated that the level of skill will be high when the analysis system is implemented for the 2000 season.

7.1.3 The 2000 Hurricane Season

M.A. Bender *R.E. Tuleya*
T. Marchok

The GFDL hurricane forecast system was successfully converted and implemented on NCEP's distributed memory computer system. The entire forecast system was converted, including pre- and post- processing stages, vortex bogussing, and forecast dissemination. Also implemented was the extension of forecast period from three to five days, which has been run successfully for tropical systems in the Atlantic and Eastern Pacific basin. The GFDL-URI (University of Rhode Island) coupled model has also been installed in parallel mode at NCEP. The POM ocean model was implemented to run in parallel with the atmospheric model, so little overhead was required in the forecast step of the coupled system.

PLANS FY01

Performance of the GFDL system in the remaining 2000 season will be monitored. The coupled model forecasts will be compared to the operational model forecasts. Alternative physics packages will be investigated and integrated with the ocean-coupled model to improve intensity prediction. A more systematic study of grid resolution and grid configurations will be attempted in an effort to identify an efficient forecast system for the 2001 hurricane season.

7.2 HURRICANE PREDICTION CAPABILITY

ACTIVITIES FY00

7.2.1 Extended Prediction

M.A. Bender *R.E. Tuleya*
T. Marchok

Extended prediction of hurricane tracks up to 120 hours using the GFDL system has been successfully implemented and has become operational at NCEP for the 2000 hurricane season. A collaborative study continues with the tropical forecast centers of the Navy, UKMET, and ECMWF in evaluating skill to 120h for the 1995 through 1998 seasons. All models, including the GFDL model, exhibit skill into days 4 and 5 when compared to a climatology and persistence reference. It was found that simple ensembles of the various forecast models yield even more skill. Interestingly, the GFDL model was found to be a key member of this ensemble; that is, the GFDL model together with any other global model gave the best track forecast.

7.2.2 Impact of Satellite-Observed Winds on GFDL Forecasts

B. Soden *C. Velden**
R. Tuleya

**University of Wisconsin*

A series of experimental forecasts was performed to evaluate the impact of enhanced satellite-derived winds on numerical hurricane track predictions (mr). The winds were derived from GOES-8 multi spectral radiance observations by tracking cloud and water vapor patterns from successive satellite images. A three-dimensional optimum interpolation method was developed to assimilate the satellite winds directly into the GFDL hurricane prediction system. A series of parallel forecasts was then performed, both with and without the assimilation of GOES winds. Except for the assimilation of the satellite winds, the model integration procedures are identical in all other respects. Over 100 cases were examined from 11 different storms covering 3 seasons (1996-1998), making it possible to account for and examine the case-to-case variability in the forecast results when performing our assessment. On average, assimilation of the GOES winds leads to statistically-significant improvements for all forecast periods, with the relative reductions in track error ranging from ~5% at 12 hours to ~12% at 36 hours. The majority of forecast cases were improved using the satellite winds, with roughly 3 improved forecasts for every 2 degraded ones. The errors in intensity forecasts for the 24-72 hour periods were also improved by 4-8%.

Inclusion of the satellite winds also dramatically reduced the westward bias which has been a persistent feature of the GFDL model forecasts, implying that much of this bias may be related to errors in the initial conditions rather than a deficiency in the model itself. A composite analysis of the deep-layer flow fields suggests that the reduction in track error and correction of the westward bias may be associated with the ability of the GOES winds to more accurately depict the strength of vorticity gyres in the environmental flow. These gyres result primarily from the interaction between the storm's vortex with the environmental gradient of vorticity. While these "β-gyres" are common features in numerical models, documenting their presence in

nature has been hampered by the lack of sufficient observations and the complex flow in the storm environment. As shown in Fig. 7.1, the assimilation of the satellite winds results in an

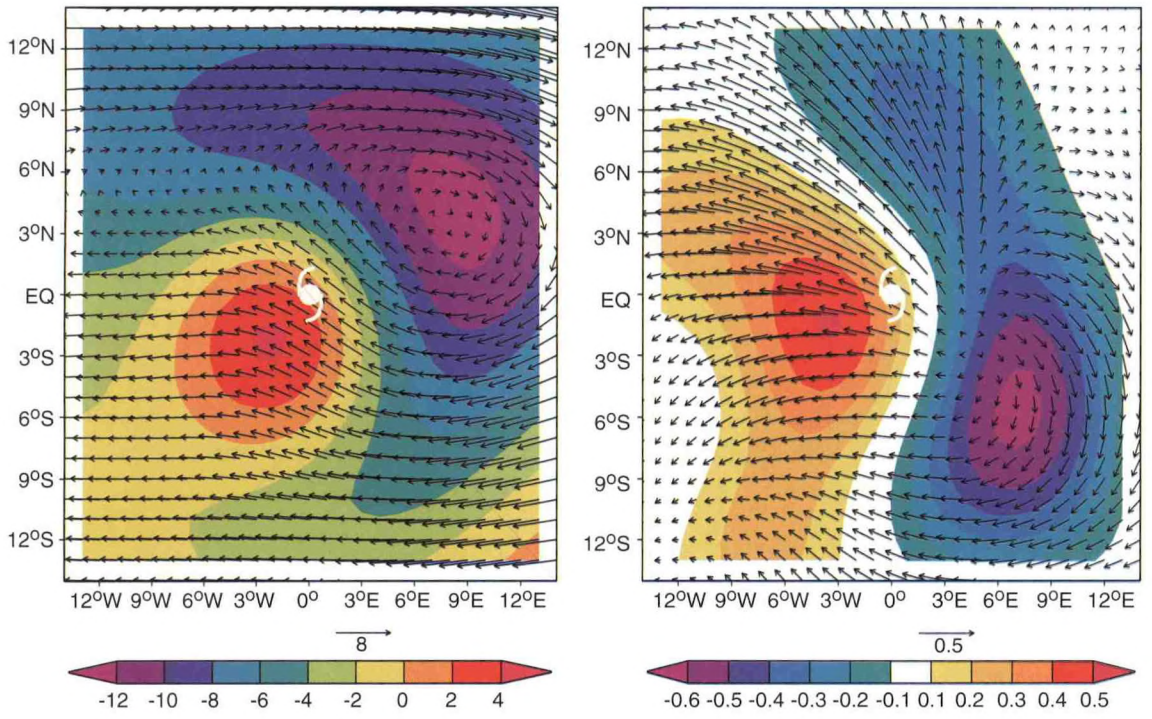

Fig. 7.1 A storm-relative composite of the large-scale steering flow from the control simulations (left) and the difference due to the assimilation of GOES winds (right) averaged over all 111 cases. Vectors depict the deep layer mean winds (in m/s) and shading depicts the corresponding vorticity field (in 10^6 s^{-1}). The hurricane symbol identifies the center of the storm used as the frame of reference to form the multi-storm composite.

enhanced gyre dipole with greater anticyclonic circulation to the northeast of the storm and greater cyclonic circulation to the southwest of the storm. This suggests that, while the initial wind field does contain a gyre-like pattern, the strength of these gyres is under-analyzed relative to that inferred from the GOES retrievals. The combination of both statistical and physical analyses thus offers compelling evidence that the assimilation of satellite winds can significantly improve the accuracy of hurricane track forecasts.

7.2.3 Sensitivity of GFDL Track Forecasts to Initial Conditions

*M.A. Bender J. Heming**

**UKMET Office*

Since 1996, the UKMET global model has also been providing operational forecast guidance for storms in the Atlantic basin. On the average, this model was the best performer for track prediction during the 1999 season. In order to evaluate the performance of the GFDL forecast system based on this global analysis, forecasts of Hurricanes Dennis, Floyd, and Gert were rerun using the UKMET analysis as input into the initial condition (designated "GFDU"). In

all of these cases, the initialization and forecast model procedures were otherwise identical to the operational GFDL. To evaluate the impact on the track forecast from the analysis alone, the lateral boundary forcing used for the GFDU forecasts was the same as that used for the operational forecasts (GFDL) obtained from the AVN model. In total, 79 cases were rerun using the GFDL model with the UKMET analysis. The GFDL forecasts initialized from the UKMET analysis showed considerable improvement compared to the operational model (Fig. 7.2). The 24, 48,

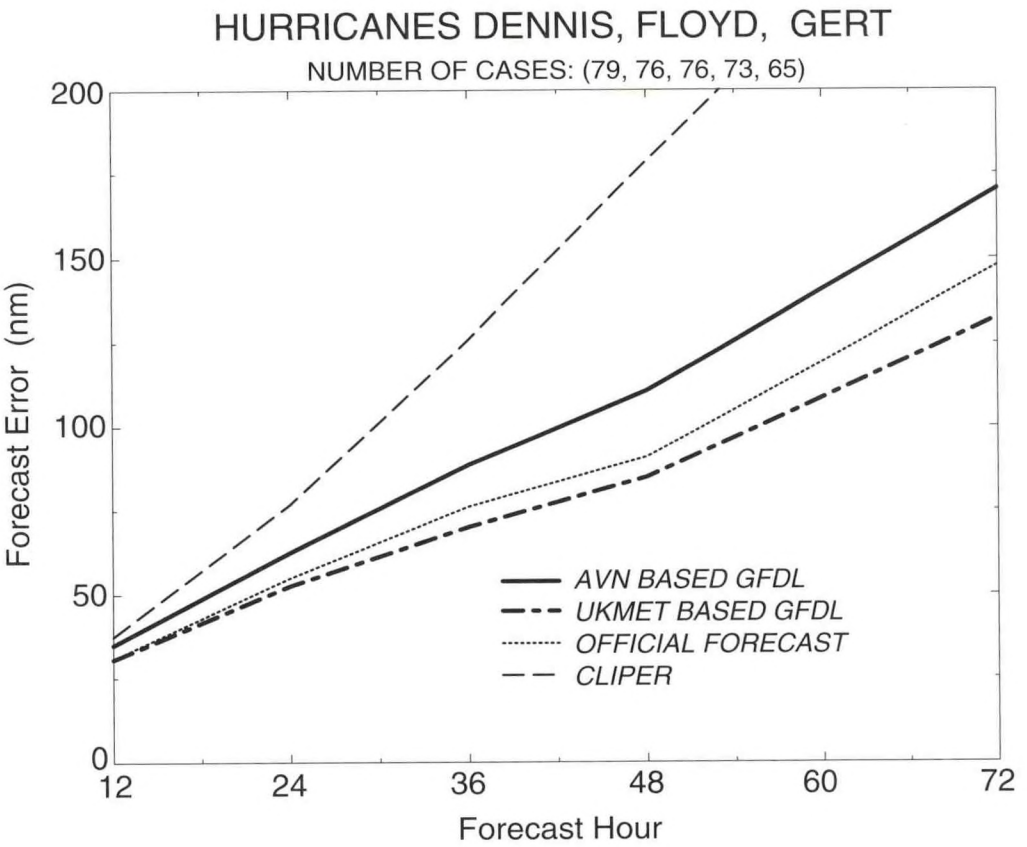

Fig. 7.2 A comparison of GFDL forecasts initiated from the operationally based NCEP AVN analysis to those based on UKMET analysis.

and 72h average track errors decreased from 63, 111, and 170 nm to 53, 85, and 132 nm, with a frequency of superior performance of 62, 71, and 60% at these time levels. Similarly, the skill relative to CLIPER increased from 38% and 39% at 48 and 72h, to 52% and 53% for GFDU. The average track error for GFDU was slightly better than the UKMET model at the longer time periods. For example, at 48h the skill relative to CLIPER was 54%, 47%, and 39% for the GFDU, UKMET, and GFDL models, respectively.

7.2.4 Evaluation of Model Forecast Errors

T. Marchok

A comprehensive study of the spatial variation of model track and intensity forecast errors across the Atlantic Basin was undertaken. Such a spatial analysis can highlight geographic regions of stronger and weaker model performance, thus providing a more

detailed look at a model's forecast biases than can be attained through average error statistics alone. Results indicate that for track, the barotropic and advection models have their regions of strongest performance in a band stretching from the deep tropics west-northwest through the Bahamas. The dynamic models, including the GFDL, Navy NOGAPS, and UKMET models, have their regions of strongest performance extending from the Bahamas and Leeward Islands northward to off the New England Coast. Almost all of the models in the study had difficulty with storms in the western Gulf of Mexico, with most models exhibiting a strong westward bias in that region. Most models also had trouble with storms in the northeastern Atlantic Ocean. For intensity, all of the models in the study exhibited an under-intensification bias for forecasts originating in the deep tropics. The GFDL model, which has an under-intensification bias across nearly the entire basin at 12 hours lead time, exhibited a wide region of relatively bias-free intensity forecasts across much of the western North Atlantic at 72 hours lead time.

PLANS FY01

Analysis of extended range 5-day forecasts will continue. The investigation of forecast skill among forecast models of the various tropical operational centers will be completed. Developmental work on the initialization methodology will proceed with evaluation of past cases. In addition, work to upgrade the GFDL system by increasing the grid resolution and improving the physical parameterizations of the model will be given higher priority.

7.3 BEHAVIOR OF TROPICAL CYCLONES

7.3.1 Hurricane Intensity in a High-CO_2 Climate

*I. Ginis** *W. Shen**
T.R. Knutson *R.E. Tuleya*

**University of Rhode Island*

ACTIVITIES FY00

The potential impact of a greenhouse gas-induced global warming on the intensity of hurricanes has been investigated in a series of studies (1527, hc, hz). The large scale atmospheric boundary conditions for a high CO_2 climate have been either derived from a global climate model (1527, hz) or explored via a systematic examination of a wide parameter space of tropical lapse rate and tropical SST changes (hc). For the global climate model-derived conditions, a modest increase (~5-10%) in the intensity of very strong hurricanes has been simulated in the high CO_2 climate, as compared to the strongest hurricanes in the control climate.

One assumption of these and other studies to date is the neglect of the effect of hurricane/ocean coupling (*i.e.*, the local SST cooling induced by the hurricane) on the intensity changes. To evaluate how a CO_2-induced enhancement of hurricane intensity could be altered by the hurricane/ocean coupling, a series of idealized hurricane experiments was performed using the GFDL Hurricane Prediction System coupled to a 1/5 degree resolution

regional version of the Princeton Ocean Model (POM). For each of a series of 72-hr experiments, a specified initial storm disturbance was placed in an idealized basic state consisting of a uniform easterly flow of 5 m/sec. The initial SST, atmospheric lapse rate, and atmospheric moisture conditions for the experiments were derived from long simulations (control and high CO_2) of a global climate model. The ocean thermal stratifications were based on observed climatologies and included the CO_2-induced stratification changes simulated by the global climate model. The results indicate that a CO_2-induced intensification still occurs even when the hurricane/ocean coupling effects are included; ocean coupling appears to have only a small impact on the magnitude of this intensification. Analysis of these experiments was completed during the past year (mv).

7.3.2 Tropical Cyclone-Ocean Interaction

M.A. Bender *I. Ginis**
*S. Frolov**

**University of Rhode Island*

Unlike the steady decline in operational forecast track errors over the past two decades, intensity prediction has shown little improvement in the forecast period of one to three days. One of the important physical components lacking in both statistically and dynamically based forecast methods is that of the role of the ocean interaction beneath the hurricane. The role of ocean interaction is becoming more accepted as an important component in forecasting tropical cyclone intensity. Therefore, the GFDL group continues to collaborate with the University of Rhode Island Oceanography group in developing a new GFDL coupled hurricane-ocean model for the Atlantic to improve hurricane intensity forecasts. For the 1999 hurricane season, the GFDL/URI forecast system produced coupled model forecast results typically available 2-4 hours after the operational NCEP GFDL product. For the 1999 season, 139 forecasts were performed including the following storms: Arlene, Brett, Cindy, Dennis, Emily, Floyd, Gert, Harvey, Irene, Jose, and Lenny. The coupled model forecasts of track and intensity were made available to the National Hurricane Center via a dedicated web site. In addition, a successful conversion was made from a research model to a fully automated real-time prediction system.

As in the 1998 season, the coupled model achieved significant improvements in the hurricane intensity forecasts compared to the operational atmosphere-only GFDL model. The mean absolute error of the sea level pressure forecasts was reduced by about 31%. Although the improvements in the minimum sea level pressure forecasts are significant, little improvement was achieved in forecasting surface winds by the coupled model. This is because the GFDL model has a tendency to underestimate the surface winds for strong hurricanes with minimum sea level pressure below 970hPa. Therefore, to gain accuracy in forecasting surface winds, the coupled model used the observed pressure-wind relationship in conjunction with the model predicted minimum sea level pressure to determine surface winds.

Work was completed in porting the coupled model to a scalable parallel design on the new NCEP IBM-SP with the goal of implementing the model for operational forecasting for the 2000 hurricane season in the Tropical Atlantic. Implementation of an improved ocean and atmospheric initialization procedure is also under way.

7.3.3 Tropical Cyclone Landfall

*M. DeMaria** *J. Persing****
*I. Ginis*** *W. Shen***
*M. Montgomery**** *R.E. Tuleya*

**NESDIS*
***University of Rhode Island*
****Colorado State University*

A suite of experiments was designed and run in collaboration with URI to investigate the role of surface water on landfalling hurricanes. This study (mt) resulted in an interesting comparison of land surface conditions, extending earlier work on the impact of surface conditions on hurricane landfall. Another study was initiated with NESDIS to evaluate the rainfall from GFDL landfall forecasts for 1995-1999. Given the flooding of Floyd and Mitch, rainfall is another important parameter to investigate, and the current studies may be the first attempt to evaluate the patterns of model produced rainfall for real cases of landfalling hurricanes. Hurricane Opal (1995) presented a challenging sequence of rapid intensification followed by filling just before landfall. A collaborative study with Colorado State University scientists indicated that trough interaction played a minimal role in Opal's intensification, and that vertical shear caused its subsequent weakening, at least in the GFDL model simulation (nb).

PLANS FY01

Other methodologies for examining the hurricane intensity/climate change issue will also be explored, such as the use of higher resolution GCMs. The sensitivity of prior results to physical parameterizations will be explored. Work will continue to improve the tropical cyclone-ocean coupled model and initialization. A plan to extensively analyze the storm behavior at landfall will be made using improved model physics.

7.4 MODEL IMPROVEMENT

ACTIVITIES FY00

M.A. Bender *R.E. Tuleya*
C. Kerr

A major activity during the past year was the successful conversion of the GFDL modeling system to a distributed memory system. This ensures the efficiency of the forecast system for operational implementation at NCEP for the 2000 tropical season, as well as for future research applications at GFDL. The conversion effort was quite difficult due to the complex nature of the GFDL moving nested grid framework. The new design incorporates two-dimensional decomposition. For operational use, the present model uses 42 processors to achieve the approximate speed attained by the Cray T90 12 processor run. Also converted were the pre- and post-processing steps of the forecast system, including the vortex bogussing step. The code was redesigned to use an arbitrary number of sub-domains. It was found that

this distributed system is highly dependent on the efficient communication between the distributed processors.

Work on the improvement in the spatial resolution of the hurricane model continues in order to cope with the increase in the global model resolution (6.1.3), as well as to represent the hurricane structure more accurately. The modeling system has been run with a doubling of resolution of 1/2°, 1/6°, and 1/12° in the horizontal and with 42 levels for a selected number of case studies of Floyd (1999), Opal (1995) and Mitch (1998). More physically realistic features have been noted. High resolution GFDL forecasts of Floyd's rainfall were quite encouraging, indicating large amounts at landfall in the Carolinas with a swath of heavy rainfall through the Mid-atlantic and up to New England (Fig. 7.3). More cases need to be evaluated to check for

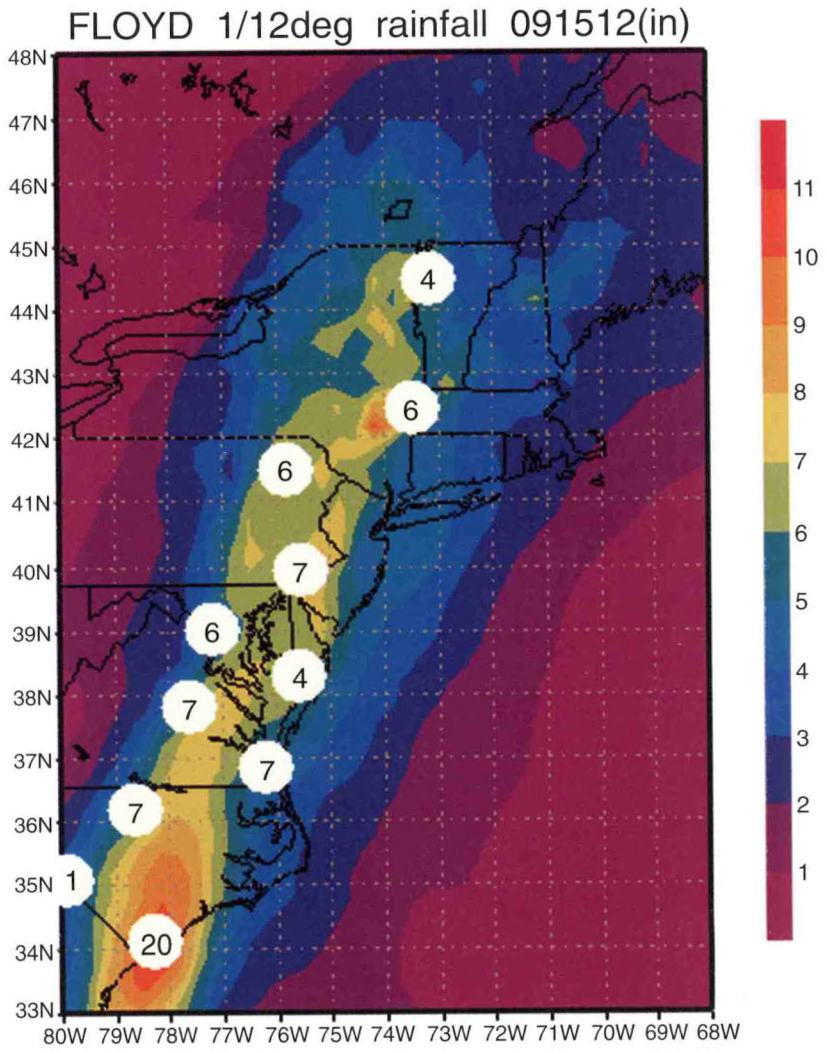

Fig. 7.3 High resolution forecast (contours) of the rainfall for Hurricane Floyd (1999). Encircled numbers are observations in inches. The copious rainfall caused disastrous flooding from the Carolinas to the Mid Atlantic.

increased forecast skill. Interestingly, the improvement in intensity error was disappointing, indicating that model physics packages may be deficient.

A comprehensive evaluation of the physical parameterizations of the GFDL model has been under way, including horizontal and vertical turbulent mixing, dissipative heating, surface exchanges, and convective parameterization. A suite of experiments using Mellor-Yamada level 2.5 mixing was tested for a 74-case suite of Dennis, Floyd, and Gert. Substantial increase in intensity skill was achieved, especially for the first two forecast days with improvements of 17 to 12, 16 to 13 and 15 to 13 knots at 12, 24, and 36h, respectively. Perhaps more impressively, the negative bias (under-forecast) for winds was reduced from ~10 knots to ~4 knots throughout the 72h forecast period. Preliminary results indicate improvements in storm structure when prediction of turbulent eddy kinetic energy is included. The model's forecasts of both track and intensity are also sensitive to different convective parameterizations.

PLANS FY01

Developmental work to improve the hurricane model initialization, ocean interaction, model physics, and resolution will continue. This is critical for improved intensity prediction skill. A significant number of case studies will be needed to evaluate the impact of these efforts on forecast skill of track and intensity. Additional work will be continued to assimilate more data into the GFDL forecast/analysis system. Physical mechanisms of evaporation of rain and sea spray together with cumulus and dissipative heating will be evaluated.

8. MESOSCALE DYNAMICS

GOALS

To produce accurate numerical simulations of storm-scale processes in order to understand the role that planetary and synoptic scale parameters play in their generation and evolution.

To understand the dynamics of synoptic and mesoscale phenomena and their interaction with larger and smaller scales.

To improve high-resolution model simulations of synoptic and smaller scale phenomena which can be used to guide parameterization development in coarser models.

8.1 ANALYSIS OF MIDLATITUDE CYCLONES AND STORM TRACKS

S. Garner *I. Orlanski*

ACTIVITIES FY00

8.1.1 The Evolution and Feedback of Cyclones in Storm Track Simulations

The life cycle of baroclinic eddies in a controlled storm track environment has been examined by means of long model integrations with the Zeta model (7.4.1) on a hemisphere (km). A time-lag regression has been applied to the last 200 days of the model integrations in order to establish a composite view of the wave-breaking process. The eddies grow, as expected, by strong poleward heat fluxes at low levels at the entrance of the storm track, where the surface baroclinicity is strong. As they evolve to a nonlinear stage, they grow deeper by fluxing energy upward, and the characteristic westward tilt in the vorticity changes to a meridional tilt. The poleward movement of the low-level vorticity is accomplished by the flux of time-mean absolute vorticity and eddy self-advection of vorticity, while the north-south orientation of the upper-level vorticity is achieved by the projection of the surface vorticity at upper levels, combined with nonlinear advection that rotates the vorticity around to the south.

Probably the most significant result of this study is the discovery of two distinct patterns of eddy evolution associated with two distinct types of storm track. These patterns can be referred to as baroclinic wave packets and quasi-stationary couplets. In baroclinic wave packets, which have been known for some time (1144), the age of the individual eddies increases from east to west, with the youngest eddy at the leading edge of the packet. The more mature eddies flux energy downstream to the younger eddies. The youngest eddies develop mainly by these fluxes until they are able to enhance their growth by surface heat fluxes. More mature eddies in the center of the packet flux as much energy downstream as they receive from upstream eddies, and also receive energy from the surface baroclinicity along their path. The oldest eddies decay by downstream energy fluxes and barotropic conversion.

The second pattern arises when the downstream surface baroclinicity cannot be maintained, as in a zonally-contracted, basin-scale storm track. High baroclinicity at the entrance (to the west) is followed by abruptly weaker baroclinicity in the middle and exit. The corresponding pattern of eddy evolution quite frequently involves the simultaneous development of upper-level, downstream eddies paired with baroclinic upstream eddies. These pairs, or couplets, are self-sustaining structures in which the upstream baroclinic eddy grows through heat fluxes in the rather stronger surface baroclinicity and fluxes energy to the upper-level downstream eddy. In contrast to the wave packet, the upstream eddy is the younger. The signature of the couplet at upper levels is an omega-like pattern with a trough in the west (principal eddy) and one to the east (downstream eddy), separated by a "building" ridge. The couplet pattern is frequently observed in storm tracks of the Northern Hemisphere winter. Wave packets are more characteristic of the zonally elongated storm tracks that are a frequent feature of the Southern Hemisphere.

8.1.2 Moist Convection in Baroclinic Life Cycles

Latent heating has long been recognized as a fundamental process for storm development. More recently, in a study concerning the interannual variability of storm tracks (1572), it has been speculated that subtropical flux of moisture over the eastern Pacific Ocean in the warm ENSO phase can explain the observed elongated shape of the storm track in this period. It has also been argued recently (km) that the dissipation of the low-level cyclone is of paramount importance in the whole life cycle of the baroclinic system. The frontal zone is the boundary of the warm air and of the poleward heat fluxes that are crucial for sustained baroclinic growth.

For perhaps the first time, a planetary scale circulation has been simulated without the standard moist parameterization. Actual individual clouds are explicitly resolved in new simulations of a baroclinic wave using explicit moist convection (8.4) in the non hydrostatic-compressible model ZETANC. A series of intercomparisons between the moist baroclinic and dry baroclinic life cycle are now being carried out. The successful simulation of the moist convective field around the development of the cyclonic circulation is displayed in Fig 8.1. The rain band ahead of the cold front and the cloud wrapping around the cyclonic circulation are realistic features.

The preliminary result of the intercomparison between the moist and dry evolution of the baroclinic life-cycle shows profound differences in all aspects of its evolution. The surface front-cyclone system is considerably more extended meridionally in the dry solution than in the moist one. A similar effect was previously found to be associated with a reduction in the zonal scale (1518). The reason here seems to be that the moist air ascends more steeply than dry air, since it tends to follow the large-scale moist adiabats. As a consequence, the eddy produces vertical motion and cyclonic vorticity sooner (farther equatorward) than in the dry case.

Perhaps the most unexpected result is the stark difference in the way the waves equilibrate. In the dry case, as has been discussed in a number of published articles (including km), the system decays via anticyclonic wave-breaking, producing poleward momentum fluxes and pulling the jet poleward from its original latitude. In the moist case, the wave seems

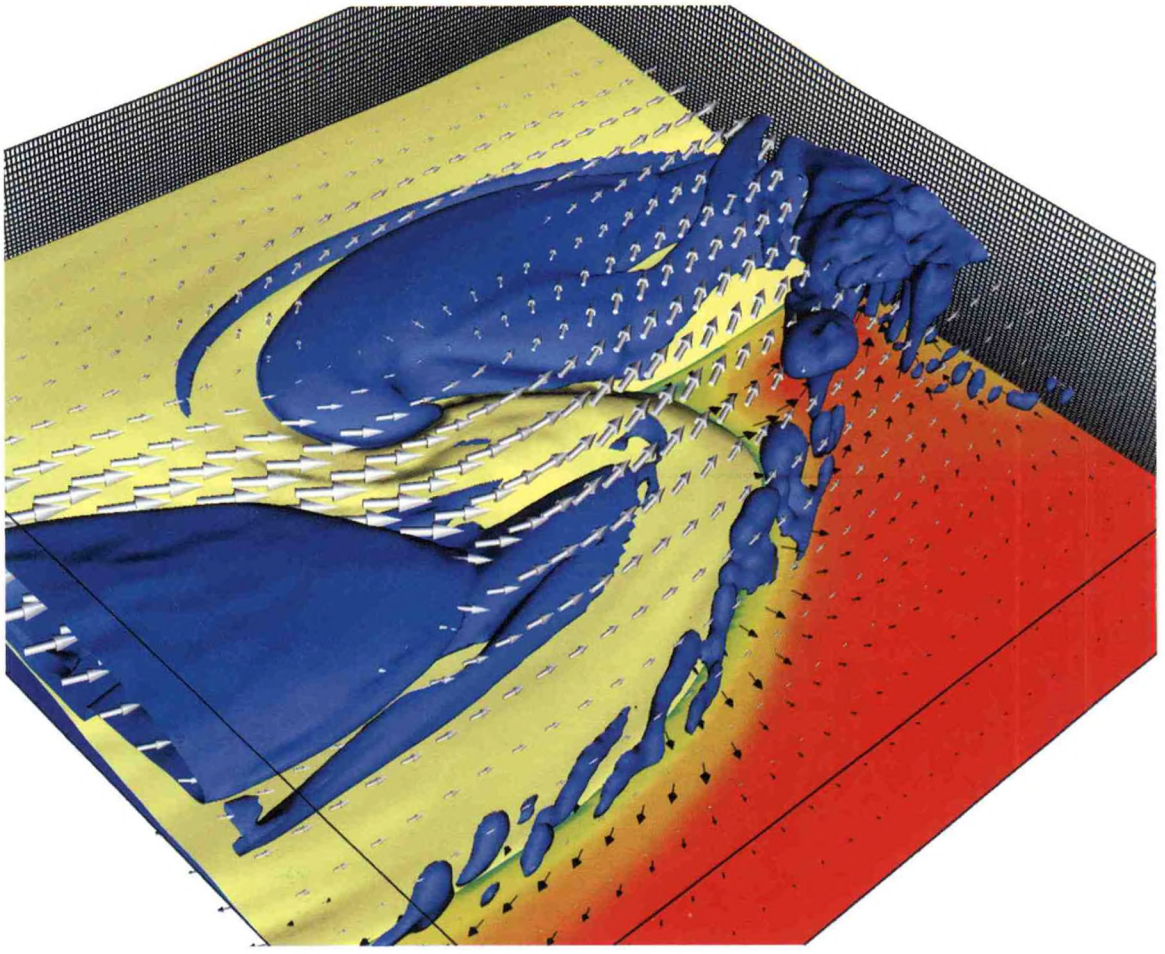

Fig. 8.1 A section of the baroclinic evolution is shown in the figure. The isentropic surface (20°C) is shown in light green, in blue is the isosurface of liquid water (1gr/kg) is blue and the vectors show the wind pattern at two different heights, 10 km (white arrows) and surface (black arrows). The surface temperature gradient is displayed from red (warm) to green (cold) and the mesh in the background shows the horizontal and vertical resolution used in the model.

to break cyclonically with weak momentum fluxes in the equatorial direction, producing a westerly jet that it lies considerably more equatorward than in the dry solution. Similar results were obtained from the dry short-wave life cycle (1518), although the connection is still not yet clear. This effect of moisture could have considerable bearing on the interannual variability of storm tracks.

PLANS FY01

The sensitivity of cyclone evolution to position within the storm track will continue to be evaluated. In particular, the mechanisms responsible for the poleward progression of low-level cyclonic eddies will be further analyzed. The moist solutions will be studied further with emphasis on a storm track environment.

8.2 TOPOGRAPHIC INFLUENCES IN ATMOSPHERIC FLOWS

S. Garner *I. Orlanski*

ACTIVITIES FY00

8.2.1 Gravity-Wave Parameterizations Over the Andes

High-resolution numerical and analytical models have been used to test the feasibility of a proposed parameterization of total mountain drag due to unresolved terrain. The parameterization assumes steady, linear gravity waves and gradual horizontal variations of the basic flow. Given the low-level buoyancy frequency and topography, it yields a map of horizontal divergence due to the terrain. The total drag on the atmosphere can then be obtained by multiplying the divergent velocity by the vertical velocity due to the resolved horizontal surface wind.

Twin experiments using the ZETA model at coarse and fine resolution showed that most of the momentum flux reaching the stratosphere from the Rocky Mountains is due to linear, hydrostatic gravity waves launched by the smallest resolved terrain feature: primarily the upstream and downstream edges of the massif. A nonlinear correction has been developed in order to parameterize the non-propagating part of the momentum forcing. However, most of the resolved drag over the Rockies in the fine-resolution experiment is linear at the source. To test the nonlinear correction, the experiments are being repeated for the Andes Mountain range.

In Fig. 8.2, surface drag vectors from coarse- and fine-resolution simulations of wintertime flow over the Andes are displayed. The thick arrows are the quasi-steady result at fine resolution and the thin arrows are the parameterized drag arising from the coarse-resolution model run. The linear parameterization is shown in the upper panel. In the lower panel, the nonlinear correction is included. The nonlinear correction improves the drag estimate in regions of greatest drag, but slightly degrades the estimate elsewhere. The large-scale flow consists of a baroclinic jet centered at 30°S, with a maximum surface wind of 7 ms^{-1} and a wind at the tropopause of about 40 ms^{-1}.

PLANS FY01

The nonlinear drag correction does not take into account the variation of mean wind over the height of the terrain. In wintertime baroclinic zones like the one in the experiments of Fig. 8.2, this correction is expected to be significant. A correction for vertical wind shear is being formulated and will be tested in the same way as the rest of the scheme, *i.e.*, with comparable high- and low-resolution experiments. The sensitivity of the drag to the treatment of the turbulent planetary boundary layer will also be examined.

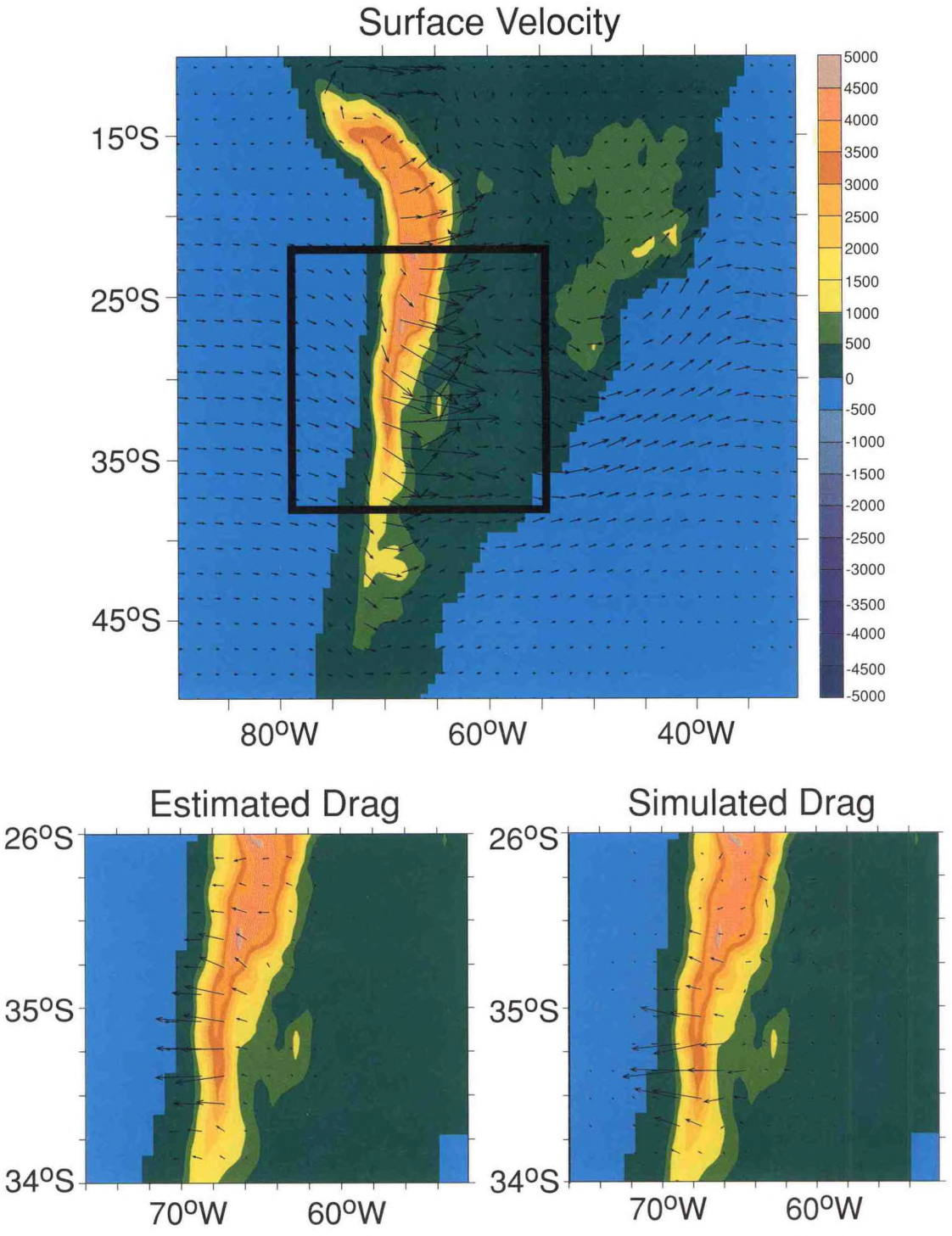

Fig. 8.2 Surface velocity and surface drag in fine-resolution and coarse-resolution simulations of wintertime flow over the Andes mountain range. The drag "estimate" is generated by the new parameterization using surface conditions from the coarse-resolution run. This estimate includes a nonlinear correction for vertical shear that considerably imnproves the result over the southern Andes, where the westerly jet is centered. The simulated drag is averaged to the coarse-resolution grid cells. The largest values of drag after the averaging are around 2 N/m^2.

8.3 MODEL DEVELOPMENT

S. Garner *I. Orlanski*
B. Gross *L. Polinsky*

ACTIVITIES FY00

8.3.1 Improvements to the Nonhydrostatic Compressible Zeta Model

The nonhydrostatic, fully compressible version of the hydrostatic Zeta model has been used to evaluate nonhydrostatic and terrain effects in mesoscale atmospheric circulations (7.3.1) and for developing physical parameterizations (7.3.2). The model has now been coded to run on the massively parallel T3E computer at GFDL. Memory swapping and the slab-oriented array structure have been eliminated. The model can run up to 10 times faster on multiple processors, even with bulk microphysics activated.

PLANS FY01

Continuing idealized storm track simulations with the spherical-coordinate models should clarify the most important processes in the development, maintenance, and decay of the storm tracks. Sensitivity studies will be undertaken to clarify the features most important to cyclone evolution within them. Ice-phase processes will be added to the bulk microphysics. Other physical processes to be added are surface boundary layer and turbulent kinetic energy schemes. The model is also being adapted to the GFDL Flexible Modeling System.

9. TECHNICAL SERVICES

GOALS

Provide a computational facility to support research conducted at GFDL with emphasis on supercomputing and networked desktop systems for developing, running, and analyzing results from numerical models.

Provide software tools for managing, manipulating, and visualizing large amounts of multi-dimensional data.

Maintain systems which provide documentation and time-sensitive information to users, create products for presentation and publication, and communicate GFDL's accomplishments to other agencies and to the public.

9.1 COMPUTER SYSTEMS

B. Gross *T. Taylor*
L. Lewis *H. Vahlenkamp*
B. Ross *R. White*
J. Sheldon *W. Yeager*

ACTIVITIES FY00

9.1.1 Current Supercomputing Systems

The Laboratory currently operates three high-performance computer systems: a Cray T932 with 24 central processors, 4 gigabytes (GB, 1 GB=1 billion bytes) of central memory, 32 GB of solid state secondary storage, and 447 GB of disk storage; a Cray T94 with 4 central processors, 1 GB of central memory, 4 GB of solid state secondary storage, and 760 GB of disk storage; and a scalable 160-processor Cray T3E-900 system with 256 megabytes (MB, 1 MB=1 million bytes) of local memory per processor and 410 GB of disk storage. All three systems are interconnected by high-speed channels and share a very large data archive hosted by the T94. The data is stored in 2 StorageTek silos with a tape capacity of up to 240 terabytes (TB, 1 TB=1 trillion bytes).

During September 1999 the original 40-processor T3E was upgraded to a 128-processor system with double the amount of memory per processor. The system was further enhanced in June 2000 with the addition of 32 more processors.

The T932 is the Laboratory's main production system. The T94 is primarily an interactive and analysis platform that also runs production jobs at night. The T3E has been an important

development platform for redesigning GFDL models to a scalable architecture paradigm and has become a major production system since being upgraded.

Table 9.1 shows the number of T932 and T3E user processor hours for each month and the cumulative amount of total archive data in trillions of bytes. The increase in T3E hours beginning July 2000 is a result of the additional 32 processors.

Table 9.1 Cray User Processor Time and Total Archive Data

Month	T932 Hours	T94 Hours	T3E Hours	Terabytes
Oct 99	15,896	1,923	70,649	86.5
Nov 99	12,633	1,880	71,318	88.1
Dec 99	14,141	1,976	75,145	88.9
Jan 00	12,727	1,895	72,795	91.7
Feb 00	13,455	1,767	69,378	93.1
March 00	13,394	1,940	72,396	95.5
April 00	11,669	1,891	70,965	97.5
May 00	11,221	1,875	71,193	100.3
June 00	12,769	2,014	77,090	101.8
Julyl 00	12,969	2,175	94,477	103.2
Aug 00	12,576	2,091	91,688	104.8
Sep 00	12,149	2,175	91,812	106.1

9.1.2 High Performance Computing System Procurement

GFDL has, for some time now, been exploring the use of scalable supercomputers for predicting and simulating geophysical fluid flows with a Cray T3E-900. The experience gained on the T3E has proven invaluable in preparing for the upgrade of the Laboratory's computing capabilities. GFDL has now completed the acquisition of an enhanced high-performance computing system (HPCS) that includes balanced capabilities in very large scalable computing, storage capacity, and analysis, visualization, and telecommunications. This HPCS will replace GFDL's current T932 and T3E supercomputers leased from SGI/Cray Research and will provide all of the facilities required by GFDL to carry out its computational research.

The effort to procure the HPCS began in earnest in January, 1999, when a working group was formed to develop the functional requirements and technical specifications that the new computing environment must satisfy. This group consisted primarily of GFDL scientists, but also included experts in computer science from the academic sector, advisors from other NOAA high-performance computing facilities, and consultants with expertise in scalable high-performance computing. The technical specifications were developed in the areas of

high-performance computational services, which include a large-scale cluster (LSC) for running GFDL's computationally intensive production workload and an analysis cluster (AC) that provides efficient execution of I/O-intensive codes and third-party software, a hierarchical storage management system (HSMS) for archiving GFDL's large datasets, and system-wide components common to the entire HPCS. Additional committees that addressed suitable benchmarks and evaluation criteria were also formed in anticipation of the full and open competition in which American high-perfomance computing vendors were expected to participate.

A Project Agreement that describes the objectives of these acquisitions was signed by appropriate parties at GFDL and in the NOAA management structure on September 9, 1999 and updated on January 24, 2000. A Request for Information (RFI) from the high-performance computing vendors, including a draft Statement of Need that describes the technical specifications for the enhanced computing environment, was posted on September 23, 1999 in Commerce Business Daily's CBDnet. Oral presentations by vendors responding to the RFI were made to members of the procurement team on November 3-5, 1999.

A comprehensive benchmark suite that includes throughput and scaling benchmarks for the LSC, a throughput analysis benchmark for the AC, and an archiving benchmark for the HSMS was completed in early March 2000. The LSC and AC benchmarks include jobs employing the Flexible Modeling System (FMS - provide reference) as well as MOM3 (provide reference). The throughput benchmarks were designed to mimic as closely as possible a typical production workload on the LSC and AC.

The Request for Proposals (RFP) was released on March 28, 2000. Offerors were given 73 days, until June 6, 2000, to respond with written proposals. These proposals were reviewed by members of the procurement team, and a Competitive Range was determined on July 5, 2000. Live Test Demonstrations were completed with Offerors in the Competitive Range on July 28, 2000. Proposal revisions were received on August 11, 2000, and further discussions were completed with Offerors on August 24, 2000. Additional proposal revisions were received on August 31, 2000 and reviewed by members of the procurement team, after which final proposals revisions were received. A consensus was reached by the procurement team on a recommendation for award on September 7, 2000, the Source Selection Official signed the Source Selection Document on September 8, 2000, and the contract awarding the HPCS contract to Raytheon Company was signed on September 27, 2000.

The initial GFDL HPCS consists of an LSC comprised of 8 sgi Origin 3800 nodes, each with 128 processors, 64GB of memory, and 720 GB of local disk, and an AC comprised of 2 sgi Origin 3800 nodes, each with 64 processors, 64GB of memory, and 4.32 TB of local disk. The LSC and AC also have access to an additional 5.76 TB of disk that is shared between the LSC and AC. The HSMS consists of three STK Powderhorn silos that is expected to hold 2000 TB of archived data which is managed by the AC nodes. The extremely high bandwidth between the LSC, AC, HSMS, and shared disk provides GFDL scientists with a balanced computing environment that focuses on the creation and analysis of large amounts of data.

9.1.3 Software Development and Technical Support Procurement

In parallel with the hardware acquisition, NOAA/GFDL also pursued support for related software and other IT development activities. These activities will involve vital research and development activities on software issues that are critical to the effective use of the HPCS, and will include component-based modular code design, code optimization, and algorithm development. In addition to ongoing university partnering, such as the collaboration being developed for joint graduate student appointments between the NOAA-supported Atmospheric and Oceanic Science Program and the Princeton University Computer Science Department, a Software Development and Technical support (SDTS) services contract was awarded to RS Information Systems for $3M over a five-year contract period. RSIS will provide services to cover a range of capabilities, including: scientific programming, code management, and conversion and optimization of software that is to run on the Laboratory's new scalable computing systems; systems administration and optimization of the various elements of the supercomputing system; data management and visualization; development of parallel programming tools; network and workstation administration; and security services. A substantial fraction of the SDTS support will be devoted to the ongoing development of the Flexible Modeling System.

While SDTS is designed to cover a variety of different task types, four tasks have been defined initially:

1. FMS Application Development
2. System Administration and Security
3. FMS Code Management
4. Application and System Optimization

Of these, only Task 4 was immediately staffed (via a subcontract to an expert in the field). For Tasks 1 and 2, personnel have been identified (former GFDL post-doctoral visitors) and are awaiting the issuance of H-1b visas. RSIS is actively recruiting for Task 3, and additional tasks are currently being considered.

9.1.4 Scientific Workstation Network

In addition to the three Cray systems, GFDL's computer facility includes five Silicon Graphics (SGI) servers, two Sun Microsystems servers, and a variety of text and graphics printers. Distributed throughout GFDL are 113 desktop workstations including 36 SGI Indigo2 R4400XZs, 34 SGI Indigo R4000XZs, 12 SGI 4D/35s, and 31 SGI 4D/25s. GFDL's anonymous FTP and web server was upgraded to an Indigo2, quadrupling its speed and disk capacity. The desktop workstations are connected to six Cabletron Fast Ethernet switches which connect to a Cabletron SmartSwitch Router via Gigabit Ethernet. The T932, T94, and T3E are attached to a Fiber Distributed Data Interface (FDDI) network which connects to the Ethernet network.

Preparations for the Year 2000 transition were completed during the final months of 1999. These included installation of software patches to the SGI IRIX operating system and upgrading the firmware in some network equipment. The actual Y2K transition went smoothly, with only a few minor problems that were corrected during the first two weeks of January.

A major upgrade of the IRIX operating system was completed on the Indigo2 and Indigo workstations. The upgrade included installation of a new software server, upgrading the memory and system disk drives on all Indigo workstations, customized configuration of the operating system, and upgrading several application software packages. New versions of many utility and application programs were installed to assure file format compatibility.

An Indigo2 was purchased in anticipation of converting Email services to the Netscape Enterprise Messaging System (NEMS). However, it is possible that the Laboratory's email services may be served by a Linux platform instead, and implementation of NEMS has been deferred temporarily. GFDL has requested assistance from OAR in implementing NEMS, but this assistance has not yet been scheduled.

Intel-based Desktop Workstation Options

A comprehencsive study has continued to evaluate the feasibility of using Intel-based platforms and the Linux operating system as alternative desktop workstations. A Dell Precision 410 Workstation with a 400 MHz Pentium II processor was purchased for this purpose in FY99 and *Linux* (an open source, Unix-like operating system) was installed. Linux on the Precision 410 has been determined to be a very viable alternative to traditional Unix systems and it interfaced well with the existing GFDL network.

Given the favorable results from these earlier investigations, two Linux-based, special-purpose servers were deployed in FY00. First, the Dell workstation used in the investigation was configured to serve data to outside users via the Distributed Ocean Data Service (DODS) protocol as well as run PMEL's Live Access Server which can select and display data interactively. Second, another Dell workstation (800 MHz Pentium III, with 1GB RAM and ~100GB disk) was purchased and deployed as a "compute server". Users can log into this platform and run their customary applications at a greatly increased speed (~6x faster than the SGI Indigo2s and up to 60x faster than the SGI 4D/25s). This platform has proven to be a boon to users.

One key application of concern as we plan a migration from SGI/Irix to Intel/Linux is Adobe FrameMaker, a high-end word processing and desktop publishing package that has become a workhorse for a large portion of the Lab's written products. Initially, FrameMaker was not going to be available for Linux, but Adobe released a beta version of FrameMaker for Linux, and it was found to work just fine. It is hoped that Adobe will decide to continue support for Linux, but in the event that they do not we would still have a backup plan whereby FrameMaker adherents could use specially configured platforms (perhaps some leftover SGI Indigo2's) or possibly the planned Citrix server (see below).

A number of FORTRAN 90 compilers were evaluated for use under Linux. Limited user testing showed that no one vendor was distinctly superior, with each having advantages and disadvantages. The conclusion was that, given the modest cost, all three of the leading vendors should be supported pending more in-depth user testing.

Providing Microsoft Windows Functionality

In order to provide users with the ability to run Windows-based applications from their Unix desktops, plans were made to deploy a Windows 2000-based platform running Citrix Metaframe. This product will allow users seated at any other platform to connect and open a window on their desktop that contains a complete Microsoft Windows desktop. A Dell 420 workstation with dual 800MHz Pentium III CPUs and 1 GB of memory was ordered for this purpose, as well as the Windows, Citrix, and Office software which will run on the machine. Trellis Network Services, a local 8(a) vendor, will assist in the configuration and deployment of this server.

PLANS FY01

The transition of users to the HPCS will commence immediately after the first systems are installed and configured in Fall 2000. The installation and acceptance of the HPCS are expected to be completed during Winter 2001. The Cray T932 and T3E will be de-installed shortly after acceptance is complete.

Migration of the desktop workstations from SGI/Irix to Intel/Linux will be a major challenge for the first half of the coming year. The workstation vendor will be selected in the fall of 2000, with deployment expected in the January-March 2001 time frame. Chief among the selection criteria will be vendor support for both the hardware and the operating system (OS). While local experience has found Linux to be a robust alternative to Irix, it is in a much more dynamic state of development than other more mature OS's and corporate support is needed to ensure continuous operation.

A limited number of copies of each of three FORTRAN 90 compilers for Linux will be purchased and installed; it is hoped that more extensive user testing will narrow the number of compilers further.

The Citrix server which will provide Microsoft Windows functionality to the Unix desktops throughout the Lab will be configured and tested. A chief concern is security, as Windows is more prone to viruses and other hazards than Unix environments, and the Lab's systems must be protected from these risks.

The Laboratory is expecting arrival of some excess Census equipment in the Fall of 2000. These desktop PCs will first serve as testbeds for client-server configuration in a Linux environment. Thereafter, csome will be configured as dual-boot Windows/Linux workstations for classroom use, and others will serve miscellaneous uses within the Lab, including a new intrusion detection system.

Recruiting on the part of RSIS will continue in an effort to fill the current FMS Code Manager position. Additional SDTS tasks are being defined and will be activated if funding permits.

The NOAA Enterprise Messaging System will be implemented for electronic mail and directory services after the new HPCS and Linux workstations are operational. Outside expertise will be required to install and configure the system. It is anticipated that there will be some disruption to electronic mail services during the transition. The current "gfdl.gov" internet domain will be converted to the "gfdl.noaa.gov" subdomain.

9.2 DATA MANAGEMENT

M. Harrison *H. Vahlenkamp*
J. Sheldon

ACTIVITIES FY00

The latest version of PMEL's "Live Access Server" has been installed for both internal and external use. The Live Access Server (LAS) is a configurable Web server designed to provide flexible access to geo-referenced scientific data. It can present distributed data sets as a unified virtual data base through the use of DODS (Distributed Oceanographic Data System) networking. DODS enables existing software to access remote data transparently and also provides tools for making local data accessible to remote locations. Ferret is the typical visualization application used by LAS, though other applications (MATLAB, IDL, GrADS, ...) can also be used. The Live Access Server enables the Web user to visualize data with on-the-fly graphics, request custom subsets of variables in a choice of file formats, and access background reference material about the data (metadata).

The first installation of LAS is on a special-purpose server visible to the Internet, with a URL of "data1.gfdl.noaa.gov". This server is a Dell 410 workstation serving approximately 35GB of atmospheric and oceanographic data from GFDL model experiments. With security a concern, this server has been stripped of all IT services except those that are necessary for DODS and LAS, and none of the rest of GFDL's network is accessible to users of this server.

The second installation of LAS is on GFDL's "compute server" discussed above (a Dell 420 Workstation with 1GB of memory and ~100GB disk). Several datasets for ongoing experiments, which change more frequently than those on the data1 server, are served from this platform, but are strictly for internal distribution.

A Dell Precision 420 PC running Windows NT 4.0 has been installed to function as a "Media Station". Intended initially to provide a means of importing and exporting large amounts of data to/from collaborators, it can currently read and write CDs, 40GB DLT tapes, and 250/100MB Zip disks. Eventually, this platform will also host animation editing and videotape production.

PLANS FY01

Depending on the traffic on the "data1" server and demand for GFDL products, additional resources may be purchased for this server. The most likely such upgrade would be additional disk space.

Over time, GFDL's collection of netCDF file manipulation software will be rebuilt using the new version 3.4 library, in order to realize the speed improvement offered by the new version. Utility updates are expected, as are new utilities, such as *"nctranspose"* which reorders the dimensions of a dataset to comply with the COARDS (Cooperative Ocean/ Atmosphere Research Data Service) conventions.

When netCDF version 3.5 is released (expected in late 2000), it will be installed and tested. Applications will be relinked using the new library, as necessary.

9.3 DATA VISUALIZATION

J. Sheldon *H. Vahlenkamp*

ACTIVITIES FY00

Following the upgrade of most of the Lab's workstations to Irix 6, new versions of several analysis/visualization packages were installed (MATLAB, Iris Explorer, S-PLUS, and IDL). These new versions offer significant new capabilities.

A number of improvements have been made to GFDL's "Gallery" web page (`http://www.gfdl.gov/~jps/GFDL_VG_Gallery.html`) over the past year. These include more animations of recent hurricanes, now including AVI formatted versions which are more appropriate for visitors using Windows platforms.

GFDL staff participated in the "Visualization Development Environments 2000" workshop and presented a variety of high-end graphics and animations that demonstrated the use of the Iris Explorer visualization package. The presentation included descriptions of the large number of locally-written modules that have been donated to the Explorer community.

GFDL has provided graphic materials in several forms to outside agencies and the media (HPCC, Science magazine, BBC, Newsweek, Discovery Channel, World Book Publishing). These interactions provide a valuable mechanism for informing the public on scientific issues related to NOAA's mission (see also section 9.5).

PLANS FY01

If, as expected, GFDL's new workstations include substantially improved graphics performance, some work will be required to adapt existing software to the new hardware. It is hoped that the graphics performance improvement of the new desktop systems (of order 20-30x) will revitalize interest in higher-end graphics within the lab. In addition, the Onyx-3 class graphics capabilities included as part of the new HPCS will be exploited, with the possible addition of special headwear (glasses) for a more immersive 3D experience.

One long-standing need that will be addressed in the coming year is an upgrade to the Lab's animation/video editing capabilities. The current hardware is approximately 10 years old, and most of the software is homegrown. Creating a videotape of even a few minutes length requires overnight processing. New technology should radically improve this situation.

9.4 INFORMATION AND PRESENTATION RESOURCES

G. Haller *T. Taylor*
C. Raphael *H. Vahlenkamp*
J. Sheldon *J. Varanyak*

ACTIVITIES FY00

A major improvement in GFDL's web pages was realized with the addition of a local-area search engine based on the *ht://Dig* search system. With a variety of configurable options, visitors to GFDL's web site can search any of the web pages and other documents available through the Lab's web server. This is a critical step toward the "Virtual Help Desk" which is envisioned to provide immediate help to users at any time of the day or night.

A second software package intended to further information dissemination has been installed. The new GFDL "Ultimate Bulletin Board" (UBB) allows for public and private forums to foster discussion about particular subjects, and maintains 'threads" of conversations for specific topics. Forums have been established for the Modular Ocean Model (MOM) and for the Flexible modeling System (FMS) to serve as a focal point for announcements about the codes and questions about its use.

GFDL's monthly "Computer Users Meetings" generally consist of several informal presentations and announcements related to various IT activities. These materials are now available on-line and are particularly useful in light of the new internal search engine. In order to provide up-to-date information between meetings, and new "Project Status" page was initiated which details the status of certain high-impact projects.

To provide access for people with disabilities, GFDL's primary web pages were made handicapped-accessible, in compliance with section 508 guidelines.

Three additional Dell laptop computers were purchased for use by GFDL staff on travel. This allows them to work on the road, but also provides a mechanism by which presentations can be made.

PLANS FY01

Updates to the existing User Guide and Visualization guide will continue as the GFDL computing environment evolves. The Laboratory's web pages will continue to evolve and improve, with the "Administrative Services" page getting early priority.

It is hoped that there will be time to begin investigating "Color Management Systems". These systems are used to calibrate monitors and printers to improve the fidelity of hard-copy printouts to that which the user sees on his workstation screen.

9.5 PUBLIC INFORMATION DISSEMINATION AND OUTREACH

M. Crane *B. Ross*
G. Haller *J. Sheldon*
J.D. Mahlman *H. Vahlenkamp*

ACTIVITIES FY00

FY00 saw NOAA's presence in the national media spotlight continue. The coverage of El Nino/La Nina, global warming, and hurricanes, served to focus national attention on several areas of research conducted at GFDL. Growing public awareness that oceanic and climate science bears directly on the economic and social well-being of our country has created new demands for the dissemination of accurate and understandable scientific information. Efforts to meet this need have been directed toward increased media attention, educational enterprises, community relations, and enhanced use of the World Wide Web. Some specific activities are listed below:

- In May, Jerry Mahlman gave a briefing to Staff Members of the Senate Commerce Committee and Testimony to a Senate Commerce Committee Hearing under Chairman John McCain on the "Science Behind Climate Change".

- In September, two symposia were held to honor the remarkable achievements of Jerry Mahlman upon the occasion of his retirement from GFDL. The first symposium "Understanding the Stratosphere: Challenges and Opportunities" provided a forum for distinguished experts on dynamics and chemistry to review recent research and outline future directions in stratospheric science, as well as to place Jerry Mahlman's contributions to this subject over the last four decades in a contemporary context. The second symposium "Beyond the Science of Climate Change" brought together renowned experts in the physical, biological and social sciences to discuss the broad human, environmental and policy implications of climate change.

- Anthony Broccoli, Thomas Delworth and Jerry Mahlman appeared on radio and television broadcasts concerning global warming and other environmental issues.

- Keith Dixon of the Climate Dynamics group provided graphics, data and background information for articles related to climate change in Newsweek magazine (January 1, 2000), Time Magazine (September 4, 2000, cover story in Canada and Europe) and Discover magazine (June 2000, cover story). Keith Dixon, Thomas Knutson and Jerry Mahlman were also quoted in the article in Discover.

- Over 100 outside seminars and lectures were presented to a wide variety of audiences by GFDL scientists in FY99 (see Appendix D). In particular, Jerry Mahlman presented a series of lectures at various colleges, universities and other organizations on global warming. Many of these were sponsored by the Sigma Xi Society.

- GFDL participated in several teacher training workshops. Key among them was the Woodrow Wilson National Fellowship Foundation's (WWNFF) Leadership Program for Teachers. As part of this program, GFDL scientists presented lectures on basic weather/climate and climate change to 55 middle and high school teachers from across the nation and one staff member mentored a subgroup of these teachers. GFDL staff also contributed two one-week units on weather and climate to QUEST, a summer science program for elementary school teachers run by the Teacher Preparation Program of Princeton University. GFDL participation in QUEST was sponsored by sponsored by the Princeton Environmental Institute (PEI). GFDL staff also participated in teacher training programs sponsored by local school districts.

- Numerous GFDL scientists volunteered to participate in educational outreach at schools (elementary school level to college), and with community groups throughout the year. These activities included classroom presentations, mentorships, and tours of GFDL.

- Effort has been increased to alert the media of significant events and research results at GFDL, including advances in hurricane prediction and the understanding of global climate change.

- The GFDL educational web page (`http://www.gfdl.gov/Science_facts.html`) has continued. In addition to presenting GFDL research in a basic, non-technical way, this page also provides links to a wide variety of web sites with facts about hurricanes, El Nino/La Nina, and climate change.

APPENDIX A

GFDL STAFF MEMBERS

and

AFFILIATED PERSONNEL

during

Fiscal Year 2000

PERSONNEL SUMMARY

September 30, 2000

GFDL/NOAA	
Full Time Permanent (FTP)	77
Part Time Permanent (PTP)	1
Part Time Temporary (PTT)	1
PRINCETON UNIVERSITY (PU)	
AOS Visiting Scientists	14
Graduate Students	15
Professors	3
Research Scholar	3
Senior Research Scholar	2
Research Staff	7
Senior Technical Staff	1
Support Staff	4
Technical Staff	1
OTHER INSTITUTIONS	
U.S. Geological Survey (USGS)	2
University Corporation for Atmospheric Research (UCAR)	2
National Centers for Environmental Prediction (NCEP)	1
VENDORS	
Cray Research Inc. Computer Support Staff	4
TOTAL	**138**

CLIMATE DYNAMICS

Held, Isaac M.	Senior Scientist at GFDL	FTP
Broccoli, Anthony J.	Meteorologist	FTP
Jackson, Charles	AOS Visiting Scientist	PU*
Delworth, Thomas L.	Meteorologist	FTP
Dixon, Keith W.	Meteorologist	FTP
Hayashi, Yoshikazu	Meteorologist	FTP**
Knutson, Thomas R.	Meteorologist	FTP
Lapeyre, Guillaume	AOS Visiting Scientist	PU
Kushner, Paul	Physical Scientist	FTP
Cash, Benjamin	AOS Visiting Scientist	PU
Marinov, Irina	Graduate Student	PU
Milly, P.C.D.	Hydrologist	USGS***
Dunne, Krista	Physical Scientist	USGS***
Shmakin, Andrey	Scientific Visitor	UCAR*
Pauluis, Olivier	Graduate Student	PU*
Phillipps, Peter J.	Meteorologist	FTP
Schneider, Tapio	Graduate Student	PU*
Stouffer, Ronald J.	Meteorologist	FTP
Golder, Donald G.	Meteorologist	FTP
Spelman, Michael J.	Meteorologist	FTP
Vallis, Geoff	Senior Research Scholar	PU
Cartwright, Cara	Graduate Student	PU
Frierson, Dargan	Graduate Student	PU
Grianik, Nadia	Gradinate Student	PU
Huck, Thierry	AOS Visiting Scientist	PU*
Scott, Robert	AOS Visiting Scientist	PU
Wetherald, Richard T.	Meteorologist	FTP
Williams, Gareth P.	Meteorologist	FTP

*Affiliation terminated prior to September 30, 2000.
**Deceased November 5, 1999.
***United States Geological Survey (USGS), on detail to GFDL.

ATMOSPHERIC PROCESSES

Ramaswamy, V.	Physical Scientist	FTP
Cooke, William	AOS Visiting Scientist	PU
Donner, Leo J.	Physical Scientist	FTP
Seman, Charles J.	Physical Scientist	FTP
Erlick, Carynelisa	AOS Visiting Scientist	PU*
Garrett, Timothy	AOS Visiting Scientist	PU
Freidenreich, Stuart	Meteorologist	FTP
Hamilton, Kevin P.	Meteorologist	FTP*
Wilson, R. John	Meteorologist	FTP
Hemler, Richard S.	Meteorologist	FTP
Klein, Steven	Meteorologist	FTP
Levy II, Hiram	Physical Scientist	FTP
Holloway, Teresa	Graduate Student	PU
Horowitz, Larry	AOS Visiting Scientist	PU
Moxim, Walter J.	Meteorologist	FTP
Wang, Sheng-Wei	AOS Visiting Scientist	PU
Yang, Huiyan	Graduate Student	PU
Schwarzkopf, M. Daniel	Meteorologist	FTP

EXPERIMENTAL PREDICTION

Anderson, Jeffrey L.	Meteorologist	FTP
Gordon, C. Tony	Meteorologist	FTP
Griffies, Stephen M.	Physical Scientist	FTP
Smith, K. Shafer	AOS Visiting Scientist	PU
Khare, Shree	Graduate Student	PU
Ploshay, Jeffrey J.	Meteorologist	FTP
Rosati, Anthony J.	Physical Scientist	FTP
Gudgel, Richard G.	Meteorologist	FTP
Harrison, Matthew	Physical Scientist	FTP
Sirutis, Joseph J.	Meteorologist	FTP
Stern, William F.	Meteorologist	FTP
Smith, Robert G.	Computer Assistant	FTP
Wyman, Bruce L.	Meteorologist	FTP
Zhang, Shaoqing	Visiting Scientist	PU

*Affiliation terminated prior to September 30, 2000.

OCEANIC CIRCULATION

Toggweiler, J. R.	Oceanographer	FTP
Bjornsson, Haldor	AOS Visiting Scientist	PU*
Carson, Steven R.	Physical Scientist	FTP
Hallberg, Robert	Oceanographer	FTP
Hotinski, Roberta	AOS Visiting Scientist	PU
Hurlin, William J.	Meteorologist	FTP
Pacanowski, Ronald C.	Oceanographer	FTP
Samuels, Bonita L.	Oceanographer	FTP
Stephens, James	AOS Visiting Scientist	PU
Winton, Michael	Oceanographer	FTP

CLIMATE DIAGNOSTICS

Lau, Ngar-Cheung	Meteorologist	FTP
Crane, Mark	Meteorologist	FTP*
Lanzante, John	Meteorologist	FTP
Nath, Mary Jo	Meteorologist	FTP
Soden, Brian J.	Physical Scientist	FTP
Tam, Chi-Yung	Graduate Student	PU
Wang, Hailan	AOS Visiting Scientist	PU

HURRICANE DYNAMICS

Tuleya, Robert E.	Meteorologist	FTP
Bender, Morris A.	Meteorologist	FTP
Marchok, Timothy	Meteorologist	NCEP**

MESOSCALE DYNAMICS

Orlanski, Isidoro	Meteorologist	FTP
Garner, Stephen	Meteorologist	FTP
Li, Di	Graduate Student	PU
Polinsky, Larry	Meteorologist	FTP

*Affiliation terminated prior to September 30, 2000.
**Science Applications International Corporation/NCEP

MANAGEMENT FRAMEWORK

Administrative and Technical Structure

Mahlman, Jerry D.	Director	FTP*
Ross, Bruce B.	Assistant Director	FTP
Balaji, V.	Applications Analyst	CRI
Byrne, James S.	Junior Technician	FTP
Gross, Brian	Physical Scientist	FTP
Kerr, Christopher L.	Scientific Visitor	UCAR
Marshall, Wendy H.	Budget Analyst	FTP
Mayle, Stephen F.	Administrative Officer	FTP
Shearn, William F.	Leader, COMPUTER OPERATIONS	FTP
Sheldon, John	Leader, TECHNICAL SERVICES	FTP
Williams, Betty M.	Secretary	FTP

Scientific Structure

Mahlman, Jerry D.	Director	FTP*
Anderson, Jeffrey L.	Leader, EXERIMENTAL PREDICTION	FTP
Held, Isaac M.	Leader, CLIMATE DYNAMICS	FTP
Lau, Ngar-Cheung	Leader, CLIMATE DIAGNOSTICS	FTP
Orlanski, Isidoro	Leader, MESOSCALE DYNAMICS	FTP
Ramaswamy, V.	Leader, ATMOSPHERIC PROCESSES	FTP
Toggweiler, J. R.	Leader, OCEANIC CIRCULATION	FTP
Tuleya, Robert E.	Leader, HURRICANE DYNAMICS	FTP

*Affiliation terminated prior to September 30, 2000.

TECHNICAL SERVICES

Sheldon, John	Graphics Specialist/Meteorologist	FTP
Haller, Gail T.	Computer Assistant	FTP
Amend, Beatrice E.	Office Automation Clerk	PTT
Urbani, Elaine B.	Transportation Assistant	FTP
Lewis, Lawrence J.	Computer Specialist	FTP
Taylor III, Thomas E.	Computer Specialist	FTP
White, Robert K.	Computer Specialist	FTP
Yeager, William T.	Computer Specialist	FTP
Raphael, Catherine	Scientific Illustrator	PTP
Vahlenkamp, Hans	Software Engineer	UCAR
Varanyak, Jeffrey	Scientific Illustrator	FTP

COMPUTER OPERATIONS SUPPORT

Shearn, William F.	Operations Manager	FTP
Deuringer, James A.	Supervisory Computer Operator	FTP
Blakemore, Geneve	Computer Operator	FTP
Krueger, Scott R.	Lead Computer Operator	FTP
Hand, Joseph S.	Supervisory Computer Operator	FTP
Cordwell, Clara L.	Lead Computer Operator	FTP
Ledden, Jay H.	Computer Operator	FTP
Russick, Deborah	Computer Operator	FTP
Henne, Ronald N.	Computer Assistant	FTP
Hopps, Frank K.	Supervisory Computer Operator	FTP
Aikin, Douglas	Computer Operator	FTP
Duggins, Marsha	Computer Operator	FTP
Harrold, Renee M.	Computer Operator	FTP
King, John T.	Lead Computer Operator	FTP
Zielenbach, Amy	Computer Operator	FTP*

*Affiliation terminated prior to September 30, 2000.

CRAY RESEARCH INCORPORATED

Siebers, Bernard	Analyst in Charge	CRI
Braunstein, Mark	Field Engineer	CRI
Balaji, V.	Applications Analyst	CRI
Weiss, Ed	Engineer in Charge	CRI

ATMOSPHERIC AND OCEANIC SCIENCES PROGRAM

Philander, S.G.H.	Professor, Program Director	PU
Boccaletti, Giulio	Graduate Student	PU
Bryan, Kirk	Senior Research Scholar	PU
Callan, Johann V.	Secretary	PU
Clark, Sandra	Systems Administrator	PU
Federov, Alexey	AOS Visiting Scientist	PU
Harper, Scott	Graduate Student	PU
Rossi, Laura	Program Manager	PU
Valerio, Anna	Technical Research Secretary	PU
Winter, Barbara	Technical Staff	PU
Wittenberg, Andrew	Gradudate Student	PU
Mellor, George	Professor Emeritus	PU
Ezer, Tal	Research Scholar	PU
Kim, Namsoug	Technical Staff	PU*
Lee, Hyun-Chul	AOS Visiting Scienitst	PU
Oey, Lie-Yauw	Research Scholar	PU
Wei, Mozheng	Research Staff	PU
Sarmiento, Jorge	Professor	PU
Armstrong, Robert	Research Scholar	PU*
Baker, David F.	Graduate Student	PU
Deutsch, Curtis	Graduate Student	PU
Fan, Song-Miao	Research Staff	PU
Gao, Yuan	Research Staff	PU
Gloor, Manuel	Research Staff	PU*
Gnanadesikan, Anand	Research Staff	PU
Gruber, Nicholas	Research Staff	PU*
Key, Robert M.	Research Scholar	PU
Matsumoto, Katsumi	Research Staff	PU
Mignone, Bryan	Graduate Student	PU
Mohr, Brian K.	Technical Staff	PU*
Slater, Richard D.	Senior Technical Staff	PU
Swathi, P.S.	Research Staff	PU
Wang, Guilian	Research Staff	PU

*Affiliation terminated prior to September 30, 2000.

APPENDIX B

GFDL

BIBLIOGRAPHY

1997-2000

GFDL PUBLICATIONS

This is a partial listing of GFDL publications. A more up-to-date version is available on-line at http://www.gfdl.gov/~gth/netscape/bibliography.html. A hardcopy of the complete bibliography can also be obtained by calling (609) 452-6502, or by writing to:

Director
Geophysical Fluid Dynamics Laboratory
Post Office Box 308
Princeton, New Jersey 08542

(1427) Mahlman, J.D., A Scientist's Perspective on Integrated Observing and Long-Term Monitoring Systems, in *First Symposium on Integrated Observing Systems*, American Meteorological Society, pp. 76-78, 1997.

(1428) Delworth, T.L., S. Manabe, and R.J. Stouffer, Multidecadal Climate Variability in the Greenland Sea and Surrounding Regions: A Coupled Model Simulation, *Geophysical Research Letters, 24(3)*, 257-260, 1997.

* (1429) Griffies, S.M., and K. Bryan, Predictability of North Atlantic Multidecadal Climate Variability, *Science, 275*, 181-184, 1997.

* (1430) Winton, M., The Damping Effect of Bottom Topography on Internal Decadal-Scale Oscillations of the Thermohaline Circulation, *Journal of Physical Oceanography, 27(1)*, 203-208, 1997.

* (1431) Knutson, T.R., S. Manabe, and D. Gu, Simulated ENSO in a Global Coupled Ocean-Atmosphere Model: Multidecadal Amplitude Modulation and CO_2 Sensitivity, *Journal of Climate, 10(1)*, 138-161, 1997.

* (1432) Gu, D., and S.G.H. Philander, Interdecadal Climate Fluctuations that Depend on Exchanges Between the Tropics and Extratropics, *Science, 275*, 805-807, 1997.

(1433) Delworth, T.L., S. Manabe, and R.J. Stouffer, Interannual to Interdecadal Variability in a Coupled Ocean-Atmosphere Model, in *Proceedings of International Workshop on Numerical Prediction of Oceanic Conditions*, Tokyo, Japan, 7-11 March 1995, pp. 99-107, 1997.

(1434) Winton, M., The Effect of Cold Climates upon North Atlantic Deep Water Formation in a Simple Ocean-Atmosphere Model, *Journal of Climate, 10(1)*, 37-51, 1997.

(1435) Bender, M.A., The Effect of Relative Flow on the Asymmetric Structure in the Interior of Hurricanes, *Journal of the Atmospheric Sciences, 54(6)*, 703-724, 1997.

(1436) Manabe, S., Early Development in the Study of Greenhouse Warming: The Emergence of Climate Models, *Ambio* (Special volume commemorating 100th year anniversary of the publication of "Arrhenius" paper on Greenhouse Warming), *26(1)*, 47-51, 1997.

(1437) Lau, N.-C., Interactions Between Global SST Anomalies and the Midlatitude Atmospheric Circulation, *Bulletin of the American Meteorological Society, 78(1)*, 21-33, 1997.

* (1438) Ramaswamy, V., and C.-T. Chen, Linear Additivity of Climate Response for Combined Albedo and Greenhouse Perturbations, *Geophysical Research Letters, 24(5)*, 567-570, 1997.

*In collaboration with other organizations

* (1439) Balasubramanian, G., and S.T. Garner, The Role of Momentum Fluxes in Shaping the Life Cycle of a Baroclinic Wave, *Journal of the Atmospheric Sciences, 54(4)*, 510-533, 1997.

* (1440) Ramaswamy, V., and C.-T. Chen, Climate Forcing-Response Relationships for Greenhouse and Shortwave Radiative Perturbations, *Geophysical Research Letters, 24(6)*, 667-670, 1997.

(1441) Hamilton, K., The Role of Parameterized Drag in a Troposphere-Stratosphere-Mesosphere General Circulation Model, in *Gravity Waves Processes, Their Parameterization in Global Climate Models*, edited by K. Hamilton, Springer-Verlag, pp.337-350, 1997.

(1442) Donner, L.J., C.J. Seman, and J.P. Sheldon, Cloud-Radiative Interactions in High-Resolution Cloud-Resolving Models, in *Preprints 9th Conference on Atmospheric Radiation*, Long Beach, CA, 2-7 February 1997, American Meteorological Society, Boston, MA, pp. 47-48, 1997.

* (1443) Swanson, K.L., P.J. Kushner, and I.M. Held, Dynamics of Barotropic Storm Tracks, *Journal of the Atmospheric Sciences, 54(7)*, 791-810, 1997.

(1444) Manabe, S., and R.J. Stouffer, Coupled Ocean-Atmosphere Model Response to Freshwater Input: Comparison to Younger Dryas Event, *Paleoceanography, 12(2)*, 321-336, 1997.

* (1445) Levy II, H., P.S. Kasibhatla, W.J. Moxim, A.A. Klonecki, A.I. Hirsch, S.J. Oltmans, and W.L. Chameides, The Global Impact of Human Activity on Tropospheric Ozone, *Geophysical Research Letters, 24(7)*, 791-794, 1997.

* (1446) Zhang, Y., *On the Mechanisms for the Mid-winter Suppression of the Pacific Stormtrack*, Ph.D. Dissertation, Atmospheric and Oceanic Sciences Program, Princeton University, 1997.

* (1447) Treguier, A.M., I.M. Held, and V.D. Larichev, Parameterization of Quasigeostrophic Eddies in Primitive Equation Ocean Models, *Journal of Physical Oceanography, 27(4)*, 567-580, 1997.

* (1448) Lanzante, J.R., and G.E. Gahrs, Examination of Some Biases in Satellite and Radiosonde Measures of Upper Tropospheric Humidity using a Framework for the Comparison of Redundant Measurement Systems, in *Proceedings of the 21st Annual Climate Diagnostics and Prediction Workshop*, Huntsville, AL, October 1996, pp. 352-355, 1997.

(1449) Anderson, J.L., A. Rosati, and R.G. Gudgel, Potential Predictability in an Ensemble of Coupled Atmosphere-Ocean General Circulation Model Seasonal Forecasts, in *Proceedings of the 21st Annual Climate Diagnostics and Prediction Workshop*, Huntsville, AL, October 1996, pp. 18-21, 1997.

(1450) Anderson, J.L., and R.G. Gudgel, Impact of Atmospheric Initial Conditions on Seasonal Predictions with a Coupled Ocean-Atmosphere Model, in *Proceedings of the 21st Annual Climate Diagnostics and Prediction Workshop*, Huntsville, AL, October 1996, pp. 61-66, 1997.

* (1451) Peng, P., and N.-C. Lau, The Impact of the Monthly-Varying Global SST Anomalies on the Northern Hemisphere Circulation as Seen in an Ensemble of NCEP GCM Simulations, in *Proceedings of the 21st Annual Climate Diagnostics and Prediction Workshop*, Huntsville, AL, October 1996, pp. 102-105, 1997.

(1452) Hayashi, Y., and D.G. Golder, United Mechanisms for the Generation of Low- and High-Frequency Tropical Waves: Part I: Control Experiments with Moist Convective Adjustment, *Journal of the Atmospheric Sciences, 54(9)*, 1262-1276, 1997.

*In collaboration with other organizations

* (1453) Hall, A., and S. Manabe, Can Local Linear Stochastic Theory Explain Sea Surface Temperature and Salinity Variability?, *Climate Dynamics, (13)*, 167-180, 1997.

(1454) Williams, G.P., Planetary Vortices and Jupiter's Vertical Structure, *Journal of Geophysical Research, 102(E4)*, 9303-9308, 1997.

* (1455) Vitart, F., J.L. Anderson, W.F. Stern, Simulation of Interannual Variability of Tropical Storm Frequency in an Ensemble of GCM Integrations, *Journal of Climate, 10(4)*, 745-760, 1997.

* (1456) Jones, P.W., K. Hamilton, and R.J. Wilson, A Very High-Resolution General Circulation Model Simulation of the Global Circulation in Austral Winter, *Journal of the Atmospheric Sciences, 54(8)*, 1107-1116, 1997.

(1457) Rosati, A., K. Miyakoda, and R. Gudgel, The Impact of Ocean Initial Conditions on ENSO Forecasting with a Coupled Model, *Monthly Weather Review, 125(5)*, 754-772, 1997.

* (1458) Li, J., S.M. Freidenreich, and V. Ramaswamy, Solar Spectral Weight at Low Cloud Tops, *Journal of Geophysical Research, 102(D10)*, 11,139-11,143, 1997.

* (1459) Soden, B., Variations in the Tropical Greenhouse Effect during El Niño, *Journal of Climate, 10(5)*, 1050-1055, 1997.

* (1460) Li, X., P. Chang, and R.C. Pacanowski, A Wave-Induced Stirring Mechanism in the Mid-depth Equatorial Ocean, *Journal of Marine Research, 54*, 487-520, 1996.

(1461) Kurihara, Y., M.A. Bender, and R.E. Tuleya, For Hurricane Intensity Forecast: Formulation of a New Initialization Method for the GFDL Hurricane Prediction Model, in *Preprints 22nd Conference on Hurricanes and Tropical Meteorology*, Ft. Collins, CO, 19-23 May 1997, American Meteorological Society, Boston, MA, pp. 543-544, 1997.

(1462) Knutson, T., R. Tuleya, and Y. Kurihara, Exploring the Sensitivity of Hurricane Intensity to CO2-Induced Global Warming using the GFDL Hurricane Prediction System, in *Preprints 22nd Conference on Hurricanes and Tropical Meteorology*, Ft. Collins, CO, 19-23 May 1997, American Meteorological Society, Boston, MA, pp. 587-588, 1997.

* (1463) Bender, M.A., C.-C. Wu, M.A. Rennick, and Y. Kurihara, Comparison of the GFDL Hurricane Model Prediction in the Western Pacific using the NOGAPS and AVN Global Analysis, in *Preprints 22nd Conference on Hurricanes and Tropical Meteorology*, Ft. Collins, CO, 19-23 May 1997, American Meteorological Society, Boston, MA, pp. 615-616, 1997.

* (1464) Wacongne, S., and R.C. Pacanowski, Seasonal Heat Transport in a Primitive Equations Model of the Tropical Indian Ocean, *Journal of Physical Oceanography, 26(12)*, 2666-2699, 1996.

* (1465) Burpee, R.W., J.L. Franklin, S.J. Lord, R.E. Tuleya, and S.D. Aberson, The Impact of Omega Dropwindsondes on Operational Hurricane Track Forecast Models, *Bulletin of the American Meteorological Society, 77(5)*, 925-933, 1996.

* (1466) Milly, P.C.D., Sensitivity of Greenhouse Summer Dryness to Changes in Plant Rooting Characteristics, *Geophysical Research Letters, 24(3)*, 269-271, 1997.

* (1467) Li, T., S.G.H. Philander, On the Annual Cycle of the Eastern Equatorial Pacific, *Journal of Climate, 9(12)*, 2986-2998, 1996

* (1468) Philander, S.G.H., D. Gu, D. Halpern, G. Lambert, N.-C. Lau, T. Li, R.C. Pacanowski, Why the ITCZ is Mostly North of the Equator, *Journal of Climate, 9(12)*, 2958-2972, 1996.

(1469) Hamilton, K., Observation of an Ultraslow Large-Scale Wave Near the Tropical Tropopause, *Journal of Geophysical Research, 102(D12)*, 13,457-13,464, 1997

* (1470) Tuleya, R.E., and S.J. Lord, The Impact of Dropwindsonde Data on GFDL Hurricane Model Forecasts using Global Analyses, *Weather and Forecasting, 12(2)*, 307-323, 1997.

*In collaboration with other organizations

* (1471) Gnanadesikan, A., and R.C. Pacanowski, Improved Representation of Flow Around Topography in the GFDL Modular Ocean Model MOM2, *International WOCE Newsletter, 27*, 23-25, 1997.

(1472) Manabe, S., and R.J. Stouffer, Climate Variability of a Coupled Ocean-Atmosphere-Land Surface Model: Implication for the Detection of Global Warming, *Bulletin of the American Meteorological Society, 78(6)*, 1177-1185, 1997.

* (1473) Haywood, J.M., R.J. Stouffer, R.T. Wetherald, S. Manabe, and V. Ramaswamy, Transient Response of a Coupled Model to Estimated Changes in Greenhouse Gas and Sulfate Concentrations, *Geophysical Research Letters, 24(11)*, 1335-1338, 1997.

* (1474) Zhang, Y., K.R. Sperber, J.S. Boyle, M.R. Dix, L. Ferranti, A. Kitoh, K.M. Lau, K. Miyakoda, D. Randall, L. Takacs, and R. Wetherald, *GCM Simulated East Asian Winter Monsoon: Results from Eight AMIP Models*, PCMDI Report No. 39, 49 pp., 1997.

* (1475) Ezer, T., and G.L. Mellor, Data Assimilation in the Gulf Stream Region: How Useful are Satellite-Derived Surface Data for Nowcasting the Subsurface Fields?, *Journal of Atmospheric and Oceanic Technology, 14(6)*, 1379-1391, 1997.

* (1476) Ezer, T., and G.L. Mellor, Simulations of the Atlantic Ocean with a Free Surface Sigma Coordinate Ocean Model, *Journal of Geophysical Research, 102(C7)*, 15,647-15,657, 1997.

* (1477) Kelley, J.G.W., F. Aikman II, L.C. Breaker, and G.L. Mellor, Coastal Ocean Forecasts, *Sea Technology, 38(5)*, 10-17, 1997.

* (1478) Cess, R.D., M.-H. Zhang, G.L. Potter, V. Alekseev, H.W. Barker, S. Bony, R.A. Colman, D.A. Dazlich, A.D. Del Genio, M. Déqué, M.R. Dix, V. Dymnikov, M. Esch, L.D. Fowler, J.R. Fraser, V. Galin, W.L. Gates, J.J. Hack, W.J. Ingram, J.T. Kiehl, Y. Kim, H. LeTreut, X.-Z. Liang, B.J. McAvaney, V.P. Meleshko, J.-J. Morcrette, D.A. Randall, E. Roeckner, M.E. Schlesinger, P.V. Sporyshev, K.E. Taylor, B. Timbal, E.M. Volodin, W. Wang, W.-C. Wang, and R.T. Wetherald, Comparison of the Seasonal Change in Cloud-Radiative Forcing from Atmospheric General Circulation Models and Satellite Observations, *Journal of Geophysical Research, 102(D14)*, 16,593-16,603, 1997.

* (1479) Koster, R.D., and P.C.D. Milly, The Interplay between Transpiration and Runoff Formulations in Land Surface Schemes used with Atmospheric Models, *Journal of Climate, 10(7)*, 1578-1591, 1997.

* (1480) Chen, T.H., A. Henderson-Sellers, P.C.D. Milly, A.J. Pitman, A.C.M. Beljaars, J. Polcher, F. Abramopoulos, A. Boone, S. Chang, F. Chen, Y. Dai, C.E. Desborough, R.E. Dickinson, L. Dumenil, M. Ek, J.R. Garratt, N. Gedney, Y.M. Gusev, J. Kim, R. Koster, E.A. Kowalczyk, K. Laval, J. Lean, D. Lettenmaier, X. Liang, J.-F. Mahfouf, H.-T. Mengelkamp, K. Mitchell, O.N. Nasonova, J. Noilhan, A. Robock, C. Rosenzweig, J. Schaake, C.A. Schlosser, J.-P. Schulz, Y. Shao, A.B. Shmakin, D.L. Verseghy, P. Wetzel, E.F. Wood, Y. Xue, Z.-L. Yang, and Q. Zeng, Cabauw Experimental Results from the Project for Intercomparison of Land-surface Parameterization Schemes (PILPS), *Journal of Climate, 10(6)*, 1194-1215, 1997.

(1481) Mahlman, J.D., Dynamics of Transport Processes in the Upper Troposphere, *Science, 276*, 1079-1083, 1997.

* (1482) Hallberg, R., Stable Split Time Stepping Schemes for Large-Scale Ocean Modeling, *Journal of Computational Physics, 135*, 54-65, 1997.

* (1483) Haywood, J.M., V. Ramaswamy, and L.J. Donner, A Limited-Area-Model Case Study of the Effects of Sub-Grid Scale Variations in Relative Humidity and Cloud Upon the Direct Radiative Forcing of Sulfate Aerosol, *Geophysical Research Letters, 24(2)*, 143-146, 1997.

*In collaboration with other organizations

* (1484) Haywood, J.M., D.L. Roberts, A. Slingo, J.M. Edwards, and K.P. Shine, General Circulation Model Calculations of the Direct Radiative Forcing by Anthropogenic Sulfate and Fossil-Fuel Soot Aerosol, *Journal of Climate, 10(7)*, 1562-1577, 1997.

* (1485) Gruber, N., J.L. Sarmiento, and T.F. Stocker, An Improved Method for Detecting Anthropogenic CO_2 in the Oceans, *Global Biogeochemical Cycles, 10*, 809-837, 1996.

* (1486) Sarmiento, J.L., and C. LeQuéré, Oceanic CO_2 Uptake in a Model of Century-Scale Global Warming, *Science, 274*, 1346-1350, 1996.

* (1487) Key, R.M., WOCE Pacific Ocean Radiocarbon Program, *Radiocarbon, 38(3)*, 415-423, 1997.

* (1488) Key, R.M., and P.D. Quay, WOCE AMS Radiocarbon I: Pacific Ocean Results: P6, P16, and P17, *Radiocarbon, 38(3)*, 425-518, 1997.

* (1489) Stuiver, M., H.G. Ostlund, R.M. Key, and P.J. Reimer, Large Volume WOCE Radiocarbon Sampling in the Pacific Ocean, *Radiocarbon, 38(3)*, 519-561, 1997.

(1490) Hayashi, Y., and D.G. Golder, United Mechanisms for the Generation of Low- and High-Frequency Tropical Waves, Part II: Theoretical Interpretations, *Journal of the Meteorological Society of Japan, 75(4)*, 775-797, 1997.

(1491) Schwarzkopf, M.D., and V. Ramaswamy, Stratospheric Climatic Effects due to CH_4, N_2O, CFCs, and the H_2O Infrared Continuum: A GCM Experiment, in *IRS 96: Current Problems in Atmospheric Radiation*, International Radiation Symposium, Fairbanks, Alaska, 19-24 August 1996, pp. 336-339, 1997.

(1492) Donner, L.J., C.J. Seman, R.S. Hemler, and J.P. Sheldon, Radiative Transfer in a Three-Dimensional Cloud-System-Resolving Model, in *IRS 96: Current Problems in Atmospheric Radiation*, International Radiation Symposium, Fairbanks, Alaska, August 1996, pp. 109-112, 1997.

* (1493) Chen, C.-T., and V. Ramaswamy, Climate Sensitivity to Solar and Greenhouse Radiative Forcings, in *IRS 96: Current Problems in Atmospheric Radiation*, International Radiation Symposium, Fairbanks, Alaska, August 1996, pp. 279-281, 1997.

(1494) Ramaswamy, V., and S.M. Freidenreich, Absorption of Solar Radiation in Overcast Atmospheres, in *IRS 96: Current Problems in Atmospheric Radiation*, International Radiation Symposium, Fairbanks, Alaska, August 1996, pp. 125-127, 1997.

(1495) Freidenreich, S.M., and V. Ramaswamy, A New Miulti-Band Solar Radiative Parameterization, preprint of the *9th Conference on Atmospheric Radiation*, Long Beach, CA, American Meteorological Society, Boston, MA, pp. 129-130, 1997.

* (1496) Hurtt, G.C., *Ocean Ecosystem Models for Use in Studies of the Air-Sea Balance of Carbon Dioxide*, Ph.D. Dissertation, Department of Ecology and Evolutionary Biology, Princeton University, 1997.

(1497) Gruber, N., and J.L. Sarmiento, Global Patterns of Marine Nitrogen Fixation and Denitrification, *Global Biogeochemical Cycles, 11(2)*, 235-266, 1997.

* (1498) Michaels, A.F., D. Olson, J.L. Sarmiento, J.W. Ammerman, K. Fanning, R. Jahnke, A.H. Knap, F. Lipschultz, J.M. Prospero, Inputs, Losses and Transformations of Nitrogen and Phosphorus in the Pelagic North Atlantic Ocean, *Biogeochemistry, 35*, 181-226, 1997.

* (1499) Sabine, C.L., D.W.R. Wallace, and F.J. Millero, Survey of CO_2 in the Oceans Reveals Clues about Global Carbon Cycle, *EOS, 78(5)*, 49, 54-55, 1997.

* (1500) Hurtt, G.C., and R.A. Armstrong, A Pelagic Ecosystem Model Calibrated with BATS Data, *Deep-Sea Research, Part II, 43(2-3)*, 653-683, 1996.

*In collaboration with other organizations

* (1501) Klonecki, A., and H. Levy II, Tropospheric Chemical Ozone Tendencies in CO-CH_4-NO_y-H_2O System: Their Sensitivity to Variations in Environmental Parameters and their Application to a Global Chemistry Transport Model Study, *Journal of Geophysical Research, 102(D17)*, 21,221-21,237, 1997.

* (1502) Donner, L.J., C.J. Seman, B.J. Soden, R.S. Hemler, J.C. Warren, J. Ström, and K.-N. Liou, Large-Scale Ice Clouds in the GFDL SKYHI General Circulation Model, *Journal of Geophysical Research, 102*(D18), 21,745-21,768, 1997.

* (1503) Nakamura, H., M. Nakamura, and J.L. Anderson, The Role of High- and Low-Frequency Dynamics in the Blocking Formation, *Monthly Weather Review, 125*(9), 2074-2093, 1997.

* (1504) Haywood, J.M., and K.P. Shine, Multi-Spectral Calculations of the Direct Radiative Forcing of Tropospheric Sulphate and Soot Aerosols using a Column Model, *Quarterly Journal of the Royal Meteorological Society, 123*, 1907-1930, 1997.

* (1505) Meehl, G.A., G.J. Boer, C. Covey, M. Latif, and R.J. Stouffer, Intercomparison Makes for a Better Climate Model, *EOS, Transactions, 78*(41), 445-446, 1997.

(1506) Christensen, N., J. Christy, R. Cooper, F. Culler, D. Hagen, R. Lindzen, J.D. Mahlman, L.D. Meeker, A. Robock, W. Schlesinger, H.H. Schmitt, M. Weidenbaum, and P. Wilcoxen, *Global Climate Change: Policy Making in the Context of Scientific and Economic Uncertainty*, The Annapolis Center, 15 pp., 1997.

* (1507) Griffies, S.M., and K. Bryan, A Predictability Study of Simulated North Atlantic Multidecadal Variability, *Climate Dynamics, 13*, 459-487, 1997.

* (1508) Spangenberg, D.A., G.G. Mace, T.P. Ackerman, N.L. Seaman, and B.J. Soden, Evaluation of Model-Simulated Upper Troposphere Humidity using 6.7 μm Satellite Observations, *Journal of Geophysical Research, 102*(D22), 25,737-25,749, 1997.

(1509) Anderson, J.L., The Impact of Dynamical Constraints on the Selection of Initial Conditions for Ensemble Predictions: Low-order Perfect Model Results, *Monthly Weather Review, 125*(11), 2969-2983, 1997.

* (1510) Haywood, J.M., K.P. Shine, and A. Slingo, Direct Radiative Forcing of Anthropogenic Sulfate and Soot Aerosol using a Flexible Radiation Code and a GCM, In *IRS '96: Current Problems in Atmospheric Radiation*, edited by William L. Smith and Knut Stamnes, A. Deepak Publishers, pp. 324-327, 1997.

* (1511) Klein, S., Synoptic Variability of Low-Cloud Properties and Meteorological Parameters in the Subtropical Trade Wind Boundary Layer, *Journal of Climate, 10*, 2018-2039, 1997.

* (1512) Hallberg, R., Localized Coupling Between Surface and Bottom-Intensified Flow Over Topography, *Journal of Physical Oceanography, 27*, 977-998, 1997.

(1513) Mahlman, J.D., Uncertainties in Projections of Human-Caused Climate Warming, *Science, 278*, 1416-1417, 1997.

(1514) Lau, N.-C., and M.W. Crane, Comparing Satellite and Surface Observations of Cloud Patterns in Synoptic-Scale Circulation Systems, *Monthly Weather Review, 125*(12), 3172-3189, 1997.

(1515) Hamilton, K., Meteorological Measurements on Ozonesonde Ascents: A Valuable Resource for Stratospheric Climatology, *SPARC Newsletter, 9*, 23, 1997.

* (1516) Forbes, J.M., M.E. Hagan, X. Zhang, and K. Hamilton, Upper Atmosphere Tidal Oscillations Due to Latent Heat Release in the Tropical Troposphere, *Annals Geophysicae, 15*, 1165-1175, 1997.

*In collaboration with other organizations

(1517) Miyakoda, K., J. Ploshay, and A. Rosati, Preliminary Study on SST Forecast Skill Associated with the 1982/83 El Niño Process using Coupled Model Data Assimilation, *Atmosphere-Ocean Special, XXXV* (No.1), 469-486, 1997.

* (1518) Balasubramanian, G., and S.T. Garner, The Equilibration of Short Baroclinic Waves, *Journal of the Atmospheric Sciences, 54*(24), 2850-2871, 1997.

* (1519) Ezer, T., and G.L. Mellor, Data Assimilation Experiments in the Gulf Stream Region: How Useful are Satellite-Derived Surface Data for Nowcasting the Subsurface Fields? *Journal of Atmospheric and Oceanic Technology, 14*(6), 1379-1391, 1997.

(1520) Broccoli, A.J., and S. Manabe, Mountains and Midlatitude Aridity, In *Tectonic Uplift and Climate Change*, edited by William F. Ruddiman, Plenum Press, pp. 89-121, 1997.

* (1521) Hayashi, Y., D.G. Golder, and P.W. Jones, Tropical Gravity Waves and Superclusters Simulated by High-Horizontal-Resolution SKYHI General Circulation Models, *Journal of the Meteorological Society of Japan, 75*(6), 1125-1139, 1997.

(1522) Hamilton, K., and R.S. Hemler, Appearance of a Super Typhoon in a Global Climate Model Simulation, *Bulletin of the American Meteorological Society, 78*(12), 2874-2876, 1997.

* (1523) Heintzenberg, J., R.J. Charlson, A.D. Clarke, C. Liousse, V. Ramaswamy, K.P. Shine, M. Wendisch, and G. Helas, Measurements and Modelling of Aerosol Single-Scattering Albedo: Progress, Problems and Prospects, *Contributions to Atmospheric Physics, 70*(4), 249-263, 1997.

(1524) Hamilton, K., "Gravity Currents in the Environment and the Laboratory", *EOS, Transactions, 79*, 71, 1998.

(1525) Knutson, T.R., and S. Manabe, Model Assessment of Decadal Variability and Trends in the Tropical Pacific Ocean, in *Preprints The Ninth Symposium on Global Change Studies and Namias Symposium on the Status and Prospects for Climate Prediction*, Phoenix, AZ, 11-16 January 1998, American Meteorological Society, Boston, MA, pp. 216-219, 1998.

(1526) Kurihara, Y., R.E. Tuleya, A Prospect of Improvement in the Forecast of Hurricane Landfall, in *Preprints 16th Conference on Weather Analysis and Forecasting and Symposium on The Research Foci of the U.S. Weather Research Program*, Phoenix AZ, 11-16 January 1998, American Meteorological Society, Boston, MA, pp. 524-525, 1998.

(1527) Knutson, T.R., R.E. Tuleya, and Y. Kurihara, Simulated Increase of Hurricane Intensities in a CO_2-Warmed Climate, *Science, 279*, 1018-1020, 1998.

(1528) Hamilton, K., Dynamics of the Tropical Middle Atmosphere, in *Proceedings of the Canadian Middle Atmosphere Project Summer School*, Cornwall, Ontario, Canada, 25-29 August 1997, edited by J.N. Koshyk and T.G. Shepherd, pp. 212-256, 1998.

* (1529) Haywood, J., and V. Ramaswamy, Global Sensitivity Studies of the Direct Radiative Forcing due to Anthropogenic Sulfate and Black Carbon Aerosols, *Journal of Geophysical Research, 103*(D6), 6043-6058, 1998.

* (1530) Holt, B., A.K. Liu, D.W. Wang, A. Gnanadesikan, and H.S. Chen, Tracking Storm-Generated Waves in the Northeast Pacific Ocean with ERS-1 Synthetic Aperture Radar Imagery and Buoys, *Journal of Geophysical Research, 103*(C4), 7917-7929, 1998.

* (1531) Hecht, A., T. Ezer, A. Huss, and A. Shapira, Wind Waves on the Dead Sea, in *The Dead Sea: The Lake and its Setting*, edited by T.M. Niemi, Z. Ben-Avraham and J.R. Gata, Monographs on Geology and Geophysics, No. 36, Oxford University Press, pp. 114-121, 1997.

* (1532) Goswami, B.N., Interannual Variations of Indian Summer Monsoon in a GCM: External Conditions versus Internal Feedbacks, *Journal of Climate, 11*, 501-522, 1998.

*In collaboration with other organizations

(1533) Kurihara, Y., R.E. Tuleya, and M.A. Bender, The GFDL Hurricane Prediction System and its Performance in the 1995 Hurricane Season, *Monthly Weather Review, 126*(5), 1306-1322, 1998.

(1534) Stouffer, R.J., and K.W. Dixon, Initialization of Coupled Models for Use in Climate Studies: A Review, in *Research Activities in Atmospheric and Oceanic Modelling*, Report No. 27, WMO/TD-No. 865, World Meteorological Organization, Geneva, Switzerland, pp. I.1-I.8, 1998.

* (1535) Griffies, S.M., A. Gnanadesikan, R.C. Pacanowski, V.D. Larichev, J.K. Dukowicz, and R.D. Smith, Isoneutral Diffusion in a Z-Coordinate Ocean Model, *Journal of Physical Oceanography, 28*(5), 805-830, 1998.

(1536) Griffies, S.M., The Gent-McWilliams Skew-Flux, *Journal of Physical Oceanography, 28*(5), 831-841, 1998.

* (1537) Andronache, C., L.J. Donner, V. Ramaswamy, C.J. Seman, and R.S. Hemler, The Effects of Atmospheric Sulfur on the Radiative Properties of Convective Clouds: A Limited Area Modeling Study, *Geophysical Research Letters, 25*(9), 1423-1426, 1998.

* (1538) Stephens, B.B., R.F. Keeling, M. Heimann, K.D. Six, R.J. Murnane, Testing Global Ocean Carbon Cycle Models using Measurements of Atmospheric O_2 and CO_2 Concentration, *Global Biogeochemical Cycles, 12*(2), 213-230, 1998.

(1539) Anderson, J.L., Impacts of Dynamically Constrained Initial Conditions on Ensemble Forecasts, in *Preprints 11th Numerical Weather Prediction Conference*, Norfolk, VA, 19-23 August 1996, American Meteorological Society, pp. 56-57, 1998.

(1540) Stern, W.F., and J.L. Anderson, Interannual Variability of Tropical Intraseasonal Oscillations in the GFDL/DERF GCM Inferred From an Ensemble of AMIP Integrations, in *Preprints 11th Numerical Weather Prediction Conference*, Norfolk, VA, 19-23 August 1996, American Meteorological Society, pp. 15-16, 1998.

(1541) Sirutis, J.J., and A. Rosati, The Impact of Cumulus Convection Parameterization in Coupled Air-Sea Models, in *Preprints 11th Numerical Weather Prediction Conference*, Norfolk, VA, 19-23 August 1996, American Meteorological Society, pp. 348-350, 1998.

(1542) Delworth, T.L., Interannual to Decadal Variability in the North Pacific of a Coupled Ocean-Atmosphere Model, in *Proceedings of the JCESS/CLIVAR Workshop on Decadal Climate Variability*, Columbia, MD, 22-24 April 1996, 1996.

* (1543) Donner, L.J., C. Andronache, and C.J. Seman, Chemistry and Radiation in Convective Cloud Systems: Transport, Transformation, and Climate Implications, *Abstracts of Papers Presented at the Rossby-100 Symposium*, Vol. 1, Department of Meteorology, University of Stockholm, Sweden, pp. 93-95, 1998.

* (1544) Gu, D., S.G.H. Philander, and M.J. McPhaden, The Seasonal Cycle and Its Modulation in the Eastern Tropical Pacific Ocean, *Journal of Physical Oceanography, 27*, 2209-2218, 1998.

* (1545) Trenberth, K.E., G.W. Branstator, D. Karoly, A. Kumar, N.-C. Lau, and C. Ropelewski, Progress During TOGA in Understanding and Modeling Global Teleconnection Associated with Tropical Sea Surface Temperatures, *Journal of Geophysical Research, 103*(C7), 14,291-14,324, 1998.

* (1546) D'Andrea, F., S. Tibaldi, M. Blackburn, G. Boer, M. Déqué, M.R. Dix, B. Dugas, L. Ferranti, T. Iwasaki, A. Kitoh, V. Pope, D. Randall, E. Roeckner, D. Straus, W. Stern, H. van den Dool, and D. Williamson, Northern Hemisphere Atmospheric Blocking as Simulated by 15 Atmospheric General Circulation Models in the Period 1979-1988, *Climate Dynamics, 14*, 385-407, 1998.

*In collaboration with other organizations

(1547) Soden, B.J., and V. Ramaswamy, Variations in Atmosphere-Ocean Solar Absorption under Clear Skies: A Comparison of Observations and Models, *Geophysical Research Letters, 25*(12), 2149-2152, 1998.

* (1548) Mellor, G.L., L.-Y. Oey, and T. Ezer, Sigma Coordinate Pressure Gradient Errors and the Seamount Problem, *Journal of Atmospheric and Oceanic Technology, 15*(5), 1122-1131,1998.

* (1549) Bush, A., and S.G.H. Philander, The Role of Ocean-Atmosphere Interactions in Tropical Cooling During the Last Glacial Maximum, *Science, 279*, 1341-1344, 1998.

* (1550) Gu, D., and S.G.H. Philander, Interdecadal Climate Fluctuations that Depend on Exchanges Between the Tropics and Extratropics, *Science, 275*, 805-807, 1997.

* (1551) Gruber, N., Anthropogenic CO_2 in the Atlantic Ocean, *Global Biogeochemical Cycles, 12*(1), 165-191, 1998.

(1552) Hamilton, K., Effects of an Imposed Quasi-biennial Oscillation in a Comprehensive Troposphere-Stratosphere-Mesosphere General Circulation Model, *Journal of the Atmospheric Sciences, 55*(14), 2393-2418, 1998.

* (1553) Klonecki, A., *Model Study of the Tropospheric Chemistry of Ozone*, Ph.D. Dissertation, Atmospheric and Oceanic Sciences Program, Princeton University, Princeton, NJ, 1998.

(1554) Soden, B.J., Tracking Upper Tropospheric Water Vapor Radiances: A Satellite Perspective, *Journal of Geophysical Research, 103*(D14), 17,069-17,081, 1998.

* (1555) Haywood, J.M., M.D. Schwarzkopf, and V. Ramaswamy, Estimates of Radiative Forcing Due to Modeled Increases in Tropospheric Ozone, *Journal of Geophysical Research, 103*(D14), 16,999-17,007, 1998.

* (1556) Haywood, J.M., V. Ramaswamy, and L.J. Donner, A Limited-Area-Model Case Study of the Effects of Sub-Grid Scale Variations in Relative Humidity and Cloud Upon the Direct Radiative Forcing of Sulfate Aerosol, *Geophysical Research Letters, 24*(2), 143-146, 1997.

(1557) Ramaswamy, V., and M.D. Schwarzkopf, Stratospheric Temperature Trends: Observations and Model Simulations, in *Stratospheric Processes and Their Role in Climate (SPARC)*, Proceedings of the 1st SPARC Assembly, Melbourne, Australia, 2-6 December 1996, World Climate Research Program, pp. 149-152, 1997.

(1558) Klein, S.A., Comments on "Moist Convective Velocity and Buoyancy Scales", *Journal of the Atmospheric Sciences, 54*, 2775-2777, 1997.

* (1559) Oltmans, S.J., A.S. Lefohn, H.E. Scheel, J.M. Harris, H. Levy II, I.E. Galbally, E.-G. Brunke, C.P. Meyer, J.A. Lathrop, B.J. Johnson, D.S. Shadwick, E. Cuevas, F.J. Schmidlin, D.W. Tarasick, H. Claude, J.B. Kerr, O. Uchino, and V. Mohnen, Trends of Ozone in the Troposphere, *Geophysical Research Letters, 25*(2), 139-142, 1998.

* (1560) Wielicki, B., B. Barkstrom, B. Baum, T. Charlock, R. Green, D. Kratz, R. Lee, P. Minnis, G. Smith, T. Wong, D. Young, R. Cess, J. Coakley, A.H. Crommelynck, L. Donner, R. Kandel, M. King, A. Miller, V. Ramanathan, D. Randall, L. Stowe, and R. Welch, Clouds and the Earth's Radiant Energy System (CERES): Algorithm Overview, *IEEE Transactions on Geoscience and Remote Sensing, 36*(4), 1127-1141, 1998.

* (1561) Sarmiento, J.L., T.M.C. Hughes, R.J. Stouffer, and S. Manabe, Simulated Response of the Ocean Carbon Cycle to Anthropogenic Climate Warming, *Nature, 393*(6682), 245-249, 1998.

(1562) Toggweiler, J.R., and B. Samuels, On the Ocean's Large-Scale Circulation at the Limit of No Vertical Mixing, *Journal of Physical Oceanography, 28*(9), 1832-1852, 1998.

*In collaboration with other organizations

* (1563) Sabine, C.L., and R.M. Key, Controls on fCO_2 in the South Pacific, *Marine Chemistry, 60,* 95-110, 1998.

* (1564) Peng, T.-H., R.M. Key, and H.G. Ostlund, Temporal Variations of Bomb Radiocarbon Inventory in the Pacific Ocean, *Marine Chemistry, 60,* 3-1, 1998.

* (1565) Broecker, W.S., S.L. Peacock, S. Walker, R. Weiss, E. Fahrbach, M. Schroeder, U. Mikolajewicz, C. Heinze, R. Key, T.-H. Peng, and S. Rubin, How Much Deep Water is Formed in the Southern Ocean?, *Journal of Geophysical Research, 103*(C8), 15,833-15,843, 1998.

(1566) Hamilton, K., Observations of Tropical Stratospheric Winds Before World War II, *Bulletin of the American Meteorological Society, 79*(7), 1367-1371, 1998.

* (1567) Hall, A., *The Role of Water Vapor Feedback in Unperturbed Climate Variability and Global Warming,* Ph.D. Dissertation, Atmospheric and Oceanic Sciences Program, Princeton University, 1998.

(1568) Lau, N.-C., El Niño: Child of the Pacific, *Twenty First Century,* bimonthly published by Institute of Chinese Studies, Chinese University of Hong Kong, *46,* 101-111, 1998.

* (1569) Boucher, O., S.E. Schwartz, T.P. Ackerman, T.L. Anderson, B. Bergstrom, B. Bonnel, P. Chylek, A. Dahlback, Y. Fouquart, Q. Fu, R.N. Halthore, J.M. Haywood, T. Iversen, S. Kato, S. Kinne, A. Kirkevag, K.R. Knapp, A. Lacis, I. Laszlo, M.I. Mishchenko, S. Nemesure, V. Ramaswamy, D.L. Roberts, P. Russell, M.E. Schlesinger, G.L. Stephens, R. Wagener, M. Wang, J. Wong, and F. Yang, Intercomparison of Models Representing Direct Shortwave Radiative Forcing by Sulfate Aerosols, *Journal of Geophysical Research,* 103(D14), 16,979-16,998, 1998.

* (1570) Delworth, T.L., and V.M. Mehta, Simulated Interannual to Decadal Variability in the Tropical-Subtropical Atlantic, *Geophysical Research Letters, 25*(15), 2825-2828, 1998.

* (1571) Latif, M., D. Anderson, T. Barnett, M. Cane, R. Kleeman, A. Leetmaa, J. O'Brien, A. Rosati, and E. Schneider, A Review of the Predictability and Prediction of ENSO, *Journal of Geophysical Research, 103*(C7), 14,375-14,393, 1998.

(1572) Orlanski, I., Poleward Deflection of Storm Tracks, *Journal of the Atmospheric Sciences, 55*(16), 2577-2602, 1998.

* (1573) Bryan, K., The Role of Mesoscale Eddies in the Poleward Transport of Heat by the Oceans, *Physica D., 98*(2-4), 249-257, 1998.

* (1574) Vitart, F., *Tropical Storm Interannual and Interdecadal Variability in an Ensemble of GCM Integrations,* Ph.D. Dissertation, Atmospheric and Oceanic Sciences Program, Princeton University, 1999.

(1575) Ramaswamy, V., and S.M. Freidenreich, A High-Spectral Resolution Study of the Near-Infrared Solar Flux Disposition in Clear and Overcast Atmospheres, *Journal of Geophysical Research, 103*(D18), 23,255-23,273, 1998.

(1576) Knutson, T.R., and S. Manabe, Model Assessment of Decadal Variability and Trends in the Tropical Pacific Ocean, *Journal of Climate, 11*(9), 2273-2296, 1998.

(1577) Mahlman, J.D., Science and Non-Science Concerning Human-Caused Climate Warming, *Annual Review of Energy and the Environment, 23,* 83-105, 1998.

* (1578) Fan, S., M. Gloor, J.D. Mahlman, S. Pacala, J. Sarmiento, T. Takahashi, and P. Tans, A Large Terrestrial Carbon Sink in North America Implied by Atmospheric and Oceanic Carbon Dioxide Data and Models, *Science, 282*(5388), 442-446, 1998.

* (1579) Winton, M., R. Hallberg, and A. Gnanadesikan, Simulation of Density-Driven Frictional Downslope Flow in Z-Coordinate Ocean Models, *Journal of Physical Oceanography, 28*(11), 2163-2174, 1998.

*In collaboration with other organizations

* (1580) Harshvardhan, W. Ridgway, V. Ramaswamy, S.M. Freidenreich, and M. Batey, Spectral Characteristics of Solar Near-Infrared Absorption in Cloudy Atmospheres, *Journal of Geophysical Research, 103*(D22), 28,793-28,799, 1998.

(1581) Broccoli, A.J., N.-C. Lau, and M.J. Nath, The Cold Ocean-Warm Land Pattern: Model Simulation and Relevance to Climate Change Detection, *Journal of Climate, 11*(11), 2743-2763, 1998.

* (1582) Yang, X.-Q., J.L. Anderson, and W.F. Stern, Reproducible Forced Modes in AGCM Ensemble Integrations and Potential Predictability of Atmospheric Seasonal Variations in the Extratropics, *Journal of Climate, 11*(11), 2942-2959, 1998.

* (1583) Kushner, P.J., and I.M. Held, A Test, Using Atmospheric Data, of a Method for Estimating Oceanic Eddy Diffusivity, *Geophysical Research Letters, 25*(22), 4213-4216, 1998.

* (1584) Pacanowski, R.C., and A. Gnanadesikan, Transient Response in a Z-level Ocean Model That Resolves Topography with Partial Cells, *Monthly Weather Review, 126*(12), 3248-3270, 1998.

(1585) Hamilton, K., Dynamics of the Tropical Middle Atmosphere: A Tutorial Review, *Atmosphere-Ocean, 36*(4), 319-354, 1998.

(1586) Hamilton, K., The Gravity Wave Parameterisation Problem for Global Simulation Models, *SPARC Newsletter, 12*, 7-14, 1999.

* (1587) Yienger, J.J., A.A. Klonecki, H. Levy II, W.J. Moxim, and G.R. Carmichael, An Evaluation of Chemistry's Role in the Winter-Spring Ozone Maximum Found in the Northern Mid-Latitude Free Troposphere, *Journal of Geophysical Research, 104*(D3), 3655-3667, 1999.

* (1588) Gnanadesikan, A., A Global Model of Silicon Cycling: Sensitivity to Eddy Parameterization and Dissolution, *Global Biogeochemical Cycles, 13*(1), 199-220, 1999.

* (1589) Andronache, C., L.J. Donner, C.J. Seman, V. Ramaswamy, and R.S. Hemler, Atmospheric Sulfur and Deep Convective Clouds in the Tropical Pacific: A Model Study, *Journal of Geophysical Research, 104*(D4), 4005-4024, 1999.

* (1590) Holland, E., S. Brown, C. Potter, S. Klooster, S-M. Fan, M. Gloor, J. Mahlman, S. Pacala, J. Sarmiento, T. Takahashi, and P. Tans, North American Carbon Sink, *Science*, (Technical Comments), *283*, 1815a, 1999.

* (1591) Kushner, P.J., and I.M. Held, Potential Vorticity Thickness Fluxes and Wave-Mean Flow Interaction, *Journal of the Atmospheric Sciences, 56*(7), 948-958, 1999.

* (1592) Klein, S.A., B.J. Soden, and N.-C. Lau, Remote Sea Surface Temperature Variations During ENSO: Evidence for a Tropical Atmospheric Bridge, *Journal of Climate, 12*(4), 917-932, 1999.

* (1593) Haywood, J.M., V. Ramaswamy, and B.J. Soden, Tropospheric Aerosol Climate Forcing in Clear-Sky Satellite Observations over the Oceans, *Science, 283*(5406), 1299-1303, 1999.

* (1594) Koshyk, J.N., K. Hamilton, and J.D. Mahlman, Simulation of the $k^{-5/3}$ Mesoscale Spectral Regime in the GFDL SKYHI General Circulation Model, *Geophysical Research Letters, 26*(7), 843-846, 1999.

* (1595) Gnanadesikan, A., A Simple Predictive Model for the Structure of the Oceanic Pycnocline, *Science, 283*(5410), 2077-2079, 1999.

* (1596) Milly, P.C.D., Factors Determining the Partitioning of Precipitation into Evaporation and Runoff, in *Global Energy and Water Cycles*, edited by K. Browning and R. Gurney, Cambridge University Press, pp. 247-253, 1999.

*In collaboration with other organizations

(1597) Schwarzkopf, M.D., and V. Ramaswamy, Radiative Effects of CH_4, N_2O, Halocarbons and the Foreign-Broadened H_2O Continuum: A GCM Experiment, *Journal of Geophysical Research, 104*(D8), 9467-9488, 1999.

(1598) Donner, L.J., and C.J. Seman, The Role of Ice Sedimentation in the Microphysical and Radiative Budgets of COARE Convective Systems, in *Proceedings of a Conference on the TOGA Coupled Ocean-Atmosphere Response Experiment (COARE)*, Boulder, CO, 7-14 July 1998, WMO/TD-No.940, pp. 227-232, 1999.

(1599) Manabe, S., and R.J. Stouffer, The Role of Thermohaline Circulation in Climate, *Tellus, 51*(A-B), 91-109, 1999.

* (1600) Wittenberg, A.T., and J.L. Anderson, Dynamical Implications of Prescribing Part of a Coupled System: Results from a Low-Order Model, *Nonlinear Processes in Geophysics, 5*(3), 167-179, 1998.

(1601) Garner, S.T., Blocking and Frontogenesis by Two-Dimensional Terrain in Baroclinic Flow, Part I: Numerical Experiments, *Journal of the Atmospheric Sciences, 56*(11), 1495-1508, 1999.

(1602) Garner, S.T., Blocking and Frontogenesis by Two-Dimensional Terrain in Baroclinic Flow, Part II: Analysis of Flow Stagnation Mechanisms, *Journal of the Atmospheric Sciences, 56*(11), 1509-1523, 1999.

* (1603) Held, I.M., and T. Schneider, The Surface Branch of the Zonally Averaged Mass Transport Circulation in the Troposphere, *Journal of the Atmospheric Sciences, 56*(11), 1688-1697, 1999.

(1604) Hamilton, K., Dynamical Coupling of the Lower and Middle Atmosphere: Historical Background to Current Research, *Journal of Atmospheric and Solar-Terrestrial Physics, 61*(1-2), 73-84, 1999.

(1605) Hemler, R.S., Key Elements of the User-Friendly GFDL SKYHI General Circulation Model, in *2nd International Workshop on Software Engineering and Code Design in Parallel Meteorological and Oceanographic Applications*, Scottsdale, Arizona, June, 1998, pp. 29-43, GSFC/CP-1998.

* (1606) Jakob, C., and S.A. Klein, The Role of Vertically Varying Cloud Fraction in the Parameterization of Microphysical Processes in the ECMWF Model, *Quarterly Journal of the Royal Meteorological Society, 125*, 941-965, 1999.

* (1607) Pincus, R., S.A. McFarlane, and S.A. Klein, Albedo Bias and the Horizontal Variability of Clouds in Subtropical Marine Boundary Layers: Observations from Ships and Satellites, *Journal of Geophysical Research, 104*(D6), 6183-6191, 1999.

* (1608) Sabine, C.L., R.M. Key, K.M. Johnson, F.J. Millero, A. Poisson, J.L. Sarmiento, D.W.R. Wallace, and C.D. Winn, Anthropogenic CO_2 Inventory of the Indian Ocean, *Global Biogeochemical Cycles, 13*(1), 179-198, 1999.

* (1609) Gnanadesikan, A., and J.R. Toggweiler, Constraints Placed by Silicon Cycling on Vertical Exchange in General Circulation Models, *Geophysical Research Letters, 26*(13), 1865-1868, 1999.

* (1610) Gnanadesikan, A., Connecting the Southern Ocean with the Rest of the World: Results from Large-Scale Ocean Models, *International WOCE Newsletter No. 35*, 30-31, 1999.

* (1611) Oey, L.-Y., A Forcing Mechanism for the Poleward Flow Off the Southern California Coast, *Journal of Geophysical Research, 104*(C6), 13,529-13,539, 1999.

(1612) Winton, M., Polar Water Column Stability, *Journal of Physical Oceanography, 29*(6), 1368-1371, 1999.

*In collaboration with other organizations

(1613) Donner, L.J., C.J. Seman, and R.S. Hemler, Three-Dimensional Cloud System Modeling of GATE Convection, *Journal of the Atmospheric Sciences, 56*(12), 1885-1912, 1999.

(1614) Dixon, K.W., and J.R. Lanzante, Global Mean Surface Air Temperature and North Atlantic Overturning in a Suite of Coupled GCM Climate Change Experiments, *Geophysical Research Letters, 26*(13), 1885-1888, 1999.

* (1615) Gruber, N., C.D. Keeling, R.B. Bacastow, P.R. Guenther, T.J. Lueker, M. Wahlen, H.A.J. Meijer, W.G. Mook, and T.F. Stocker, Spatiotemporal Patterns of Carbon-13 in the Global Surface Oceans and the Oceanic Suess Effect, *Global Biogeochemical Cycles, 13*(2), 307-335, 1999.

* (1616) Hurtt, G.C., and R.A. Armstrong, A Pelagic Ecosystem Model Calibrated with BATS and OWSI Data, *Deep Sea Research, 46*, 27-61, 1999.

* (1617) Murnane, R.J., J.L. Sarmiento, and C. LeQuéré, Spatial Distribution of Air Sea-CO_2 Fluxes and the Interhemispheric Transport of Carbon by the Oceans, *Global Biogeochemical Cycles, 13*(2), 287-305, 1999.

(1618) Milly, P.C.D., and K.A. Dunne, Non-Detectability of 20th Century Trends in River Discharge from Large Basins--Observational and Model-Based Results, in *Proceedings of the 9th Symposium Global Change Studies*, American Meteorological Society, Phoenix, AZ, 11-16 January 1998, pp. 162-163, 1998.

(1619) Milly, P.C.D., Comment on "Antiphasing Between Rainfall in Africa's Rift Valley and North America's Great Basin", *Quaternary Research, 51*, 104-107, 1999.

(1620) Donner, L.J., C.J. Seman, and R.S. Hemler, Ice Microphysics and Radiative Transfer in Deep Convective Systems, in *Proceedings of the 10th Conference on Atmospheric Radiation*, 28 June-2 July 1999, American Meteorological Society, Boston, MA, pp. 611-614, 1999.

* (1621) Armstrong, R.A., Stable Food Web Structures for Pelagic Ecosystem Models with Multiple Phytoplankton Taxa, *Journal of Plankton Research, 21*(3), 445-464, 1999.

* (1622) Joussaume, S., K.E. Taylor, P. Braconnot, J.F.B. Mitchell, J.E. Kutzbach, S.P. Harrison, I.C. Prentice, A.J. Broccoli, A. Abe-Ouchi, P.J. Bartlein, C. Bonfils, B. Dong, J. Guiot, K. Herterich, C.D. Hewitt, D. Jolly, J.W. Kim, A. Kislov, A. Kitoh, M.F. Loutre, V. Masson, B. McAvaney, N. McFarlane, N. de Noblet, W.R. Peltier, J.Y. Peterschmitt, D. Pollard, D. Rind, J.F. Royer, M.E. Schlesinger, J. Syktus, S. Thompson, P. Valdes, G. Vettoretti, R.S. Webb, U. Wyputta, Monsoon Changes for 6000 Years Ago: Results of 18 Simulations from the Paleoclimate Modeling Intercomparison Project (PMIP), *Geophysical Research Letters, 26*(7), 859-862, 1999.

* (1623) Andronache, C., L.J. Donner, V. Ramaswamy, C.J. Seman, and R.S. Hemler, Possible Impact of Atmospheric Sulfur Increase on Tropical Convective Systems: A TOGA COARE Case, in *Proceedings of a Conference on the TOGA Coupled Ocean-Atmosphere Response Experiment (COARE)*, Boulder, CO, 7-14 July 1998, WMO/TD-940, pp. 243-244, 1999.

(1624) Harrison, M.J., and A. Rosati, Simulating the Tropical Pacific Ocean Using Prescribed Forcing, in *Proceedings of a Conference on the TOGA Coupled Ocean-Atmosphere Response Experiment (COARE)*, Boulder, CO, 7-14 July 1998, WMO/TD-940, pp. 377-378, 1999.

(1625) Harrison, M.J., and A. Rosati, Coupled Model Simulation and Prediction of the Tropical Pacific - Impact of Ocean Model Physics, in *Proceedings of a Conference on the TOGA Coupled Ocean-Atmosphere Response Experiment (COARE)*, Boulder, CO, 7-14 July 1998, WMO/TD-940, pp. 381-382,1999.

*In collaboration with other organizations

* (1626) Anderson, J., H. van den Dool, A. Barnston, W. Chen, W. Stern, and J. Ploshay, Present Day Capabilities of Numerical and Statistical Models for Atmospheric Extratropical Seasonal Simulation and Prediction, *Bulletin of the American Meteorological Society, 80*(7), 1349-1361, 1999.

(1627) Held, I.M., The Macroturbulence of the Troposphere, *Tellus, 51A-B*(1), 59-70, 1999.

* (1628) Denning, A.S., M. Holzer, K.R. Gurney, M. Heimann, R.M. Law, P.J. Rayner, I.Y. Fung, S-M. Fan, S. Taguchi, P. Friedlingstein, Y. Balkanski, M. Maiss, and I. Levin, Three-Dimensional Transport and Concentration of SF_6: A Model Intercomparison Study (TransCom 2), *Tellus, 51B*(2), 266-297, 1999.

(1629) Toggweiler, J.R., Oceanography: An Ultimate Limiting Nutrient, *Nature, 400(6744)*, 511-512, 1999.

(1630) Soden, B.J., How Well Can We Monitor and Predict an Intensification of the Hydrological Cycle?, *GEWEX News*, 9(3), 1, 4-5, 1999.

(1631) Chanin, M-L., V. Ramaswamy, D.J. Gaffen, W. Randel, R.B. Rood, and M. Shiotani, Trends in Stratospheric Temperatures, in *Scientific Assessment of Ozone Depletion: 1998*, WMO Global Ozone Research and Monitoring Project, Report #44, WMO Geneva, pp. 5.1-5.59, 1999.

(1632) Knutson, T.R., and R.E. Tuleya, Increased Hurricane Intensities with CO_2-Induced Global Warming as Simulated using the GFDL Hurricane Prediction System, *Climate Dynamics, 15*, 503-519, 1999.

(1633) Stouffer, R.J., and S. Manabe, Response of a Coupled Ocean-Atmosphere Model to Increasing Atmospheric Carbon Dioxide: Sensitivity to the Rate of Increase, *Journal of Climate, 12(8)*, 2224-2237, 1999.

(1634) Dixon, K.W., T.L. Delworth, M.J. Spelman, and R.J. Stouffer, The Influence of Transient Surface Fluxes on North Atlantic Overturning in a Coupled GCM Climate Change Experiment, *Geophysical Research Letters, 26(17)*, 2749-2752, 1999.

(1635) Manabe, S., and R.J. Stouffer, Are Two Modes of Thermohaline Circulation Stable?, *Tellus, 51A(3)*, 400-411, 1999.

* (1636) Fan, S-M., J.L. Sarmiento, M. Gloor, and S.W. Pacala, On the Use of Regularization Techniques in the Inverse Modeling of Atmospheric Carbon Dioxide, *Journal of Geophysical Research, 104(D17)*, 21,503-21,512,1999.

* (1637) Mellor, G., Comments on "On the Utility and Disutility of JEBAR", *Journal of Physical Oceanography, 29(8)*, 2117-2118, 1999.

* (1638) Waliser, D.E., Z. Shi, J.R. Lanzante, and A.H. Oort, The Hadley Circulation: Assessing NCEP/NCAR Reanalysis and Sparse In-Situ Estimates, *Climate Dynamics - Abstract 15(10)*, 719-735, 1999.

(1639) Delworth, T.L., J.D. Mahlman, and T.R. Knutson, Changes in Heat Index Associated with CO_2-induced Global Warming, *Climatic Change, 43(2)*, 369-386, 1999.

(1640) Zhang, Y., and I.M. Held, A Linear Stochastic Model of a GCM's Midlatitude Storm Tracks, *Journal of the Atmospheric Sciences, 56(19)*, 3416-3435, 1999.

* (1641) Klein, S.A., and C. Jakob, Validation and Sensitivities of Frontal Clouds Simulated by the ECMWF Model, *Monthly Weather Review, 127(10)*, 2514-2531, 1999.

(1642) Lau, N.-C., and M.J. Nath, Observed and GCM-Simulated Westward-Propagating, Planetary-Scale Fluctuations with Approximately Three-week Periods, *Monthly Weather Review, 127(10)*, 2324-2345, 1999.

*In collaboration with other organizations

(1643) Toggweiler, J.R., Variation of Atmospheric CO_2 by Ventilation of the Ocean's Deepest Water, *Paleoceanography, 14(5)*, 571-588, 1999.

* (1644) Hall, A., and S. Manabe, The Role of Water Vapor Feedback in Unperturbed Climate Variability and Global Warming, *Journal of Climate, 12(8)*, 2327-2346, 1999.

* (1645) Pitman, A.J., A. Henderson-Sellers, C.E. Desborough, Z.-L. Yang, F. Abramopoulos, A. Boone, R.E. Dickinson, N. Gedney, R. Koster, E. Kowalczyk, D. Lettenmaier, X. Liang, J.-F. Mahfouf, J. Noilhan, J. Polcher, W. Qu, A. Robock, C. Rosenzweig, C.A. Schlosser, A.B. Shmakin, J. Smith, M. Suarez, D. Verseghy, P. Wetzel, E. Wood, and Y. Xue, Key Results and Implications from Phase 1(c) of the Project for Intercomparison of Land-Surface Parameterization Schemes, *Climate Dynamics, 15*, 673-684, 1999.

* (1646) Bryan, K., J.K. Dukowicz, and R.D. Smith, On the Mixing Coefficient in the Parameterization of Bolus Velocity, *Journal of Physical Oceanography, 29(9)*, 2442-2456, 1999.

* (1647) Fung, K.K., and V. Ramaswamy, On Shortwave Radiation Absorption in Overcast Atmospheres, *Journal of Geophysical Research, 104(D18)*, 22,233-22,241, 1999.

* (1648) Schneider, T., and S.M. Griffies, A Conceptual Framework for Predictability Studies, *Journal of Climate, 12(10)*, 3133-3155, 1999.

* (1649) Vitart, F., J.L. Anderson, and W.F. Stern, Impact of Large-Scale Circulation on Tropical Storm Frequency, Intensity, and Location Simulated by an Ensemble of GCM Integrations, *Journal of Climate, 12(11)*, 3237-3254, 1999.

(1650) Bush, A.B.G., and S.G.H. Philander, The Climate of the Last Glacial Maximum: Results from a Coupled Atmosphere-Ocean General Circulation Model, *Journal of Geophysical Research, 104(D20)*, 24,509-24,525, 1999.

(1651) Pauluis, O., Entropy Budget of an Atmosphere in Radiative-Convective Equilibrium, Ph.D. Dissertation, Atmospheric and Oceanic Sciences Program, Princeton University, 1999.

(1652) Hamilton, K., R.J. Wilson, and R.S. Hemler, Middle Atmosphere Simulated with High Vertical and Horizontal Resolution Versions of a GCM: Improvements in the Cold Pole Bias and Generation of a QBO-Like Oscillation in the Tropics, *Journal of the Atmospheric Sciences, 56(22)*, 3829-3846, 1999.

(1653) Wetherald, R.T., and S. Manabe, Detectability of Summer Dryness Caused by Greenhouse Warming, *Climatic Change, 43(3)*, 495-511, 1999.

(1654) Polyakov, I.V., A.Y. Proshutinsky, and M.A. Johnson, Seasonal Cycles in Two Regimes of Arctic Climate, *Journal of Geophysical Research, 104(C11)*, 25,761-25,788, 1999.

(1655) Hamilton, K., Convective Excitation of Gravity Waves Experiment-CEGWE, in *Mesoscale Processes in the Stratosphere*, Proceedings of the European Workshop, Bad Tölz, Bavaria, Germany, 8-11 November 1998, edited by K.S. Carslaw and G.T. Amanatidis, pp. 93-98, 1999.

* (1656) Levy II, H., W.J. Moxim, A.A. Klonecki, and P.S. Kasibhatla, Simulated Tropospheric NO_x: Its Evaluation, Global Distribution and Individual Source Contributions, *Journal of Geophysical Research, 104(D21)*, 26,279-26,306, 1999.

* (1657) Vinnikov, K.Y., A. Robock, R.J. Stouffer, J.E. Walsh, C.L. Parkinson, D.J. Cavalieri, J.F.B. Mitchell, D. Garrett, V.F. Zakharov, Global Warming and Northern Hemisphere Sea Ice Extent, *Science, 286(5446)*, 1934-1937, 1999.

* (1658) Anderson, J.L., and S.L. Anderson, A Monte Carlo Implementation of the Nonlinear Filtering Problem to Produce Ensemble Assimilations and Forecasts, *Monthly Weather Review, 127(12)*, 2741-2758, 1999.

*In collaboration with other organizations

* (1659) Norris, J.R., and S.A. Klein, Low Cloud Type Over the Ocean from Surface Observations, Part III: Relationship to Vertical Motion and the Regional Surface Synoptic Environment, *Journal of Climate, 13(1)*, 245-256, 2000.

* (1660) Wang, S.W., H. Levy II, G. Li, and H. Rabitz, Fully Equivalent Operational Models for Atmospheric Chemical Kinetics within Global Chemistry-Transport Models, *Journal of Geophysical Research, 104(D23)*, 30,417-30,426, 1999.

* (1661) Masina, S., and S.G.H. Philander, An Analysis of Tropical Instability Waves in a Numerical Model of the Pacific Ocean, 1. Spatial Variability of the Waves, *Journal of Geophysical Research, 104(C12)*, 29,613-29,635, 1999.

(1662) Perliski-Bruhwiler, L., and K. Hamilton, A Numerical Simulation of the Stratospheric Ozone Quasi-biennial Oscillation Using a Comprehensive General Circulation Model, *Journal of Geophysical Research, 104(D23)*, 30,525-30,557, 1999.

* (1663) Ezer, T., Decadal Variabilities of the Upper Layers of the Subtropical North Atlantic: An Ocean Model Study, *Journal of Physical Oceanography, 29(12)*, 3111-3124, 1999.

* (1664) Koshyk, J.N., B.A. Boville, K. Hamilton, E. Manzini, and K. Shibata, Kinetic Energy Spectrum of Horizontal Motions in Middle-Atmosphere Models, *Journal of Geophysical Research, 104(D22)*, 27,177-27,190, 1999.

* (1665) Shen, W., R.E. Tuleya, and I. Ginis, A Sensitivity Study of the Thermodynamic Environment on GFDL Model Hurricane Intensity: Implications for Global Warming, *Journal of Climate, 13(1)*, 109-121, 2000.

* (1666) Gnanadesikan, A., Numerical Issues for Coupling Biological Models with Isopycnal Mixing Schemes, *Ocean Modeling, 1*, 1-15, 1999.

(1667) Held, I.M., Planetary Waves and Their Interaction with Smaller Scales, in *The Life Cycles of Extratropical Cyclones*, edited by M. Shapiro and S. Grons, American Meteorological Society, pp. 101-109, 1999.

* (1668) Park, Y.-G., The Stability of Thermohaline Circulation in a Two-Box Model, *Journal of Physical Oceanography, 29(12)*, 3101-3110, 1999.

* (1669) Ghan, S.J., D. Randall, K.-M. Xu, R. Cederwall, D. Cripe, J. Hack, S. Iacobellis, S. Klein, S. Krueger, U. Lohmann, J. Pedretti, A. Robock, L. Rotstayn, R. Somerville, G. Stenchikov, Y. Sud, G. Walker, S. Xie, J. Yio, and M. Zhang, A Comparison of Single Column Model Simulations of Summertime Midlatitude Continental Convection, *Journal of Geophysical Research, 105(D2)*, 2091-2124, 2000.

* (1670) Stouffer, R.J., G. Hegerl, and S. Tett, A Comparison of Surface Air Temperature Variability in Three 1000-Year Coupled Ocean-Atmosphere Model Integrations, *Journal of Climate, 13(3)*, 513-537, 2000.

(1671) Soden, B.J., The Sensitivity of the Tropical Hydrological Cycle to ENSO, *Journal of Climate, 13(3)*, 538-549, 2000.

(1672) Freidenreich, S.M., and V. Ramaswamy, A New Multiple Band Solar Radiative Parameterization for General Circulation Models, *Journal of Geophysical Research, 104(D24)*, 31,389-31,409, 1999.

(1673) Knutson, T.R., T.L. Delworth, K. Dixon, and R.J. Stouffer, Model Assessment of Regional Surface Temperature Trends (1949-1997), *Journal of Geophysical Research, 104(D24)*, 30,981-30,996, 1999.

* (1674) Mehta, V.M., M.J. Suarez, J. Manganello, T.L. Delworth, Oceanic Influence on the North Atlantic Oscillation and Associated Northern Hemisphere Climate Variations: 1959-1993, *Geophysical Research Letters, 27(1)*, 121-124, 2000.

*In collaboration with other organizations

(1675) Manabe, S., and R.J. Stouffer, A Study of Abrupt Climate Change by a Coupled Ocean-Atmosphere Model, *Quaternary Science Review, 19*, 285-299, 1999.

(1676) Griffies, S.M., R.C. Pacanowski, and R.W. Hallberg, Spurious Diapycnal Mixing Associated with Advection in a Z-Coordinate Ocean Model, *Monthly Weather Review, 128(3)*, 538-564, 2000.

(1677) Broccoli, A.J., Tropical Cooling at the Last Glacial Maximum: An Atmosphere-Mixed Layer Ocean Model Simulation, *Journal of Climate, 13(5)*, 951-976, 2000.

* (1678) Stephens, J.C., and D.P. Marshall, Dynamical Pathways of Antarctic Bottom Water in the Atlantic, *Journal of Physical Oceanography, 30(3)*, 622-640, 2000.

* (1679) Park, Y.-G., and K. Bryan, Comparison of Thermally Driven Circulations from a Depth Coordinate Model and an Isopycnal-Layer Model, Part I. Scaling-Law Sensitivity to Vertical Diffusivity, *Journal of Physical Oceanography, 30(3)*, 590-605, 2000.

* (1680) Murnane, R.J., and J.L. Sarmiento, Roles of Biology and Gas Exchange in Determining the ^{13}C Distribution in the Ocean and the Preindustrial Gradient in Atmospheric ^{13}C, *Global Biogeochemical Cycles, 14(1)*, 389-405, 2000.

* (1681) Gloor, M., S-M. Fan, S. Pacala, and J. Sarmiento, Optimal Sampling of the Atmosphere for Purpose of Inverse Modeling: A Model Study, *Global Biogeochemical Cycles, 14(1)*, 407-428, 2000.

* (1682) Suntharalingam, P., and J.L. Sarmiento, Factors Governing the Oceanic Nitrous Oxide Distribution: Simulations with an Ocean General Circulation Model, *Global Biogeochemical Cycles, 14(1)*, 429-454, 2000.

(1683) Delworth, T.L., and T.R. Knutson, Simulation of Early 20th Century Global Warming, *Science, 287(5461)*, 2246-2250, 2000.

* (1684) Galanter, M., H. Levy II, G.R. Carmichael, Impacts of Biomass Burning on Tropospheric CO, NO_x, and O_3, *Journal of Geophysical Research, 105(D5)*, 6633-6653, 2000.

* (1685) Hall, A., and S. Manabe, Effect of Water Vapor Feedback on Internal and Anthropogenic Variations of the Global Hydrologic Cycle, *Journal of Geophysical Research, 105(D5)*, 6935-6944, 2000.

* (1686) Meehl, G.A., D.R. Easterling, T. Karl, S. Changnon, R. Pielke, D. Changnon, J. Evans, P. Groisman, T. Knutson, K.E. Kunkel, L.O. Mearns, C. Parmesan, R. Pulwarty, T. Root, R.T. Sylves, P. Whetton, and F. Zwiers, An Introduction to Trends in Extreme Weather and Climate Events: Observations, Socioeconomic Impacts, Terrestrial Ecological Impacts, and Model Projections, *Bulletin of the American Meteorological Society, 81(3)*, 413-416, 2000.

* (1687) Meehl, G.A., F. Zwiers, J. Evans, T. Knutson, L. Mearns, and P. Whetton, Trends in Extreme Weather and Climate Events: Issues Related to Modeling Extremes in Projections of Future Climate Change, *Bulletin of the American Meteorological Society, 81(3)*, 427-436, 2000.

* (1688) Meehl, G.A., G.J. Boer, C. Covey, M. Latif, and R.J. Stouffer, The Coupled Model Intercomparison Project (CMIP), *Bulletin of the American Meteorological Society, 81(2)*, 313-318, 2000.

* (1689) Paulius, O., V. Balaji, and I. Held, Frictional Dissipation in a Precipitating Atmosphere, *Journal of the Atmospheric Sciences, 57(7)*, 989-994, 2000.

* (1690) Pawson, S., K. Kodera, K. Hamilton, T.G. Shepherd, S.R. Beagley, B.A. Boville, J.D. Farrara, T.D.A. Fairlie, A. Kitoh, W.A. Lahoz, U. Langematz, E. Manzini, D.H. Rind, A.A. Scaife, K. Shibata, P. Simon, R. Swinbank, L. Takacs, R.J. Wilson, J.A. Al-Saadi, M. Amodei, M. Chiba, L. Coy, J. de Grandpré, R.S. Eckman, M. Fiorino, W.L. Grose, H. Koide,

*In collaboration with other organizations

J.N. Koshyk, D. Li, J. Lerner, J.D. Mahlman, N.A. McFarlane, C.R. Mechoso, A. Molod, A. O'Neill, R.B. Pierce, W.J. Randel, R.B. Rood, and F. Wu, The GCM-Reality Intercomparison Project for SPARC (GRIPS): Scientific Issues and Initial Results, *Bulletin of the American Meteorological Society, 81(4)*, 781-796, 2000.

* (1691) Bender, M.A., and I. Ginis, Real Case Simulations of Hurricane-Ocean Interaction Using a High Resolution Coupled Model: Effects on Hurricane Intensity, *Monthly Weather Review, 128(4)*, 917-946, 2000.

* (1692) Soden, B., S. Tjemkes, J. Schmetz, R. Saunders, J. Bates, B. Ellingson, R. Engelen, L. Garand, D. Jackson, G. Jedlovec, T. Kleespies, D. Randel, P. Rayer, E. Salathe, D. Schwarzkopf, N. Scott, B. Sohn, S. de Souza-Machado, L. Strow, D. Tobin, D. Turner, P. van Delst, and T. Wehr, An Intercomparison of Radiation Codes for Retrieving Upper Tropospheric Humidity in the 6.3-micron Band: A Report from the First GvaP Workshop, *Bulletin of the American Meteorological Society, 81(4)*, 797-808, 2000

* (1693) Giorgi, F., G.A. Meehl, A. Kattenberg, H. Grassl, J.F.B. Mitchell, R.J. Stouffer, T. Tokioka, A.J. Weaver, and T.M.L. Wigley, Simulation of Regional Climate Change with Global Coupled Climate Models and Regional Modeling Techniques, in *The Regional Impacts of Climate Change, An Assessment of Vulnerability*, edited by R.T. Watson, M.C. Zinyowere, R.H. Moss, and D.J. Dokken, Intergovernmental Panel on Climate Change, Cambridge University Press, pp. 429-437, 2000.

* (1694) Goddard, L., and S.G.H. Philander, The Energetics of El Niño and La Niña, *Journal of Climate, 13(9)*, 1496-1516, 2000.

* (1695) Delworth, T.L., and R.J. Greatbatch, Multidecadal Thermohaline Circulation Variability Driven by Atmospheric Surface Flux Forcing, *Journal of Climate, 13(9)*, 1481-1495, 2000.

(1696) Winton, M., A Reformulated Three-Level Sea Ice Model, *Journal of Atmospheric and Oceanic Technology, 17(4)*, 525-531, 2000.

* (1697) Vinnikov, K.Y., A. Robock, R.J. Stouffer, J.E. Walsh, C.L. Parkinson, D.J. Cavalieri, J.F.B. Mitchell, D. Garrett, and V.F. Zakharov, Northern Hemisphere Sea Ice Extent (Response to comments by Moritz and Bitz), *Science, 288*, 927a, 2000. (Available at www.sciencemag.org/cgi/conten/full/288/5468/927a).

* (1698) Redelsperger, J.L., P.R. Brown, F. Guichard, C. Hoff, M. Kawasima, S. Lang, T. Montmerle, K. Nakamura, K. Saito, C. Seman, W.K. Tao, and L.J. Donner, A GCSS Model Intercomparison for a Tropical Squall Line Observed during TOGA-COARE. I: Cloud-Resolving Models, *Quarterly Journal of the Royal Meteorological Society, 126(564)*, 823-863, 2000.

* (1699) Gaffen, D.J., M.A. Sargent, R.E. Habermann, and J.R. Lanzante, Sensitivity of Tropospheric and Stratospheric Temperature Trends to Radiosonde Data Quality, *Journal of Climate, 13(10)*, 1776-1796, 2000.

* (1700) Vallis, G.K., Large-Scale Circulation and Production of Stratification: Effects of Wind, Geometry and Diffusion, *Journal of Physical Oceanography, 30(5)*, 933-954, 2000.

* (1701) Holloway, T., H. Levy II, and P. Kasibhatla, Global Distribution of Carbon Monoxide, *Journal of Geophysical Research, 105(D10)*, 12,124-12,147, 2000.

(1702) Gordon, C.T., A. Rosati, and R. Gudgel, Tropical Interannual Variability Response of a Coupled Model to Specified Low Clouds, in *Proceedings of the Twenty-Fourth Annual Climate Diagnostics and Prediction Workshop*, Tucson, AZ, 5-9 November 1999, pp. 331-334, 1999.

*In collaboration with other organizations

(1703) Gudgel, R.G., A. Rosati, and C.T. Gordon, The Impact of Prescribed Tropical land and Ocean Clouds on the Walker Circulation in the GFDL Coupled Ocean-Atmosphere GCM, in *Proceedings of the Twenty-Fourth Annual Climate Diagnostics and Prediction Workshop*, Tucson, AZ, 5-9 November 1999, pp. 307-310, 1999.

(1704) Anderson, J.L., Why are Statistical Models for Seasonal Prediction Competitive with Current Generation GCM Predictions? in *Proceedings of the Twenty-Fourth Annual Climate Diagnostics and Prediction Workshop*, Tucson, AZ, 5-9 November 1999, pp. 176-178, 1999.

(1705) Anderson, J.L., and J.J. Ploshay, Impacts of Land Surface Initial Conditions on Seasonal Lead GCM Simulations, in *Proceedings of the Twenty-Fourth Annual Climate Diagnostics and Prediction Workshop*, Tucson, AZ, 5-9 November 1999, pp. 319-322, 1999.

(1706) von Storch, J-S., P. Muller, R.J. Stouffer, R. Voss, and S.F.B. Tett, Variability of Deep-Ocean Mass Transport: Spectral Shapes and Spatial Scales, *Journal of Climate, 13(11)*, 1916-1935, 2000.

(1707) Hallberg, R., Time Integration of Diapycnal Diffusion and Richardson Number Dependent Mixing in Isopycnal Coordinate Ocean Models, *Monthly Weather Review, 128(5)*, 1402-1419, 2000.

* (1708) Yang, X-Q, and J.L. Anderson, Correction of Systematic Errors in Coupled GCM Forecasts, *Journal of Climate, 13(12)*, 2072-2085, 2000.

* (1709) Wilson, R.J., and M.I. Richardson, The Martian Atmosphere During the Viking Mission, I: Infrared Measurements of Atmospheric Temperatures Revisited, *Icarus, 145(2)*, 555-579, 2000.

* (1710) Federov, A.V., and S.G.H. Philander, Is El Niño Changing?, *Science, 288(5473)*, 1997-2000, 2000.

* (1711) Barnett, T.P., G. Hegerl, T. Knutson, and S. Tett, Uncertainty Levels in Predicted Patterns of Anthropogenic Climate Change, *Journal of Geophysical Research, 105(D12)*, 15,525-15,542, 2000.

(1712) Delworth, T.L., S. Manabe, and R.J. Stouffer, Simulations of Natural and Forced Variability in the North Atlantic, in *Proceedings of the Atlantic Climate Change Program Meeting*, Lamont-Doherty Earth Observatory, Palisades, NY, 24-26 September 1999, pp. 33-36, 1999.

* (1713) Rodin, A.V., R.T. Clancy, R.J. Wilson, Dynamical Properties of Mars Water Ice Clouds and Their Interaction with Atmospheric Dust and Radiation, *Advances in Space Research, 23*, 1577-1585, 1999.

* (1714) Toggweiler, J.R., and H. Bjornsson, Drake Passage and Paleoclimate, *Journal of Quaternary Science, 15(4)*, 319-328, 2000.

* (1715) Ezer, T., and G. Mellor, Sensitivity Studies with the North Atlantic Sigma Coordinate Princeton Ocean Model, *Dynamics of Atmospheres and Oceans, 32(3-4)*, 185-208, 2000.

* (1716) Chassignet, E.P., H. Arango, D. Dietrich, T. Ezer, D.B. Haidvogel, M. Ghil, C.C. Ma, A. Mehra, A.M. Paiva, and Z. Sirkes, DAMEE-NAB, The Base Experiments, *Dynamics of Atmospheres and Oceans, 32*, 155-184, 2000.

* (1717) Ezer, T., On the Seasonal Mixed-Layer Simulated by a Basin-Scale Ocean Model and the Mellor-Yamada Turbulence Scheme, *Journal of Geophysical Research, 105(C7)*, 16,843-16,855, 2000.

*In collaboration with other organizations

(1718) Moxim, W.J., and H. Levy II, A Model Analysis of the Tropical South Atlantic Ocean Tropospheric Ozone Maximum: The Interaction of Transport and Chemistry, *Journal of Geophysical Research, 105(D13)*, 17,393-17,415, 2000.

(1719) Gordon, C.T., A. Rosati, and R. Gudgel, Tropical Sensitivity of a Coupled Model to Specified ISCCP Low Clouds, *Journal of Climate, 13(13)*, 2239-2260, 2000.

(1720) Griffies, S.M., and R.W. Hallberg, Biharmonic Friction with a Smagorinsky-like Viscosity for Use in Large-Scale Eddy-Permitting Ocean Models, *Monthly Weather Review, 128(8)*, 2935-2946, 2000.

* (1721) Fan, S-M., T.L. Blaine, and J.L. Sarmiento, Terrestrial Carbon Sink in the Northern Hemisphere Estimated from the Atmospheric CO_2 Difference Between Mauna Loa and the South Pole Since 1959, *Tellus, 51B*, 863-870, 1999.

(1722) Soden, B.J., Enlightening Water Vapour, *Nature, 406(6793)*, 247-248, 2000.

(1723) Soden, B.J., The Diurnal Cycle of Convection, Clouds, and Water Vapor in the Tropical Upper Troposphere, *Geophysical Research Letters, 27(15)*, 2173-2176, 2000.

* (1724) Kasibhatla, P., H. Levy II, W.J. Moxim, S.N. Pandis, J.J. Corbett, M.C. Peterson, R.E. Honrath, G.J. Frost, K. Knapp, D.D. Parrish, and T.B. Ryerson, Do Emissions from Ships Have a Significant Impact on Concentrations of Nitrogen Oxides in the Marine Boundary Layer?, *Geophysical Research Letters, 27(15)*, 2229-2232, 2000.

* (1725) Burnett, W.H., V.M. Kamenkovich, G.L. Mellor, and A.L. Gordon, The Influence of the Pressure Head on the Indonesian Seas Circulation, *Geophysical Research Letters, 27(15)*, 2273-2276, 2000.

* (1726) Larson, K., D.L. Hartmann, and S.A. Klein, The Role of Clouds, Water Vapor, Circulation and Boundary Layer Structure in the Sensitivity of the Tropical Climate, *Journal of Climate*, Part I: *12(8)*, 2359-2374, 2000.

* (1727) Klein, S.A., C. Jakob, and J.J. Morcrette, An Examination of Frontal Clouds Simulated by the ECMWF Model, in *Workshop on Cloud Processes and Cloud Feedbacks in Large-Scale Models*, World Climate Research Programme, WMO-TD-No.993, ECMWF, Reading, UK, 9-13 November 1998, pp. 76-83, 2000.

* (1728) Gnanadesikan, A., and R.W. Hallberg, On the Relationship of the Circumpolar Current to Southern Hemisphere Winds in Coarse-Resolution Ocean Models, *Journal of Physical Oceanography, 30(8)*, 2013-2034, 2000.

(1729) Anderson, J.L., and J.J. Ploshay, Impact of Initial Conditions on Seasonal Simulations with an Atmospheric General Circulation Model, *Quarterly Journal of the Royal Meteorological Society, 126(567)*, 2241-2264, 2000.

* (1730) Hall, A., and S. Manabe, Suppression of ENSO in a Coupled Model Without Water Vapor Feedback, *Climate Dynamics, 16(5)*, 393-403, 2000.

* (1731) Jakob, C., and S.A. Klein, A Parameterization of the Effects of Cloud and Precipitation Overlap for Use in General Circulation Models, *Quarterly Journal of the Royal Meteorological Society, 126(568)*, 2525-2544, 2000.

* (1732) Hamilton, K., and S. Fan, Effects of the Stratospheric Quasi-biennial Oscillation on Long-Lived Greenhouse Gases in the Troposphere, *Journal of Geophysical Research, 105(D16)*, 20,581-20,587, 2000.

* (1733) Chai, F., S.T. Lindley, J.R. Toggweiler, and R.T. Barber, Testing the Importance of Iron and Grazing in the Maintenance of the High Nitrate Condition in the Equatorial Pacific Ocean: A Physical-Biological Model Study, in *The Changing Ocean Carbon Cycle*, edited by R.B. Hanson, H.W. Ducklow, and J.G. Field, Cambridge University Press, pp. 155-186, 2000.

*In collaboration with other organizations

* (1734) Burnett, W.H., V.M. Kamenkovich, D.A. Jaffe, A.L. Gordon, G.L. Mellor, Dynamical Balance in the Indonesian Seas Circulation, *Geophysical Research Letters, 27(17)*, 2705-2708, 2000.

* (1735) Delworth, T.L., and M.E. Mann, Observed and Simulated Multidecadal Variability in the Northern Hemisphere, *Climate Dynamics, 16(9)*, 661-676, 2000.

* (1736) Sabine, C.L., R.M. Key, K. Johnson, F.J. Millero, A. Poisson, J. Sarmiento, D. Wallace, and C. Winn, Anthropogenic CO_2 Inventory of the Indian Ocean, *Global Biogeochemical Cycles, 13(1)*, 179-198, 1999.

* (1737) Hemler, R.S., Key Elements of the User-Friendly, GFDL SKYHI General Circulation Model, *Journal of Scientific Programming, 8*, 39-47, 2000.

* (1738) Ortiz, J.D., A.C. Mix, P. Wheeler, and R.M. Key, Anthropogenic CO_2 Invasion into the Northeast Pacific Based on Concurrent $\delta^{13}C_{DIC}$ and Nutrient Profiles from the California Current, *Global Biogeochemical Cycles, 14(3)*, 917-929, 2000.

* (1739) Harper, S., Thermocline Ventilation and Pathways of Tropical-Subtropical Water Mass Exchange, *Tellus, 52A(3)*, 330-345, 2000.

* (1740) Eluszkiewicz, J., R.S. Hemler, J.D. Mahlman, L. Bruhwiler, and L. Takacs, Sensitivity of Age-of-Air Calculations to the Choice of Advection Scheme, *Journal of the Atmospheric Sciences, 57(19)*, 3185-3201, 2000.

* (1741) Soden, B.J., and S.R. Schroeder, Decadal Variations in Tropical Water Vapor: A Comparison of Observations and a Model Simulation, *Journal of Climate*, 13(19), 3337-3341, 2000.

*In collaboration with other organizations

MANUSCRIPTS SUBMITTED FOR PUBLICATION

* (ez) Gnanadesikan, A., Representing the Bottom Boundary Layer in the GFDL Ocean Model: Model Framework, Dynamical Impacts, and Parameter Sensitivity, *Journal of Physical Oceanography*, May 1997.

* (fp) Armstrong, R.A., J.L. Sarmiento, G.C. Hurtt, and S.W. Pacala, Food Web Models for Ocean Biogeochemistry, in *Marine Food Webs*, edited by A. Solow and D. DeAngelis, September 1997.

* (ip) Mellor, G., S. Hakkinen, and T. Ezer, A Generalization of a Sigma Coordinate Ocean Model and an Intercomparison of Model Vertical Grids, Ocean Forecasting: Theory and Practice, Springer Publishing Co., edited by N. Pinardi, August 1998.

* (jh) Hallberg, R., and P.B. Rhines, Boundary Sources of Potential Vorticity in Geophysical Circulations, in *Developments in Geophysical Turbulence*, edited by Kerr and Kimura, Kluwer Publishing, October 1998.

* (jr) Wu, C.-C., M. Bender, and Y. Kurihara, On the Performance of the GFDL Hurricane Prediction System in the Western North Pacific and a Comparison Using the NOGAPS and AVN Global Analysis, *Weather and Forecasting*, December 1998.

* (ju) Andronache, C., L.J. Donner, T.G. Reisin, C.J. Seman, and R.S. Hemler, Cloud Condensation Nuclei-Sulfate Relationship Simulated with a Dynamic Cloud Model with Explicit Microphysics, *Geophysical Research Letters*, January 1999.

* (jz) Erlick, C., L.M. Russell, and V. Ramaswamy, A Microphysics-Based Investigation of the Radiative Effects of Aerosol-Cloud Interactions for Two MAST Experiment Case Studies, *Journal of Geophysical Research*, February 1999.

* (kf) Bjornsson, H., A.J. Willmott, L.A. Mysak, M.A. Maqueda, Polynya Simulations: A Comparison of a Flux Model with a High Resolution Dynamic-Thermodynamic Sea Ice Model, *Journal of Physical Oceanography*, March 1999.

* (kj) Wang, S.W., H Levy II, G. Li, and H. Rabitz, Fully Equivalent Operational Models for Atmospheric Chemical Kinetics within Global Chemistry-Transport Models, *Journal of Geophysical Research*, April 1999.

(kl) Hayashi, Y., and D.G. Golder, Cloud-Feedback Sensitivity of Tropical Intraseasonal Oscillations Simulated by a GFDL General Circulation Model, *Journal of the Atmospheric Sciences*, April 1999.

(km) Orlanski, I., and B. Gross, On the Life-Cycle of Baroclinic Eddies in a Storm Track Environment, *Journal of the Atmospheric Science*, April 1999.

* (kp) Ramaswamy, V., M-L. Chanin, J. Angell, J. Barnett, D. Gaffen, M. Gelman, P. Keckhut, Y. Koshelkov, K. Labitzke, J-J.R. Lin, A. O'Neill, J. Nash, W. Randel, R. Rood, K. Shine, M. Shiotani, R. Swinbank, Stratospheric Temperature Trends: Observations and Model Simulations, *Reviews of Geophysics*, May 1999.

(ku) Hamilton, K., The Quasi-biennial Oscillation, in *Encyclopedia of Global Environmental Change*, Wiley and Sons, Publishers, June 1999.

(kw) Ramaswamy, V., Stratospheric Temperature Trends: Observations and Model Simulations, in *Proceedings of the LTACT 99 Conference*, Pune, India, February 1999.

* (ky) Mellor, G.L., One-Dimensional, Ocean Surface Layer Modeling, A Problem and a Solution, *Journal of Physical Oceanography*, April 1999.

* (la) Offermann, D., H.-H. Graef, M. Donner, M. Bittner, and K. Hamilton, An 18 Year Time Series of OH Rotational Temperatures and Middle Atmosphere Decadal Variations, *Journal of Geophysical Research*, July 1999.

*In collaboration with other organizations

* (Ib) Broecker, W., J.L. Stieglitz, D. Archer, M. Hofmann, E. Maier-Reimer, O. Marchal, T. Stocker, and N. Gruber, How Strong is the Harvardton-Bear Constraint?, *Global Biogeochemical Cycles*, June 1999.

* (Ic) Gruber, N., and C.D. Keeling, The Isotopic Air-Sea Disequilibrium and the Oceanic Uptake of Anthropogenic CO_2, in *Proceedings of the 2nd International CO_2 in the Ocean*, Tsukuba, Japan, July 1999.

* (Id) Coatanoan, C., C. Goyet, N. Gruber, C.L. Sabine, and M. Warner, Comparison of Two Approaches to Quantify Anthropogenic CO_2 in the Ocean: Results from the Northern Indian Ocean, *Global Biogeochemical Cycles*, July 1999.

* (Ih) Barnett, T.P., K. Hasselmann, M. Chelliah, T. Delworth, G. Hegerl, P. Jones, E. Rasmusson, E. Roeckner, C. Ropelewski, B. Santer, S. Tett, Detection and Attribution of Recent Climate Change: A Status Report, *Bulletin of the American Meteorological Society*, July 1999.

* (Ik) Huck, T., G.K. Vallis, and A.C. de Verdiere, On the Robustness of the Interdecadal Modes of the Thermohaline Circulation, *Journal of Climate*, July 1999.

(Il) Mahlman, J.D., Human-Caused Climate Warming: Implications for Practically Everything, in *Environment in Peril*, Vol.II, Johns Hopkins University Press, July 1999.

(Im) Lau, N.-C., and M.J. Nath, Impact of ENSO on the Variability of the Asian-Australian Monsoons as Simulated in GCM Experiments, *Journal of Climate*, August 1999.

(In) Griffies, S.M., An Introduction to Linear Predictability Analysis, in *Global Climate, Barcelona, 1999*, Proceedings of Global Climate Conference, Barcelona, Spain, September 1999.

(Io) Griffies, S.M., An Introduction to Ocean Climate Modeling, in *Global Climate, Barcelona 1999*, Proceedings of Global Climate Conference, Barcelona, Spain, September 1999.

* (Iq) Vitart, F., and J.L. Anderson, Sensitivity of Atlantic Tropical Storm Frequency to ENSO and Interdecadal Variability of SSTs in an Ensemble of GCM Integrations, *Journal of Climate*, September 1999.

* (Is) Baldwin, M.P., L.J. Gray, T.J. Dunkerton, K.P. Hamilton, P.H. Haynes, W.J. Randel, J.R. Holton, M.J. Alexander, I. Hirota, T. Horinouchi, D.B.A. Jones, J.S. Kinnersley, C. Marquardt, K. Sato, and M. Takahashi, The Quasi-Biennial Oscillation, *Reviews of Geophysics*, September 1999.

* (It) Griffies, S.M., R.C. Pacanowski, M. Schmidt, and V. Balaji, The Explicit Free Surface Method in the GFDL Modular Ocean Model, *Monthly Weather Review*, October 1999.

* (Iu) Koster, R.D., P.A. Dirmeyer, P.C.D. Milly, and G.L. Russell, Comparing GCM-Generated Land Surface Water Budgets Using a Simple Common Framework, in *Observations and Modeling of Land Surface Hydrological Processes*, October 1999.

(Iv) Hamilton, K., Free and Forced Interannual Variability of the Circulation in the Extratropical Northern Hemisphere Middle Atmosphere, *AGU Geophysical Monographs*, October 1999.

(Iw) Delworth, T.L., A.J. Broccoli, K. Dixon, I. Held, T.R. Knutson, P.J. Kushner, M.J. Spelman, R.J. Stouffer, K.Y. Vinnikov, and R.T. Wetherald, Coupled Climate Modeling at GFDL: Recent Accomplishments and Future Plans, CLIVAR Exchanges Newsletter, November 1999.

* (Ix) Lanzante, J.R., and G.E. Gahrs, On the "Clear Sky Bias" of TOVS Upper Tropospheric Humidity, *Journal of Climate*, November 1999.

*In collaboration with other organizations

* (lz) Smith, K.S., and G.K. Vallis, The Scales and Equilibration of Mesoscale Ocean Eddies. Part I: Freely Evolving Flow, *Journal of Physical Oceanography*, December 1999.

* (ma) Koshyk, J.N., and K. Hamilton, The Horizontal Kinetic Energy Spectrum and Spectral Budget Simulated by a High-Resolution Troposphere-Stratosphere-Mesosphere GCM, *Journal of the Atmospheric Sciences*, December 1999.

(mc) Griffies, S.M., Review of the Book, Ocean Modeling and Parameterization, E.P. Chassignet and J. Verron, Eds., NATO Science Series C: Mathematical and Physical Sciences, Vol. 516, Kluwer Academic Publishers, Dordrecht, 1998, *Bulletin of the American Meteorological Society*, 1999.

* (mf) Ramachandran, S., V. Ramaswamy, G.L. Stenchikov, and A. Robock, Radiative Impact of the Mt. Pinatubo Volcanic Eruption: Lower Stratospheric Response, *Journal of Geophysical Research*, December 1999.

(mg) Broccoli, A.J., T.L. Delworth, and N.-C. Lau, An Assessment of the Relationship Between the Arctic Oscillation and Northern Hemisphere Temperature, *Journal of Climate*, January 2000.

(mh) Held, I.M., and B.J. Soden, Water Vapor Feedback and Global Warming, *Annual Reviews of Energy and the Environment*, January 2000.

(mi) Carson, S.R., and J.R. Toggweiler, Effect of Tracer Advection Schemes on Biogeochemical Models, *Global Biogeochemical Cycles*, February 2000.

* (mj) Pincus, R., and S.A. Klein, Unresolved Spatial Variability and Microphysical Process Rates in Large Scale Models, *Journal of Geophysical Research*, February 2000.

(mk) Soden, B.J., Water Vapor Observations, in *Frontiers in the Science of Climate Modeling*, February 2000

(ml) Mahlman, J.D., Scientific Biography of Dr. Syukuro Manabe, Pioneer and World Leader in Mathematical Modeling of Human-Caused Climate Change, in *Encyclopedia of Global Environmental Change*, February 2000.

(mm) Kushner, P.J., I.M. Held, and T.L. Delworth, Southern-Hemisphere Atmospheric Circulation Response to Global Warming, *Journal of Climate*, February 2000.

* (mn) Donner, L.J., C.J. Seman, R.S. Hemler, and S. Fan, A Cumulus Parameterization Including Mass Fluxes, Convective Vertical Velocities, and Mesoscale Effects: Thermodynamic and Hydrological Aspects in a General Circulation Model, *Journal of Climate*, February 2000.

(mo) Delworth, T.L., and K.W. Dixon, Implications of the Recent Trend in the Arctic/North Atlantic Oscillation for the North Atlantic Thermohaline Circulation, *Journal of Climate*, March 2000.

* (mq) Huck, T., and G.K. Vallis, The Use of a Tangent Linear Model for Predicting Oscillations of the Three-Dimensional Thermohaline Circulation, *Tellus*, March 2000.

* (mr) Soden, B.J., C.S. Velden, and R.E. Tuleya, The Impact of Satellite Winds on Experimental GFDL Hurricane Model Forecasts, *Monthly Weather Review*, March 2000.

(ms) Lau, N.-C., Impact of ENSO on the Variability of the Asian-Australian Monsoons, in *Proceedings of the Fourth Conference on East Asia and Western Pacific Meteorology and Climate*, April 2000.

* (mt) Shen, W., I. Ginis, and R.E. Tuleya, A Numerical Investigation of Land Surface Water on Landfalling Hurricanes, *Journal of the Atmospheric Sciences*, April 2000.

* (mv) Knutson, T.R., R.E. Tuleya, W. Shen, and I. Ginis, Impact of CO_2-Induced Warming on Hurricane Intensities as Simulated in a Hurricane Model with Ocean Coupling, *Journal of Climate*, April 2000.

*In collaboration with other organizations

(mw) Held, I., The Partitioning of the Poleward Energy Transport between the Tropical Ocean and Atmosphere, *Journal of the Atmospheric Sciences*, April 2000.

(mx) Wetherald, R.T., R.J. Stouffer, and K.W. Dixon, Committed Warming and Its Implications for Climate Change, *Geophysical Research Letters*, April 2000.

(my) Hallberg, R., Reply, *Journal of Physical Oceanography*, April 2000.

* (mz) Toggweiler, J.R., and R.M. Key, Thermohaline Circulation, in *Encyclopedia of Atmospheric Sciences*, Academic Press, May 2000.

* (na) Harrison, M.J., A. Rosati, B.J. Soden, E. Galanti, and E. Tziperman, An Evaluation of Air-Sea Flux Products for ENSO Simulation and Prediction, *Monthly Weather Review*, May 2000.

* (nb) Persing, J., M.T. Montgomery, and R.E. Tuleya, An Illustration of Hurricane-Trough Interaction in the GFDL Hurricane Model, *Monthly Weather Review*, May 2000.

* (nc) Hallberg, R., and A. Gnanadesikan, An Exploration of the Role of Transient Eddies in Determining the Transport of a Zonally Reentrant Current, *Journal of Physical Oceanography*, May 2000.

* (nd) Vitart, F., J.L. Anderson, J. Sirutis, and R.E. Tuleya, Sensitivity of Tropical Storms Simulated by a GCM to Changes in Cumulus Parameterization, *Climate Dynamics*, May 2000.

* (ne) Garner, S.T., and A.J. Thorpe, Note on "A Simplified Squall-Line Model Revisited", *Quarterly Journal of the Royal Meteorological Society*, June 2000.

* (nf) Schneider, T., and I.M. Held, Discriminants of Twentieth-Century Changes in Earth Surface Temperatures, *Nature*, June 2000.

(ng) Milly, P.C.D., A Minimalist Probabilistic Description of Root-Zone Soil Water, *Water Resources Research*, June 2000.

(ni) Williams, G.P., Jovian Dynamics, Part II: The Genesis and Equilibration of Vortex Sets, *Journal of the Atmospheric Sciences*, June 2000.

(nj) Mahlman, J.D., and R.J. Stouffer, Projection of Future Changes in Climate, in *Encyclopedia of Global Environmental Change*, June 2000.

(nk) Lau, N.-C., and M.J. Nath, Impact of ENSO on SST Variability in the North Pacific and North Atlantic: Seasonal Dependence and Role of Extratropical Air-Sea Coupling, *Journal of Climate*, July 2000.

(nl) Gudgel, R.G., A. Rosati, and C.T. Gordon, The Impact of Prescribed Land and Ocean Low-Level Tropical Clouds on the Tropical Circulation in a Coupled Atmospheric-Ocean GCM, *Monthly Weather Review*, July 2000.

* (nm) Griffies, S.M., C. Böning, F.O. Bryan, E.P. Chassignet, R. Gerdes, H. Hasumi, A. Hirst, A. Treguier, and D. Webb, Developments in Ocean Climate Modeling, *Ocean Modeling*, July 2000.

(nn) Manabe, S., T.R. Knutson, R.J. Stouffer, and T.L. Delworth, Exploring Natural and Anthropogenic Variation of Climate, *Quarterly Journal of the Royal Meteorological Society*, July 2000.

(no) Schwarzkopf, M.D., and V. Ramaswamy, Sensitivity to Changes in Cloud Prediction Schemes in a General Circulation Model, in *Proceedings of the International Radiation Symposium 2000*, 24-29 July 2000, St. Petersburg, Russia, month year.

* (np) Milly, P.C.D., and K.A. Dunne, Trends in Evaporation and Surface Cooling in the Mississippi River Basin, *Nature*, July 2000.

(nq) Jackson, C.S., and A.J. Broccoli, Response of Arctic Climate to Changes in Earth's Orbit, *Science*, July 2000.

*In collaboration with other organizations

* (nr) Hamilton, K., and R.A. Vincent, International Field Experiment to Examine Middle Atmospheric Gravity Waves in Relation to Possible Convective Sources, *EOS*, August 2000.

* (ns) Lee, H.-C., and G.L. Mellor, Numerical Simulation of the Gulf Stream System. Part I: The Gulf Stream and the Deep Circulation, *Monthly Weather Review*, August 2000.

* (nt) Lee, H.-C., and G.L. Mellor, Numerical Simulation of the Gulf Stream System. Part II: The Loop Current and Deep Circulations, *Monthly Weather Review*, August 2000.

* (nu) van Dam, T., J. Wahr, P.C.D. Milly, A.B. Shmakin, G. Blewitt, D. Lavalee, Crustal Displacements Due to Continental Water Loading, *Geophysical Research Letters*, August 2000.

* (nv) Cooke, W.F., V. Ramaswamy, and P. Kasibhatla, A GCM Study of the Global Carbonaceous Aerosol Distribution, *Journal of Geophysical Research*, August 2000.

(nw) Hamilton, K., Semiannual Oscillation, in *Encyclopedia of Atmospheric Sciences*, August 2000.

* (nx) Allan, R.P., V. Ramaswamy, and A. Slingo, Interannual Variability of the Hydrological Cycle in the Hadley Centre and GFDL Climate Models and the ECMWF Re-analysis, *Journal of Climate*, August 2000.

* (ny) Mehta, V., E. Lindstrom, A. Busalacchi, T. Delworth, C. Deser, L.-L. Fu, J. Hansen, G. Lagerloef, K.-M. Lau, S. Levitus, G. Meehl, G. Mitchum, E. Sarachik, J. Susskind, and W. White, Summary of the Proceedings of the NASA Workshop on Decadal Climate Variability, *Bulletin of the American Meteorological Society*, August 2000.

(nz) Anderson, J.L., An Ensemble Adjustment Filter for Data Assimilation, *Monthly Weather Review*, September 2000.

* (oa) Federov, A., and S.G.H. Philander, A Stability Analysis of Tropical Ocean-Atmosphere Interactions (Bridging Measurements of, and Theories for El Niño), *Journal of Climate*, September 2000.

* (ob) Deutsch, C., N. Gruber, R.M. Key, J.L. Sarmiento, and A. Ganachaud, Denitrification and N2 Fixation in the Pacific Ocean, *Global Biogeochemical Cycles*, September 2000.

* (oc) Gruber, N., K. Keller, and R.M. Key, Recent Changes in Oceanic Tracer Concentrations: Biological or Physical Explanation?, *Science*, September 2000.

* (od) Key, R.M., Ocean Process Tracers: Natural Radiocarbon, in *Encyclopedia of Ocean Sciences*, edited by J. Steele, S. Thorpe, and K. Turekian, Academic Press Ltd., London, September 2000.

* (oe) Key, R.M., Ocean Process Tracers: Anthropogenic Radiocarbon, in *Encyclopedia of Ocean Sciences*, edited by J. Steele, S. Thorpe, and K. Turekian, Academic Press Ltd., London, September 2000.

* (of) Lamb, M.F., C.L. Sabine, R.A. Feely, R. Wanninkhof, R.M. Key, G.C. Johnson, F.J. Millero, K. Lee, T.-H. Peng, A. Kozyr, J.L. Bullister, D. Greeley, R.H. Byrne, D.W. Chipman, A.G. Dickson, C. Goyet, P.R. Guenther, M. Ishii, K.M. Johnson, C.D. Keeling, T. Ono, K. Shitashima, B. Tilbrook, T. Takahashi, D.W.R. Wallace, Y. Watanabe, C. Winn, and C.S. Wong, Consistency and Synthesis of Pacific Ocean CO_2 Survey Data, *Deep-Sea Research*, September 2000.

* (og) Keller, K., R.D. Slater, M. Bender, and R.M. Key, Decadal Scale Trends in North Pacific Nutrient and Oxygen Concentrations: Biological or Physical Explanation, *Deep Sea Research*, September 2000.

*In collaboration with other organizations

* (oh) Orr, J.C., E. Maier-Reimer, U. Mikolajewicz, P. Monfray, J.L. Sarmiento, J.R. Toggweiler, N.K. Taylor, J. Palmer, N. Gruber, C.L. Sabine, C. LeQuéré, R.M. Key, and J. Boutin, Estimates of Anthropogenic Carbon Uptake from Four 3-D Global Ocean Models, *Global Biogeochemical Cycles*, September 2000.

* (oi) Sabine, C.L., R. Wanninkhof, R.M. Key, C. Goyet, and F.J. Millero, Seasonal CO_2 Fluxes in the Tropical Indian Ocean, *Marine Chemistry*, September 2000.

* (oj) Schlosser, P., J.L. Bullister, R. Fine, W.J. Jenkins, R. Key, J. Lupton, W. Roether, and W.M. Smethie, Jr., Transformation and Age of Water Masses, in *Proceedings of the WOCE Conference*, Halifax, Nova Scotia, Canada, January 2000.

* (ok) Gnanadesikan, A., R.D. Slater, and J.L. Sarmiento, New Production as a Constraint on Oceanic Vertical Exchange, *Deep Sea Research*, September 2000.

* (ol) Roff, G., S. Pawson, U. Langmatz, K. Hamilton, A. Scaife, T. Horinouchi, and R.J. Wilson, Systematic Errors Found in GRIPS, in *Proceedings of the ECRP Symposium on Systematic Errors*, Melbourne, Australia, October 2000.

* (om) Andronache, C., L.J. Donner, C.J. Seman, and R.S. Hemler, A Study of the Impact of ITCZ on Aerosols During INDOEX, *Journal of Geophysical Research*, September 2000.

*In collaboration with other organizations

BIBLIOGRAPHY
1997-2000
CROSS REFERENCE BY AUTHOR

ABE-OUCHI, A. (1622),

ABERSON, S.D. (1465),

ABRAMOPOULOS, F. (1480),(1645),

ACKERMAN, T.P. (1508),(1569),

AIKMAN II, F. (1477),

ALEKSEEV, V. (1478),

ALEXANDER, M.J. (ls),

ALLAN, R.P. (nx),

AI-SAADI, J.A. (1690),

AMMERMAN, J.W. (1498),

AMODEI, M. (1690),

ANDERSON, D. (1571),

ANDERSON, J.L. (1449),(1450),(1455),(1503),(1509),(1539),(1540),
(1582),(1600),(1626),(1649),(1658),(1704),(1705),
(1708),(1729),(lq),(nd),(nz),

ANDERSON, S.L. (1658),

ANDERSON, T.L. (1569),

ANDRONACHE, C. (1537),(1543),(1589),(1623),(ju),(om),

ANGELL, J. (kp),

ARANGO, H. (1716),

ARCHER, D. (lb),

ARMSTRONG, R.A. (1500),(1616),(1621),(fp),

BACASTOW, R.B. (1615),

BALAJI, V. (1689),(lt),

BALASUBRAMANIAN, G. (1439),(1518),

BALDWIN, M.P. (ls),

BALKANSKI, Y. (1628),

BARBER, R.T. (1733),

BARKER, H.W. (1478),

BARKSTROM, B. (1560),

BARNETT, J. (kp),

BARNETT, T.P. (1571),(1711),(lh),

BARNSTON, A. (1626),

BARTLEIN, P.J. (1622),

BATES, J. (1692),

BATEY, M. (1580),

BAUM, B. (1560),

BEAGLEY, S.R. (1690),

BELJAARS, A.C.M. (1480),

BENDER, M. (og),

BENDER, M.A. (1435),(1461),(1463),(1533),(1691),(jr),

BERGSTROM, B. (1569),

BITTNER, M. (la),

BJORNSSON, H. (1714),(kf),

BLACKBURN, M. (1546),

BLAINE, T.L. (1721),

BLEWITT, G. (nu),

BOER, G.J. (1505),(1546),(1688),

BONFILS, C. (1622),

BONNEL, B. (1569),

BÖNING, C. (nm),

BONY, S. (1478),

BOONE, A. (1480),(1645),

BOUCHER, O. (1569),

BOUTIN, J. (oh),

BOVILLE, B.A. (1664),(1690)

BOYLE, J.S. (1474),

BRACONNOT, P. (1622),

BRANSTATOR, G.W. (1545),

BREAKER, L.C. (1477),

BROCCOLI, A.J. (1520),(1581),(1622),(1677),(lw),(mg),(nq),

BROECKER, W.S. (1565),(lb),

BROWN, P.R.A. (1698),

BROWN, S. (1590),

BRUHWILER, L. (1740),

BRUNKE, E.-G. (1559),
BRYAN, F.O. (nm),
BRYAN, K. (1429),(1507),(1573),(1646),(1679),
BULLISTER, J.L. (of),(oj),
BURNETT, W.H. (1725),(1734),
BURPEE, R.W. (1465),
BUSALACCHI, A. (ny),
BUSH, A.B.G. (1549),(1650),
BYRNE, R.H. (of),
CANE, M. (1571),
CARMICHAEL, G.R. (1587),(1684),
CARSON, S.R. (mi),
CAVALIERI, D.J. (1657),(1697),
CEDERWALL, R. (1669),
CESS, R.D. (1478),(1560),
CHAI, F. (1733),
CHAMEIDES, W.L. (1445),
CHANG, P. (1460),
CHANG, S. (1480),
CHANGNON, D. (1686),
CHANGNON, S. (1686),
CHANIN, M-L. (1631),(kp),
CHARLOCK, T. (1560),
CHARLSON, R.J. (1523),
CHASSIGNET, E.P. (1716),(nm),
CHELLIAH, M. (lh),
CHEN, C.-T. (1438),(1440),(1493),
CHEN, F. (1480),
CHEN, H.S. (1530),
CHEN, T.H. (1480),
CHEN, W. (1626),
CHIBA, M. (1690),
CHIPMAN, D.W. (of),
CHRISTENSEN, N. (1506),

CHRISTY, J. (1506),

CHYLEK, P. (1569),

CLANCY, R.T. (1713),

CLARKE, A.D. (1523),

CLAUDE, H. (1559),

COAKLEY, J. (1560),

COATANOAN, C. (ld),

COLMAN, R.A. (1478),

COOKE, W.F. (nv),

COOPER, R. (1506),

CORBETT, J.J. (1724),

COVEY, C. (1505),(1688),

COY, L. (1690),

CRANE, M.W. (1514),

CRIPE, D. (1669),

CROMMELYNCK, A.H. (1560),

CUEVAS, E. (1559),

CULLER, F. (1506),

DAHLBACK, A. (1569),

D'ANDREA, F. (1546),

DAI, Y. (1480),

DAZLICH, D.A. (1478),

de GRANDPRÉ, J. (1690),

Del GENIO, A.D. (1478),

DELWORTH, T.L. (1428),(1433),(1542),(1570),(1634),(1639),(1673),(1674),(1683),(1695),(1712),(1735),(lh),(lw),(mg),(mm),(mo),(nn),(ny),

DENNING, A.S. (1628),

de NOBLET, N. (1622),

DÉQUÉ, M. (1478),(1546),

DESBOROUGH, C.E. (1480),(1645),

DESER, C. (ny),

de SOUZA-MACHADO, S. (1692),

DEUTSCH, C. (ob),

de VERDIERE, A.C. (lk),

DICKINSON, R.E. (1480),(1645),

DICKSON, A.G. (of),

DIETRICH, D. (1716),

DIRMEYER, P.A. (lu),

DIX, M.R. (1474),(1478),(1546),

DIXON, K.W. (1534),(1614),(1634),(1673),(lw),(mo),(mx),

DONG, B. (1622),

DONNER, L.J. (1442),(1483),(1492),(1502),(1537),(1543),(1556),
(1560),(1589),(1598),(1613),(1620),(1623),(1698),
(ju),(mn),(om),

DONNER, M. (la),

DUGAS, B. (1546),

DUKOWICZ, J.K. (1535),(1646),

DUMENIL, L. (1480),

DUNKERTON, T.J. (ls),

DUNNE, K.A. (1618),(np),

DYMNIKOV, V. (1478),

EASTERLING, D.R. (1686),

ECKMAN, R.S. (1690),

EDWARDS, J.M. (1484),

EK, M. (1480),

ELLINGSON, B. (1692),

ELUSZKIEWICZ, J. (1740),

ENGELEN, R. (1692),

ERLICK, C. (jz),

ESCH, M. (1478),

EVANS, J. (1686),(1687),

EZER, T. (1475),(1476),(1519),(1531),(1548),(1663),(1715),
(1716),(1717),(ip),

FAHRBACH, E. (1565),

FAIRLIE, T.D.A. (1690),

FAN, S-M. (1578),(1590),(1628),(1636),(1681),(1721),(1732),
(mn),

FANNING, K. (1498),

FARRARA, J.D. (1690),

FEDEROV, A.V. (1710),(oa),

FEELY, R.A. (of),
FERRANTI, L. (1474),(1546),
FINE, R. (oj),
FIORINO, M. (1690),
FORBES, J.M. (1516),
FOUQUART, Y. (1569),
FOWLER, L.D. (1478),
FRANKLIN, J.L. (1465),
FRASER, J.R. (1478),
FREIDENREICH, S.M. (1458),(1494),(1495),(1575),(1580),(1672),
FRIEDLINGSTEIN, P. (1628),
FROST, G.J. (1724),
FU, L.-L. (ny),
FU, Q. (1569),
FUNG, I.Y. (1628),
FUNG, K.K. (1647),
GAFFEN, D.J. (1631),(1699),(kp),
GAHRS, G.E. (1448),(lx),
GALANTER, M. (1684),
GALANTI, E. (na),
GALBALLY, I.E. (1559),
GALIN, V. (1478),
GANACHAUD, A. (ob),
GARAND, L. (1692),
GARNER, S.T. (1439),(1518),(1601),(1602),(ne),
GARRATT, J.R. (1480),
GARRETT, D. (1657),(1697),
GATES, W.L. (1478),
GEDNEY, N. (1480),(1645),
GELMAN, M. (kp),
GERDES, R. (nm),
GHAN, S.J. (1669),
GHIL, M. (1716),
GINIS, I. (1665),(1691),(mt),(mv),

GIORGI, F. (1693),

GLOOR, M. (1578),(1590),(1636),(1681),

GNANADESIKAN, A. (1471),(1530),(1535),(1579),(1584),(1588),(1595),
(1609),(1610),(1666),(1728),(ez),(nc),(ok),

GODDARD, L. (1694),

GOLDER, D.G. (1452),(1490),(1521),(kl),

GORDON, A.L. (1725),(1734),

GORDON, C.T. (1702),(1703),(1719),(nl),

GOSWAMI, B.N. (1532),

GOYET, C. (ld),(of),(oi),

GRAEF, H.-H. (la),

GRASSL, H. (1693),

GRAY, L.J. (ls),

GREATBATCH, R.J. (1695),

GREELEY, D. (of),

GREEN, R. (1560),

GRIFFIES, S.M. (1429),(1507),(1535),(1536),(1648),(1676),(1720),
(ln),(lo),(lt),(mc),(nm),

GROISMAN, P. (1686),

GROSE, W.L. (1690),

GROSS, B. (km),

GRUBER, N. (1485),(1497),(1551),(1615),(lb),(lc),(ld),(ob),(oc),
(oh),

GU, D. (1431),(1432),(1468),(1544),(1550),

GUDGEL, R.G. (1449),(1450),(1457),(1702),(1703),(1719),(nl),

GUENTHER, P.R. (1615),(of),

GUICHARD, F. (1698),

GUIOT, J. (1622),

GURNEY. K.R. (1628),

GUSEV, Y.M. (1480),

HABERMANN, R.E. (1699),

HACK, J.J. (1478),(1669),

HAGAN, M.E. (1516),

HAGEN, D. (1506),

HAIDVOGEL, D.B. (1716),

HAKKINEN, S. (ip),

HALL, A. (1453),(1567),(1644),(1685),(1730),

HALLBERG, R.W. (1482),(1512),(1579),(1676),(1707),(1720),(1728),(jh),(my),(nc),

HALPERN, D. (1468),

HALTHORE, R.N. (1569),

HAMILTON, K.P. (1441),(1456),(1469),(1515),(1516),(1522),(1524),(1528),(1552),(1566),(1585),(1586),(1594),(1604),(1652),(1655),(1662),(1664),(1690),(1732),(ku),(la),(ls),(lv),(ma),(nr),(nw),(ol),

HANSEN, J. (ny),

HARPER, S. (1739),

HARRIS, J.M. (1559),

HARRISON, M.J. (1624),(1625),(na),

HARRISON, S.P. (1622),

HARSHVARDHAN (1580),

HARTMANN, D.L. (1726),

HASSELMANN, K. (lh),

HASUMI, H. (nm),

HAYASHI, Y. (1452),(1490),(1521),(kl),

HAYNES, P.H. (ls),

HAYWOOD, J.M. (1473),(1483),(1484),(1504),(1510),(1529),(1555),(1556),(1569),(1593),

HECHT, A. (1531),

HEGERL, G. (1670),(1711),(lh),

HEIMANN, M. (1538),(1628),

HEINTZENBERG, J. (1523),

HEINZE, C. (1565),

HELAS, G. (1523),

HELD, I.M. (1443),(1447),(1583),(1591),(1603),(1627),(1640),(1667),(1689),(lw),(mh),(mm),(mw),(nf),

HEMLER, R.S. (1492),(1502),(1522),(1537),(1589),(1605),(1613),(1620),(1623),(1652),(1737),(1740),(ju),(mn),(om),

HENDERSON-SELLERS, A. (1480),(1645),

HERTERICH, K. (1622),

HEWITT, C.D. (1622),

HIROTA, I. (ls),

HIRSCH, A.I. (1445),
HIRST, A. (nm),
HOFF, C. (1698),
HOFMANN, M. (lb),
HOLLAND, E. (1590),
HOLLOWAY, T. (1701),
HOLT, B. (1530),
HOLTON, J.R. (ls),
HOLZER, M. (1628),
HONRATH, R.E. (1724),
HORINOUCHI, T. (ls),(ol),
HUCK, T. (lk),(mq),
HUGHES, T.M.C. (1561),
HURTT, G.C. (1496),(1500),(1616),(fp),
HUSS, A. (1531),
IACOBELLIS, S. (1669),
INGRAM, W.J. (1478),
ISHII, M. (of),
IVERSEN, T. (1569),
IWASAKI, T. (1546),
JACKSON, C.S. (nq),
JACKSON, D. (1692),
JAFFE, D.A. (1734),
JAHNKE, R. (1498),
JAKOB, C. (1606),(1641),(1727),(1731),
JEDLOVEC, G. (1692),
JENKINS, W.J. (oj),
JOHNSON, B.J. (1559),
JOHNSON, G.C. (of),
JOHNSON, K.M. (1608),(1736),(of),
JOHNSON, M.A. (1654),
JOLLY, D. (1622),
JONES, D.B.A. (ls),
JONES, P. (lh),

JONES, P.W.	(1456),(1521),
JOUSSAUME, S.	(1622),
KAMENKOVICH, V.M.	(1725),(1734)
KANDEL, R.	(1560),
KARL, T.	(1686),
KAROLY, D.	(1545),
KASIBHATLA, P.S.	(1445),(1656),(1701),(1724),(nv),
KATO, S.	(1569),
KATTENBERG, A.	(1693),
KAWASIMA, M.	(1698),
KECKHUT, P.	(kp),
KEELING, C.D.	(1615),(lc),(of),
KEELING, R.F.	(1538),
KELLER, K.	(oc),(og),
KELLEY, J.G.W.	(1477),
KERR, J.B.	(1559),
KEY, R.M.	(1487),(1488),(1489),(1563),(1564),(1565),(1608),(1736),(1738),(mz),(ob),(oc),(od),(oe),(of),(og),(oh),(oi),(oj),
KIEHL, J.T.	(1478),
KIM, J.W.	(1480),(1622),
KIM, Y.	(1478),
KING, M.	(1560),
KINNE, S.	(1569),
KINNERSLEY, J.S.	(ls),
KIRKEVAG, A.	(1569),
KISLOV, A.	(1622),
KITOH, A.	(1474),(1546),(1622),(1690),
KLEEMAN, R.	(1571),
KLEESPIES, T.	(1692),
KLEIN, S.A.	(1511),(1558),(1592),(1606),(1607),(1641),(1659),(1669),(1726),(1727),(1731),(lf),(mj),
KLONECKI, A.A.	(1445),(1501),(1553),(1587),(1656),
KLOOSTER, S.	(1590),
KNAP, A.H.	(1498),

KNAPP, K.R. (1569),(1724),

KNUTSON, T.R. (1431),(1462),(1525),(1527),(1576),(1632),(1639),
(1673),(1683),(1686),(1687),(1711),(lw),(mv),(nn),

KODERA, K. (1690),

KOIDE, H. (1690),

KOSHELKOV, Y. (kp),

KOSHYK, J.N. (1594),(1664),(1690),(ma),

KOSTER, R.D. (1479),(1480),(1645),(lu),

KOWALCZYK, E.A. (1480),(1645),

KOZYR, A. (of),

KRATZ, D. (1560),

KRUEGER, S. (1669),

KUMAR, A. (1545),

KUNKEL, K.E. (1686),

KURIHARA, Y. (1461),(1462),(1463),(1526),(1527),(1533),(jr),

KUSHNER, P.J. (1443),(1583),(1591),(lw),(mm),

KUTZBACH, J.E. (1622),

LABITZKE, K. (kp),

LACIS, A. (1569),

LAGERLOEF, G. (ny),

LAHOZ, W.A. (1690),

LAMB, M.F. (of),

LAMBERT, G. (1468),

LANG, S. (1698),

LANGEMATZ, U. (1690),(ol),

LANZANTE, J.R. (1448),(1614),(1638),(1699),(lx),

LARICHEV, V.D. (1447),(1535),

LARSON, K. (1726),

LASZLO, I. (1569),

LATHROP, J.A. (1559),

LATIF, M. (1505),(1571),(1688),

LAU, K.M. (1474),(ny),

LAU, N.-C. (1437),(1451),(1468),(1514),(1545),(1568),(1581),
(1592),(1642),(lm),(mg),(ms),(nk),

LAVAL, K. (1480),

LAVALEE, D. (nu)

LAW, R.M. (1628),

LEAN, J. (1480),

LEE, H.-C. (ns),(nt),

LEE, K. (of),

LEE, R. (1560),

LEETMAA, A. (1571),

LEFOHN, A.S. (1559),

LeQUÉRÉ, C. (1486),(1617),(oh),

LERNER, J. (1690),

LeTREUT, H. (1478),

LETTENMAIER, D. (1480),(1645),

LEVIN, I. (1628),

LEVITUS, S. (ny),

LEVY II, H. (1445)(1445),(1501),(1559),(1587),(1656),(1660),
(1684),(1701),(1718),(1724),

LI, D. (1690),

LI, G. (1660),

LI, J. (1458)

LI, T. (1467),(1468),

LI, X. (1460),

LIANG, X.-Z. (1478),(1480),(1645),

LIN, J-J.R. (kp),

LINDLEY, S.T. (1733),

LINDSTROM, E. (ny),

LINDZEN, R. (1506),

LIOU, K.-N. (1502),

LIOUSSE, C. (1523),

LIPSCHULTZ, F. (1498),

LIU, A.K. (1530),

LOHMANN, U. (1669),

LORD, S.J. (1465),(1470),

LOUTRE, M.F. (1622),

LUEKER, T.J. (1615),

LUPTON, J. (oj),

MA, C.C. (1716),

MACE, G.G. (1508),

MAHFOUF, J.-F. (1480),(1645),

MAHLMAN, J.D. (1427),(1481),(1506),(1513),(1577),(1578),(1590),
(1594),(1639),(1690),(1740),(ll),(ml),(nj),

MAIER-REIMER, E. (lb),(oh),

MAISS, M. (1628),

MANABE, S. (1428),(1431),(1433),(1436),(1444),(1453),(1472),
(1473),(1520),(1525),(1561),(1576),(1599),(1633),
(1635),(1644),(1653),(1675),(1685),(1712),(1730),(nn),

MANGANELLO, J. (1674),

MANN, M.E. (1735),

MANZINI, E. (1664),(1690),

MAQUEDA, M.A. (kf),

MARCHAL, O. (lb),

MARSHALL, D.P. (1678),

MARQUARDT, C. (ls),

MASINA, S. (1661),

MASSON, V. (1622),

McAVANEY, B.J. (1478),(1622),

McFARLANE, N.A. (1622),(1690),

McFARLANE, S.A. (1607),

McPHADEN, M.J. (1544),

MEARNS, L.O. (1686),(1687),

MECHOSO, C.R. (1690),

MEEHL, G.A. (1505),(1686),(1687),(1688),(1693),(ny),

MEEKER, L.D. (1506),

MEHRA, A. (1716),

MEHTA, V.M. (1570),(1674),(ny),

MEIJER, H.A.J. (1615),

MELESHKO, V.P. (1478),

MELLOR, G.L. (1475),(1476),(1477),(1519),(1548),(1637),(1715),
(1725),(1734),(ip),(ky),(ns),(nt),

MENGELKAMP, H.-T. (1480),

MEYER, C.P. (1559),

MICHAELS, A.F. (1498),

MIKOLAJEWICZ, U. (1565),(oh),
MILLER, A. (1560),
MILLERO, F.J. (1499),(1608),(1736),(of),(oi),
MILLY, P.C.D. (1466),(1479),(1480),(1596),(1618),(1619),(lu),(ng),(np),(nu),
MINNIS, P. (1560),
MISHCHENKO, M.I. (1569),
MITCHELL, J.F.B. (1622),(1657),(1693),(1697),
MITCHELL, K. (1480),
MITCHUM, G. (ny),
MIYAKODA, K. (1457),(1474),(1517),
MIX, A.C. (1738),
MOHNEN, V. (1559),
MOLOD, A. (1690),
MONFRAY, P. (oh),
MONTGOMERY, M.T. (nb),
MONTMERLE, T. (1698),
MOOK, W.G. (1615),
MORCRETTE, J.-J. (1478),(1727),
MOXIM, W.J. (1445),(1587),(1656),(1718),(1724),
MULLER, P. (1706),
MURNANE, R.J. (1538),(1617),(1680),
MYSAK, L.A. (kf),
NAKAMURA, H. (1503),
NAKAMURA, K. (1698),
NAKAMURA, M. (1503),
NASH, J. (kp),
NASONOVA, O.N. (1480),
NATH, M.J. (1581),(1642),(lm),(nk),
NEMESURE, S. (1569),
NOILHAN, J. (1480),(1645).
NORRIS, J.R. (1659).
O'BRIEN, J. (1571),
OEY, L.-Y. (1548),(1611),
OFFERMAN, D.N. (la),

OLSON, D. (1498),
OLTMANS, S.J. (1445),(1559),
O'NEILL, A. (1690),(kp),
ONO, T. (of),
OORT, A.H. (1638),
ORLANSKI, I. (1572),(km),
ORR, J.C. (oh),
ORTIZ, J.D. (1738),
OSTLUND, H.G. (1489),(1564),
PACALA, S.W. (1578),(1590),(1636),(1681),(fp),
PACANOWSKI, R.C. (1460),(1464),(1468),(1471),(1535),(1584),(1676),(lt),
PANDIS, S.N. (1724),
PAIVA, A.M. (1716),
PALMER, J. (oh),
PARK, Y.-G. (1668),(1679),
PARKINSON, C.L. (1657),(1697),
PARMESAN, C. (1686),
PARRISH, D.D. (1724),
PAULIUS, O. (1651),(1689),
PAWSON, S. (1690),(ol),
PEACOCK, S.L. (1565),
PEDRETTI, J. (1669),
PELTIER, W.R. (1622),
PENG, P. (1451),
PENG, T.-H. (1564),(1565),(of),
PERLISKI-BRUHWILER, L. (1662),
PERSING, J. (nb),
PETERSCHMITT, J.Y. (1622),
PETERSON, M.C. (1724),
PHILANDER, S.G.H. (1432),(1467),(1468),(1544),(1549),(1550),(1650),
(1661),(1694),(1710),(oa),
PIELKE, R. Jr. (1686),
PIERCE, R.B. (1690),
PINCUS, R. (1607),(mj),
PITMAN, A.J. (1480),(1645),

PLOSHAY, J.J. (1517),(1626),(1705),(1729),

POISSON, A. (1608),(1736),

POLCHER, J. (1480),(1645),

POLLARD, D. (1622),

POLYAKOV, I.V. (1654),

POPE, V. (1546),

POTTER, G.L. (1478),(1590),

PRENTICE, I.C. (1622),

PROSHUTINSKY, A.Y. (1654),

PROSPERO, J.M. (1498),

PULWARTY, R. (1686),

QU, W. (1645),

QUAY, P.D. (1488),

RABITZ, H. (1660),

RAMACHANDRAN, S. (mf),

RAMANATHAN, V. (1560),

RAMASWAMY, V. (1438),(1440),(1458),(1473),(1483),(1491),(1493),
(1494),(1495),(1523),(1529),(1537),(1547),(1555),
(1556),(1557),(1569),(1575),(1580),(1589),(1593),
(1597),(1623),(1631),(1647),(1672),(jz),(kp),(kw),
(mf),(no),(nv),(nx),

RANDALL, D.A. (1474),(1478),(1546),(1560),(1669),

RANDEL, D. (1692),

RANDEL, W.J. (1631),(1690),(kp),(ls),

RASMUSSON, E. (lh),

RAYER, P. (1692),

RAYNER, P.J. (1628),

REDELSPERGER, J.L. (1698),

REIMER, P.J. (1489),

REISIN, T.G. (ju),

RENNICK, M.A. (1463),

RHINES, P.B. (jh),

RICHARDSON, M.I. (1709),

RIDGWAY, W. (1580),

RIND, D.H. (1622),(1690)

ROBERTS, D.L. (1484),(1569),

ROBOCK, A. (1480),(1506),(1645),(1657),(1669),(1697),(mf),

RODIN, A.V. (1713),

ROECKNER, E. (1478),(1546),(lh),

ROETHER, W. (oj),

ROFF, G. (ol),

ROOD, R.B. (1631),(1690),(kp),

ROOT, T. (1686),

ROPELEWSKI, C. (1545),(lh),

ROSATI, A. (1449),(1457),(1517),(1541),(1571),(1624),(1625),
(1702),(1703),(1719),(na),(nl),

ROSENZWEIG, C. (1480),(1645),

ROTSTAYN, L. (1669),

ROYER, J.F. (1622),

RUBIN, S. (1565),

RUSSELL, G.L. (lu),

RUSSELL, L.M. (jz),

RUSSELL, P. (1569),

RYERSON, T.B. (1724),

SABINE, C.L. (1499),(1563),(1608),(1736),(ld),(of),(oh),(oi),

SAITO, K. (1698),

SALATHE, E. (1692),

SAMUELS, B. (1562),

SANTER, B. (lh),

SARACHIK, E. (ny),

SARGENT, M.A. (1699),

SARMIENTO, J.L. (1485),(1486),(1497),(1498),(1561),(1578),(1590),
(1608),(1617),(1636),(1680),(1681),(1682),(1721),
(1736),(fp),(ob),(oh),(ok),

SATO, K. (ls),

SAUNDERS, R. (1692),

SCAIFE, A.A. (1690),(ol).

SCHAAKE, J. (1480),

SCHEEL, H.E. (1559),

SCHLESINGER, M.E. (1478),(1569),(1622),

SCHLESINGER, W. (1506),

SCHLOSSER, C.A. (1480),(1645),
SCHLOSSER, P. (oj),
SCHMETZ, J. (1692),
SCHMIDLIN, F.J. (1559),
SCHMIDT, M. (lt),
SCHMITT, H.H. (1506),
SCHNEIDER, E. (1571),
SCHNEIDER, T. (1603),(1648),(nf),
SCHROEDER, S.R. (1565),(1741),
SCHULZ, J.-P. (1480),
SCHWARTZ, S.E. (1569),
SCHWARZKOPF, M.D. (1491),(1555),(1557),(1597),(1692),(no),
SCOTT, N. (1692),
SEAMAN, N.L. (1508),
SEMAN, C.J. (1442),(1492),(1502),(1537),(1543),(1589),(1598),
(1613),(1620),(1623),(1698),(ju),(mn),(om),
SHADWICK, D.S. (1559),
SHAO, Y. (1480),
SHAPIRA, A. (1531),
SHELDON, J.P. (1442),(1492),
SHEN, W. (1665),(mt),(mv)
SHEPHERD, T.G. (1690),
SHI, Z. (1638),
SHIBATA, K. (1664),(1690),
SHINE, K.P. (1484),(1504),(1510),(1523),(kp),
SHIOTANI, M. (1631),(kp),
SHITASHIMA, K. (of),
SHMAKIN, A.B. (1480),(1645),(nu),
SIMON, P. (1690),
SIRKES, Z. (1716),
SIRUTIS, J.J. (1541),(nd),
SIX, K.D. (1538),
SLATER, R.D. (og),(ok),
SLINGO, A. (1484),(1510),(nx),
SMETHIE, Jr., W.M. (oj),

SMITH, G. (1560),

SMITH, J. (1645),

SMITH, R.D. (1535),(1646),

SMITH, K.S. (lz),

SODEN, B.J. (1459),(1502),(1508),(1547),(1554),(1592),(1593),
(1630),(1671),(1692),(1722).(1723),(1741),(mh),
(mk),(mr),(na),

SOHN, B. (1692),

SOMERVILLE, R. (1669),

SPANGENBERG, D.A. (1508),

SPELMAN, M.J. (1634),(lw),

SPERBER, K.R. (1474),

SPORYSHEV, P.V. (1478),

STENCHIKOV, G.L. (1669),(mf),

STEPHENS, B.B. (1538),

STEPHENS, G.L. (1569),

STEPHENS, J.C. (1678),

STERN, W.F. (1455),(1540),(1546),(1582),(1626),(1649),

STIEGLITZ, J.L. (lb),

STOCKER, T.F. (1485),(1615),(lb),

STOUFFER, R.J. (1428),(1433),(1444),(1472),(1473),(1505),(1534),
(1561),(1599),(1633),(1634),(1635),(1657),(1670),
(1673),(1675),(1688),(1693),(1697),(1706),(1712),(lw),
(mx),(nj),(nn),

STOWE, L. (1560),

STRAUS, D. (1546),

STRÖM, J. (1502),

STROW, L. (1692),

STUIVER, M. (1489),

SUAREZ, M.J. (1645),(1674),

SUD, Y. (1669),

SUNTHARALINGAM, P. (1682),

SUSSKIND, J. (ny),

SWANSON, K.L. (1443),

SWINBANK, R. (1690),(kp),

SYKTUS, J. (1622),

SYLVES, R.T. (1686),

TAGUCHI, S. (1628),

TAKACS, L. (1474),(1690),(1740),

TAKAHASHI, M. (ls),

TAKAHASHI, T. (1578),(1590),(of),

TANS, P. (1578),(1590),

TAO, W.K. (1698),

TARASICK, D.W. (1559),

TAYLOR, K.E. (1478),(1622),

TAYLOR, N.K. (oh),

TETT, S.F.B. (1670),(1706),(1711),(lh),

THOMPSON, S. (1622),

THORPE, A.J. (ne),

TIBALDI, S. (1546),

TILLBROOK, B. (of),

TIMBAL, B. (1478),

TJEMKES, S. (1692),

TOBIN, D. (1692),

TOGGWEILER, J.R. (1562),(1609),(1629),(1643),(1714),(1733),(mi),(mz),
(oh),

TOKIOKA, T. (1693),

TREGUIER, A.M. (1447),(nm),

TRENBERTH, K.E. (1545),

TULEYA, R.E. (1461),(1462),(1465),(1470),(1526),(1527),(1533),
(1632),(1665),(mr),(mt),(mv),(nb),(nd),

TURNER, D. (1692),

TZIPERMAN, E. (na),

UCHINO, O. (1559),

VALDES, P. (1622),

VALLIS, G.K. (1700),(lk),(lz),(mq),

van DAM, T. (nu),

van DELST, P. (1692),

van den DOOL, H. (1546),(1626),

VELDEN, C.S. (mr),

VERSEGHY, D.L. (1480),(1645),

VETTORETTI, G. (1622),

VINCENT, R.A. (nr),

VINNIKOV, K.Y. (1657),(1697),(lw),

VITART, F. (1455),(1574),(1649),(lq),(nd),

VOLODIN, E.M. (1478),

von STORCH, J-S. (1706),

VOSS, R. (1706),

WACONGNE, S. (1464),

WAGENER, R. (1569),

WAHLEN, M. (1615),

WAHR, J. (nu),

WALISER, D.E. (1638),

WALKER, G. (1669),

WALKER, S. (1565),

WALLACE, D.W.R. (1499),(1608),(1736),(of),

WALSH, J.E. (1657),(1697),

WANG, D.W. (1530),

WANG, M. (1569),

WANG, S.W. (1660),(kj),

WANG, W. (1478),

WANG, W.-C. (1478),

WANNINKHOF, R. (of),(oi),

WARNER, M. (ld),

WARREN, J.C. (1502),

WATANABE, Y. (of),

WEAVER, A.J. (1693),

WEBB, D. (nm),

WEBB, R.S. (1622),

WEHR, T. (1692),

WEIDENBAUM, M. (1506),

WEISS, R. (1565),

WELCH, R. (1560),

WENDISCH, M. (1523),

WETHERALD, R.T. (1473),(1474),(1478),(1653),(lw),(mx),

WETZEL, P. (1480),(1645),
WHEELER, P. (1738),
WHETTON, P. (1686),(1687),
WHITE, W. (ny),
WIELICKI, B. (1560),
WIGLEY, T.M.L. (1693),
WILCOXEN, P. (1506),
WILLIAMS, G.P. (1454),(ni),
WILLIAMSON, D. (1546),
WILLMOTT, A.J. (kf),
WILSON, R.J. (1456),(1652),(1690),(1709),(1713),(ol),
WINN, C.D. (1608),(1736),(of),
WINTON, M. (1430),(1434),(1579),(1612),(1696),
WITTENBERG, A.T. (1600),
WONG, C.S. (of),
WONG, J. (1569),
WONG, T. (1560),
WOOD, E.F. (1480),(1645),
WU, C.-C. (1463),(jr).
WU, F. (1690),
WYPUTTA, U. (1622),
XIE, S. (1669),
XU, K.-M. (1669)
XUE, Y. (1480),(1645),
YANG, F. (1569),
YANG, X.-Q. (1582),(1708),
YANG, Z.-L. (1480),(1645),
YIENGER, J.J. (1587),
YIO, J. (1669),
YOUNG, D. (1560),
ZAKHAROV, V.F. (1657),(1697),
ZENG, Q. (1480),
ZHANG, M.-H. (1478),(1669),
ZHANG, X. (1516),

ZHANG, Y. (1446),(1474),(1640),
ZWIERS, F. (1686),(1687),

APPENDIX C

Seminars Given at GFDL

During Fiscal Year 2000

October 1, 1999	Antarctic Sea Ice Ocean Mixing, and the Origin of Pleistocene Climate Instability, by Prof. Ralph Keeling, Scripps Institute of Oceanography, University of California-San Diego, La Jolla, CA
October 6, 1999	Gravity Waves Generated by Tropospheric Convection: Recent Observations Analyses and Their Interpretation, by Dr. Joan Alexander, Colorado Research Associates, Boulder, CO
October 12, 1999	The Walker Circulation Problem, by Dr. Jun-Ichi Yano, Monash University, Melbourne, Australia
October 13, 1999	How El Niño Changes When Climate Changes, by Dr. Alexey Fedorov, Atmospheric and Oceanic Sciences Program, Princeton University, Princeton, NJ
October 14, 1999	Eddies in the Antarctic Circumpolar Current and Their Influence on the Mean Flow, by Dr. Vladimir Ivchenko, Jet Propulsion Laboratory, California Institute of Technology, Pasadena, CA
October 19, 1999	The OMEGA Atmospheric Simulation System: From A to W, by David P. Bacon, Science Applications International Corporation (SAIC), McLean, VA
October 20, 1999	What REALLY Sets the Transport of the Circumpolar Current, by Dr. A. Gnanadesikan and Dr. Robert Hallberg, Atmospheric and Oceanic Sciences Program, Princeton University, Princeton, NJ
October 21, 1999	Climate During the Past Millennium, by Prof. Michael Mann, Department of Environmental Sciences, University of Virginia, Charlottesville, VA
November 3, 1999	Z Level, Coordinate and Ocean Models, by Prof. George Mellor, Atmospheric and Oceanic Sciences Program, Princeton University, Princeton, NJ
November 10, 1999	Fluctuating Within the Monsoon Season of 1998: Buoy Data from Bay of Bengal, by Dr. Debasis Sengupta, Atmospheric and Oceanic Sciences Program, Princeton University, Princeton, NJ
November 17, 1999	A New Set of Software Tools for Visualizing and Evaluating GCM Output, by Ngar-Cheung Lau, Jeffrey Ploshay, Paul Kushner and Anthony Broccoli, Geophysical Fluid Dynamics Laboratory, Princeton, NJ
November 22, 1999	Use of Adjoint Physics with 4D Variational Data Assimilation in the NCEP Global Spectral Model, by Dr. Shaoqing Zhang, Florida State University, Tallahassee, FL
December 3, 1999	Fact or Fiction: Radar Clouds or Clouds in Models, by Timothy Schneider, Environmental Technology Laboratory/NOAA, Boulder, CO
December 6, 1999	Vertical Heat Transports in the Ocean and their Effect on Time-Dependent Climate Change, by Dr. Jonathan Gregory, Hadley Center Meteorological Office, Bracknell, United Kingdom

December 7, 1999	The Role of Cloud for Seasonal Variation in the East Pacific, by John Bergman, NOAA/CIRES Climate Diagnostic Center, Boulder, CO
December 22, 1999	Earth's Orbital Configuration and Cryogenesis Over the Past 135,000 Years, by Charles Jackson, Atmospheric and Oceanic Sciences Program, Princeton University, Princeton, NJ
January 7, 2000	Stratospheric Influence on Natural Variability, by Dr. Drew Shindell, Goddard Institute for Space Studies/NASA, New York, NY
January 19, 2000	Interannual and Interdecadal Variability over the Summertime North Pacific, by Dr. Joel Norris, Atmospheric and Oceanic Sciences Program, Princeton University, Princeton, NJ
January 20, 2000	Indian Ocean Experiment: New Insights into the Role of Aerosols in Climate, by Prof. V. Ramanathan, Scripps Institution of Oceanography, University of California at San Diego, La Jolla, CA
January 21, 2000	Scale Dependence of Cloud Spatial Structure and their Thermodynamic Forcing, by Prof. V. Ramanathan, Scripps Institution of Oceanography, University of California at San Diego, La Jolla, CA
January 26, 2000	GFDL: Past, Present, and Future, by Dr. Jerry D. Mahlman, Geophysical Fluid Dynamics Laboratory, Princeton, NJ
February 2, 2000	The Radiative Properties and Direct Effect of Saharan Dust, by Dr. James Haywood, Meteorological Research Flight, UK Meteorological Office, Farnborough, United Kingdom
February 3, 2000	Statistical Models for Predicting the Spreading Phase of Open Ocean Convection, by Prof. Andy Majda, Courant Institute, New York University, New York, NY
February 3, 2000	The Role of Angular Momentum Constraints in Statistical Models for Baroclinic Vortices, by Dr. Mark DiBattista, Courant Institute, New York University, New York, NY
February 9, 2000	Crime Prevention at GFDL: An Informal and Interactive Discussion, by Officer Fred Lyle, Plainsboro Police Department, Plainsboro, NJ
March 1, 2000	Resistance is Futile: A Practical Monte Carlo Filter for Data Assimilation, by Dr. Jeffrey Anderson, Geophysical Fluid Dynamics Laboratory, Princeton, NJ
March 7, 2000	SMS: A High Level Directive-Based Alternative to MPI, by Dan Schaffer, Tom Henderson, Mark Govett, and Leslie Hart, Forecast Systems Laboratory, Boulder, CO
March 9, 2000	Efficient Numerical Procedures for High-Resolution Prediction Models and Data Assimilation, by Dr. R. James Purser, National Centers for Environmental Prediction/NOAA, Camp Springs, MD

March 10, 2000	Climate Observation from Space: The Role of Sensor Accuracy, by Dr. David Keith, Carnegie Mellon University, Pittsburgh, PA
March 22, 2000	Dynamics of Small Scale Tracer Structures in Geophysical Turbulence, by Mr. Guillaume Lapeyre, Laboratoire de Physique des Oceans, Ifremer, Brest, France
March 24, 2000	Caspian Sea Level Variations by MPI ECHAM4/OPYC and NCAR CCM Models, 1850-2100, by Dr. George Golitsyn, Institute of Atmospheric Science, Russian Academy of Sciences, Moscow, Russia
March 29, 2000	Mean Field Theory for Tropical Precipitation, by Dr. Adam Sobel, Department of Applied Physics and Applied Mathematics, Columbia University, New York, NY
March 31, 2000	Constraining Climate System Properties using an Intermediate Climate Model and Optimal Fingerprint Detection Techniques, by Dr. Christopher Forest, Joint Program for the Science and Policy of Global Change, Massachusetts Institute of Technology, Cambridge, MA
April 5, 2000	Radiative Characteristics of Arctic Clouds, by Tim Garrett, Department of Atmospheric Sciences, University of Washington, Seattle, WA
April 5, 2000	Intensity and Structure of Hurricanes, by Dr. Yoshio Kurihara, Frontier Research System for Global Change, Tokyo, Japan
April 6, 2000	Dynamics of Extratropical Cyclones and FASTEX, by Prof. Alan J. Thorpe, Climate Research, Hadley Centre Meteorological Office, Bracknell, United Kingdom
April 7, 2000	Progress in Wind-Driven Circulation: Analytical Solutions and Interior Communication Window, by Dr. Rue Xin Huang, Woods Hole Oceanographic Institution, Woods Hole, MA
April 11, 2000	Vortex Asymmetries in the Midlatitude Atmosphere, by Prof. David Muraki, Courant Institute, New York University, New York, NY
April 12, 2000	Impact of Satellite Winds on GFDL Hurricane Forecasts, by Dr. Brian Soden and Mr. Robert Tuleya, Geophysical Fluid Dynamics Laboratory, Princeton, NJ
April 13, 2000	Subtropical/Tropical Exchanges in the Atlantic Ocean, by Prof. Paola Malanotte-Rizolli, Department of Physical Oceanography, Massachusetts Institute of Technology, Cambridge, MA
April 26, 2000	GFDL HPCS RFP (Supercomputing Procurement), by Dr. Brian Gross, Geophysical Fluid Dynamics Laboratory, Princeton, NJ
April 27, 2000	Climate Change Since the Mid-Holocene Under the Influence of Solar, Orbital and Greenhouse Gas Radiative Forcing, by Prof. Andrew Weaver, School of Earth and Ocean Sciences, University of Victoria, Victoria, British Columbia, Canada

April 28, 2000	Predictability and the Relationship Between Subseasonal and Interannual Variability During the Asian Summer Monsoon, by Dr. Kenneth Sperber, PCMD, Lawrence Livermore National Laboratory, Livermore, CA
May 3, 2000	Simulations of Water Mass Formation in the Black Sea using a High Resolution Version of MOM, by Prof. Emil Stanev, Department of Geosciences, University of Sofia, Sofia, Bulgaria
May 4, 2000	Atmospheric Composition and Climate on the Early Earth?, by Dr. James Kasting, Department of Geophysics, Pennsylvania State University, University Park, PA
May 5, 2000	The Transmission and Transformation of Baroclinic Rossby Waves by Topography, by Prof. Joseph Pedlosky, Department of Physical Oceanography, Woods Hole Oceanographic Institute, Woods Hole, MA
May 10, 2000	Build Your Own Atlantic Conveyor, by Dr. Haldor Bjornsson and Dr. Robert Toggweiler, Geophysical Fluid Dynamics Laboratory, Princeton, NJ
May 11, 2000	Thermohaline Circulation and Climate, by Dr. Uwe Mikolajewicz, Max-Planck Institute for Meteorology, Hamburg, Germany
May 12, 2000	Stochastic Climate Models, by Dr. Timothy DelSole, Center for Ocean-Land-Atmosphere Studies, Calverton, MD
May 17, 2000	CVS: A Version Central System for FMS, by Peter Phillipps, Geophysical Fluid Dynamics Laboratory, Princeton, NJ
May 18, 2000	The Deep Ocean and Its Influence on Climate Signals, by Prof. Susan Lozier, Earth and Ocean Sciences, Duke University, Durham, NC
May 19, 2000	Arctic Sea Ice Variability in the Context of Recent Atmospheric Circulation Changes, by Dr. Clara Deser, Climate and Global Dynamics Division, National Center for Atmospheric Research, Boulder, CO
May 23, 2000	Clouds and Convection: Development and Evaluation of a Parameterization for Climate Models, by Dr. Sandrine Bony-Lena, Department of Earth Sciences, Massachusetts Institute of Technology, Cambridge, MA
May 25, 2000	Recent Work on Global Modeling of Tropospheric Chemistry, by Prof. Daniel Jacob, Department of Earth and Planetary Sciences, Harvard University, Cambridge, MA
May 26, 2000	Evaluation of Height-Dependent Moisture Variability in the GFDL and Hadley Centre Climate Models using Re-Analysis and Observational Data, by Dr. Richard Allan, Hadley Centre Meteorological Office, Bracknell, United Kingdom
May 26, 2000	What Forces Deep Convection? by Prof. David Raymond, Physics Department, New Mexico Technical College, Socorro, NM

June 5, 2000	A Shallow Water Model for De-aliasing High-Frequency Barotropic Sea Level Variations, by Naoki Hirose, Jet Propulsion Laboratory, California Institute of Technology, Pasadena, CA
June 6, 2000	Spectral Microphysics Hebrew University Cloud Model and its Application for Simulation of Cloud-Aerosol Interaction, by Prof. Alexander Khain, Institute of Earth Sciences, The Hebrew University of Jerusalem, Jerusalem, Israel
June 7, 2000	Improved Cloud Diagnostic Techniques Applied to the GFDL FMS and the NCAR CCM3, by Joel Norris, Atmospheric and Oceanic Sciences Program, Princeton University, Princeton, NJ
June 8, 2000	Warming of World Ocean, by Mr. Sydney Levitus, National Oceanographic Data Center/NOAA, Washington, DC
June 12, 2000	Using Effective Diffusivity to Quantify Mixing and Transport in the Upper Troposphere and Lower Stratosphere, by Dr. Emily Shuckburgh, Centre for Atmospheric Science, University of Cambridge, Cambridge, United Kingdom
June 13, 2000	On the Structure of the Zonal-Mean Zonal Wind in the Southern Hemisphere, by Dr. Hyun-kyung Kim, Pennsylvania State University, University Park, PA
June 15, 2000	Observed Nonmodal Growth of the PNA, by Ben Cash, Pennsylvania State University, University Park, PA
June 22, 2000	A Study on Interhemispheric Interactions in the Atlantic Ocean, by Dr. Holger Brix, Alfred-Wegener Institute for Polar and Marine Research, Bremerhaven, Germany
June 29, 2000	An Overview of Cyclic Mesocyclogenesis and Tornadogenesis: Some New Results and Questions, by Dr. Edwin Adlerman, School of Meteorology, University of Oklahoma, Norman, OK
July 20, 2000	Dansgaard-Oeschger and Heinrich Events Simulated with the CLIMBER-2 Model, by Dr. Stefan Rahmstorf, Potsdam Institute for Climate Impact Research, Potsdam, Germany
August 17, 2000	Studies of Interannual Tropical-Extratropical Interactions, by Dr. Xavier Rodo, University of Barcelona, Barcelona, Spain
August 23, 2000	The Response of Ice Microphysics in Extra-tropical Continental Storms to Atmospheric Aerosol Concentrations, Drop Freezing, and Dynamical Forcings, by Mr. Vaughan Phillips, UMIST, Manchester, United Kingdom
September 6, 2000	Seasonal Forecasting at ECMWF, by Dr. David Anderson, European Centre for Medium-Range Weather Forecasts, Reading, United Kingdom
September 26, 2000	A Study of the Heat Flux Carried by the ACC Mean Flow, by Dr. Che Sun, School of Oceanography, University of Rhode Island, Narragansett, RI

September 27, 2000 GFDL's New High-Performance Computing System, by Dr. Brian Gross, Geophysical Fluid Dynamics Laboratory, Princeton, NJ

APPENDIX D

Talks, Seminars, and Papers Presented Outside GFDL

During Fiscal Year 2000

October 4, 1999	Dr. Anthony J. Broccoli "Extratropical Influences on Interhemispheric Asymmetry of LGM Tropical Climate", Third PMIP Workshop, Saint-Michel-Des-Saints, Quebec, Canada
October 8, 1999	Dr. Paul Kushner "Southern Hemisphere Response to Global Warming", Lamont-Doherty Geological Observatory, Palisades, NY
October 12, 1999	Dr. Brian Soden "How Well Can We Monitor and Predict an Intensification of the Hydrological Cycle?", Chapman Conference on Water Vapor in the Climate System, Potomac, MD
October 14, 1999	Dr. Jerry D. Mahlman "Human-Caused Climate Warming: Implications for Practically Everything", 1999 Norman J. Field Lecture in Science, Monmouth University, West Long Branch, NJ
October 15, 1999	Dr. Kevin P. Hamilton "Maintenance of the Mesoscale Spectral Regime", University of Washington, Seattle, WA
October 18, 1999	Dr. Kevin P. Hamilton "An Imposed QBO in a Dynamical/Chemical GCM", University of Victoria, Victoria, British Columbia, Canada
October 18, 1999	Mr. Ronald J. Stouffer "An Interesting 8.2 KBP-like Event in a 12,000 Year Coupled Model Control Integration", Workshop on 8.2 KBP Event, Lamont-Doherty Geological Observatory, Palisades, NY
October 19, 1999	Dr. Jerry D. Mahlman "Human-Caused Climate Warming: Implications for Practically Everything", Planet Earth Lecture Series, Princeton Adult School, Princeton, NJ
October 19, 1999	Dr. V. Ramaswamy "Radiative Forcing by Stratospheric Aerosols", Symposium on Frontiers in the Science of Climate Modeling, Scripps Institution for Oceanography, La Jolla, CA
October 19, 1999	Dr. Brian Soden "Water Vapor Observations", Symposium on Frontiers in the Science of Climate Modeling, Scripps Institution for Oceanography, La Jolla, CA
October 25, 1999	Dr. Kevin P. Hamilton "Introduction to the Effects of Tropical Convection Experiment", 3rd Planning Meeting of the SPARC-sponsored Effects of Tropical Convection Experiment, Boulder, CO
October 25, 1999	Dr. Jerry D. Mahlman "Global Warming", 18th Symposium on Fusion Engineering, Albuquerque, NM

October 26, 1999	Dr. Jerry D. Mahlman "Human-Caused Climate Warming: Implications for Practically Everything", Sigma Xi Lecture, University of New Mexico, Albuquerque, NM
October 26, 1999	Dr. Bruce B. Ross "High Performance Computing: Progress and Plans", NOAA HPCC Council Meeting, Silver Spring, MD
October 27, 1999	Dr. J.R. Toggweiler "Energizing the Ocean's Meridional Overturning Circulation", State University of New York-Stony Brook, Marine Sciences Research Center, Stony Brook, Long Island, NY
October 29, 1999	Dr. Bruce B. Ross "Reviews of Premises for Computing Requirements and Technology Trends", NOAA HPCC Study Meeting, Silver Spring, MD
November 1, 1999	Dr. Ngar-Cheung Lau "Impact of El Niño on the Asian-Australian Monsoons", Hong Kong Observatory, Hong Kong, China
November 1, 1999	Mr. Richard Gudgel "The Impact of Prescribed Tropical Land and Ocean Clouds on the Walker Circulation in the GFDL Coupled Ocean-Atmosphere GCM", 24th Climate Diagnostics and Prediction Workshop, Tucson, AZ
November 1, 1999	Dr. Charles T. Gordon "Tropical Interannual Variability Response of a Coupled Model to Specified Low Clouds", 24th Climate Diagnostics and Prediction Workshop, Tucson, AZ
November 2, 1999	Dr. Jeffrey Anderson 1. "Impact of Local Surface Initial Conditions on Seasonal Land GCM Predictions", 2. "Why are Statistical Models for Seasonal Prediction Competitive with Current Generation GCMs", 24th Climate Diagnostics and Prediction Workshop, Tucson, AZ
November 2, 1999	Dr. V. Ramaswamy "Activities and Developments Related to Stratospheric Temperature Trends", SPARC SSG Meeting, Paris, France
November 5, 1999	Dr. Paul Kushner "Southern Hemisphere Extratropical Circulation Response to Global Warming", Goddard Institute for Space Studies/NASA, New York, NY
November 12, 1999	Dr. Jerry D. Mahlman "Global Warming: Implications for Practically Everything", Yale University, New Haven, CT
November 15, 1999	Dr. Bruce B. Ross "Demo: Computational Challenges in Climate and Weather Research", SC99 Conference, Portland, OR

November 15, 1999	Dr. Brian D. Gross "Hurricane Forecasting", SC99 Conference, Portland, OR
November 16, 1999	Dr. Jerry D. Mahlman "Regional Implications of Climate Warming", Conference on the Delaware River Basin, Philadelphia, PA
November 16, 1999	Dr. Leo Donner "LAN Sulfate Model", Center for Clouds in Chemistry and Climate, Scripps Institution of Oceanography, La Jolla, CA
November 19, 1999	Dr. Jerry D. Mahlman "Human-Caused Climate Warming: Implications for Practically Everything", Rutgers University, New Brunswick, NJ
November 22, 1999	Dr. V. Ramaswamy "Stratospheric Temperature Changes", Workshop on Climate Change of the Past Fifty Years, Goddard Institute for Space Studies/NASA, New York, NY
November 22, 1999	Mr. Thomas Knutson "Model Assessment of Regional Surface Temperature Trends (1949-1997)", Workshop on Climate Change of the Past Fifty Years, Goddard Institute for Space Studies/NASA, New York, NY
November 22, 1999	Dr. Thomas Delworth "GCM Simulation of Decadal Climate Variability and Change", Workshop on Climate Change of the Past Fifty Years, Goddard Institute for Space Studies/NASA, New York, NY
November 22, 1999	Dr. Brian Soden "Water Vapor Overview", Workshop on Climate Change of the Past Fifty Years, Goddard Institute for Space Studies/NASA, New York, NY
November 23, 1999	Dr. Jerry D. Mahlman "What's Driving Climate Change in the 20th Century-Changing Solar Output or Greenhouse Gases?", U.S. GCRP Seminar on Capitol Hill, Washington, DC
December 1, 1999	Dr. Stephen Griffies "Aspects of MOM", National Center for Environmental Prediction, Camp Springs, MD
December 2, 1999	Dr. Isidoro Orlanski "The Future of Atmospheric Sciences in Argentina", University of Argentina, Buenos Aires, Argentina
December 4, 1999	Dr. Isaac M. Held "Problems in the Theory of Stormtracks", Courant Institute, New York University, New York, NY
December 6, 1999	Dr. Bruce B. Ross "Computational Challenges in Climate and Weather Research", IT2 Demo, Asheville, NC

December 8, 1999	Mr. William Stern "MJO Behavior in the GFDL-DERF GCM During the 1997-1998 ENSO", Monsoon/CLIVAR Conference, Honolulu, HI
December 10, 1999	Dr. Stephen Griffies "Aspects of MOM", Courant Institute, New York University, New York, NY
December 13, 1999	Dr. Kevin P. Hamilton "Aspects of GCM Simulation of the Residual Circulation", Oxford Workshop on the Brewer-Dobson Circulation, Oxford, United Kingdom
December 13, 1999	Mr. Robert J. Wilson "GCM Simulations of the Mars Aphelion Season Tropical Cloud Belt", American Geophysical Union's 1999 Fall Meeting, San Francisco, CA
December 14, 1999	Dr. V. Ramaswamy "Natural Versus Anthropogenic Aerosol Forcing Estimates of Climate Change", Aerosol Radiative Forcing, Panel Meeting, San Francisco, CA
December 14, 1999	Dr. Anthony J. Broccoli "An Assessment of the Association Between the Arctic Oscillation and Northern Hemisphere Temperature", American Geophysical Union's 1999 Fall Meeting, San Francisco, CA
December 14, 1999	Dr. Paul Kushner "The Southern-Hemisphere Response to Global Warming, and its Relation to the Antarctic Oscillation", American Geophysical Union's 1999 Fall Meeting, San Francisco, CA
December 16, 1999	Dr. Thomas L. Delworth "Can a Combination of Internal Climate Variability and Anthropogenic Forcing Account for the Observed Global Warming of the Early 20th Century?", American Geophysical Union's 1999 Fall Meeting, San Francisco, CA
December 16, 1999	Mr. Keith W. Dixon "Transient Climate Change Responses Simulated in a Set of Nine Coupled GCM Experiments", American Geophysical Union's 1999 Fall Meeting, San Francisco, CA
December 16, 1999	Mr. Thomas R. Knutson "Model Assessment of Regional Surface Temperature Trends (1949-1997)", American Geophysical Union's 1999 Fall Meeting, San Francisco, CA
January 5, 2000	Dr. V. Ramaswamy "New GFDL Radiation Parameterizations", National Center for Environmental Prediction, Camp Springs, MD
January 10, 2000	Dr. John R. Toggweiler "Glacial-Interglacial Changes in Atmospheric CO_2", Weizmann Institute, Tel Aviv, Israel

January 10, 2000	Dr. Thomas L. Delworth "Can a Combination of Internal Climate Variability and Anthropogenic Forcing Account for the Observed Global Warming of the Early 20th Century?", American Meteorological Society's Eleventh Symposium on Global Change Studies, Long Beach, CA
January 10, 2000	Mr. Thomas Knutson "Impact of CO_2-Induced Warming on Hurricane Intensities as Simulated in a Hurricane Model with Ocean Coupling", American Meteorological Society's Eleventh Symposium on Global Change Studies, Long Beach, CA
January 12, 2000	Dr. Anthony J. Broccoli "An Assessment of the Association Between the Arctic Oscillation and Northern Hemisphere Temperature", American Meteorological Society's Eleventh Symposium on Global Change Studies, Long Beach, CA
January 24, 2000	Dr. John R. Toggweiler "Response to the ACC and the Antarctic Pycnocline to a Meridional Shift of the S.H. Westerlies", American Geophysical Union's 2000 Ocean Sciences Meeting, San Antonio, TX
January 24, 2000	Dr. Robert Hallberg "An Exploration of the Role of Transient Eddies in Determining the Transport of a Zonally Re-entrant Current", American Geophysical Union's 2000 Ocean Sciences Meeting, San Antonio, TX
January 24, 2000	Ms. Meredith Galanter "Impact of Asian Emissions on the North Pacific", American Geophysical Union's 2000 Ocean Sciences Meeting, San Antonio, TX
January 25, 2000	Mr. Ronald J. Stouffer "Climate Change and the Thermohaline Circulation", American Geophysical Union's 2000 Ocean Sciences Meeting, San Antonio, TX
February 3, 2000	Dr. Jerry D. Mahlman "The Science of Global Climate Change: Future Implications", The Nature Conservancy Board Retreat, International Headquarters, Arlington, VA
February 11, 2000	Dr. Jerry D. Mahlman "Human-Caused Climate Warming: Implications for Practically Everything", Lamont-Doherty Earth Observatory, Palisades, NY
February 14, 2000	Dr. V. Ramaswamy "Radiative Forcing of Climate Change", IPCC 3rd Drafting Meeting, Auckland, New Zealand
February 15, 2000	Mr. Morris Bender "Sensitivity of GFDL Hurricane Prediction System to Initial Conditions", Interdepartmental Hurricane Conference, Houston, TX

February 15, 2000	Mr. Robert E. Tuleya "Improvements to the GFDL Hurricane Forecast System", Interdepartmental Hurricane Conference, Houston, TX
February 23, 2000	Dr. Stephen Griffies "Aspects of MOM", Courant Institute, New York University, New York City, NY
February 23, 2000	Dr. V. Ramaswamy "Developments in Simulation of Stratospheric Aerosol Climatic Effects", SAGE III Science Team Meeting, Hampton, VA
February 24, 2000	Mr. Bruce Wyman "The Current Status of GFDL's Flexible Modeling System", Second International Workshop on Next Generation Climate Models for Advanced High Performance Computing Facilities, Toulouse, France
February 24, 2000	Dr. Jerry D. Mahlman "Human-Caused Climate Warming: Implications for Practically Everything", Sigma Xi Lecturer, Iowa State University, Ames, Iowa
February 25, 2000	Dr. Ngar-Cheung Lau "Interaction Between Global SST Anomalies and the Atmospheric Circulation", Spring 2000 Seminar Series, Goddard Institute for Space Studies/NASA, New York, NY
February 28, 2000	Dr. Robert Hallberg "An Improved Treatment of the Coriolis Term in C-grid Layered Ocean Models", Layer Ocean Model Users Workshop, Miami, FL
February 29, 2000	Dr. Brian Soden "Applications of GOES Winds for Climate Studies and Numerical Hurricane Prediction", Fifth International Winds Workshop, Lorne, Australia
February 29, 2000	Dr. Stephen Griffies "Aspects of MOM", Layered Ocean Model Meeting, Miami, FL
February 29, 2000	Mr. Keith Dixon "Coupled Climate Modeling at GFDL: Recent, Ongoing, and Planned Experiments", International ad hoc Detection Group Meeting, Livermore, CA
February 29, 2000	Dr. Jerry D. Mahlman "Human-Caused Climate Warming: Implications for Practically Everything", Associated Faculty Seminar Series, Guyot Hall, Princeton University, Princeton, NJ
March 1, 2000	Dr. Stephen Griffies "Report on MESO", Meeting of Working Group on Ocean Model Development, Miami, FL
March 1, 2000	Dr. Isaac M. Held "Thoughts on Water Vapor Feedback", Massachusetts Institute of Technology, Cambridge, MA

March 2, 2000	Dr. Jerry D. Mahlman "Human-Caused Climate Warming: Implications for Practically Everything", American Meteorological Society/Sigma Xi Lecture, East Tennessee State University, Johnson City, TN
March 8, 2000	Dr. Stephen Griffies "Aspects of MOM", Massachusetts Institute of Technology, Cambridge, MA
March 10, 2000	Dr. Jerry D. Mahlman "Human-Caused Climate Warming: Implications for Practically Everything", Sigma Xi Lecture, Ramapo College of New Jersey, Mahwah, NJ
March 13, 2000	Dr. Stephen Klein "Sub-grid Scale Spatial Variability of Clouds and its Impact on Microphysical Process Rates in Large-Scale Models", Atmospheric Radiation Measurement Program's Science Team Meeting, San Antonio, TX
March 13, 2000	Dr. Bruce B. Ross "Status of GFDL HPCS Acquisition", Oceanic and Atmospheric Research, Silver Spring, MD
March 13, 2000	Dr. Brian Soden "Satellite Measurements of Upper Tropospheric Water Vapor for ARM", Atmospheric Radiation Measurement Program's Science Team Meeting, San Antonio, TX
March 15, 2000	Dr. Anthony J. Broccoli "Simulating the Response of Holocene Climate to Orbital Forcing", 35th Annual Meeting of the Northeastern Section of the Geological Society of America, New Brunswick, NJ
March 17, 2000	Dr. John R. Toggweiler "Glacial to Interglacial Changes in Atmospheric CO_2", Atlantic Oceanographic and Meteorological Laboratory, Miami, FL
March 20, 2000	Dr. Bruce B. Ross "NOAA/GFDL Activities/Plans under IT2 Initiative", PITAC Committee Meeting, Washington, DC
March 27, 2000	Dr. Brian D. Gross "A Nonhydrostatic Modeling Strategy for GFDL", The 2nd USWRP Science Symposium, Boulder, CO
March 27, 2000	Dr. Isaac M. Held "Some Recent Results from GFDL on Global Warming", Department of Energy Climate Change Prediction Program Meeting, Bethesda, MD
April 4, 2000	Dr. Jerry D. Mahlman "Human-Caused Climate Warming: Implications for Practically Everything", Duke University, Durham, NC

April 5, 2000	Dr. Anthony J. Broccoli 1. "Tropical Temperatures at the Last Glacial Maximum: Results from Climate Simulations", 2. "Tropical Climate Anomalies Forced From the Extratropics", Woods Hole Oceanographic Institution Seminar Series, Climate and Paleoclimate Modeling, Woods Hole, MA
April 6, 2000	Dr. Ngar-Cheung Lau "Modes of Climate Variability", Spring 2000 Meeting of the NOAA Panel on Abrupt Change, Oracle, AZ
April 12, 2000	Dr. Kevin P. Hamilton "Simulation of the Mesoscale Regime and Other Aspects of High Resolution Global Modeling", Institute for Terrestrial and Planetary Atmospheres, State University of New York, Stony Brook, NY
April 12, 2000	Dr. John R. Toggweiler "Drake Passage and Paleoclimate", Department of Earth, Atmospheric and Planetary Sciences, Massachusetts Institute of Technology, Cambridge, MA
April 12, 2000	Mr. Thomas Knutson "20th Century Surface Temperature Trends: Models vs. Observations", USBDRP Seminar Series, Washington, DC
April 12, 2000	Dr. Jerry D. Mahlman "Human-Caused Climate Warming: Implications for Practically Everything", Sigma Xi Lecture, East Stroudsburg University, East Stroudsburg, PA
April 13, 2000	Dr. Jerry D. Mahlman "Human-Caused Climate Warming: Implications for Practically Everything", Sigma Xi Lecture, Indiana University of Pennsylvania, Indiana, PA
April 14, 2000	Dr. Jerry D. Mahlman "Human-Caused Climate Warming: Implications for Practically Everything", Sigma Xi Lecture, West Virginia University, Morgantown, WV
April 25, 2000	Dr. Bruce B. Ross "Review of GFDL IT Activities and Future Directions", OAR IT Management Meeting, Boulder, CO
April 26, 2000	Dr. Leo J. Donner 1. "Sulfate Transport and Chemistry in INDOEX Deep Convection", 2. "Radiative Impacts of Mesoscale Circulations Associated with Deep Convection", European Geophysical Society, General Assembly, Nice, France
May 2, 2000	Dr. Leo J. Donner "Ice Clouds and Deep Convection in General Circulation Models", Laboratoire de Meteorologie Dynamique, Paris, France
May 2, 2000	Dr. Jerry D. Mahlman "Human-Caused Climate Warming: Implications for Practically Everything", Chadron State College, Chadron, NE

May 16, 2000	Dr. Jerry D. Mahlman "The Science Behind Global Warming", Staffers of the Senate Commerce, Science, and Transportation Committee, Washington, DC
May 17, 2000	Dr. Jerry D. Mahlman "The Science Behind Global Warming", Testimony Presented Before the Senate Commerce, Science, and Transportation Committee, Washington, DC
May 18, 2000	Dr. Hiram Levy II "Transcontinental Air Pollution Research at GFDL", CENR Air Quality Research Sub-committee Meeting, Washington, DC
May 23, 2000	Dr. Thomas L. Delworth "Simulations of Climate Change in the 20th Century", Brookhaven National Laboratory, Upton, NY
May 24, 2000	Dr. Bruce B. Ross "GFDL Computing Infrastructure: Current Status and Future Direction", OAR Mini-Review of GFDL, Silver Spring, MD
May 30, 2000	Mr. Donald G. Golder "A Testimonial to the Memory of Dr. Yoshikazu Hayashi", 24th American Meteorological Society's Hurricanes and Tropical Meteorology Conference, Fort Lauderdale, FL
May 30, 2000	Dr. Anthony J. Broccoli "Response of Arctic Climate to Changes in Earth's Orbit", Hadley Centre, Bracknell, United Kingdom
May 31, 2000	Mr. Ronald J. Stouffer "THC and Climate", Hadley Centre, Bracknell, United Kingdom
May 31, 2000	Dr. Kevin P. Hamilton 1. "Interannual Variations in Stratospheric Transport and Effects on Stratospheric and Tropospheric Trace Constituent Concentrations", 2. "Geophysical Turbulence in the Real World - How is the Observed Mesoscale Energy Spectrum Maintained?", Annual Charney Lecture, American Geophysical Society Spring Meeting, Washington, DC
June 1, 2000	Mr. Robert E. Tuleya 1. "Improvements to the GFDL Forecast System", 2. "Impact of CO_2-Induced Warming on Tropical Cyclone Intensities in a Model with Ocean Coupling", 24th American Meteorological Society's Hurricane and Tropical Meteorology Conference, Fort Lauderdale, FL
June 1, 2000	Mr. Morris Bender "Comparison of the Performance of the GFDL Hurricane Model using the AVN and UK Meteorological Analysis", 24th American Meteorological Society's Hurricane and Tropical Meteorology Conference, Fort Lauderdale, FL

June 2, 2000	Dr. John R. Toggweiler "Sequence of Events Leading to Atmospheric CO_2 Changes During the Holocene and Glacial-Interglacial Transition", American Geophysical Union Spring Meeting, Washington, DC
June 6, 2000	Dr. Anthony J. Broccoli "Response of Arctic Climate to Changes in Earth's Orbit", Sea Ice in the Climate System: The Record of the North Atlantic Arctic Meeting, Kirkjubaejarklaustur, Iceland
June 8, 2000	Dr. Jerry D. Mahlman "Human-Caused Climate Warming: Implications for Practically Everything", New York Academy of Dentists, New York, NY
June 12, 2000	Mr. Robert John Wilson 1. "MGCM Simulations of the Martian Tropical Cloud Belt", 2. "Identification of Diurnal Period Kelvin Waves in the Lower Atmosphere and Thermosphere of Mars", Mars Global Surveyor Workshop, Boulder, CO
June 13, 2000	Dr. V. Ramaswamy "Forcing of Climate Change", Conference on Chemistry-Climate Interactions, International Center for Theoretical Physics, Trieste, Italy
June 13, 2000	Mr. Mark W. Crane "Overview of GFDL Web-Site", OAR Outreach Coordinators Workshop, Mystic, CN
June 14, 2000	Dr. Anthony J. Broccoli "Future Climate Projections: What Will the 21st Century Bring?", Speaker in USRA Public Lecture Series, Greenbelt, MD
June 19, 2000	Dr. Robert Hallberg 1. "An Introduction to Isopycnal Coordinate Ocean Models", 2. "Ocean Model Intercomparisons in Process Studies", WOCE Young Investigator Workshop, Boulder, CO
June 19, 2000- August 25, 2000	Dr. Isaac M. Held Present ten lectures on "The General Circulation of the Atmosphere", Woods Hole GFD Summer School, Woods Hole, MA
June 20, 2000	Dr. Jeffrey Anderson "FMS Programming Principles and Philosophy", NCEP Model Infrastructure Meeting, Camp Springs, MD
June 24, 2000	Mr. Stuart Freidenreich "Analysis of BSRN Data", Gordon Research Conference on Solar Radiation and Climate, New London, CT
June 25, 2000	Mr. M. Daniel Schwarzkopf "Sensitivity to Changes in Cloud Prediction Schemes in a General Circulation Model", International Radiation Symposium, 2000 Conference, St. Petersburg, Russia

June 26, 2000	Dr. Brian Soden "Interannual Variability of the Hydrologic and Energy Cycles", Gordon Research Conference on Solar Radiation and Climate, New London, CN
June 26, 2000	Dr. Jeffrey L. Anderson "The Non-Linear Filtering Problem and its Relation to Adjoint Assimilation", Workshop on Adjoint Applications in Dynamic Meteorology, Moliets, France
June 28, 2000	Dr. Kevin P. Hamilton "Interannual Circulation Variations in the Stratosphere and Effects on Trace Constituents", Climate Monitoring and Diagnostics Laboratory/NOAA, Boulder, CO
June 28, 2000	Dr. Leo J. Donner "Preliminary Experiments with Linked Parameterizations for Deep Convection, Mesoscale Ice Cloud and Prognostic Large-Scale Microphysics in CCM", CCSM Meeting, Breckenridge, CO
July 5, 2000	Dr. Brian Gross "Determination of Competitive Range for GFDL HPCS Acquisition", HPCS Acquisition Briefing, Silver Spring, MD
July 5, 2000	Dr. Bruce B. Ross "Determination of Competitive Range for GFDL HPCS Acquisition", HPCS Acquisition Briefing, Silver Spring, MD
July 9, 2000	Dr. V. Ramaswamy "Simulated Natural Variability of Cirrus Cloud Distributions and Its Implications for Aerosol Radiative Forcing", ICAO/European Commission Workshop on Aviation, Aerosols, Contrails, and Cirrus Clouds, Frankfurt, Germany
July 10, 2000	Dr. Jerry D. Mahlman "Overview of GFDL Programs and Issues", Present GFDL Mini Review to OAR Headquarters Staff, Silver Spring, MD
July 10, 2000	Mr. Richard T. Wetherald "Climate Models", Teachers Forum, Annapolis, MD
August 2, 2000	Dr. Jeffrey L. Anderson "An Ensemble Adjustment Filter for Atmospheric and Oceanic Data Assimilation", National Center for Atmospheric Research, Boulder, CO
August 14, 2000	Dr. Ngar-Cheung Lau 1. "Impact of ENSO on Asian-Australian Monsoons", 2. "Relationships Between ENSO and Atmospheric Variability on Synoptic and Intraseasonal Time Scales", International Pacific Research Center, University of Hawaii, Honolulu, HI
August 24, 2000	Dr. Thomas L. Delworth "The Science of Global Warming", The Pennsylvania Cable Network, Harrisburg, PA

August 29, 2000	Dr. Jerry D. Mahlman "GFDL: current Status and Future Plans", Department of Commerce and OMB Budget Examiners, Washington, DC
September 18, 2000	Dr. Isidoro Orlanski "Baroclinic Life-Cycle in Storm Track Environments", University of Buenos Aires, Buenos Aires, Argentina
September 20, 2000	Dr. Leo J. Donner "Characteristics of Mesoscale Convective Systems in a General Circulation Model", CERES Science Team Meeting, Huntsville, AL
September 29, 2000	Dr. Jeffrey Anderson "FMS Infrastructure Overview", NCEP Global Model Development Working Group, Camp Springs, MD

APPENDIX E

ACRONYMS

ACRONYMS

AASE	Arctic Airborne Stratospheric Experiment
ABLE	Atmospheric Boundary Layer Experiment
AC	Analysis Cluster
ACC	Antarctic Circumpolar Current
AEROCE	Air Ocean Chemistry Experiment
AGCM	Atmospheric General Circulation Model
AMEX	Australian Monsoon Experiment
AMIP	Atmospheric Model Intercomparison Project
AO	Arctic Oscillation
AOGCM	Atmosphere-Ocean General Circulation Model
AOML	Atlantic Oceanographic and Meteorological Laboratory/NOAA
AOU	Apparent Oxygen Utilization
API	Application Programming Interface
ARL	Atmospheric Research Laboratory/NOAA
ARCS	Applied Research Centers
ARM	Atmospheric Radiation Measurements
ASCII	American Standard Code for Information Interchange
A99/P00	GFDL Activities FY99, Plans FY00
BC	Black Carbon
BSRN	Baseline Surface Radiation Network
CAPE	Convective Available Potential Energy
CCN	Cloud Condensation Nuclei
CCNUMA	Cache Coherent Non-Uniform Memory Architecture
CDC	Climate Diagnostic Center
CGCM	Coupled General Circulation Model
CEM	Cumulus Ensemble Model
CERES	Clouds and the Earth's Radiant Energy System
CFC	Chlorofluorocarbon
CGRER	Center for Global and Regional Environmental Research
CHAMMP	Computer Hardware, Advanced Mathematics and Model Physics project
CIMA	Centro de Investigaciones para el Mar y La Atmosfera, Buenos Aires, Argentina

CIRA	COSPAR International Reference Atmosphere
CLD	Fraction of upper tropospheric CLouD cover.
CLIPER	A simple model combining CLImatology and PERsistence used in hurricane prediction.
CM	CONTROL Coupled General Circulation Model (CGCM) experiment
CMC	Carbon Modeling Consortium
CMDL	Climate Monitoring and Diagnostics Laboratory/NOAA
CMEP	Coupled Model Ensemble Prediction
CMIO	CGCM experiment utilizing prescribed low-level clouds from ISCCP
CMIOL	CGCM experiment utilizing prescribed low-level clouds from ISCCP
COADS	Comprehensive Ocean-Atmosphere Data Set
COARDS	Cooperative Ocean/Atmosphere Research Data Service
COARE	Coupled Ocean-Atmosphere Response Experiment
COFS	Coastal Ocean Forecast System
COLA	Center for Ocean, Land and Atmosphere Studies
COSPAR	Congress for Space Research
CPU	Central Processing Unit
CRAY	Cray Research, Inc.
CRF	Cloud Radiative Forcing
CSIRO	Commonwealth Scientific & Industrial Research Organization
CVS	Concurrent Versions System
DAMEE	Data Assimilation and Model Evaluation Experiments
DC	Deep Convective Cloud Cover
DJF	December, January, February (winter)
DODS	Distributed Oceanographic Data Systems
DTEP	Deep Tropical Eastern Pacific
DTEPOGA	Deep Tropical Eastern Pacific Ocean-Global Atmosphere
DU	Dobson units
DWBC	Deep Western Boundary Current
E	A physical parametrization package in use at GFDL. E physics includes a high-order closure scheme for subgrid turbulence.
ECMWF	European Centre for Medium-Range Weather Forecasts
ED	Ecosystem Demography

E"n"	Horizontal model resolution corresponding to "n" points between a pole and the equator on the E-grid.
ENSO	El Niño - Southern Oscillation
EOF	Empirical Orthogonal Function
EPOCS	Equatorial Pacific Ocean Climate Studies
ERBE	Earth Radiation Budget Experiment
FDDI	Fiber Distributed Data Interface
FDH	Fixed Dynamic Heating model
FEOM	Fully Equivalent Operational Model
FIRE	First ISCCP Regional Experiment
FMS	Flexible Modeling System
FTP	File Transfer Protocol
FY"yy"	Fiscal Year "yy" where "yy" are the last two digits of the year.
GAIM	Global Analysis Interpretation and Modeling
GARP	Global Atmospheric Research Program
GATE	GARP Atlantic Tropical Experiment
GB	Gigabyte, equal to 1 billion bytes
GCM	General Circulation Model
GCTM	Global Chemical Transport Model
GEOSAT	Geodetic Satellite
GEWEX	Global Energy and Water Experiment
GFD	Geophysical Fluid Dynamics
GFDL	Geophysical Fluid Dynamics Laboratory/NOAA
GHG	Greenhouse Gases
GMT	Greenwich Mean Time
GOES	Geostationary Operational Environmental Satellite
GRS	Great Red Spot
GTE	Global Tropospheric Experiment
GUI	Graphical User Interface
HCM	Hybrid Coupled Model
HIBU	Federal Hydrological Institute and Belgrade University
HIM	Hybrid Isopycnal Model
HPCC	High Performance Computing and Communications

HPCS	High Performance Computing System
HRD	Hurricane Research Division/AOML
HSMS	Hierarchical Storage Management System
ICRCCM	InterComparison of Radiation Codes in Climate Models
IGBP/PAGES	International Geosphere-Biosphere Project/Past Global Changes
I/O	Input/Output
ICTP	International Center for Theoretical Physics, Trieste, Italy
INDOEX	Indian Ocean Experiment
IPCC	Intergovernmental Panel on Climate Change
IRI	International Research Institute for Climate Prediction
IRIX	SGI's Operating System
ISCCP	International Satellite Cloud Climatology Project
IT	Information Technology
ITCZ	Intertropical Convergence Zone
JGOFS	Joint Global Ocean Flux Study
JJA	June, July, August (summer)
JPL	Jet Propulsion Laboratory
KPP	K-Profile Parameterization
KS	Kolmogorov-Smirnov
LaD	Land Dynamics
LAHM	Limited Area HIBU Model
LAI	Leaf Area Index
LAN	Limited Area Nonhydrostatic
LAN	Local Area Network
LAS	Live Access Server
LBL	Line By Line
LC	Loop Current
LGM	Last Glacial Maximum
LIMS	Limb Infrared Monitor of the Stratosphere
L"n"	Vertical model resolution of "n" levels.
LSC	Large-Scale Cluster
LW	Long Wave

LWC	Liquid Water Content
LWP	Liquid Water Path
MAST	Monterey Area Ship Track
MB	Megabyte, equal to 1 million bytes
MESO	Modeling Eddies in the Southern Ocean
MGCM	Mars General Circulation Model
MGS	Mars Global Surveyor
MJO	Madden-Julian Oscillation
MLM	Mixed Layer Model
MLS	Microwave Limb Sounder
MMIP	Monsoon/ENSO Intercomparison Project
MMM	Multiply-nested Movable Mesh
MOM	Modular Ocean Model
MOM2	Modular Ocean Model, Version 2
MOM3	Modular Ocean Model, Version 3
MOM4	Modular Ocean Model, Version 4
MOODS	Master Oceanographic Observations Data Set
MOZART	Model for Ozone and Related Chemical Tracers
MPI	Message-Passing-Inferface
MPP	Massively Parallel Processor
MRF	Meteorological Research Flight
MSc	Marine Stratocumulus Clouds
MSU	Microwave Sounding Unit
NAB	North Atlantic Basin
NABE	North Atlantic Bloom Experiment
NADW	North Atlantic Deep Water
NAO	North Atlantic Oscillation
NARE	North Atlantic Regional Experiment
NASA	National Aeronautics and Space Administration
NB	Narrow Band
NCAR	National Center for Atmospheric Research
NCDC	National Climate Data Center/NOAA

NCEP	National Centers for Environmental Prediction
NEMS	Netscape Enterprise Messaging System
NERSC	National Energy Research Scientific Computing Center
netCDF	Unidata's NETwork Common Data Format
NH	Northern Hemisphere
NHC	National Hurricane Center
NMC	National Meteorological Center/NOAA
NOAA	National Oceanic and Atmospheric Administration
NODC	National Oceanographic Data Center/NOAA
NOPP	National Ocean Partnership Program
NP	North Pacific
NRG	Northern Recirculation Gyre
NVAP	NASA Water Vapor Project
NWS	National Weather Service
OAR	Oceanic and Atmospheric Research
OCMIP	Ocean Carbon-Cycle Model Intercomparison Project
ODA	Ocean Data Assimilation
OLR	Outgoing Longwave Radiation
ONR	Office of Naval Research
OS	Operating System
OTL	Ocean Tracers Laboratory/Princeton University
PCMDI	Program for Climate Model Diagnosis and Intercomparison
PE	Processing Element
PEI	Princeton Environmental Institute
PFC	Perfluorocarbon
PILPS	Project for Intercomparison of Land-Surface Parameterization Schemes
PMEL	Pacific Marine Environmental Laboratory
PMIP	Paleoclimate Model Intercomparison Project
PNA	Pacific-North American
POM	Princeton Ocean Model
PPPL	Princeton Plasma Physics Laboratory
PSCs	Polar Stratospheric Clouds

QBO	Quasi-Biennial Oscillation
QG	Quasi-Geostrophic
QUEST	Query Underlies Effective Science Teaching
RAINS-Asia	Regional Air Pollution Information System - Asia
RAOB	RAdiosonde OBservation
RAS	Relaxed Arakawa-Schubert
RCM	Radiative-Convective Model
RFI	Request for Information
RFP	Request for Proposal
R"n"	Horizontal resolution of spectral model with rhomboidal truncation at wavenumber "n".
SAGE	Stratospheric Aerosol and Gases Experiment
SAMS	Stratospheric Aerosol Measurement System
SAMW	Subarctic Mode Water
SAO	South Atlantic Ocean
SAT	Surface Air Temperature
SAVE	South Atlantic Ventilation Experiment
SB	Single Band
SBUV	Solar Backscatter Ultraviolet (satellite)
SCM	Single Column Model
SDTS	Software Development and Technical Support
SGI	Silicon Graphics, Inc.
SH	Southern Hemisphere
SHMEM	Shared Memory
SiB	Simple Biosphere
SIS	Sea Ice Simulator
SKYHI	The GFDL Troposphere-Stratosphere-Mesosphere GCM
SLT	Semi-Lagrangian Transport
SME	Solar Mesosphere Explorer
SMP	Symmetric Multiprocessors
SOI	Southern Oscillation Index
SPCZ	South Pacific Convergence Zone
SPECTRE	Spectral Radiation Experiment

SST	Sea Surface Temperature
SUN	Sun Microsystems, Inc.
SVD	Singular Vector Decomposition
SW	Simulated Wave
TB	Terabyte, equal to 1 trillion bytes
TCO	Tropospheric Column Ozone
TES	Thermal Emission Spectrometer
THC	Thermohaline Circulation
TIO	Tropical Intraseasonal Oscillations
T"n"	Horizontal resolution of spectral model with triangular truncation at wavenumber "n".
TOA	Top-of-the-Atmosphere
TOGA	Tropical Ocean and Global Atmosphere project
TOMS	Total Ozone Mapping Spectrometer
TOPEX	Topographic Experiment
TOVS	Tiros Operational Vertical Sounder
TRACEA	Transport and Atmospheric Chemistry near the Equator-Atlantic
TRW	Topographic Rossby Waves
TTO	Transient Tracers in the Oceans
UARS	Upper Atmosphere Research Satellite
UBB	Ultimate Bulletin Board
UNICOS	Cray's Operating System
URI	University of Rhode Island
UTH	Upper Tropospheric Relative Humidity
WCRP	World Climate Research Program
VLAN	Virtual Local Area Network
WGNE	Working Group on Numerical Experimentation
WMO	World Meteorological Organization
WOCE	World Ocean Circulation Experiment
WWB	Westerly Windburst
WWNFF	Woodrow Wilson National Fellowship Foundation
XBT	Expendable Bathythermograph
ZODIAC	Gridpoint Climate Model